Christos Lampris

Solidification/Stabilisation of Air Pollution Control Residues from Municipal Solid Waste Incineration

A thesis submitted for the degree of
Doctor of Philosophy from Imperial College London
2013

Department of Civil and Environmental Engineering

Imperial College London

In loving memory of my father, Ioannis Lampris

DECLARATION OF ORIGINALITY

I hereby declare that the present thesis titled

"Solidification/Stabilisation of Air Pollution Control Residues from Municipal Solid Waste Incineration"

is the product of my own work and that any work of others presented herein has been fully cited and referenced.

COPYRIGHT DECLARATION

ABSTRACT

Air pollution control (APC) residues are by-products of the flue gas cleaning process in energy-from-waste (EfW) plants treating municipal solid waste. They are classified as a hazardous waste in the EU Waste Catalogue and are a priority hazardous waste stream in the UK due to high alkalinity, concentrations of volatile heavy metals and soluble salts. Plans currently exist to increase the number of EfW plants in the UK, with the potential to increase future arisings of APC residues. Stabilisation/solidification (S/S) is an inexpensive treatment technology, involving mixing of the waste with cementitious binders. The main objective of this research is to assess the effectiveness of CEM I and ground granulated blast furnace slag (GGBS) as S/S binders for the treatment of APC residues. The ultimate goal is to expand existing knowledge on S/S systems and assist development of more sustainable treatment methods for APC residues. S/S APC residue specimens were prepared varying the waste-to-binder and water-to-solids ratios and subsequently tested for physical properties and contaminant leaching according to international standards. Geochemical modelling was used to assess contaminant release-controlling processes and contribute to more efficient mix and treatment design.

Results from this study indicate that mechanical properties of 50 wt.% CEM I and GGBS mixes exceed UK landfill disposal criteria (1.0 MPa), achieving unconfined compressive strength (UCS) values of up to 21 MPa. CEM I mixes with 10 and 20 wt.% binder addition also met the criterion of 1.0 MPa, achieving UCS values of up to 10 MPa. In contrast, 10 and 20 wt.% GGBS mixes exhibited inferior mechanical properties (UCS < 1.0 MPa). S/S is hampered predominantly by high concentrations of chloride in APC residues. All monolithic S/S samples exceeded relevant UK waste acceptance criteria (monWAC) for chloride (20,000 mg/m^2) within the first two days of the 64-day monolithic leaching test. Altough partial immobilisation occurs through the formation of chloro-complexes, S/S of APC residues would require binder additions greater than 50 wt.% to meet UK requirements for landfill disposal. Leaching of Pb also becomes problematic for mixes with 10 and 20 wt.% binder addition, exceeding UK monWAC (20 mg/m^2). Nevetheless, the amphoteric nature of heavy metals and the high solubility of chloride salts could favour extraction of potentially valuable elements through washing procedures. Modelling results indicate that a simple washing step may be able to extract 650 mg of Pb and 120 mg of Zn per kg of APC residues treated, while removing approximately 90% of available chloride.

ACKNOWLEDGEMENTS

I would first like to thank my supervisors, Professor Chris Cheeseman and Dr. Geoff Fowler, for their trust in me to start and finish a part-time PhD while working full-time. Professor Cheesemans' support has been unwavering and his guidance has been instrumental to see me through to the end. Dr. Fowler has provided good insights and analytical expertise and the discussions on topics beyond science have always been interesting. Now at the end, and after eight years of knowing them both, I undoubtedly consider them good friends.

I would like to thank my mother, Ioanna Karakaidou, and my sister, Maria Lampri for their love and faith in me. My mother has been a constant source of inspiration and along with my father are the reasons that I became an engineer in the first place. I owe everything to them. Maria has a fascinating ability to make laugh even through the toughest times, and has provided me with all the support a brother can wish for.

I would like to thank my partner, Karine Cung, for all her patience and loving support throughout this challenging endeavour. I hope that I will be able to be as supportive in years to come, through good times and bad.

I would also like to thank Dr. Julia Stegemann for her advice and contribution to publications resulting from this work. It has been a fantastic experience working on the *ProCeSS* project led by Dr. Stegemann and learnt a lot while working as part of a group of talented and knowledgeable individuals.

Finally, the work required to complete this thesis as part of a part-time PhD took place in five countries over the last seven years. I have made many good friends over this time that provided me with support and motivation to complete this thesis. I would like to thank all those friends and hope that we can cross paths again the near future.

TABLE OF CONTENTS

LIST OF FIGURES

LIST OF TABLES

LIST OF ABBREVIATIONS

AES	Acid Extraction Sulphide Stabilisation
ANC	Acid Neutralisation Capacity
ANOVA	Analysis of Variance
APC	Air Pollution Control
BREF	Best available technique reference document. Refers to European Commission documents that have been adopted under the Industrial Emissions (2010/75/EU) and Integrated Pollution Prevention and Control (2008/1/EC) Directives.
BSE	Backscattered Scanning Electron (refers to microscopy techniques)
CHC	Coefficient of Hygroscopic Contraction
CHE	Coefficient of Hygroscopic Expansion
CSA	Calcium Sulphoaluminate (refers to type of cement)
DEFRA	UK Department of Food and Rural Affairs
DHA	Dissolved Humic Acid
DIC	Dissolved Inorganic Carbon
DOC	Dissolved Organic Carbon
ECN	Energy Research Centre of the Netherlands
EDS	Energy Dispersive Spectrometry
EfW	Energy from Waste
EKS	Electro-Kinetic Stabilisation
EPA	Environmental Protection Agency
EU	European Union
FOM	Figure of Merit
FTIR	Fourier Transform Infrared Spectroscopy
GGBS	Ground granulated blast furnace slag
HFO	Hydrous Ferric Oxides
IBA	Incinerator Bottom Ash
ICP-OES	Inductively Coupled Plasme Optical Emission Spectroscopy
IR	Infrared Spectroscopy
LeachXS	Leaching Expert System (refers to software package by ECN)
L/S	Liquids-to-Solids ratio
monWAC	Monolithic Waste Acceptance Criteria

MSW	Municipal Solid Waste
MSWI	Municipal Solid Waste Incineration
OLS	Ordinary Least Squares (refers to regression method)
OPC	Ordinary Portland Cement
PAH	Polyaromatic Hydrocarbons
PCB	Polychlorinated biphenyls
PFA	Pulverised Fuel Ash
ProCeSS	Process Envelopes for Cement-based Stabilisation/Solidification
RMSE	Root Mean Square Error
SELCHP	South East London Combined Heat and Power
SEM	Scanning Electron Microscopy
SEM-EDS	Scanning Electron Microscopy-Energy Dispersive Spectrometry
SI	Saturation Index
S/S	Stabilisation/Solidification
SUC	Shrinking Unreacted Core (refers to leaching model)
TCLP	Toxicity Characteristic Leaching Procedure
UCS	Unconfined Compressive Strength
XANES	X-ray Absorption Near Edge Structure
XAS	X-ray Spectroscopy
XRD	X-Ray Diffractrometry
XRF	X-Ray Fluorescence
w/b	Waste-to-Binder Ratio
w/s	Water-to-Solids Ratio
WAC	Waste Acceptance Criteria
WtE	Waste to Energy

CEMENT CHEMISTRY NOTATION

C_3S	Tricalcium silicate or alite – C_3SiO_5 or ($3CaO.SiO_2$)
C_2S	Dicalcium silicate or belite – C_2SiO_4 or ($2CaO.SiO_2$)
C_3A	Tricalcium aluminate – $Ca_3Al_2O_6$ or ($3CaO.Al_2O_3$)
C_4FA	Calcium aluminoferrite – $2(Ca_2AlFeO_5)$ or $4CaO.Al_2O_3.Fe_2O_3$
CSH	$3CaO.2SiO_2.8H_2O$
Ettringite	$[Ca_3Al(OH)_6.12H_2O]_2.(SO_4)_3.2H_2O$ or $C_3A.3CaSO_4.32H_2O$
Friedel's Salt	$Ca_4Al_2(OH)_{12.05}(Cl)_{1.95}.4H_2O$
Kuzel's Salt	$Ca_4Al_2\ (SO_4)_{0.5}(Cl)(OH)_{12}.6H2O$
AFm	AFm (Al_2O_3-Fe_2O_3-mono) refers to a family of hydrated calcium aluminates structurally related to hdyrocalumite with the general formula $[Ca_2(Al,Fe)(OH)_6]\cdot X\cdot xH_2O$, where X is a singly charged (e.g. Cl^-) or half of a double charged (SO_4^{2-}, CO_3^{2-}) anion. Examples of AFm phases are monosulphate ($C_3A.CaSO_4.12H_2O$), Friedel's Salt and monocarbonate.
AFt	AFt (Al_2O_3-Fe_2O_3-tri) are also hydration products with the general formula $[Ca_3(Al,Fe)(OH)_6]\cdot X_3\cdot xH_2O$. They are formed under broadly similar conditions as the AFm phases but the difference is that they have a higher ratio of CaX to C_3(A, F). For example ettringite (AFt phase) contains 3 molecules of anhydrite compared to monosulphate (AFm phase) which contains one.
LDH	Layered Double Hydroxides

Note that the following solution species in the document with and without their charge are used interchangeably: Al: Al^{3+}, OH: OH^-, SO_4: SO_4^{2-}, CO_3: CO_3^{2-}, Cl: Cl^-

1. INTRODUCTION

1.1 EU Waste Management Strategy and Status

The European Commission published in December 2005 the Thematic Strategy on the Prevention and Recycling of Waste (Waste TS) (COM(2005)666), together with a proposal for the revision of the Waste Framework Directive (2006/12/EC), which ultimately became Directive 2008/98/EC on Waste. The Waste TS included a number of actions to modernise the legal framework and promote waste prevention, re-use, recycling and recovery. The long-term goal is for the EU to become a recycling society that seeks to avoid waste and uses waste as a resource (European Commission, 2011). The revised Waste Framework Directive (2008/98/EC) aims to implement actions set out in the Waste TS. It highlights that for Member States to better protect the environment, measures should be taken for the treatment of wastes which are aligned with the hierarchy depicted in Figure 1.1. This hierarchy demonstrates that the basis for the development of any waste management/treatment strategy should be the prevention of waste generation, with disposal being the least sustainable option. This waste management framework is commonly referred to as "Reduce – Reuse –Recycle". The aim to divert waste from landfill and reduce its environmental impact is also clearly communicated to the Member States in Directive 1999/31/EC on the Landfill of Waste. This Directive includes among other measures, targets for Member States to achieve in relation to the amount of waste landfilled. In particular, Member States should reduce the fraction of biodegradable waste landfilled by i) 75% of that produced in 1995 by 2010, ii) 50% of that produced in 1995 by 2013 and iii) 35% of that produced in 1995 by 2020.

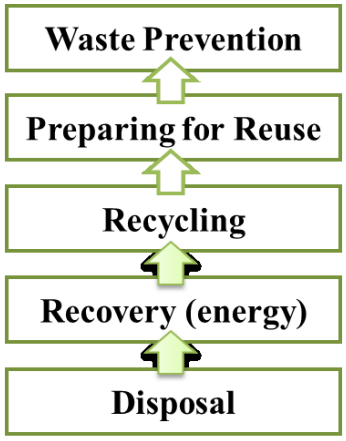

Figure 1.1 EU Waste Management Hierarchy

Despite the EU focus on waste prevention, waste generation in the EU has exhibited an increase over the recent decades, including increases in municipal solid waste (MSW), construction and demolition waste, hazardous and packaging waste. According to a recent report for the review of the Waste TS (European Commission, 2010), modelling results based on an assumption of no great future changes to policies or implementation mechanisms (legislative and market-based), predict that per capita rates of waste generation will peak for the EU-27 around 2016, then plateau until 2030 but not decline. Figure 1.2 shows the variation observed in EU-27 Member States in terms of waste generation. The differences observed are indicative of the economic development, as well the social and environmental conditions in the different member states. These differences pose a significant challenge for an EU-wide movement up the waste management hierarchy and diversion of waste from landfill. An additional challenge is the implementation of the Waste Framework Directive to the management of waste in Member States where significant infrastructure investments may be needed. The ability of certain EU Member States to make such investments will also determine their progress towards implementation of the Waste Framework Directive.

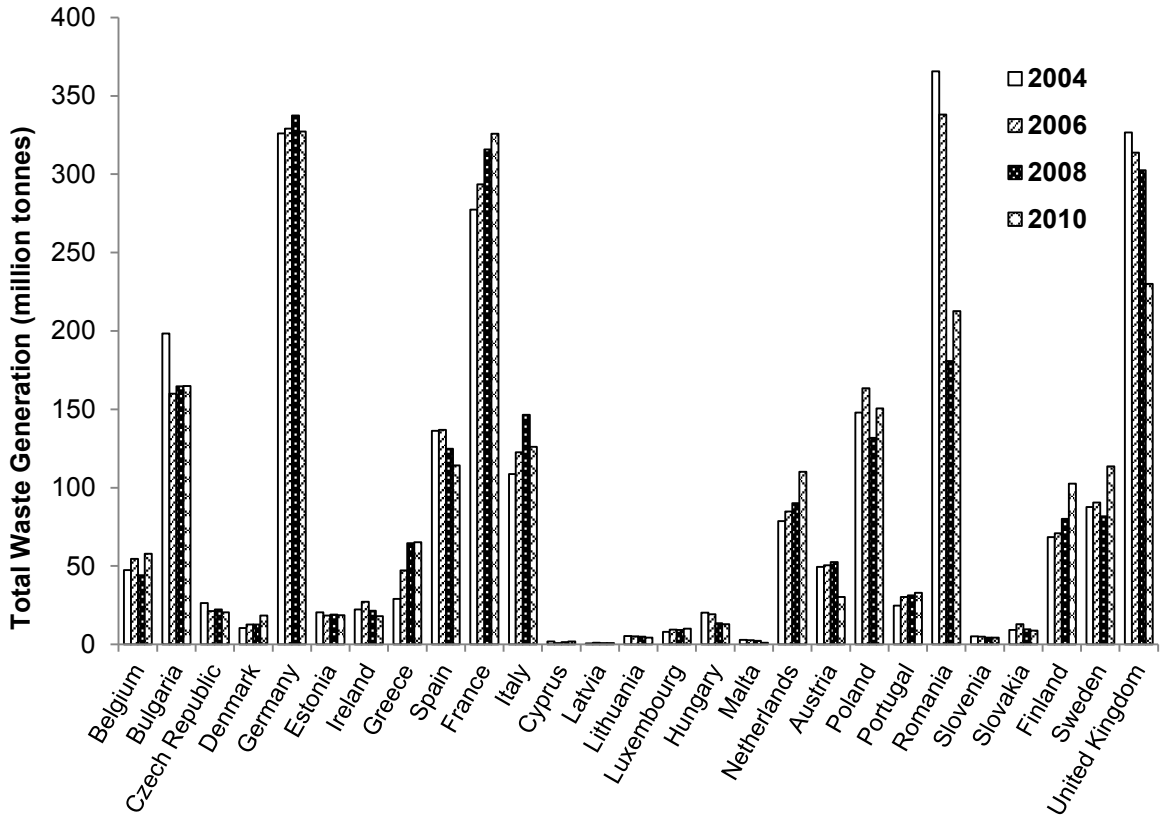

Figure 1.2 Total waste generation in EU-27 member states (Eurostat, 2013)

1.1.1 Municipal Solid Waste (MSW)

MSW is a waste stream which has exhibited an increase in quantities in the EU. Increased population and affluence, modern day consumerism, as well as other socioeconomic (e.g. 2008 financial crisis) and environmental factors can affect MSW generation. According to the report by the European Commission (2010), MSW generation per capita in the EU-27 had been increasing until recently (from 499kg in 1997 to 523kg in 2006, with a peak of 527kg in 2002), but since 2006 appears to be stabilising at between 523 and 525kg. However, the total amount of MSW generated by the EU continues to increase, as shown in Figure 1.3, associated with a slight increase in EU-27 population. On the whole, EU-12 Member States generate less MSW per capita than the EU-15, and less than the EU-27 average. This may also be indicative of differences in the implementation and focus on the Waste Framework Directive between developed Member States and newer and less developed members.

Current management options for MSW include reuse/recycling, composting/digestion, incineration and landfill disposal. Figure 1.4 shows the percentage utilisation of different options since 2005. It can be observed that recycling percentages within the EU are increasing with a concurrent reduction in landfilling percentages, which is aligned with a movement up the waste management hierarchy. It is noted however, that recycling is not increasing at the same rate in all Member States and MSW management practices and preferred treatment options vary significantly across the EU. Data for the EU-25 in 2005 (EU, 2010) demonstrate that three distinct groups of Member States can be identified: i) Member states with high levels of recycling and incineration (i.e. Switzerland, Netherlands, Sweden), ii) Member States with intermediate levels of recycling, substantial levels of landfilling and limited amounts of energy recovery (i.e. UK, Portugal, Italy) and iii) a group of Member States with low levels of recycling and high levels of landfilling (i.e. Greece, Cyprus, Romania).

It is evident that in order to achieve the objectives of the Waste Framework Directive the challenges faced by the individual Member States differ. Member States with low levels of recycling need to put in place the appropriate infrastructure, policies and incentives to increase recycling rates and reduce their dependence on landfill. Members with high levels of recycling should aim to improve recycling and material recovery/reuse mechanisms and focus on waste prevention which is the optimal level in the waste management hierarchy.

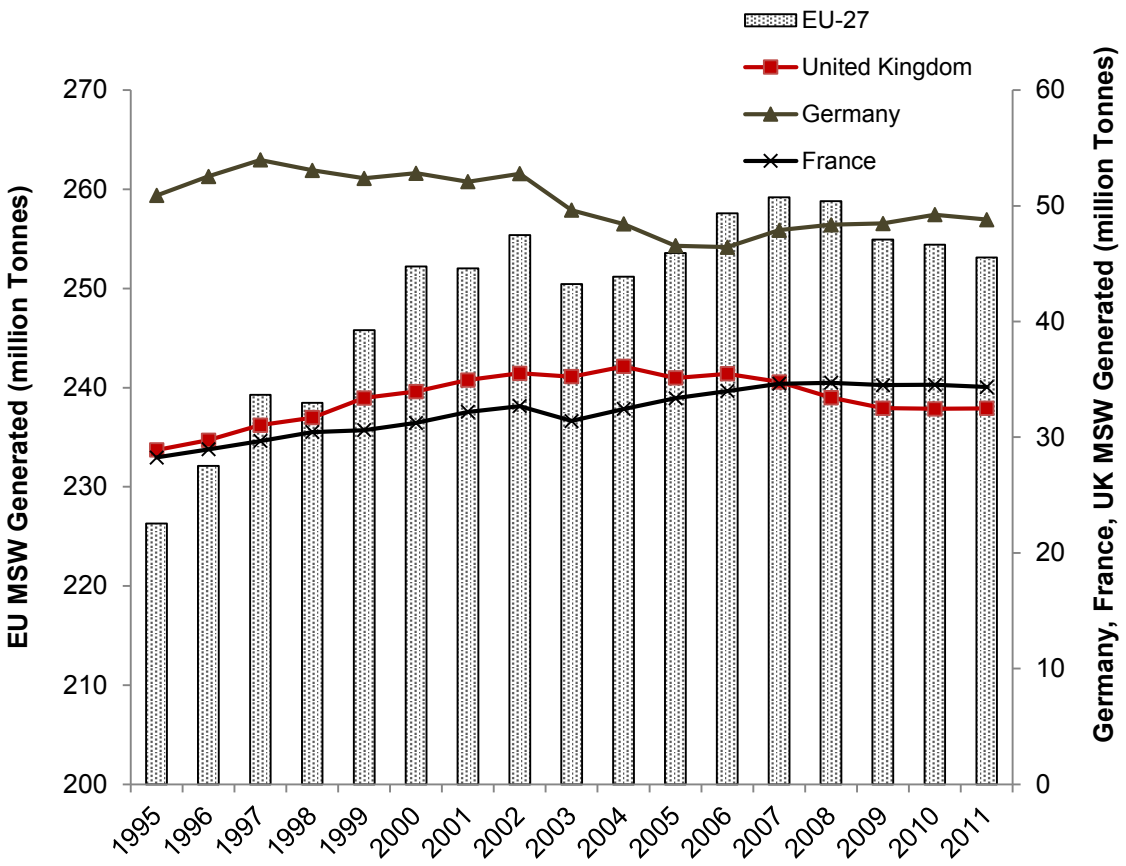

Figure 1.3 MSW Generation in the EU (Eurostat, 2013)

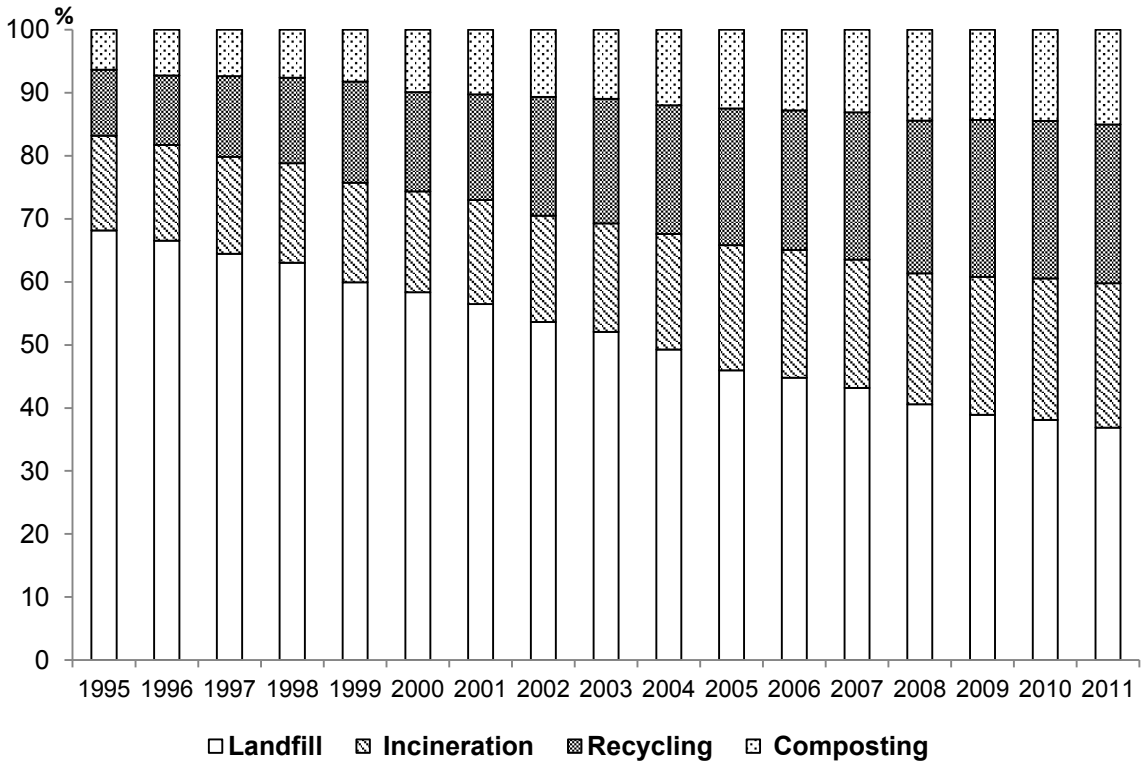

Figure 1.4 MSW treatment routes in EU-27 (Eurostat, 2013)

It is expected that increases in MSW generation will place significant emphasis on management/treatment of this waste stream over the next years, while addressing waste prevention. Despite significant focus on MSW reuse and recycling, technological advances in MSW incineration have increased its attractiveness and use of the last decade.

1.2 Incineration of Municipal Solid Waste

Incineration is a thermal treatment method which involves the combustion of waste at high temperatures. Modern incinerators are referred to as waste-to-energy (WtE) or energy-from-waste (EfW) plants, as energy is recovered in the form of heat during the treatment process and utilised to provide power and heat to local communities. The incineration and energy recovery process is described in further detail below. EU Directive 2008/98/EC on the management of wastes sets specific criteria about the efficiency levels (energy output) at which an incinerator can be considered as an energy recovery facility.

The volumes of MSW produced, coupled with the constant limitations on landfill space have increased the use of incineration as a treatment method for MSW in the EU, as shown in Figure 1.5. This increase has been observed in spite of the low priority of treatment of waste via energy recovery in the EU waste management hierarchy (Figure 1.1). Current worldwide emphasis on viable alternative energy sources may also make incineration with energy recovery an increasingly attractive option for the treatment of MSW. This causes concerns about the impact of incineration on recycling or other material recovery options as well as the contribution of incineration to emissions of greenhouse gases (GHG).

The majority of incineration is currently taking place in the financially developed EU member states such as Germany, France, Netherlands and the UK. According to Eurostat data, in 2011, 66% of total MSW incinerated in the EU is attributed to these countries. It is also noteworthy that the countries with the greatest use of incineration also ranked among the top waste producers in the EU in the period 2004-2010, as demonstrated in Figure 1.2. Figure 1.5 shows that the amount of MSW treated via incineration in the UK has increased steadily over the last decade. There are currently 24 EfW plants in the UK and plans exist to increase the use of incineration in the near future.

Although the vast majority of incineration in the EU involves energy recovery, there is still a fraction of MSW incinerated without (significant) energy recovery as shown in Figure 1.6. More than 90% of EU MSW treated in incinerators without energy recovery is found in Germany. It is noted that energy recovery may actually occur in some of these facilities but their energy efficiency level may be lower than the thresholds at which treatment can be deemed as energy recovery rather than disposal (European Commission, 2010). In addition, data presented in relation to energy recovery originate from before the adoption of the specific requirements about the efficiency level. According to a report covering the period from 2004 to 2007, an estimated 40% of municipal waste incinerators in the EU might be able to achieve the energy efficiency criteria for municipal waste incinerators set by Directive 2008/98/EC (European Commission, 2010).

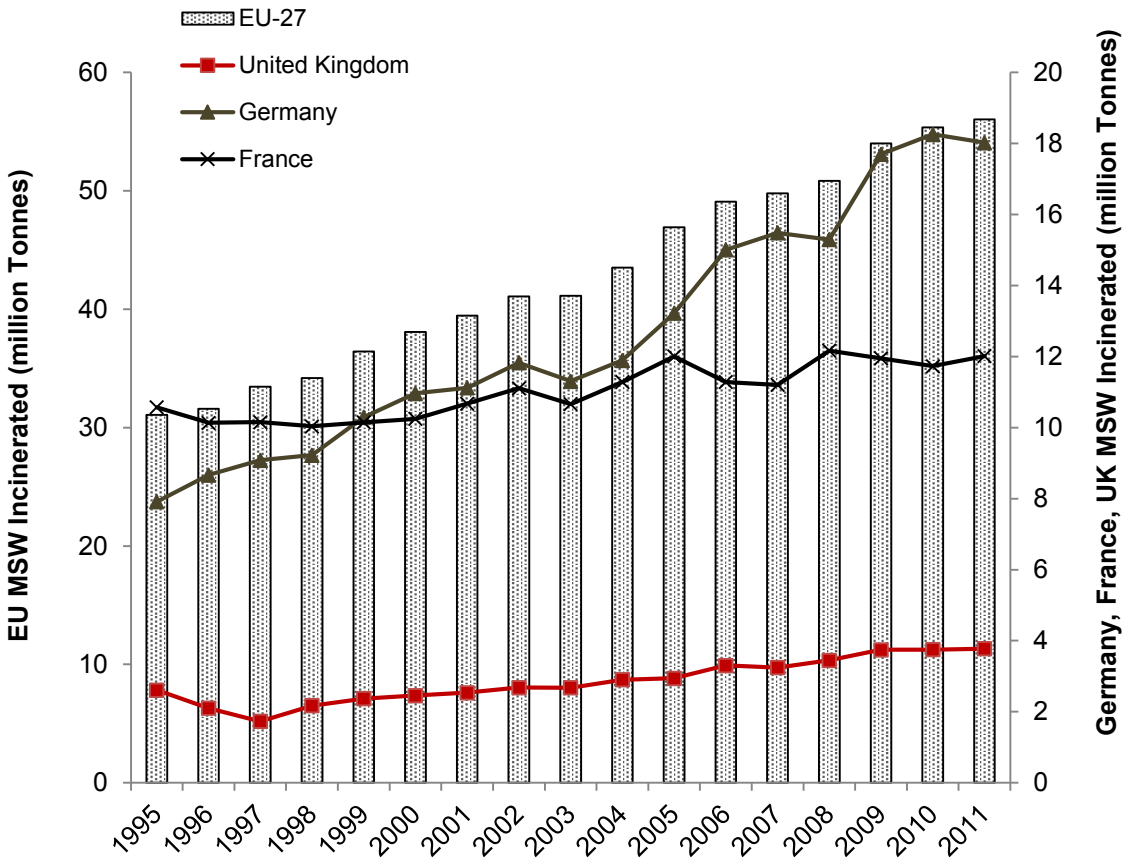

Figure 1.5 EU MSW Incineration (Source: Eurostat, 2013)

Incineration with energy recovery has the obvious advantage of electricity or heat production while significantly reducing the volume of waste to be landfilled. However, there is a negative public perception due to concerns about potential environmental and health impacts from hazardous compounds that can be emitted in the flue gases, such as dioxins and furans.

Incineration in the UK and the European Community is regulated by the EU Directive 2000/97/EC on the Incineration of Waste. The Directive sets strict limits on the emission of organic pollutants including dioxins and furans (0.1 ng I-TEQ/Nm^3), as well as the levels of NOx gases (daily average of 400 mg/m^3) and heavy metals (average of 0.5 or 0.05 mg/m^3 depending on the metal).

Rapid technological developments in the incineration sector with respect to air pollution control and tightening of emission standards have resulted in CO_2 emissions from incineration decreasing by 45% between 1990 and 2007. CO_2 emissions from incineration in this period contributed only 0.1% of total EU-15 greenhouse gas emissions. Although the Waste Incineration Directive does not include CO_2 limit values, the waste incineration best available technique reference document (BREF) under the Integrated Pollution Prevention Control (IPPC) Directive does make reference to CO_2 emissions. (European Commission, 2010).

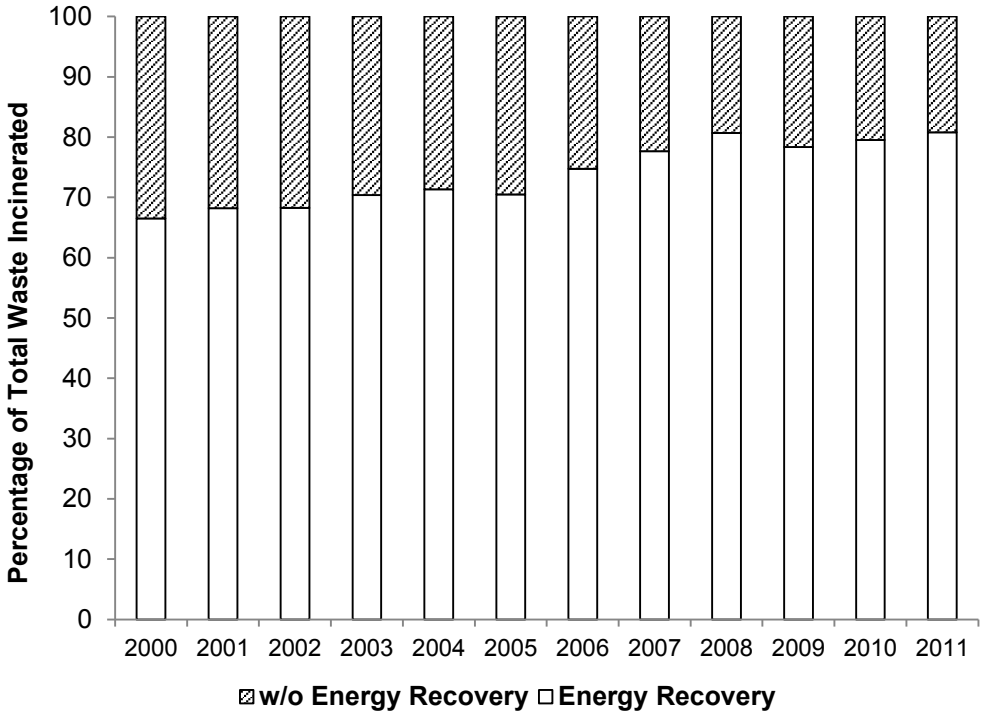

Figure 1.6 Fractions of MSW incinerated with and without energy recovery (Eurostat, 2013)

The layout of a standard EfW plant are presented in Figure 1.7. It is the schematic of the SE London combined heat and power plant (SELCHP) with a capacity of 420,000 tonnes of

MSW per annum. A summary of the incineration process at SELCHP is provided here. A typical EfW plant can be divided into five main areas (Williams, 2005):

a. Waste delivery, bunker and feeding system
b. Furnace
c. Heat recovery
d. Emissions control
e. Energy recovery via district heating and electricity generation

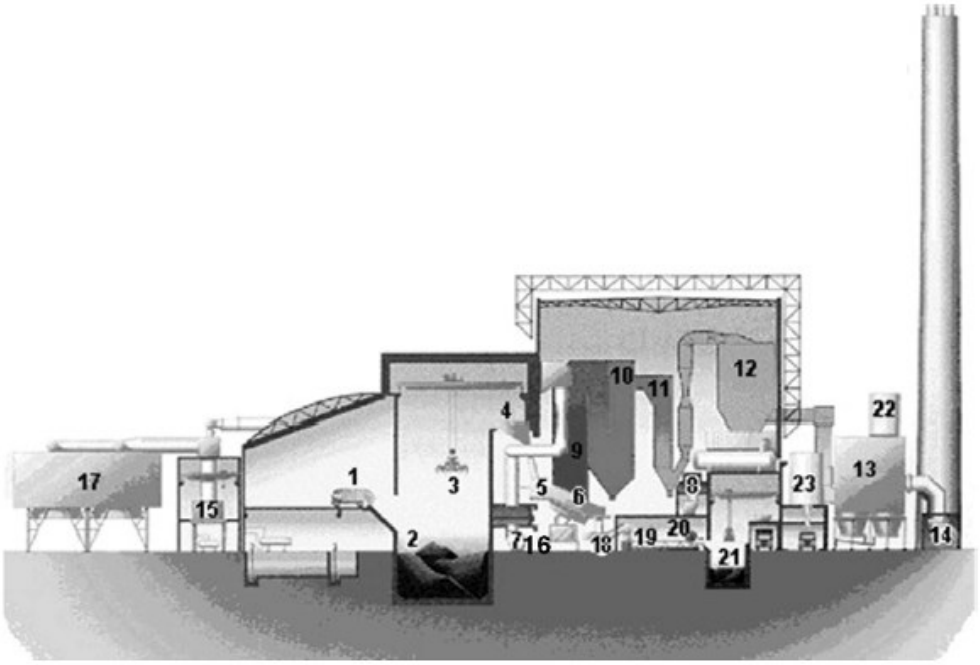

Figure 1.7 SELCHP facility (reproduced from Amutha Rani et al., 2008a)

The incineration process starts with the collection of waste in the waste storage pit (bunker) as shown in Figure 1.7. Crane grabs are used to transfer the waste to the feed hopper and down the feed chutes. Waste is then fed to the incineration grate where it burns at temperatures greater than 850 ºC. Incinerators treating clinical or hazardous wastes utilise temperatures greater than 1200 ºC due to the nature of the waste treated. Rotary grates are

used to ensure thorough burning and that enough oxygen is supplied to avoid incomplete combustion. Hot gases produced during the combustion process pass through a water tube boiler where they are cooled. This generates steam which leaves the boilers at a temperature of 395 ºC and pressure of 46 bar, and is fed directly into a single 35MW steam turbine generator. Steam from the turbine is also used to pre-heat the combustion air to 125 ºC for the waste combustion process.

Cooled gases from the boiler contain acid gases as well as heavy metals and organic compounds which can have a significant detrimental effect to human health. As mentioned above, compliance with the EU Waste Incineration Directive requires advanced air pollution control systems. These typically involve particulate removal systems such as electrostatic precipitators and neutralisation of acid gases using wet, dry or semi-dry lime or sodium bicarbonate scrubbers. Activated carbon is used to absorb heavy metals and dioxins and injection of dilute ammonia solution to reduce nitrogen oxides to nitrogen. Bag house filters are also used for the removal of dust particles prior to the emission of the clean gases to the atmosphere. A more detailed description of EfW plants is provided by Williams (2005).

The MSW incineration process produces two types of solid residues (by-products), incinerator bottom ash (IBA) and air pollution control (APC) residues. IBA is a residue from the combustion of wastes and is a heterogeneous mixture of slag, metals, ceramics, glass and other non-combustible organics. APC residues are fine particulates produced and collected from the flue gas treatment process and are a mixture of fly ash, alkaline reagents and carbon (Xiaomin, 2006). APC residues from MSW incineration are also often incorrectly referred to in the literature as MSWI fly ash. IBA has found use as a construction material in applications such as road paving applications and is being commercially exploited. Recent developments however have shown that IBA may exhibit eco-toxic effects in the long-term depending on the surrounding environment following application (Ore et al, 2007). Management of APC residues is more problematic due to the nature of the waste which is described below.

1.3 Air Pollution Control Residues

APC residues represent 3-5% by weight of the waste incinerated (Todorovic, 2003). Their composition can vary depending on the type of incinerator, the composition of the waste

treated and the flue gas treatment process. APC residues are classified as hazardous waste according to the European Waste Catalogue (19 01 07*), predominantly due to the high alkalinity. APC residues also contain high concentrations of soluble salts and volatile heavy metals such as cadmium, copper, lead and zinc. They also contain trace levels of organic pollutants such as dioxins and furans. Furthermore, compounds in APC residues produce a highly alkaline environment, which can increase the solubility and release in the environment of amphoteric heavy metals (Figure 1.8).

The amount of APC residues from MSW incineration in the UK has been reported to have increased from 170,000 tonnes in 2006 to 190,000 in 2009 (Johnson, 2012). According to the UK Department of Food and Rural Affairs (DEFRA), EfW plants currently under construction will increase APC residue generation in England by a further 77,000 tonnes per annum. Additional EfW plants have also obtained planning approval which indicates that generation of APC residues will increase by at least a further 95,000 tonnes per annum (total increase of 172,000 tonnes) if all the plants become operational (Department of Environment, Food and Rural Affairs, 2010). The possibility of the development of additional EfW capacity in the near future would lead to even greater quantities being produced. By far the majority of APC residues is produced by MSW EfW plants, but clinical waste incineration and sewage sludge incineration also contribute to the generation of APC residues.

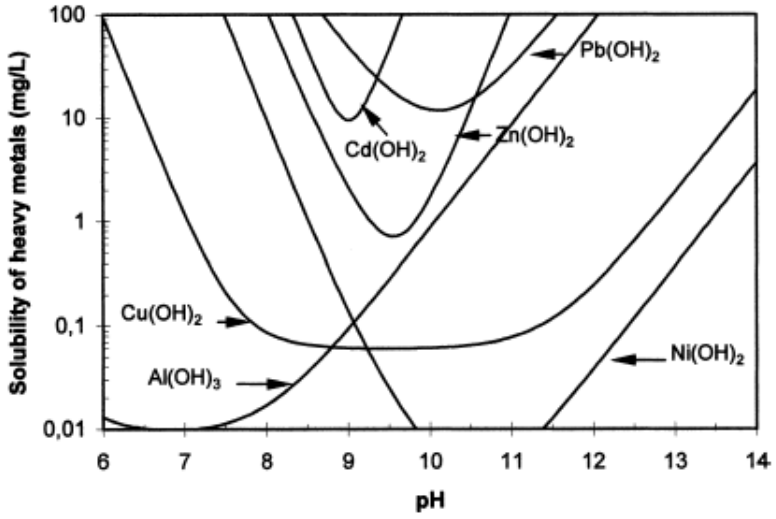

Figure 1.8 Solubility of the most common metal hydroxides as a function of pH

1.3.1 Relevant Legislation and Developments

APC residues are a hazardous waste which is included in the EU Waste Catalogue (19 01 07*). Hazardous wastes in the EU Waste Catalogue are denoted with an asterisk following the waste code number. Management of APC residues should be in accordance with the EU Waste Framework Directive (2008/98/EC). In terms of disposal in landfills, APC residues are governed by the EU Landfill Directive (1999/31/EC). This requires the pre-treatment of hazardous wastes before landfill to an appropriate level. The Landfill Directive has been implemented in England and Wales through the 2002 Landfill Regulations. These set specific criteria for acceptance of waste in landfills with respect to contaminant leaching.

DEFRA published in March 2010 a policy document including the strategy for the management of hazardous wastes in the UK. This strategy aims to align UK objectives, as well as waste treatment and management legislation with the waste management hierarchy in the Waste Framework Directive (2008/98/EC). The DEFRA strategy document sets the priority as the development of treatment facilities for a number of problematic hazardous waste streams, including APC residues. This strategy sets six (6) high level principles for the management of hazardous wastes which are summarised as follows (Department of Environment, Food and Rural Affairs, 2010):

1. Hazardous waste should be managed in accordance with the Waste Framework Directive hierarchy with landfill disposal being the last resort.
2. Infrastructure provision for the treatment of hazardous wastes should be in accordance with the waste management hierarchy. Such infrastructure should constitute the UK self-sufficient in terms of hazardous waste recovery and disposal.
3. Reduce UK reliance on landfill for hazardous wastes, which should only be used when there is no recovery or better disposal option.
4. No mixing or dilution. Hazardous wastes shall not be mixed with different categories of hazardous wastes, or any other waste, substances or materials, unless under the terms of an environmental permit, and the mixing operation conforms to Best Available Techniques.
5. Hazardous organic wastes that cannot be reused, recycled or recovered shall be subject to destruction using best available techniques, with energy recovery for all

appropriate treatments. No hazardous organic waste shall be landfilled unless the requirements of the Landfill Directive are met.

6. End of the Landfill Waste Acceptance Criteria (WAC) derogation (3x WAC) which allowed hazardous wastes to continue to be landfilled.

These principles demonstrate the emphasis of the revised UK waste management strategy on the EU waste management hierarchy, value recovery from waste and diversion from landfill. Banning of mixing and dilution as well as the end of the three times (3x) WAC derogation will significantly affect current management practices of certain hazardous waste streams, including APC residues.

An important aspect is also the provision of infrastructure required to treat hazardous wastes. The DEFRA policy document states with respect to APC residues that there is a need for at least five (5) facilities that can recycle APC residues to other materials that can be re-used. Each facility should have a capacity of 33,000 tonnes per annum. A significant number of additional facilities may be needed if further EfW plants are developed. Other treatments for APC residues, which simply enable the waste stream to meet Landfill Directive requirements, are lower down the hierarchy (Department of Environment, Food and Rural Affairs, 2010).

1.3.2 Management Options and Treatment Technologies for APC residues

The main disposal method for APC residues in the UK until recently involved conditioning with aqueous wastes prior to placement directly into monofill cells at a hazardous waste landfill (Environment Agency, 2002). Mixing with wastewater is used to adjust the pH to the lower alkaline range and form a treated product that solidifies and has some strength. This also aids handling of APC residues, as it prevents wind-blown dispersal at the landfill.

APC residues have been the focus of several studies over recent years, and different treatment methods have been suggested for the immobilisation/removal of contaminants of concern. These technologies range from stabilisation/solidification processes to thermal treatment and electrokinetic extraction. Each technology exhibits advantages and disadvantages in relation to contaminant immobilisation/removal efficiency, cost, by-products and carbon footprint. Recent review papers (Amutha Rani et al, 2008a; Quina et al, 2008) provide a thorough assessment of current management/treatment options for APC residues. Although this study

focuses on stabilisation/solidification (S/S) using cementitious binders as a treatment method for APC residues, alternative technologies and relevant recent studies are presented here for completeness. Management/treatment options for APC residues are presented in Figure 1.9. This list is not exhaustive but includes major areas of study over recent years. In addition, S/S includes a wide range of techniques for the treatment of APC residues, including S/S using hydraulic binders. In the following chapters however, the S/S notation will refer only to the latter.

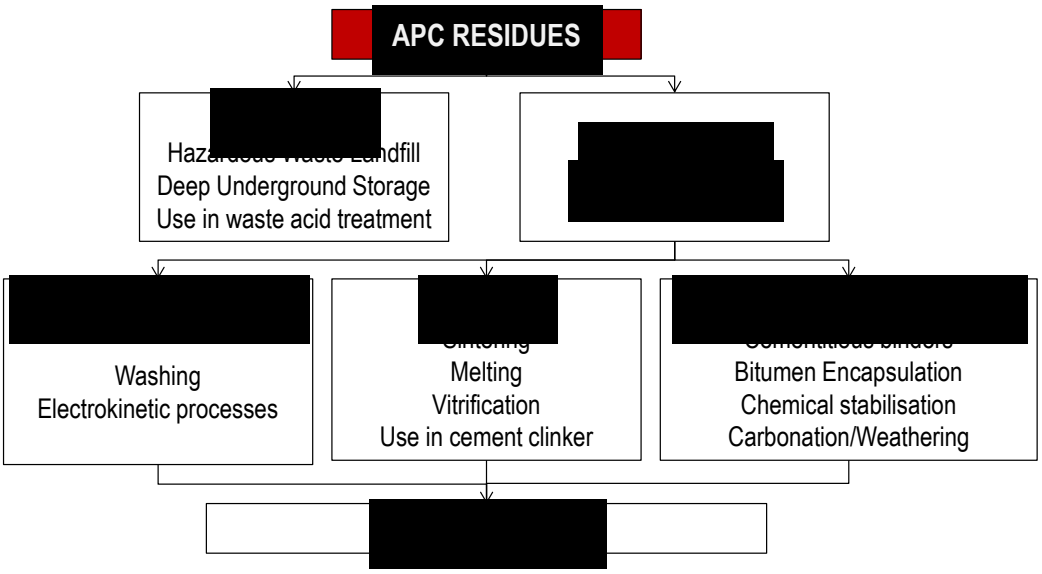

Figure 1.9 Management/Treatment Options for APC residues

a) Disposal in Hazardous Waste Landfill

As mentioned in previous sections, APC residues in the UK are conditioned with aqueous wastes prior to landfilling directly into monofill cells at a hazardous waste landfill. The DEFRA strategy (DEFRA, 2010) aims to divert APC residues from landfill and considers such disposal options as the last resort. Banning of mixing with other waste streams (unless stipulated in the terms of a permit) may potentially limit the use of this method. Furthermore, APC residues treated in this way leach total dissolved solids at more than three times the waste acceptance criteria (WAC). Although this is currently considered acceptable, the revised DEFRA strategy aims to end the three times WAC derogation, which may constitute the APC residues treated this way unacceptable for landfilling.

b) Deep Underground Storage

Significant fractions of UK APC residues are being sent for underground storage in a salt mine in Cheshire, England. APC residues are collected from the EfW plant and loaded into sealed transit capsules and transferred to the mine floor, 170 m below the surface. According to DEFRA (Department of Environment, Food and Rural Affairs, 2010), this option which is currently applied to problematic waste streams such as APC residues and metallic mercury, is also considered as a landfill operation in the UK. Therefore the same limitations may apply as with the disposal in hazardous waste landfill option.

c) Use of APC Residues for Waste Acid Treatment

A number of hazardous waste companies in the UK are using APC residues to treat waste acids. This converts the lime content of APC residues into compounds which are less hazardous and uses approximately equal weights of waste acid, typically HCl, and APC residues as:

$$2HCl + Ca(OH)_2 \rightarrow CaCl_2 + 2H_2O$$

The pH is maintained at a high level to prevent the salts being released into solution. The $CaCl_2$ formed has a lower risk classification than $Ca(OH)_2$. As a consequence of adding acid to the APC residues, the concentration of metals such as Pb and Zn is reduced through incidental dilution. The resultant mixture is no longer described as an APC residue but as sludge from a physico/chemical treatment, which is considered non-hazardous according to the classification and code in the EU Waste Catalogue (19 02 06). This allows this sludge to be disposed in non-hazardous waste landfills. However, there are no data available on the long-term leaching and effectiveness of this process (Amutha Rani et al, 2008a). The revised DEFRA strategy may also limit application of this treatment method, as it involves mixing of wastes and landfill disposal of the end product.

d) APC Residue Washing

Several studies have attempted to optimize washing of APC residues using single or multiple-stage processes, using water and/or acid solution as the washing liquid, and achieving significant removal efficiencies of soluble salts and heavy metals. The liquids-to-solids (L/S)

ratio and treatment time and pH were found to be the most important parameters affecting the performance of single or multiple-stage processes.

Rouchotas and Cheeseman (2001) investigated the removal of impurities from APC residues using a two-step washing process including a water-wash step, varying the liquid-to-solids ratio (L/S) and an acid-wash step using nitric acid. Trial washes of APC residues with distilled water at L/S ratios of 5, 10, 20, 40 and 60 (l/kg) were completed and it was found that an L/S ratio of 20 and washing time of 30 minutes was optimum for removing large quantities of soluble cations. In addition, concentrations of heavy metals in the leachate were only significant for pH < 6.0.

Chimenos et al (2005) used a two-stage water-washing process, followed by a further rinse, varying the solids-to-liquids ratio (1/10 to 1/1 g/L) and treatment time (1-24h). The researchers concluded that the optimum conditions taking into account water consumption and process economics were an S/L ratio of 1/3 g/L and 1 hour of treatment time. APC residues treated in this manner were classified as non-special according to Catalonian (Spanish) standards. The same research also investigated the potential of using $MgSO_4$ during washing in order to consume the lime in APC residues, reduce the initial ash pH and thus solubility of heavy metals. Leaching tests according to German DIN 38414-S4 showed improved leaching of heavy metals and chloride. Reduction in chloride and metal leaching was also attributed to the formation of Sorel cement ($5Mg(OH)_2 \cdot MgCl_2 \cdot 5H_2O$), which, coupled with the production of gypsum, was thought to have resulted in curing reactions and thus improved physical encapsulation.

Kung-Yuh Chiang et al (2008) investigated treatment of APC residues and extraction of heavy metals, utilising the flue gas during MSWI incineration (reducing CO_2 emissions) and waste acid. APC residues were mixed with water at a constant L/S ratio (L/S=40). CO_2 4% v/v was injected, reducing the initial pH of the ash (11.4-12.0) to 7.2-7.5. The targeted pH of 3-5 was achieved using 1N HCl. CO_2 was used to simulate gaseous emissions during MSWI, while HCl was used to simulate the waste acid. The effect of varying particle sizes and pH was investigated. Metals in the leachant were extracted via chemical precipitation. Metal extraction capacity increased with decreasing pH and the authors reported recoveries ranging between 0.5% and 1% of initial APC residue dry mass for Cd and Zn. After treatment, APC

residues were classified as non-hazardous and metals were not detected in the leachant complying with Taiwan regulatory standards. However, results for chloride were not reported.

Aguiar Del Toro et al (2009) investigated a wet extraction method coupled with a carbonation step for the removal of heavy metals and chlorides from MSWI and straw combustion fly ashes. The experimental programme involved suspending fly ash in water at a defined Liquid-to-Solids (L/S) ratio and then bubbling CO_2 until the solution reached a stable pH for 30 minutes. Experimental controlling factors were L/S, time, CO_2 treatment and pH. The authors concluded that the most significant factors for MSWI fly ash were pH and L/S ratio. A model optimisation showed that the optimum conditions for the extraction of the elements studied for MSWI fly ash would be:

- L/S ratio: 18;
- pH: 3;
- No CO_2 treatment; and
- Leaching time: 120 minutes

These conditions achieved removal of 90% of Cl, 60% of Cd, 4% of Pb, 44% of Cu and 70% of Zn.

Fenfen Zhu et al (2010) investigated the behaviour of chloride during washing of MSWI fly ash using X-ray Diffraction (XRD) and X-ray absorption near edge structure (XANES). Approximately 15% of the chlorine in the fly ash was in the form of NaCl, 10% was in the form of KCl, 51% was $CaCl_2$, and the remainder was in the form of Friedel's salt ($Ca_4Al_2(OH)_{12.05}(Cl)_{1.95}.4H_2O$). They concluded that both the mole percentage and the amount of soluble chlorides including NaCl, KCl and $CaCl_2$ decrease quickly with the increase of liquid to solid (L/S) ratio or washing frequency. Friedel's salt and the related compound ($11CaO{\cdot}7Al_2O_3{\cdot}CaCl_2$) were reliable standards for the insoluble chlorides which decrease at a slower rate during washing.

Hyks et al (2007) using pH-static leaching tests and geochemical modelling suggested the same solubility controlling minerals for the elements Al, Ca, Mg, Si, S, Mo, Zn, Cd, and Cu, regardless of the untreated/washed character of the APC residues. In addition, they concluded that 57% of total Pb was found to be rather mobile in the initial stages of the leaching tests.

Washing of APC residues can improve the leaching characteristics of the waste, especially in terms of soluble salts and it exhibits heavy metal recovery potential. However, there may be a difficulty with the management of the resultant chloride-rich wastewater. This can be sent for treatment prior to discharge, and evaporation/crystallisation processes can be used to recover salts such as NaCl, $CaCl_2$, KCl and gypsum (Amutha Rani et al, 2008a).

e) Electrokinetic Processes

Electrokinetic remediation/stabilisation (EKS) methods have been extensively used in contaminated soil remediation. The process is also being used as a non-destructive method for chloride removal from hardened concrete to avoid steel corrosion. There has been a growing interest recently and efforts are made to utilise the electrokinetic phenomenon for the treatment of waste materials such as MSWI bottom ash and APC residues (Traina et al, 2009; Ferreira et al, 2008; Ottosen et al, 2006; Pedersen et al, 2005), sewage sludge (Ferri et al, 2009) and others (i.e. mine tailings).

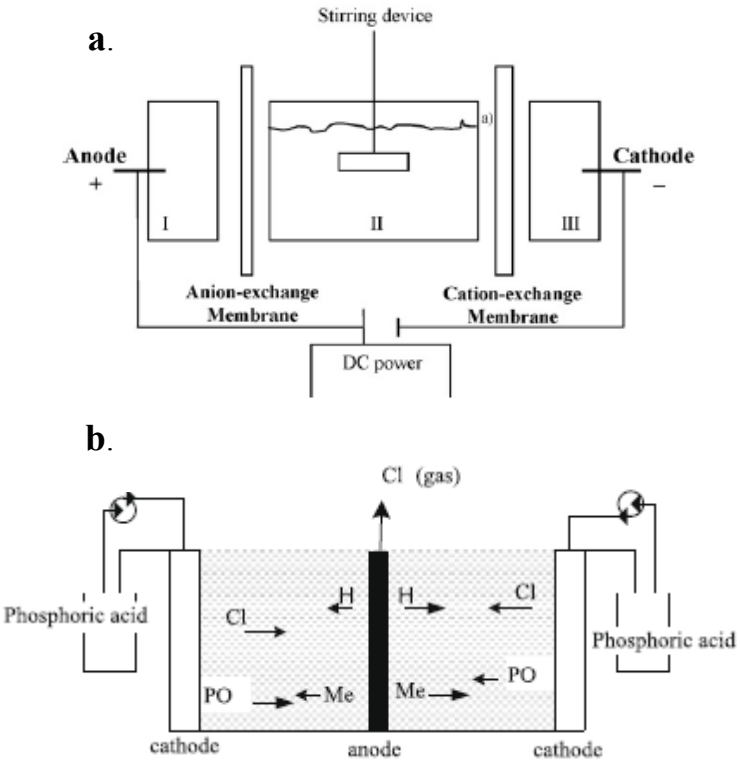

Figure 1.10 Schematic diagrams of EKS design a. Lima et al (2010) b. Traina et al (2009)

The process involves placing the waste material under the influence of an electric field. The electric field is provided by a direct current (DC) power supply and two electrodes. Under the influence of the electric field the anions move towards the anode and the cations towards the cathode. Transport occurs due to the hydraulic flow induced by the electric field (electro-osmosis), the movement of ions to the electrode of the opposite charge (electro-migration) and the movement of charged particles or colloids due to the presence of the electric field which can carry bound contaminants (electro-phoresis) (Ferri et al, 2009). A schematic of EKS design cells are presented in Figures 1.10a-b. The process has the ability to rapidly remove soluble salts and heavy metals simultaneously. Highly mobile anions such as chlorides will be transported towards the anode while heavy metals will be transported towards the cathode. In addition, heavy metals transported to the cathode can be subsequently recovered using methods such as electroplating, precipitation or co-precipitation at the electrode and complexing with ion-exchange resins (Al-Hamdan and Reddy, 2008).

Ottosen et al (2006) used a cell similar to the one shown in Figure 1.10a to remove Pb, Cu and Cl from APC residues. The material was continuously stirred and $NaNO_3$ was used as anolyte and catholyte with a pH < 2, adjusted using HNO_3. Ion exchange membranes were used to ensure current efficiency by allowing ions from the ash suspension to electro-migrate to the electrolytes, but preventing ions (with opposite charge) from the electrolytes from entering the ash suspension (Pedersen et al, 2005). Experiments were conducted varying the L/S ratio in the waste compartment (II), while treatment duration and cell voltage were fixed at 15 days and 7V respectively. At the end of the experiments, the suspension was filtered and the water-extractable concentrations of Pb and Cu were measured in the ash. Concentrations in the electrolytes, electrodes and ion exchange membranes were also measured. Concentrations of Pb in the ash increased from 8560 to 16800 mg/kg indicating that Pb is present in the least soluble fraction of the ash. Cu concentrations in the ash decreased from 2200 to 860 mg/kg. Removal of chloride was more effective with removal efficiencies greater than 98%.

Traina et al, (2009) used the cell shown in Figure 1.10b for the removal of chloride and heavy metals from MSWI bottom ash. Phosphoric acid was used at the cathodes which had a twofold role; i) maintain a catholyte pH < 5.0 and ii) aid removal of heavy metals via phosphation. The water content of the ash was adjusted to 25% and experiments were conducted varying the cell voltage while treatment time was fixed at 24 hours. Heavy metal

precipitation was observed in the cathodes in the form of phosphates (metal hydroxyl-apatite, chloro-apatite, calcium-apatite minerals). Significant leaching reduction was reported for Ba, Pb and Fe (97%, 92% and 92% respectively), compared to the untreated material according to leaching test EN 12457-2:2004. Leaching of Cu and Cl was reduced by 90% and 80% respectively, but was still above regulatory requirements for reuse.

Other studies have investigated the use of assisting agents such as ammonium or sodium citrate, ammonia (Pedersen et al, 2005) or pre-treatment of APC residues through acid washing to improve heavy metal removal efficiency (Ferreira et al, 2008). Lima et al (2010) conducted statistical analyses on results obtained from EKS treatment of different ashes and concluded that the factors affecting the efficiency of the process are the ash type, treatment duration and dissolution of the ash (percentage of initial wet mass). For the latter and with respect to APC residues, Ferreira et al (2008) reported that removal of soluble salts results in reduced fouling of the ion exchange membranes and increases heavy metal removal. In addition pH effects during the process may affect heavy metal removal efficiency for APC residues. Hydrolysis (water-splitting) occurs at the anode and cathode according to the following reactions:

Cathode: $2H_2O + 2e^- \rightarrow 2OH^- + H_2\ (g)$

Anode: $2H_2O \rightarrow 4H^+ + O_2\ (g) + 4e^-$

Hydronium ions move towards the cathode while hydroxyl ions move towards the anode. When the two fronts meet there is a pH jump occurring which is usually closer to the cathode due to the faster mobility of protons (Traina et al, 2009; Al-Hamdan and Reddy, 2008). The acid front may result in a reduction of the natural pH of APC residues (>11) to a range where heavy metals exhibit low solubility, thus affecting removal efficiency (Ferreira et al, 2005).

Although most studies have used a single cell where electrolytes are circulated treating small amounts of waste, Kirkelund et al (2010) investigated treatment of APC residues on a pilot scale able to treat batches of 8 kg of APC residues in a continuous process. The process involves circulating APC residues in suspension (diluate) and tap water (concentrate) through an electrodialytic stack consisting of flow spacers and ion exchange membranes as well as electrodes at each end. During the process, contaminants migrate from the diluate to the concentrate. Different experiments were conducted varying the treatment time, applied

voltage and the shape of diluate tank, treating raw or carbonated APC residues. Treatment of carbonated APC residues achieved Danish criteria for reuse except for Cr, while raw APC residue failed to meet limits for Pb, Zn and depending on the experiment, Cl. Power consumption in the different experiments ranged between 0.5 and 13 kWh.

Electrokinetic processes exhibit promising results for the removal of heavy metals and especially chloride from APC residues which can enable reuse. Considerations however for commercial large-scale application include the treatment time, power consumption, aqueous by-products that may require further treatment and of course the capacity for material recovery and/or reuse.

f) Thermal Treatment

Thermal treatment of incinerator residues normally involves heating to temperatures above 1000 ºC. This induces changes in physicochemical properties that reduce the volume and leaching and produces a stable and non-hazardous slag (Amutha Rani et al, 2008a). Thermal treatment technologies can be divided into i) vitrification (conventional and plasma vitrification), ii) melting (or fusion) and iii) sintering.

Vitrification is the process where a mixture of glass precursor materials and waste are melted at high temperatures (>1100 ºC) to produce an amorphous and homogeneous glassy solid. Heavy metal retention is achieved by chemical bonding and encapsulation. Vitrification processes vary from conventional electric furnaces to DC plasma arc technology (Amutha Rani et al, 2008a).

Andreaola et al (2008) vitrified mixes of bottom ash and MSWI fly ash with inert materials such as feldspar waste and glass cullet at 1400 ºC. The end products showed significantly reduced leaching of contaminants and properties comparable with commercial soda-lime glasses. It is noted that this study utilised relatively low amounts of MSWI fly ash in the mixes between 4-5 wt.%.

Amutha Rani et al (2008b) investigated the vitrification of APC residues blended with silica and alumina using DC arc plasma technology, as shown in Figure 1.11. The mix was vitrified at 1600 ºC producing an amorphous homogeneous glass and reducing the volume of waste by

70—75%. Release of contaminants for concern such as Pb, Zn and Cl decreased significantly below UK limits for disposal to inert waste landfill. The theoretical energy input was calculated at 700kWh/ton of APC residues.

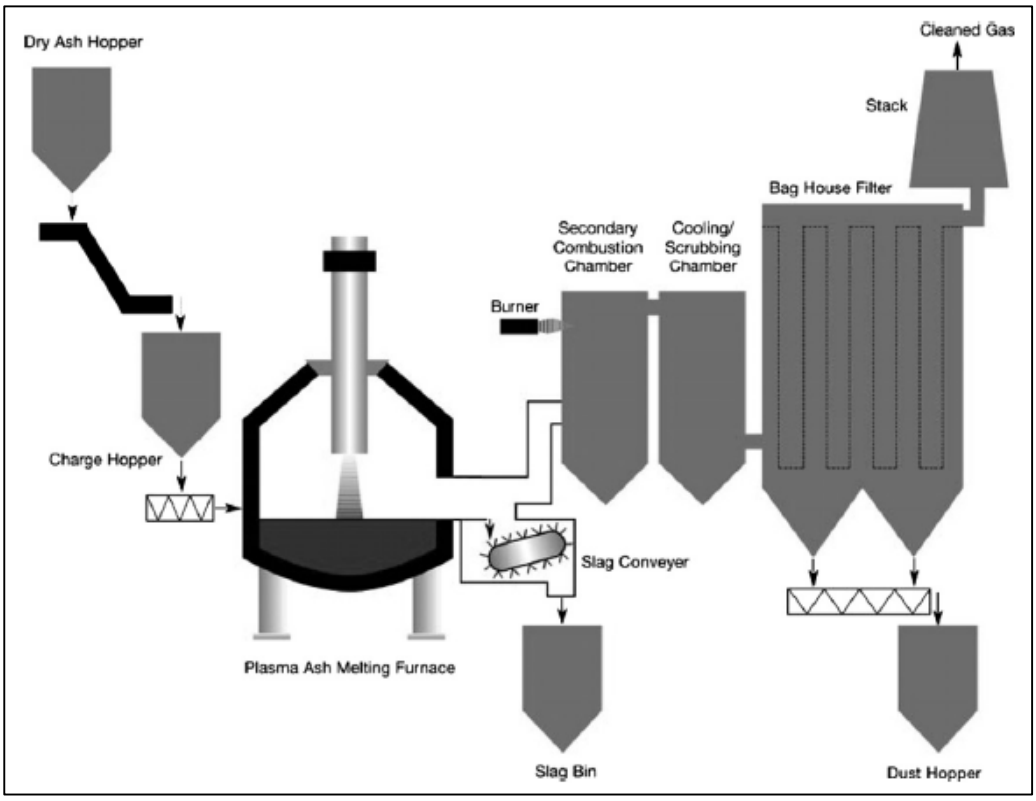

Figure 1.11 Process flow diagram for the plasma vitrification of incinerator ashes (Amutha Rani et al, 2008b)

Peng Zhao et al, (2010) also investigated the effect of plasma vitrification and different cooling methods on the leachability of heavy metals in MSWI fly ash. Heavy metal concentration in the slags reduced for Pb, Zn and Cd by up to 94%, 85% and 97% respectively but increased for Cr. Leaching of these contaminants was far below regulatory limits. Water-cooled and composite-cooled (cooled in air and quenched in water) slags exhibited better leaching results compared to air cooled slags.

Recent studies have evaluated the reuse potential of the glass produced from vitrification of APC residues to produce construction materials or glass ceramics. Kourti et al (2010) used glass from DC plasma treatment of APC residues to produce geopolymers with high compressive strengths (up to 130MPa), high density and low porosity. Roether et al, (2010)

have investigated the production of sintered glass ceramics from DC plasma treated APC residues and reported that products with properties comparable to porcelain and marble.

Melting (fusion) is similar to vitrification but in this case no additives are used and less emphasis is given to process chemistry. The end product includes crystalline phases and may be heterogeneous (Quina et al, 2008; Chandler et al, 1997).

According to Trujilo-vazquez et al (2009), the French power supply company EDF investigated treatment of APC residues using a melting thermal process where the waste is placed in an electric arc furnace at 1450 ºC for 15 minutes. The end product was a melilite-type solid solution with significantly lower leaching of contaminants.

The presence of chlorides during thermal treatment can enhance the formation of volatile metal chlorides and HCl gas and therefore result in secondary pollution and/or equipment corrosion. All thermal process systems are equipped with air pollution control systems for the treatment of the flue gas produced during treatment. Kung-Yuh Chiang and Yu-Hsin Hu (2010) studied the effect of washing MSWI fly ash prior to melting. Concentrations of metals in the flue gas were measured and metal retention efficiencies in the slag were calculated based on the heavy metal amount in the water-washed ash and the amount in the slag. Lower concentrations of metals in the flue gas and higher metal retention ratios were reported for Pb and Cu for the washed fly ash, which was attributed to the removal of chlorides during washing (up to 99.7 wt.%). The process however had a negligible effect on Zn volatility and retention in the slag.

Sintering is an alternative thermal method for treating/recycling MSW incinerator ashes. Temperature is increased during the process until chemical phases in the solid achieved reconfiguration (Chandler et al, 1997). Organic residues can be decomposed and heavy metal compounds stabilised by incorporating them into a ceramic material (Amutha Rani et al, 2008a).

Karamanov et al (2003) studied the sintering behaviour of a mix consisting of 70% MSWI fly ash and feldspar waste. Crystallisation was influenced by the heating rate. At high rates, surface crystallisation was the predominant mechanism while at low heating rates (<2 ºC/min), bulk crystallisation occurred. Heating at low rates formed glass–ceramics containing

open and closed porosity. Non-porous sintered samples were obtained using heating rates of 30 ºC /min followed by isothermal treatment at 1120 ºC for 40 minutes.

Zhang Haiying et al (2011) utilised MSWI fly ash in blends with red ceramic clay, feldspar and gangue sand for the production of ceramic bricks. The optimum fly ash addition and sintering temperature were 20 wt.% and 950 ºC respectively. Contaminant leaching from the sintered bricks decreased compared to the green (prior to sintering) bricks, to levels below Chinese limits for hazardous waste identification. The authors recommended use of MSWI fly ash in ceramic brick manufacturing based on physical properties and leaching characteristics.

A recent study by Sun-Yu Chou et al (2009) investigated the use of microwave energy for the sintering of raw and water-washed MSWI fly ash. Samples were treated with a microwave frequency of 2.45GHz at 600W varying the treatment time (10-50 minutes). The authors reported high heavy metal immobilisation efficiencies which increased with treatment time, and decreased sintering efficiency when soluble salts were removed with water-washing. However, flue gas emissions during the process were not reported.

Studies have also attempted to reuse MSWI fly ash in the production of cement clinker (Saikia, et al, 2007; Jill R. Pan et al, 2008; Hui-Sheng Shi et al, 2009a; Lei Wang et al, 2010a). Raw and/or washed fly ash was used in varying amounts between 1.75% and 48% of the raw meal. These studies suggested that volatisation of heavy metals occurs during heating of the raw meal and that the remaining amount of heavy metals is immobilised in clinker phases. The resulting products exhibited potential for practical use, having similar mineralogy and physical properties (i.e. compressive strength) with commercial cements. Issues requiring further investigation include kiln corrosion due to Cl in raw fly ash and long-term durability.

Thermal techniques have the advantage of stabilizing all contaminants of concern in APC residues, reducing the volume of waste and producing potentially re-usable materials. The major drawback of these methods is the partial volatisation of some heavy metals at high temperatures. These thermal treatment systems require air pollution technologies whose end product is a highly concentrated ash with heavy metals (Sakai and Hiraoka, 2000). Thermal

treatment methods also require high power and therefore higher cost compared to other treatment methods and do not involve currently any energy recovery.

g) Chemical Stabilisation Processes

Chemical stabilisation processes involve the use of chemicals such as hydroxides, sulphides, silicates, carbonates, phosphates and chelating agents. Chelates are complexes with multidentate ligands (i.e. ligands with various positions to bind the same cation) (Appelo and Postma, 2005). Contaminants of concern are bound in the resulting products due to precipitation, adsorption, microencapsulation and detoxification (Quina et al, 2010). Addition of phosphates for example can result in the formation of insoluble metal phosphates, thus reducing metal mobility (Geyzen et al, 2004a). Bournoville et al, (2004) suggested that addition of soluble phosphates in water-washed MSWI fly ash can result in the precipitation of apatite, which can in turn form solid solutions with heavy metals.

Zhao Youcai et al (2002) used NaOH, ethylene-diamine-tetra-acetate (EDTA), sodium sulphide and thiourea to treat MSWI fly ash. Fly ash was mixed with varying amounts of the different additives and stirred for 8 hours at 25 ºC. Leaching of treated fly ash samples was assessed via the Chinese leachability toxicity method. It was observed that leaching of Pb and Cd increased with increasing addition of EDTA, while the opposite effect occurred for sodium sulphide and thiourea. The authors concluded that thiourea and sodium sulphide achieved the best results in terms of Pb and Cd immobilisation, meeting Chinese regulatory standards and requiring smaller amounts of reagents to be added. They also suggested that immobilisation of Pb in thiourea occurs through precipitation of an insoluble solid according to the following reaction:

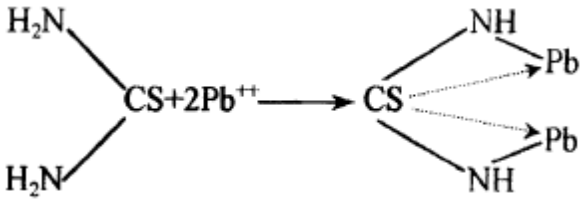

Park (2006) used a colloidal silica solution to treat a chlorine-rich (>35 wt.%) fly ash. Fly ash samples were mixed with a 4 wt.% colloidal solution and treated at temperatures ranging

from 50 to 800 ºC. Samples treated with H_3PO_4 as well as cement were also prepared for comparison. All samples were tested for leaching according to the Toxicity Characteristic Leaching Procedure (TCLP). Products with fly ash and colloidal silica at temperatures of more than 700 ºC exhibited heavy metal leaching below Korean regulatory standards, with Pb^{2+} <0.02 ppm, Zn^{2+} <0.52 ppm, and Cd^{2+}, Cr^{2+}, Cu^{2+}, Mn^{2+}<0.01 ppm. Treatment with cement also yielded leaching concentrations below Korean regulatory limits for all heavy metals tested but did not solidify and remained a friable powder. Addition of H_3PO_4 increased leaching of heavy metals compared to the raw fly ash.

Bayuseno et al (2009) also used a hydrothermal method to produce stable mineral phases with the capacity to immobilise heavy metals, using MSWI fly ash as a source of Si^{4+} and Al^{3+}. Raw and washed fly ash was mixed in 0.5M NaOH or KOH alkali solutions and then treated at temperatures from 90 to 180 ºC for 48 hours. Release of heavy metals was assessed according to the TCLP test and it was lower than TCLP limits for Pb, Cu, Cr and Ni for both raw and washed fly ash. Reduction in leaching was suggested to have occurred due to incorporation in less soluble and more stable phases formed during hydrothermal treatment.

Quina et al (2010) investigated the effect of different stabilising agents for the treatment of APC residues, including NaHS, H_3PO_4, Na_2CO_3, $C_5H_{10}NNaS_2{\cdot}3H_2O$ and $Na_2O{\cdot}SiO_2$. The researchers concluded that all additives had a positive effect on the leaching characteristics but H_3PO_4 and $Na_2O{\cdot}SiO_2$ were selected as the most reliable and economical. Phosphates and silicates achieved Zn release as low as 1 mg/kg, but increased leaching of Cr(VI). Treatment with phosphates at specific L/S ratios can result in a non-hazardous waste classification with respect to heavy metals. All additives investigated had a negligible effect on the release of soluble salts.

Treatment of APC residues using stabilising agents is already applied on a large scale and examples include the *Ferrox* process, the *VKI* process, the *WES-Phix* process, acid extraction and phosphate based stabilization processes. Amutha Rani et al (2008a) describes these processes in more detail, however a summary of each is presented here.

The Ferrox process is comprised of three units. The mixing tank where ferrous sulphate solution is mixed with water and APC residues, the process tank where oxidation of ferrous

iron occurs followed by pH adjustment and the plate filter-place where the treated residue is dewatered. The process is claimed to fully immobilize heavy metals in the treated residue.

The VKI process is a one-stage treatment process involving the removal of soluble salts by aqueous extraction, chemical stabilisation of the washed product with carbon dioxide (CO_2) or phosphoric acid (H_3PO_4), washing the product and final dewatering. A process schematic of the VKI process is presented in Figure 1.12.

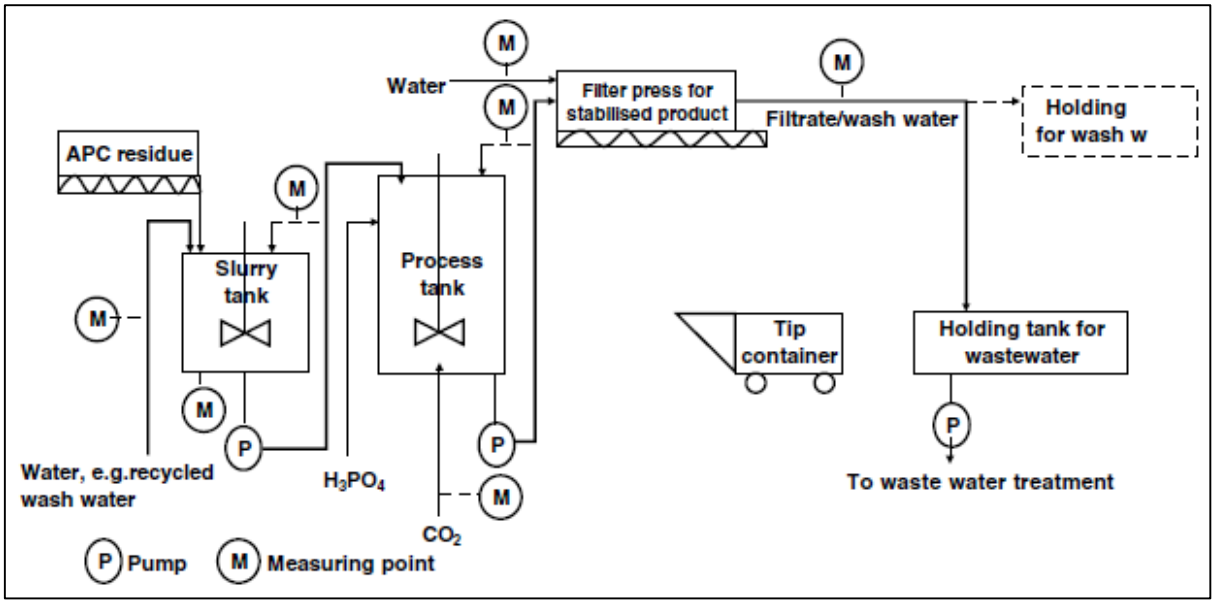

Figure 1.12 Outline for the pilot plant for the VKI process (Amutha Rani et al, 2008a)

The WES-Phix involves the addition of phosphate for the stabilisation of heavy metals in APC and is completed without washing. Stabilisation occurs due to precipitation of metal phosphates rather than by adsorption of metals onto phosphates.

In the acid extraction sulphide stabilisation (AES) process, incinerator fly ash is acid-extracted and stabilised by NaHS to change residual heavy metals into insoluble heavy metal sulphides. Soluble heavy metals are extracted by the acidic agent and sodium sulphide is added to stabilize the remaining heavy metals.

h) Carbonation

Carbonation is the process where Ca-containing minerals react with CO_2 to produce carbonates. A typical example is the reaction of portlandite with CO_2 according to the following simplified reaction, where $CO_{2(g)}$ is first dissolved in water:

$$Ca(OH)_2 + CO_{2(aq)} \rightarrow CaCO_3 + H_2O$$

Carbonation can occur naturally for waste such as bottom ash and APC residues from MSWI, (also termed as aging or weathering), and it is also a deterioration mechanism for reinforced concrete. Recently, treatment of waste ashes with high calcium content via carbonation has been considered not only for the mitigation of their environmental impact but also as a means of carbon sequestration and storage. Reaction routes for carbonation include (Baciocchi et al, 2009):

i) Aqueous or wet route where the waste is humidified and moderate temperatures (20-50 ^oC) and CO_2 pressures (1-10 bar) are applied. The reaction takes place in a three phase system.
ii) Gas-solid route, in which the reactions are rapid and completion can be achieved in short periods at temperatures above 350 °C and ambient CO_2 pressure.

Todorovic and Ecke (2006) treated bottom ashes, one APC residue and one MSWI fly ash by pumping CO_2 in closed containers (gasbags or plastic buckets) where the ash was stored. The effect of the treatment was evaluated in terms of leaching of eight critical contaminants according to NEN 7374. The impact was greater on bottom ash compared to APC residues and releases of Cr, Se and Pb remained unaffected or increased for the latter. Cl and SO_4 remained mobile in all ashes.

Xiaomin Li et al (2007) investigated the effect of accelerated carbonation on APC residues by adjusting the water content of the waste and placing it in carbonation reactors. Parameters investigated were the water-to-solids ratio (w/s), reaction temperature and treatment time. An optimum w/s ratio of 0.3 was reported as well as significant decrease in the leaching of Pb, up to 2-3 orders of magnitude. Leaching of Cl and SO_4 also decreased but remained greater than the UK Landfill WAC for granular waste.

Similar results were obtained by Lei Wang et al (2010b) who also investigated accelerated and natural carbonation of MSWI fly ash. The optimum w/s ratio was 0.25 while leaching of Pb and Zn reduced by 2-3 and one order of magnitude respectively. Leaching of Cd and Sb however, increased compared to the untreated waste. Carbonation also had a negligible effect on leaching of Cl. The authors attributed the immobilisation capacity of the process to:

- Reduction of the natural ash pH (12.1) to a range where heavy metals exhibit low solubility (9.5-10.5), possibly forming heavy metal carbonates.
- Possible sorption of heavy metals to calcite leading to co-precipitation.
- Physical retention of contaminants by reducing the porosity of monolithic samples.

Baciocchi et al, (2009) investigated and compared both the gas-solid and wet route for carbonation. Similar results were obtained for both routes with respect to contaminant leaching. Pb release was below the limits for non-hazardous waste landfills while leaching of Zn and Cu was below limits for inert waste landfills. As with other studies, leaching of Sb increased after carbonation and Cl largely exceeded limits for hazardous waste landfills. The two routes achieved a similar maximum calcium conversion to carbonates (around 65%) corresponding to a potential CO_2 storage capacity of 250 g/kg residues.

Carbonation as a treatment method for APC residues can be effective in reducing leaching of heavy metals such as Pb and Zn and could potentially be applied on-site at EfW plants. In addition, the capacity of the process for CO_2 storage is aligned with global climate change objectives and GHG emission reduction. However, further process optimisation or combination with other treatment methods may be required to address leaching of heavy metals such as Cd and Sb (depending on ash composition) and soluble salts.

Accelerated carbonation has been recently commercialised in the UK. The company Carbon8 Systems Ltd provides accelerated carbonation technologies for the treatment of industrial wastes and contaminated soils. APC residues are also among the wastes that the company claims to have successfully treated. Carbon8 Systems Ltd currently has a pilot plant in operation in the UK which produces aggregates from APC residues via accelerated carbonation.

i) Solidification/stabilization using Binders (S/S)

S/S involves mixing wastes into a cementitious binder system. S/S systems have been widespread due to benefits such as low cost and ease of application. The focus of this study is S/S technologies and application to APC residues from MSWI. A background to the S/S process and a review of recent developments with respect to S/S of APC residues are presented and discussed in the following chapter.

2. REVIEW OF STABILISATION/SOLIDIFICATION: BASIC CONCEPTS, APPLICATION TO APC RESIDUES AND RECENT DEVELOPMENTS

2.1 Definitions and EU Status

Stabilisation/solidification (S/S) comprises a wide range of techniques and methods for the treatment of hazardous waste. As the name suggests, it includes two processes (solidification and stabilisation) that can sometimes be interrelated. These terms are occasionally used interchangeably, however they are distinctly different.

- **Solidification** refers to techniques that aim to encapsulate the waste in a monolithic solid with structural integrity. The encapsulation may be of fine waste particles (micro-encapsulation) or of a large block or container of wastes (macro-encapsulation) (Chandler et al, 1997). Contaminant migration is restricted due to a dense matrix with low porosity and high tortuosity, as well as reduced surface area available for leaching.
- **Stabilisation** refers to techniques that aim to reduce environmental impact by converting contaminants in the waste material into less soluble, mobile or toxic forms. They do not necessarily involve a change in the physical nature of the waste.

These two processes are often used in combination such as in S/S using hydraulic binders, altering both the physical and chemical characteristics of the waste. This provides an additional barrier in case for example that the solidified matrix deteriorates.

S/S using hydraulic binders was used to treat nuclear wastes in the 1950s and was widely applied to hazardous wastes in the early 1970s (Conner, 1990). It has been used both to treat wastes as a pre-treatment stage prior to disposal, as well as soils and sediments contaminated by previous improper disposal. According to Batchelor (2006) S/S has been identified by the US EPA as the Best Demonstrated Available Technology for 57 regulated hazardous wastes and is one of the most commonly applied technologies at Superfund sites in the US, being used at 24% of sites between 1982 and 2002.

S/S has also been adopted by certain EU Member States as a pre-treatment method for waste prior to landfill to comply with the requirements of the Landfill Directive (1999/31/EC). Figure 2.1 provides information on the quantities of hazardous waste treated using S/S in the EU as well as selected Member States (Eurostat). It is noted that quantities presented in Figure 2.1 pertaining to treatment via S/S, may be skewed as Eurostat includes quantities of vitrified waste in the same treatment category as S/S waste. Quantities of hazardous waste treated via S/S have increased in the EU-27 between 2004 and 2008[1].

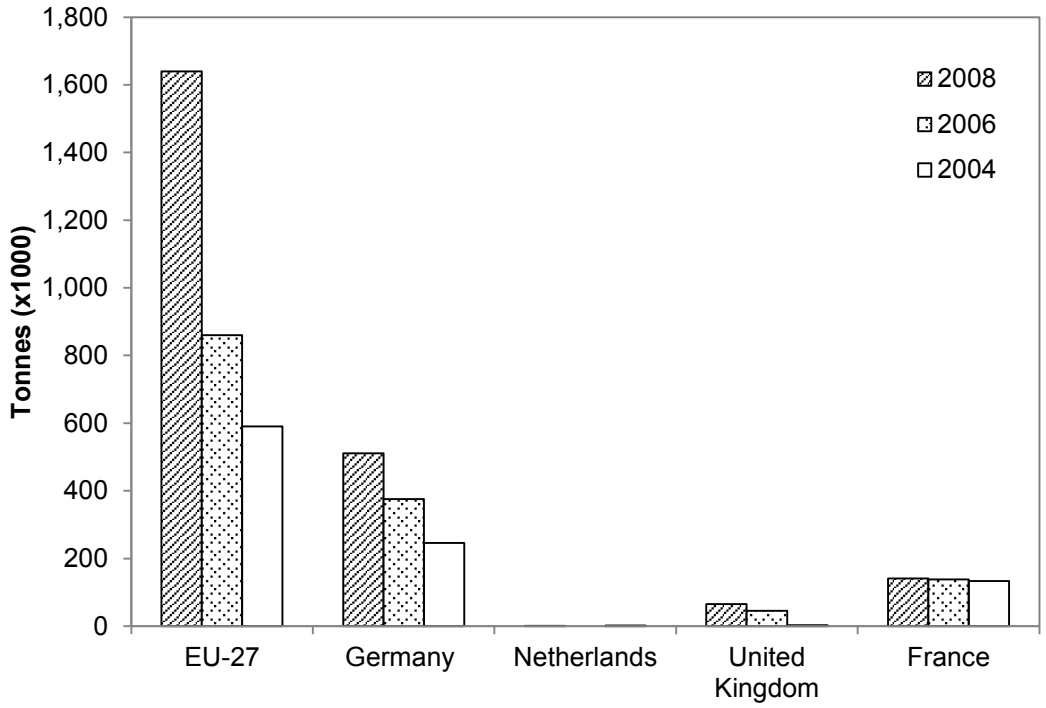

Figure 2.1 S/S (including vitrification) in the EU (Eurostat, 2013)

Germany and France have been utilising S/S extensively for the treatment of hazardous waste. In contrast, the UK has been fairly slow in the adoption of S/S as a treatment method compared to the other Member States. A sharp increase was however observed in the use of S/S in the UK between 2006 and 2008 according to Eurostat data, with quantities increasing from 3,225 to 65,077 tonnes. A guidance document on the cement S/S of contaminated soils published in 2004 by the UK Environment Agency (Environment Agency, 2004) explains that the poor uptake of S/S technologies up to 2004 was due to the following barriers:

- Relatively low cost and widespread use of disposal to landfill
- Lack of authoritative technical guidance on S/S in the UK

[1] 2010 Eurostat data for S/S waste were not available by the time this thesis was finalised

- Uncertainty over the durability and rate of contaminant release from S/S-treated material
- Experiences of past poor practice in the application of cement stabilisation processes used in waste disposal in the 1980s and 1990s
- Residual liability associated with immobilised contaminants remaining on-site, rather than their removal or destruction

Recent developments in EU waste management policies may pose an additional barrier to the application of S/S as a treatment method for hazardous wastes. In particular and as described in Chapter 1, treatment methods that do not involve material reuse or recovery will be given less priority compared to other alternatives. Hence, S/S prior to landfill disposal may be a less preferred option as Member States are aiming to move up the waste management hierarchy included in the Waste Framework Directive.

S/S using cementitious binders has the advantage that it may provide a route for utilisation of certain types of waste in cement or concrete matrices. Such an approach is dependent on the type of hazardous waste and the effect of constituents on cement hydration and would require rigorous testing for compliance with international standards. The economics of a working process also play an important role as well as the presence of a market for the products of the treatment process. The nature of S/S using cementitious binders is such that product properties could be tailored by varying key parameters of the mix formulations, assuming that this results in environmentally and economically viable products.

2.1.1 Binders used in S/S

S/S using hydraulic binders has previously been used for the treatment of wastes containing a variety of organic and inorganic contaminants such as metals and metalloids, asbestos, inorganic cyanides, radionuclides, solid organics, polyaromatic hydrocarbons (PAHs), polychlorinated biphenyls (PCBs) and dioxins (Environment Agency, 2004). S/S binders used for treating various types of wastes include Portland cement, lime, pulverised fuel ash, ground granulated blast furnace slag (GGBS), and these are often used in combination.

Lime is available in the form of quicklime (calcium oxide), hydrated lime (calcium hydroxide) or milk of lime (calcium hydroxide suspension). Lime can be used to raise the pH of the S/S

matrix with favourable effects on the solubility of contaminants as will be demonstrated in the following sections. It can be used either alone or in combination with cement or other pozzolanic materials.

PFA is a by-product of coal fired electricity generation with pozzolanic properties due to the amount of silica (SiO_2) and alumina (Al_2O_3). It has a history of use spanning over 50 years, being used as a concrete additive, structural fill, for grouting, in soil stabilisation and for the production of lightweight aggregates. Different types of PFA include dry, classified and conditioned PFA.

GGBS is a by-product from the steel industry. The molten slag from a blast furnace is quenched in water and this produces amorphous calcium silicate and aluminosilicates. This is ground to a fine powder to form GGBS which has excellent pozzolanic properties and is increasingly used to partially substitute Portland cement in concrete.

Thermoplastics such as bitumen or bitumen emulsions and asphalt can also be used for the treatment of waste. Bitumen is thought to have minimal interaction with waste constituents (Environment Agency, 2004) and therefore the main contaminant retention mechanism is physical encapsulation. The physical integrity of the matrix is therefore critical when such binders are used.

S/S technologies provide several routes for contaminant immobilization. The most critical parameter in most S/S systems for determining if inorganic contaminants are in a mobile or immobile form is pH. Chemical mechanisms such as precipitation, adsorption and ion exchange produce immobile contaminant forms and are strongly influenced by pH. The success of S/S is dependent on the interactions between binder and waste resulting in the formation of pH-controlling hydration phases as well as the pH-dependent reactions that determine the extent of contaminant immobilisation (Batchelor, 2006).

2.2 Chemistry of Cementitious Stabilised/Solidified Waste Forms

Cement chemistry and chemistry of S/S waste forms have been fields of extensive study. An extensive review of cement chemistry is not in the scope of this study, therefore only fundamentals are presented and focus is given on the contaminant binding capacity of cements. Hewlett (1998) and Taylor (1997) provide more details on cement chemistry.

Portland cement is a mixture containing predominantly tricalcium (C_3S) and dicalcium (C_2S) silicates, with smaller amounts of tricalcium aluminate (C_3A), calcium aluminoferrite (C_4AF) and gypsum ($CaSO_4$). The reaction of cement with water is referred to as *hydration* during which each constituent reacts (hydrates) at a different rate to produce a range of hydration products. According to Bullard et al (2011), hydration involves a collection of coupled chemical processes, the rate of which depends on their nature, as well as the state of the overall system at a given time. These processes fall into one of the following categories:

1. ***Dissolution/dissociation*** involves detachment of molecular units from the surface of a solid in contact with water.
2. ***Diffusion*** describes the transport of solution components through the pore volume of cement paste or along the surfaces of solids in the adsorption layer.
3. ***Growth*** involves surface attachment, the incorporation of molecular units into the structure of a crystalline or amorphous solid within its self-adsorption layer.
4. ***Nucleation*** initiates the precipitation of solids heterogeneously on solid surfaces or homogeneously in solution, when the bulk free energy driving force for forming the solid outweighs the energetic penalty of forming the new solid–liquid interface.
5. ***Complexation***, reactions between simple ions to form ion complexes or adsorbed molecular complexes on solid surfaces.
6. ***Adsorption***, the accumulation of ions or other molecular units at an interface, such as the surface of a solid particle in a liquid.

The rate of hydration has been described based on a plot of heat evolution versus time. Such a plot for a cement paste (CEM I) prepared at a water-to-solids ratio of 0.5 is presented in Figure 2.2. The reaction rate of the different clinker constituents is according to the following increasing order: $C_3A > C_3S \approx CA > C_4AF > C_2S$ (Chen et al, 2009). Four distinct phases can be identified in the plot:

Stage I - Initial Reaction: The early heat evolution and behaviour of cement is governed by the aluminate phases, although according to Bullard et al, (2011) significant heat is also released from the dissolution of C_3S. Soon after mixing the most reactive of the clinker phases, the C_3A, reacts with water producing an exothermic signal, and forming a calcium-aluminium-rich gel, which in turn reacts with sulphate in solution to form ettringite (AFt) crystals. Sulphate is introduced in unhydrated cement in the form of gypsum to control the rapid setting of hydrated C_3A.

Stage II – Dormant Period: The initial reaction of clinker phases is followed by a period of low heat evolution during which cement paste still retains plasticity. The low reaction rate and deceleration after the initial reaction has been the subject of debate and different theories have been proposed. One theory is the metastable barrier hypothesis according to which a metastable thin layer of calcium silicate hydrate is rapidly formed which passivates the surface of C_3S grains by restricting access to water, or restricts diffusion of detaching ions away from the surface (Chen et al, 2009). This theory assumes that dissolution of C_3S would continue to be rapid if it were not for the formation of the passivating layer.

Other researchers have proposed alternative theories for the decrease in the dissolution rate of C_3S. According to Barrett et al, (1983), as cited by Bullard et al, (2011), a "superficially hydroxylated layer" forms on C_3S surfaces in contact with water. The dissociation of ions from this layer occurs much more slowly than would be otherwise expected for a mineral in highly under-saturated solutions. A review by Bullard et al, (2011) provides additional information on the slow dissolution step hypothesis.

Stage III – Acceleration Period: This is the main period of cement hydration. At the end of the dormant period C_3S or alite (alite includes impurities, mainly Mg and Al) and C_2S or belite, begin to hydrate with cement grains reacting from the surface inwards, producing CSH, $Ca(OH)_2$ and heat. The principal contributors to longer term strength are the calcium silicates. C_3S is most reactive, giving early strength but C_2S has a better longer term contribution. The shoulder peak observed between stages III and IV is attributed to the reaction of C_3A phases to produce ettringite (Bullard et al, 2011). The acceleration period is characterised mainly by nucleation and growth processes and different hypotheses have been made to date regarding what initiates the onset of the two. The four hypotheses existing in the literature are presented in Table 2.1.

Table 2.1. Hypotheses on the onset of the nucleation and growth period (reproduced from Bullard et al, 2011)

Hypothesis	Brief Description
Nucleation and Growth of CSH	Nucleation and growth of a stable CSH happen at the end of the slow reaction period and are rate-controlling during the acceleration period as a metastable protective layer of hydrate becomes chemically unstable and exposes the high-solubility C_3S.
Growth of Stable CSH	Nuclei of stable CSH, already formed during initial reaction, grow at a nearly exponential rate. CSH growth is rate controlling. No metastable hydrate barrier layer is invoked.
Rupture of initial barrier	Metastable CSH barrier layer is semipermeable. Solution inside is close to saturation with respect to C_3S. Osmotic pressure leads to its rupture.
Nucleation of portlandite	Nucleation and growth of portlandite become rate-controlling (and thus indirectly control the rate of growth of CSH)

Stage IV – Deceleration and Curing Period: The deceleration period is characterised by slow heat evolution by C_2S. It is important for structural applications as it contributes to the long-term strength of concrete. It is generally considered that this period is controlled by diffusion although other parameters may also be important such as consumption of small particles leaving only large particles to react, lack of space, or lack of water.

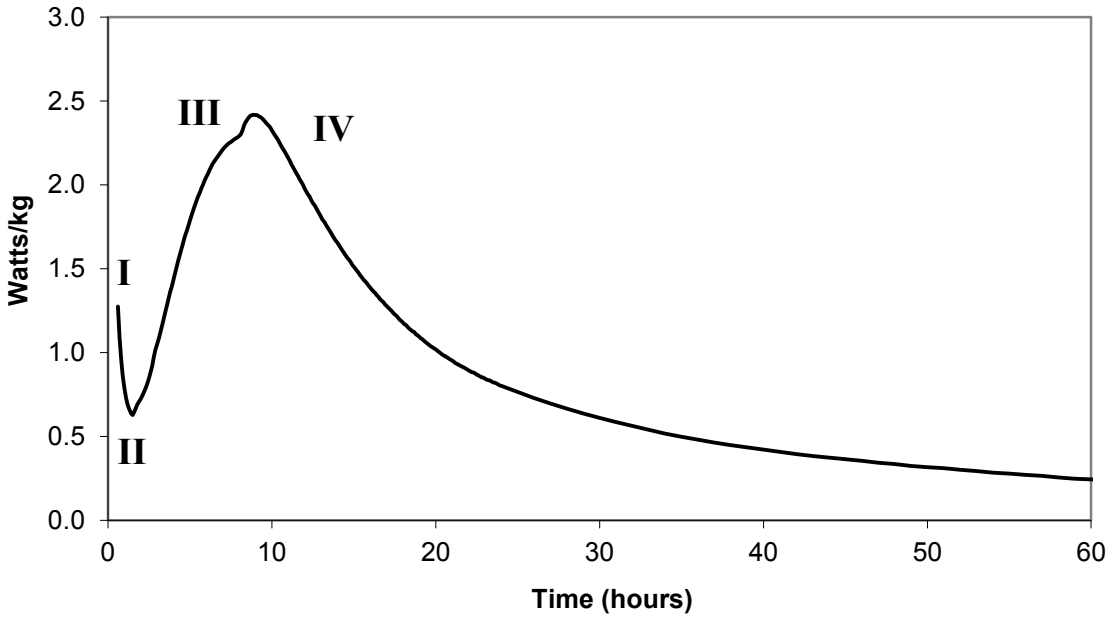

Figure 2.2 Heat evolution of a CEM I paste at a water-to-solids ratio of 0.5

The stages of cement hydration are also summarised in Table 2.2. The hydration products of Portland cement comprise approximately 20–25% $Ca(OH)_2$, 60–70% C–S–H and 5–15% other phases, including grains of unhydrated cement.

Table 2.2 Cement hydration kinetics (Adapted from Chen et al, 2009)

Stage	Reactions	Remarks
Initial reaction	Surface wetting, dissolution of cement phases, nucleation of ettringite and hexagonal crystals of $Ca(OH)_2$, which occurs homogeneously from the solution phase, or heterogeneously at solid solution interfaces	0–15 min, chemical reaction control, heavy metals may influence the nucleation of C–S–H, $Ca(OH)_2$ and ettringite
Dormant period	Growth of ettringite needles and precipitation of CSH gel onto C_3S grains or slower C_3S and C_3A dissolution rate.	15 min–4 h, chemical reaction control, heavy metals may show accelerating or retarding effects
Acceleration period	Disruption of the hydrate protective layer by osmotic pressure or transformation of the hydrates or change in C_3S dissolution rate; CSH and CH growth rapidly	4–8 h, chemical reaction control, heavy metals may co-precipitate with C–S–H, CH and ettringite
Deceleration and hardening	Slow heat evolution of C_2S. AFt transformation into AFm. Important stage for final strength development.	8–24 h, diffusion control, heavy metals may influence this conversion process and setting, and promote atmospheric carbonation
Curing period	Further hydration, conversions of hydration products	A few days, diffusion control, Heavy metals may influence the mechanical strength and permeability

Portland cement and other commercial binders exhibit mechanical properties (compressive strength, porosity, permeability etc.) and chemical features that are responsible for their widespread use in S/S treatment processes. The addition of waste products in cement can affect hydration reactions in various ways through different mechanisms depending on the nature of the waste. Different compounds can inhibit or accelerate setting/curing, retard hydration reactions or alter the properties of the final products by coating cement grains, disrupting the cementitious matrix or by interfering with the reactions and acting as flocculants, dispersants, or complexing agents. Conner (1993) and Asavapisit (1998) have reported in detail the effects of different compounds on cement hydration.

2.2.1 Effect of Metals on Cement Hydration

a) Heavy Metals

A review of the effect of heavy metals on cement hydration was carried out and Table 2.3 provides a summary of findings for selected studies. This review shows that effects of heavy metals include acceleration or retardation of cement hydration reactions, impacting physical properties such as compressive strength and setting time.

Table 2.3 Review of the effect of heavy metals on cement hydration

Study	Year	Study Description	Study Highlights
Hills et al	1994	Calorimetric and microstructural study of the effects of heavy metals on Ordinary Portland Cement (OPC)	An individual metal compound was not found to have a poisoning effect, but could accelerate or retard hydration. Cu, Ni and Zn were found to retard cement hydration and reduce the total heat evolved. Pb and Cd modified the first hydration peak. Pb was also found to increase the total heat evolved. However, combination of compounds produce synergistic effects that can poison hydration. The authors suggested that metal additions can modify the gel produced during the induction period rendering it impermeable, and thus leading to an indefinite induction period.
Asavapisit et al	1997	Studied the effect of synthetic metal wastes (Cd, Pb and Zn) on the hydration of OPC	Hydration peak occurred later for Pb-doped wastes suggesting retardation of hydration. No hydration peak was observed for Zn-doped wastes and this effect was attributed to calcium zincate hydrate, which precipirates on cement clinker phases, creating a membrane and preventing further hydration. The same was also observed by Yousuf et al (1993). Cd was found to accelerate cement hydration at the additions investigated (metal sludge addition of 10% of OPC mass)
Hamilton and Sammes	1999	Properties of S/S steel foundry bag house dusts	As with Asavapisit et al (1999), XRD results showed that presence of Zn in cement leads to the formation of calcium zincate hydrate. No Pb compounds were detected. In contrast, Ortego (1990) suggested that Pb forms sulphate or hydrosulphate phases, consuming available SO_4^{2-}. This hypothesis can be related to findings by Tashiro et al (1979), who reported that ettringite is not formed in the presence of Pb.

Study	Year	Study Description	Study Highlights
Olmo et al	2001	Effect of Pb, Zn and Fe on the setting time and strength development of cement pastes	Zn strongly retarded the setting time of cement and reduces early strength development. The effect on strength is less pronounced at later hydration stages. Fe did not have significant effects on the setting and compressive strength at early hydration stages but it reduced compressive strength at later stages. Pb did not affect compressive strength at late hydration stages but was shown to retard cement setting.
Li et al	2001	S/S of a circuit board factory sludge with high concentrations of Cu, Pb and Zn	The study used a geochemical modelling approach using MINTEQA2 and determined that heavy metals like Cu, Pb and Zn are present in S/S matrics as metal hydrated phases or metal hydroxides precipitating on the surface of matrix constituents.
Ouki and Hills	2002	Effect of Ba, Cu, Ni, Zn, Cr(III), Pb and Cd on cement hydration	All metal–doped mixes showed a lower degree of cement hydration, with the mix with the combination of metals at 1.0 wt.% having the most pronounced effect (74% decrease compared to the control mix). At the same time all metal-doped mixes apart from those with Ba, Cu or Cr at 0.1% addition, exhibited a decrease in porosity compared to the control mix. The authors concluded that combination of metal contaminants does not always exert the most significant adverse effect on microstructural development when compared to individual metal additions.
Trezza and Ferraiuelo	2003	Effect of hazardous waste containing Cr(VI) on the hydration of limestone-blended cement	The authors determined that Cr(VI) retards hydration of pure and limestone blended cement. It was also found that Cr(VI) in the presence of limestone retards formation of monocarboaluminate. In addition, presence of Cr(VI) resulted in reduced compressive strengths for both pure and limestone-blended cement.
Trezza	2007	Effect of Zn addition (as nitrate) on cement hydration	In contrast to the grain coating hypothesis, The author suggested that Ca and OH ions are consumed during the induction period, forming metal-containing calcium hydrates ($CaZn_2(OH)_6.2H_2O$). The supersaturation of Ca and OH is then delayed and so is the subsequent precipitation of CSH and portlandite. Therefore, the greater the amount of Zn in the mix the greater the retardation effect would be.

Study	Year	Study Description	Study Highlights
Chen et al	2007	Characterisation of products from C_3S hydration in the presence of Cr, Cu Pb and Zn (as nitrates)	Heavy metals investigated were found to have an accelerating effect on C_3S hydration apart from Zn which exhibited a severe retardation effect at early stages. Heavy metals were found to have a retarding effect on the precipitation of portlandite. This was attributed to the reduction of pH resulting from the hydrolysis of heavy metal ions during C_3S hydration. Finally metals were also found to co-precipitate with calcium as layered double hydroxides such as $CaZn_2(OH)_6.2H_2O$.
Qiao et al	2007	Investigate the S/S performance of Portland cement through cement clinker phases	Addition of Cu, Pb and Zn hydroxides in cement paste led to a reduction in compressive strength (28 days) of 15.5% compared to the control mix. Addition of $Zn(OH)_2$ completely prevents hydration of C_3S at early stages due to a coating effect from the formation of calcium zincate hydrate. Addition of $Pb(OH)_2$ and $Cu(OH)_2$ was not found to have a retarding effect. Cu, Pb and Zn hydroxides were found to affect hydration of C_3A at early hydration stages only in the presence of gypsum. This is due to formation of heavy metal aluminate carbonate hydrates and a subsequent coating effect.
Evans	2008	Overview of binding mechanisms of radionuclides in cement	The review from Evans suggested that Pb and Zn can form compounds that coat cement grains having a retarding effect on cement hydration.
Gineys et al	2010	Interactions of cement paste and Cu, Cd, Ni, Pb and Zn, added as soluble nitrate salts	Additions (at 0.018 and 0.18 mol/kg) of heavy metals had a detrimental effect on compressive strength after 2 days of curing but 28-day strengths were comparable to the control mixes for all heavy metals. Different heavy metals affected early hydration to varying extents which was demonstrated by differences in 2-day compressive strengths. Differences at 28 days were attributed to different microstructure and density of CSH as the degree of hydration was the same of all metal-doped mixes. SEM showed that Cu and Pb are absorbed in CSH and had the greatest effect on compressive strength.Cd, Ni and Zn precipitated as hydroxides in the intergranular porosity.

This review demonstrates that heavy metals can have a detrimental effect on the hydration of cement and its physical properties. According to Gineys et al (2010), the prevailing theory that precipitation of heavy metal hydrates or hydroxides coats cement grains preventing

further hydration at early stages was recently disputed. Weeks et al (2008), as cited by Gineys et al (2010), proposed that the retardation of setting was attributed to the conversion of a metal hydroxide to a metal hydroxyl-species. This reaction consumes calcium and hydroxide ions and delays the supersaturation of the solution and subsequent precipitation of C–S–H and portlandite.

b) Group I – Alkalis (Na, K)

Apart from heavy metals, Group I alkalis, namely sodium and potassium can also influence cement hydration and its products. A recent FTIR study by Lodeiro et al (2009) on the effect of alkalis on fresh CSH gels concluded that:

- High NaOH concentrations in fresh CSH gels may result in gel modification even in the first 72 hours of hydration
- CSH carbonation is enhanced by alkali content
- Modification of CSH gels in the presence of NaOH can be attributed to the following two factors:
  - Carbonation induced by high alkalinity which leads in silicate polymerisation, resulting in a silica-rich gel residue.
  - Modification of the original CSH gel favouring the formation of a Ca-containing NSH gel.

In addition the presence of alkalis can strongly affect the pH and solubility of cement hydration phases such as portlandite (Polettini et al, 2001). Alkalis can induce a rise in pH as the Na^+ - OH^- (or K^+ - OH^-) ion pair replaces the less alkaline Ca^{2+} - OH^- in solution. Alkalis can decrease the solubility of portlandite and CSH and increase the solubility of silica gel. Other studies have also determined that alkalis can have a marked effect on the rheological properties of fresh cement pastes (Röβler et al, 2008)

2.2.2 Effect of Chlorides and Sulphates

Chlorides and sulphates can affect cement hydration and the resulting hydration products. Chlorides have been widely used in the past as additives (i.e. $CaCl_2$) due to their accelerating effects on cement hydration when added in quantities 1.0-3.0 wt.% of cement. Addition in

greater quantities however has been reported to retard cement hydration (Lampris et al, 2009). Chlorides and sulphates can affect fresh and hardened cement and concrete pastes, both when part of the constituents of the mix (internal attack) and when part of a solution in contact with cement or concrete (external attack).

Both chlorides and sulphates can alter the nature and structure of hydration products (notably the calcium aluminate hydrates) and affect their stability. These anions, as well as carbonates can compete with and replace OH^- in AFm/AFt phases altering their composition and properties. Studies have reported the formation of compounds such as Friedel's and Kuzel's salt depending on the pore-water concentrations of the chlorides, sulphates and carbonates present. Friedel's salt is a hydrated chloride-containing calcium aluminate analogous to monosulphate in hydrated ordinary Portland cement. It forms from the reaction of chloride with aluminate phases and is considered as the main sink of chloride ions in cement.

High concentrations of chloride have been reported (Loser et al, 2010; Birmin-Yauri and Glasser, 1998) to destabilise AFm and AFt phases in favour of the production of Friedel's salt The competition between hydroxyl, sulphate, carbonate and chloride ions may also lead to a preferential formation of Friedel's salt and potentially destabilisation of ettringite or monosulphate. A destabilisation effect has also been reported for cement hydrates such as portlandite and CSH, whose solubility may increase in the presence of high chloride concentrations. Loser et al (2010) reported that in the presence of high chloride concentrations, portlandite, CSH and Friedel's salt can be leached reducing the chloride binding capacity of cement. The results agreed with past studies and established that depletion of Friedel's salt and portlandite occurs near the surface of cement samples exposed to NaCl solutions.

Sulphate-bearing solutions or sulphates present in the original mix can also have significant detrimental effects on cement-based materials. Sulphate ions in the pore solutions can react with ionic species leading to the formation of phases such as gypsum ($CaSO_4$), ettringite ($[Ca_3Al(OH)_6.12H_2O]_2.(SO_4)_3.2H_2O$) or thaumasite ($Ca_3[Si(OH)_6 \cdot 12H_2O] \cdot (CO_3) \cdot SO_4$) or mixtures of these phases.

In the case of external sulphate attack, penetration of sulphate ions in a cement-based matrix induces a series of reactions between these ions and cement hydration products. Sulphate ions

react with portlandite to form gypsum and with calcium aluminates to form ettringite. Gypsum can in turn react with calcium aluminates to form ettringite. Initially, calcium ions are supplied by portlandite but when this is not available CSH dissociates into silica gel, releasing calcium ions. Expansive solid compounds such as gypsum and ettringite can fill pores within the cement matrix until strain develops eventually leading to stress and cracking (Sarkar, 2010).

2.2.3 Immobilisation Mechanisms

Major factors and immobilisation or containment mechanisms for contaminants in stabilised/solidified waste are presented in Table 2.3 (Conner, 1993; Asavapisit, 1998).

Table 2.4 S/S immobilization mechanisms

Mechanism	Description
pH control	S/S waste forms rely heavily on pH for metal containment. Metal hydroxides exhibit minimum solubility in the pH range of 7.5 to 11. Certain heavy metals exhibit amphoteric behaviour and have high solubility both at low and high pH values. Chemical stabilisation of solid or liquid wastes occurs by controlling the pH of the mixed wastes between 8 and 9.5 (Asavapisit, 1998). Nevertheless, all heavy metals do not exhibit low solubility at the same pH, therefore there has to be compromise in terms of the optimum pH of the system.
Redox potential	The redox potential (E_h) is the oxidation-reduction potential referred to the hydrogen scale, expressed in millivolts. It establishes the ratio of oxidants and reductants existing in the waste-environment system, and may affect the valence state of a metal in that system. An example of the influence of the valence state on solubility is chromium (Cr^{+6} vs. the less toxic Cr^{3+}).
Precipitation	It refers to reactions leading to the formation of relatively insoluble species and it is directly related to the solubility of metals in aqueous solution. Some alkali metals (e.g. Na, K) have solubilities that are little affected by pH. Others precipitate at high pH values into insoluble forms, while others exhibit amphoteric behaviour. These are acid soluble, but as the pH increases they undergo initial precipitation. Their solubility passes through a minimum and it rises again at higher pH values (Glasser, 1993). Determination of precipitation reactions and products in S/S processes requires knowledge of the nature of the solubility –limiting phases for waste species.
Adsorption	Adsoption occurs when a molecule or ion becomes attached to a surface, usually as a monolayer. The adsorbing ability of a material or system is directly related to its surface area (Conner, 1993). CSH, the main cement hydration product has a high specific surface area (10-50 m^2/g) (Glasser, 1993) which creates a strong potential for sorption.

Mechanism	Description
Chemisorption	There is no sharp boundary between adsorption and chemisorption, and some of the mechanisms described as adsorption can be classified as the latter. Functionally, the major difference is that chemisorbed species do not desorb easily.
Passivation	Metal ions dissolving from a solid surface may precipitate on the surface after contacting an anion in solution which forms a less soluble species. If the precipitate forms a tight, impermeable layer, it may block or inhibit further reaction at the surface. Such phenomena are specific to the constituents of the system and may operate only temporarily.
Ion exchange	It refers to the ability of certain natural materials such as soils and zeolites, as well as various synthetics to exchange ions which they contain for others in solution. Removal efficiency of an ion from solution is directly proportional to its charge and inversely proportional to its size.
Diodochy	Also termed as isomorphous substitution it occurs when one element substitutes for another of similar size and charge in a crystalline lattice (crystallochemical incorporation).
Encapsulation	Encapsulation refers to the ability of the solidified matrix to continue to isolate the waste from the environment according to its physical properties such as permeability. It is divided into micro and macro-encapsulation.

Chen et al (2007) reported that the possible immobilisation mechanisms in cementitious waste could be (1) sorption, (2) chemical incorporation including surface complexation, precipitation, co-precipitation and diodochy and (3) encapsulation including micro- and macro-encapsulation. Diodochy or isomorphous substitution in particular is considered an important barrier to the migration of contaminants. It occurs when elements are incorporated in minerals via substitution. Such an example is the substitution of OH^- by Cl^- in double layered hydroxide phases, such as aluminium cement hydrates. Studies have also suggested that Cr and Pb may be bound into the silica matrix in cement waste forms, possibly as "silicates" (Conner, 1993). Factors that affect substitution are mainly the size and charge of the ions. In particular (Jensen, 1982):

i) Of two ions having the same charge but different ionic radii the ion with the smaller radius is preferably incorporated.
ii) Of two ions having the similar radii but different charges, the ion with the higher charge is preferably incorporated.

Chen et al (2007) also reported that the dominant immobilisation mechanism in cementitious waste is precipitation or co-precipitation. Heavy metals in cementitious systems can precipitate as hydroxides, carbonates, silicates or sulphates.

Recent studies also show the potential of cement hydrates such as CSH and AFt phases (i.e. ettringite) for the immobilisation of contaminants. Vespa et al (2006) used techniques such as X-ray Spectroscopy (XAS) and XRF to investigate the uptake of Co and Ni in hardened CEM I paste. It was found that Ni(II) forms predominantly Ni-Al layered double hydroxide phases. In contrast to Ni, Co was found to be present in the oxidation states II and III. Co(II) is predominately incorporated into newly formed Co(II) hydroxide-like phases ($Co(OH)_2$), Co-LDH or Co-phyllosilicates, whereas Co(III) tends to be incorporated into a Co(III)O(OH)-like phase or a Co-phyllomanganate. A review (Evans, 2008) of studies on the binding mechanisms of radionuclides in cement also reported that Zn has a strong affinity for hydrate ferrite phases and is also retained in CSH. This retention was attributed to the linkage of tetrahedral Zn to tetrahedral CSH silicate chains. The same study suggested three potential mechanisms for the binding of Pb in cement matrices: i) isomorphous substitution of Pb^{2+} for Ca^{2+} in CSH, ii) retention in hydrate phases coming from C_4AF and iii) precipitation as basic lead compounds.

Johnson (2002) conducted a review of studies on the binding mechanisms of heavy metals in cement and the conclusions are summarised in Table 2.4.

Table 2.5 Binding mechanisms of metals in cement (reproduced from Johnson, 2002)

Binding Mechanism	**Ions**
Significant precipitation as simple or mixed hydroxide	Co^{+2}, Ni^{2+}, Cu^{2+}, Cd^{2+}
Significant incorporation in CSH	Pb^{2+}, Zn^{2+}, Cr^{3+}
Significant precipitation as Ca metallate	MoO_4^{2-}, WO_4^{2-}, AsO_4^{3-}, (VO_4^{3-})
Significant incorporation in AFm, Aft	CrO_4^{2-}, SeO_4^{2-}, SeO_3^{2-}, AsO_3^{3-}
Unclear	Hg^{2+}, VO^{2+}, (VO_4^{3-}), SbO_3^{2-}, $Sb(OH)_3$, $S_b(OH)_6$-

2.3 Cement and Concrete Degradation Mechanisms

Although constituents of APC residues can negatively affect cement hydration, cementitious waste products are also susceptible to other deterioration/degradation effects when exposed to the environment that can affect the ability of the S/S matrices to retain the pollutants of concern. It has been shown that S/S products exposed to the environment can undergo the same degradation processes as concrete (Klich et al, 1999). Such processes include decalcification, carbonation, alkali-aggregate reaction and sulphate attack and are described below.

2.3.1 Decalcification

Studies have shown that the physical properties of cementitious matrices such as compressive strength and porosity may be severely affected under leaching conditions. Calcium leaching from the dissolution of $Ca(OH)_2$ from cementitious materials in contact with water, and the successive decalcification of CSH gel has been extensively studied and relative findings are presented in this section.

Decalcification is the mechanism of loss of calcium through chemical processes. It is one of the most important mechanisms of degradation of cementitious materials. For cement pastes and concrete, decalcification occurs by various means including leaching by soft or acidic waters, carbonation, and sulphate attack. Decalcification occurs due to coupled dissolution of portlandite and CSH. Some studies have reported that CSH gel begins to dissolve only after complete dissolution of portlandite, i.e., dissolution reactions do not occur concurrently. However, other authors have reported that portlandite does not have to dissolve completely for CSH dissolution to occur, and this is a function of the mass (or volume) ratios of the leachant to the solid (Jain and Neithalath, 2009). Well-known detrimental effects of calcium leaching include increase in porosity with subsequent decrease in strength and increase in ionic diffusivities by an order of magnitude, if the extent of leaching is such to create a percolated porous structure (Chen et al, 2006).

Adenot and Buil (1992) studied and modelled the effects of deionized water on cement paste. It was found that the leaching of calcium is governed by diffusion and the pore solution is in equilibrium with the solid at every point in the cement paste. An unaltered core was observed

followed by degraded calcium depleted zones separated by dissolution/precipitation from. Progressive decalcification of CSH was also observed. A model was developed based on the assumptions of diffusion governed kinetics and local chemical equilibrium of the species of interest.

Due to the fact that decalcification reactions are slow, many studies have used an ammonium nitrate solution, which is a more aggressive leachant, removing calcium in order to study the effects of loss of calcium. Ammonium nitrate is very soluble in water and reacts first with cement paste by reactions which lead to the formation of a highly soluble calcium salt and gaseous ammoniac (NH_3). Then an expansive calcium nitro-aluminate is formed from the reaction of calcium nitrate with the hydrated aluminates from the cement paste. This compound is formed only when the material is dried (Carde and François, 1999).

Carde and François (1997) characterised the deterioration of the mechanical properties of concrete encapsulating radioactive waste due to water infiltration. The results of immersion of cement specimens in ammonium nitrate solution for a certain period of time showed the presence of three zones; an unleached sound zone, a dissolution front of calcium hydroxide and a degraded peripheral zone containing less amounts of calcium compared to the sound zone. The results also indicated the loss of calcium and the successive degradation to be governed by a diffusion mechanism with the degradation thickness showing a linear variation with the square root of time. Both compressive strength and porosity showed a linear relationship with the ratio of peripheral degraded area over total specimen area with an average increase in porosity of 19.3%.

The same researchers in a later study (Carde and François, 1999) investigated the individual contribution of the two different mechanisms of loss of calcium in the decrease in compressive strength and the increase in porosity. These mechanisms as previously mentioned involve: i) the dissolution and leaching of calcium hydroxide and ii) the decalcification of CSH. In order to study these two mechanisms the researchers used pure cement paste and cement combined with silica fume in order for the latter to totally consume the calcium hydroxide. In the case of silica fume cement paste, where in the absence of calcium hydroxide decalcification occurs due to the dissolution of CSH, the percentage loss of Ca is a linear function (negatively correlated) of the depth of the degraded thickness. In the presence of calcium hydroxide (pure cement paste), the percentage loss of Ca is negatively

correlated with the thickness of the degraded zone only for the first half due to the dissolution of both CSH and portlandite. In the remaining half of the degraded zone, the percentage loss is constant and attributed to the dissolution of portlandite only.

The researchers produced a model to describe the decrease in compressive strength and increase in porosity in relation to the degraded area ratio. It was concluded that leaching of calcium hydroxide crystals creates a macro-porosity (capillary porosity) whereas decalcification of CSH creates micro-porosity. In the presence of portlandite the increase of porosity (≈ 13%) resulted primarily from the dissolution of calcium hydroxide and to a lesser extent from the decalcification of CSH although its contribution was not negligible.

Heukamp et al (2003) studied the effects of decalcification on poroplastic properties of cement pastes and mortars also using an aggressive ammonium nitrate solution. The position of the portlandite dissolution front was found to be governed by the form $x_d = 2mm/\sqrt{d}$. The porosity after leaching increased from 39.7% to 63.2% for cement pastes and from 27.5% to 40.1% for mortars. The perforated structure of leached cement paste is presented in Figure 2.3. It was also shown that decalcified CSH (low Ca/Si ratio) is highly plastically deformable with large pores created during Portlandite dissolution collapsing during hydrostatic loading, hence reducing porosity.

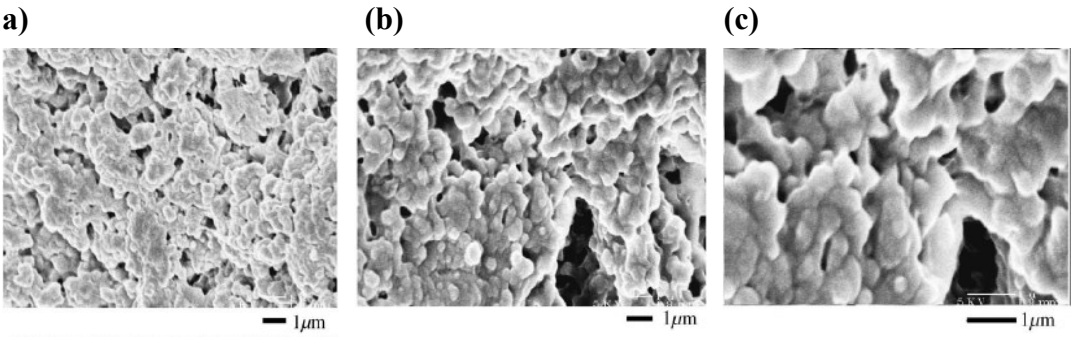

Figure 2.3 SEM micrographs of microstructure of leached cement paste. (a) Uniform washed-out appearance of the leached microstructure with a large density of new pores in the range of 100nm. (b and c) Pores in the micrometre range created by the dissolution of Portlandite crystals (reproduced from Heukamp et al, 2003).

Gallé et al (2004) also studied the effects of accelerated degradation on cement-based materials. As in previous studies total dissolution of portlandite was considered the complete

degradation criterion. The decalcification front propagation was similar ($x_d = 1.74 mm/\sqrt{d}$) to the one observed by Heukamp et al. Porosity results showed that increase after leaching was approximately 90% for both cement paste and concrete. The researchers also measured water permeability of the leached specimens and it was found to increase by two orders of magnitude.

A more recent study (Jain and Neithalath, 2009) examined the decalcification effects of plain cement pastes and pastes modified with fly ash, glass powder and silica fume in contact with deionised water. Porosity increased with increase in leaching duration for all pastes. Porosity increase was greater for plain cement pastes (porosity increase up to approx. 11%), whereas the least change was observed for glass powder-modified pastes (porosity increase up to approx. 5.5%). The authors determined that the largest contribution to porosity increase comes from leaching of portlandite, whereas at short leaching duration (i.e. 28 days) contribution by leaching of CSH is negligible. At longer leaching durations (i.e. 90 days) however, its contribution is not insignificant as porosity created due to CSH leaching was approximately 2.8% for plain cement pastes. In addition, plain cement pastes exhibited the greatest leaching depths after 90 days (1.22 mm) whereas glass powder-modified pastes had the best leaching resistance with a leaching depth of approximately 0.8 mm.

2.3.2 Carbonation

Accelerated carbonation as a treatment method for APC residues has been described in the previous chapter. This section refers to effects of natural carbonation on cement/concrete and S/S matrices. Carbonation involves the penetration of gaseous CO_2 in partially saturated cement or concrete which initiates a series of reactions with ions dissolved in the pore solution and the hydrated cement paste. Carbonation can be explained based on the carbonate system and it has been found to decrease the pH and increase dissolution of portlandite in cement and concrete matrices.

When in solution, CO_2 dissociates into different ionic species according to the following reactions:

$$CO_{2(aq)} + H_2O \rightarrow H^+ + HCO_3^-$$
$$HCO_3^- \rightarrow H^+ + CO_3^{2-}$$

Using the equilibrium constant equations and combining with the water dissociation relationship $[(H^+)(OH^-) = 10^{-14}]$ the fractionation of carbonate ions can be expressed as a function of pH as shown in Figure 2.4 (curves calculated using ORCHESTRA).

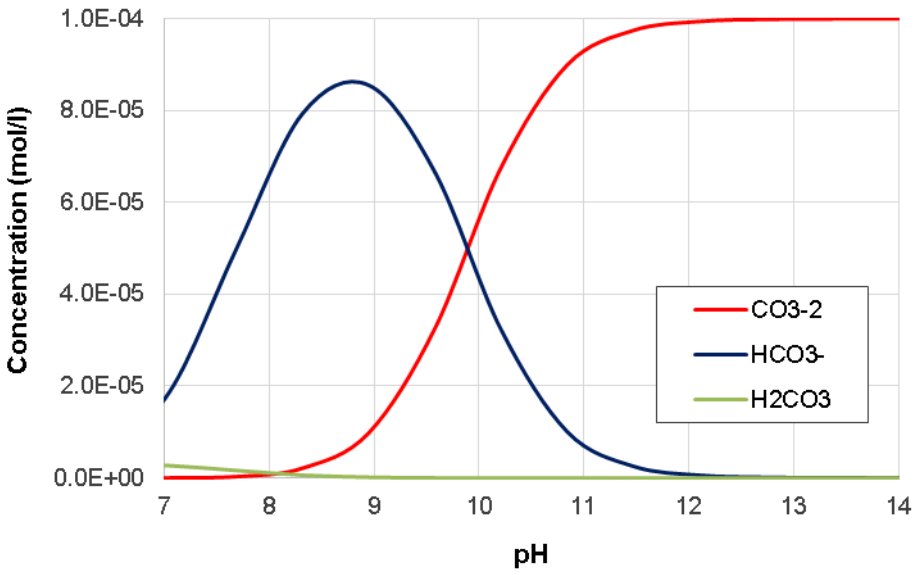

Figure 2.4 Fractionation of carbonate ions as a function of pH.

A review by Glasser et al (2008) reported that carbonation reactions can be summarised with the following reaction which demonstrates the pH-reducing effect of carbonation by consuming available hydroxyl ions:

$$CO_{2(aq)} + OH^- \rightarrow CO_3^{2-} + H_2O$$

Peter et al (2008) using a numerical model reported that other cement hydrates (i.e. CSH) and unreacted constituents (i.e C_3S, C_2S) can compete with portlandite for available CO_2. The authors reported that the amount of CO_2 consumed by portlandite was three times greater than the amount consumed by CSH, 20 times greater than that by C_2S and 50 times greater than the amount consumed by C_3S. The same authors suggested the following reactions for the carbonation of CSH and tricalcium and dicalcium silicates:

$$(3CaO.2SiO_2.3H_2O) + 3CO_2 \rightarrow (3CaCO_3.2SiO_2.3H_2O)$$
$$(2CaO.SiO_2) + 2CO_2 + nH_2O \rightarrow (SiO_2.nH_2O) + 2CaCO_3$$
$$(3CaO.SiO_2) + 3CO_2 + nH_2O \rightarrow (SiO_2.nH_2O) + 3CaCO_3$$

where n is an arbitrary positive number to describe the amount of water molecules that are conserved by the reactions. The authors suggested that unhydrated cement constituents can be excluded from carbonation calculations/models due to their little influence. The effect of CSH, especially under natural conditions depends on its accessibility to CO_2 and the amount of CSH present.

Carbonation is important in concrete applications as the pH drop (reduction in alkalinity) is associated with the disruption of the layer that passivates reinforcement bars, thus making them more prone to corrosion. Carbonation may also result in positive effects such as the precipitation of calcite which in turns reduces porosity and forms a protective layer on the surface of concrete. Carbonation is also important in S/S systems and as with concrete applications it can have both positive and detrimental effects such as the pH drop which may affect release of constituents of concern whose solubility is strongly related to pH. Positive effects include as mentioned above the reduction in porosity, thus restricting migration of contaminants and also the possible formation of less soluble metal carbonates.

The above effects on S/S waste forms were confirmed by Garrambrants et al (2004) by comparing the carbonated and non-carbonated states of ground cement-based material containing metal oxide powders. The authors reported a pH reduction of 1.5 units after carbonation compared to the parent material. Carbonation resulted in a decrease in Pb solubility, an increase in As solubility while Cu and Zn remained unaffected. The increase in As solubility was attributed by the authors to the loss of adsorptive phases for As(V) at high pH as Ca-bearing mineral phases were dissolved or decalcified.

Van Gerven et al, (2007) investigated the combined effect of carbonation and leaching on the porosity of MSWI bottom ash-cement mortar with bottom ash replacing the sand fraction and a cement paste with 30% of cement substituted by flue gas cleaning residue. The authors reported that carbonation decreases porosity (up to 12%) while leaching has the opposite effect (up to 16%) as expected. A net increase in porosity was observed for the mixes tested. In addition, both pH and porosity reduction have an effect on soluble constituents such as Na and K, associated with an increase and decrease in leaching respectively. The authors reported that the effect of porosity on these elements is more pronounced than that of pH resulting in a net decrease in the leaching of Na and K.

Antemir et al (2010) examined long-term disposal effects on metal-containing soils treated via S/S. Cores were extracted from selected sites in the US and the UK and were examined for physical properties (i.e. UCS and permeability) and microstructural characteristics. The authors identified the presence of carbonates in voids and micro-cracks within specimens demonstrating the effect of carbonation. Following evaluation of contaminant immobilisation they concluded that the effect of carbonation was inconsequential.

2.3.3 Sulphate Attack

Sulphate attack and its associated reactions have been discussed in previous sections but are repeated briefly in this section for completeness. Sulphate-bearing solutions or sulphates present in the original mix have been shown to affect cement hydration and the resulting hydration products. Formation of phases such as gypsum, ettringite or thaumasite has been found to result in expansion, spalling, strength loss and severe degradation of cement and concrete pastes due to the ingress of sulphate ions. Formation of ettringite in particular is

often considered the predominant reason for volumetric changes and expansion in hardened cement pastes. However, according to Glasser et al, (2008) formation of gypsum was shown to cause expansion of C_3S hydrated pastes and can probably contribute to the degradation of concrete in sulphate-laden environments.

In the case of cement-bound wastes exposed to sulphate-rich solutions, ettringite formation and subsequent cracking can affect the diffusivity of constituents of concern. Under real-life leaching conditions, properties of S/S matrices such as porosity may change with time due to processes taking place during leaching (i.e. diffusion of ions, mechanical damage etc.). Sarkar et al, (2010) used a numerical model to assess cement degradation during sulphate attack, taking into account chemical reactions, changes in porosity attributed to leaching (diffusion of ions), as well as mechanical damage caused by expansive solids and related changes in diffusion properties. The authors used their numerical model to simulate damage accumulation in a cement mortar (US Type I) in contact with a 0.35M Na_2SO_4 solution. Modelling results showed that formation of gypsum from the reaction of portlandite with sulphate ions was the prominent contributor to volumetric expansion. In addition, hydrogarnet (calcium aluminate phase) was found to be completely consumed in favour of the production of ettringite.

2.4 Application of S/S to APC Residues

This section contains a review of the literature on S/S of APC residues. Different binders have been used in the various studies comprising mainly Portland cement, blended and alkali-activated cements. A number of studies have also utilised one or more pre-treatment stages prior to S/S for the removal of soluble salts which as described above can have a detrimental effect on the S/S process. The following sub-sections are presented according to the nature of the binder used for the S/S process.

2.4.1 S/S Using Commercial Hydraulic Binders

Barna et al (2000a, 200b) investigated the use of APC residues and a mixture of hydraulic binders for the construction of the bottom slab of a water storage reservoir. 29% water and 12% hydraulic binder were added to the APC residues and the leaching performance and transfer mechanisms were assessed on a laboratory scale via a monolithic leaching test. The

researchers achieved significantly reduced leaching of metals such as Cd, As, Zn and Pb using an acid solution to reduce pH to 7. Solubilisation of heavy metals (Pb, Zn and Cd) was strongly dependent on pH, with minimum solubility occurring in the pH range 8–10. Leaching of alkalis (Na, K), Ca and Cl^- remained high and release was described using a diffusional model incorporating physico-chemical characteristics. The model and the laboratory leaching results were validated by means of a field pilot study also showing that air carbonation does not fundamentally affect mass transfer processes.

A study by Polettini et al (2001) assessed the properties of four different MSWI fly ashes stabilised with class 42.5R OPC. Mixes were prepared with MSWI fly ash addition varying between 0 and 80 wt.% and water addition between 29 and 40 wt.% (dry weight). The effect of activators such as $CaCl_2$ and $Na_2SiO_3 \cdot 9H_2O$ was also investigated. Products were tested for setting time, compressive strength and bulk density, as well as Acid Neutralisation Capacity (ANC). The majority of fly ashes tested delayed initial setting beyond 24 hours and only the fly ash with the lower alkali and chloride content had setting times similar to OPC control mixes. Compressive strengths were up to 30MPa depending on type and % addition of MSWI fly ash. The authors suggested that the adverse effects of MSWI fly addition on cement hydration were not to be attributed solely to the presence of heavy metals and anions but also to alkalis which reduce the solubility of CaO and increase the solubility of Al_2O_3. ANC was reduced with increasing MSWI fly ash addition which was ascribed to the reduced formation of pH-controlling hydration phases.

Collivignarelli and Sorlini (2002) investigated a combined washing-immobilisation treatment for MSWI fly ash. MSWI fly ash was washed at a L/S of 10 and then mixed with reagents including cement, lime, sodium silicate, blast furnace slag, bentonite and water. The resulting products were milled to a minimum diameter of 1.5mm and were subsequently used as partial replacements (11% to 22% of total aggregates) of natural aggregates in concrete. Compressive strengths achieved for all mixes were greater than 15 MPa which was required by Italian regulations for structural concrete applications. The best results in terms of physical properties and leaching were achieved using cement, lime and sodium silicate, while no significant improvement was observed with blast furnace slag and bentonite addition. Leaching of heavy metals also complied with Italian regulations except for mercury. Results for mercury however may not be realistic as the laboratory detection limit was used to calculate emissions.

Mangialardi (2003) investigated a combined process, comprising a two-step washing stage and subsequent S/S using ASTM Type I cement for the treatment of two MSWI fly ashes with low and high alkali chloride and sulphate contents respectively. Mixes were prepared using cement, washed or unwashed fly ash, or a combination of washed fly ash with the slurry produced from the washing process. Cement addition was at 25 wt.% of total solids and the water-to-solids ratio was 0.4. Leaching was evaluated via the US EPA TCLP. Washed fly ash mixes had lower setting times compared to unwashed fly ash demonstrating the retarding effect of constituents removed by washing (i.e chlorides and sulphates). Leaching results of washed fly ash mixes cured for 7 days complied with Italian regulations for Cd, Cr(VI), Cu and Pb, while unwashed fly ash mixes failed to meet limit concentrations. The author also suggested a pH treatment in the range of 6.5-7.5 for the wastewater from the washing process to remove Al, Cd, Pb and Zn.

The same researcher (2004) also investigated the effects of a four-step washing stage on the S/S of MSWI fly ash using CEM I 42.5. Mixes were prepared with unwashed or washed fly ash addition of 55 wt.% and the minimum water-to-solids ratio for each mix above which no workability issues were observed. Similar results with the previous research were obtained in terms of setting with washed fly ash exhibiting lower setting times. Unwashed fly ash mixes exhibited greater expansion (up to 0.39%) while washed fly ash mixes had similar expansion behaviour with a control mix comprising 55 wt.% quartz sand and 45 wt.% CEM I. The expansion was attributed to the formation of hydration products such as ettringite and calcium monochloroaluminate. Compressive strength of washed fly ash mixes was greater compared to unwashed fly ash, both before and after water immersion. Results of a leaching test with acetic acid showed that only the washed fly ash-cement mix met Italian standards for solid waste disposal, with all other mixes and raw and washed fly ash failing in terms of Cd and Pb.

Cinquepalmi et al (2008) used S/S washed MSWI fly ash as an artificial aggregate in Portland cement mortars. The S/S product was prepared by using 48 wt.% washed fly ash, 20 wt.% CEM I, 32 wt.% water and was cured for 365 days at 100% RH. Cement mortars were prepared using cement, S/S fly ash and natural sand varying the replacement level of sand with S/S fly ash (0, 10 and 50 wt.%). Compressive strengths of up to 36MPa after 90 days of curing were achieved, while monolithic leaching test results for Cr, Cu, Pb and Zn for specimens with 10 and 50 wt.% sand replacement were lower than the control sample. The

authors concluded that there is potential for reuse of MSWI fly ash in concrete applications as coarse aggregates. It is noted that a combination of washing and S/S was used in this study.

Qian et al (2008) assessed the feasibility of using a cementitious matrix comprising MSWI fly ash and calcium sulphoaluminate cement (CSA) for the S/S of high concentrations of heavy metals. CSA (70%)-MSWI fly ash (30%) mixes were prepared and doped with Pb or Zn amounts varying between 0.5% and 2%. Addition of MSWI fly ash had a negative effect on strength development but showed better early strength development in the case of Zn doped mixes compared to OPC control mixes. All mixes however achieved strengths greater than 20 MPa. TCLP leaching performance in terms of Pb and Zn was dramatically improved compared to OPC mixes. Leaching of Pb was far below TCLP limit (5 mg/L) even for Pb-doped CSA-MSWI fly ash mixes. XRD phases included ettringite and Friedel's salt while Fourier Transform Infrared (FTIR) analysis suggested that Pb and Zn incorporation in the ettringite structure may have occurred. However, chloride leaching results were not reported in this study.

Further studies have evaluated the potential of reusing APC residues in concrete. Aubert et al (2004) utilised pre-treated APC residues in CEM I 52.5R concrete. Pre-treatment comprised of washing, phosphation and calcination (>600ºC). The treated APC residues were found to behave like inert sand in the concrete mixes in terms of mechanical properties, while leaching of contaminants was also low. Bertolini et al (2004) used a 30 wt.% replacement of CEM I 52.5R with washed MSWI fly ash. Addition of MSWI fly ash led to compressive strengths similar with mixes containing coal fly ash, demonstrating a potential hydraulic behaviour. The authors however concluded that MSWI bottom ash would be more suitable for the partial replacement of cement in concrete, as MSWI fly ash did not yield significant improvement to the properties of concrete and it also requires pre-treatment. Hui-Sheng Shi and Li-Li Kan (2009b) used a mixture of 40% MSWI fly ash and 60% OPC and achieved leaching of heavy metals compliant with Chinese regulatory standards. The authors concluded that reuse of the waste in concrete mixes is feasible. Chloride leaching results however were not reported.

2.4.2 S/S Using Alkali-Activated Cements and/or Admixtures

Geysen et al (2004b) used different types of cement (CEM I, CEM II, CEM III etc.) as well as silica containing materials (water-glass, microsilica, pyrogenic silica etc.) as additives to improve the leaching properties of five different air pollution control residues. Leaching performance was assessed according to the German DIN 38414-S4. Use of cement only could reduce Pb leaching by a factor between 3 and 50 depending on cement type and curing time. However, regulatory limits for landfill (2 mg/L) were not attained. Addition of micro-silica reduced Pb leaching from 101.3 to 0.7mg/l, while use of aerosol (pyrogenic silica) reduced leaching to below detection limits. pH-dependent leaching tests showed that at pH 2.5, Pb leaching is 250 times lower for the micro-silica-treated residue than for the cement-treated residue and almost 7 times lower at pH 12.4. The authors attributed reduction of Pb leachability to the formation of Ca-silicates.

Dajie Zhang et al (2007) investigated solidification of MSWI fly ash using Na_2SiO_3-activated GGBS. MSWI fly ash addition varied between 25 and 45 wt.% (dry mass) with a w/s ratio of 0.30 and a 5 wt.% addition Na_2SiO_3. Leaching was assessed according to the TCLP test. The study focused on the leaching of Pb and Cr, as the leaching of Zn, Cu and Cd from the raw MSWI fly ash was below the limits of the Chinese toxicity discriminate standard for hazardous wastes. Compressive strength of all mixes was greater than the 1.0 MPa threshold for landfill disposal after 7 days of curing. Samples cured for 28 and 60 days showed reduced leaching of Pb and Cr to levels lower than the Chinese regulatory limits (3.0 and 1.5 mg/L respectively). The authors attributed retention of Pb and Cr to the formation of hydration products such as CSH and ettringite. They suggested immobilisation occurs by isomorphous substitution of Ca in CSH, adsorption on CSH or by precipitation as hydroxides.

Geopolymerisation is a method that has received increased attention over the recent years for the reuse of aluminosilicate waste materials. It involves mixing of the waste with an activating solution comprising using an alkali hydroxide (NaOH, or KOH) and sodium or potassium silicate solution. This results in the formation of a –Si-O-Al-O- polymeric network where the negative charge from Al^{3+} in IV coordination can be balanced by Na^+, K^+ and Ca^{2+} cations. Geopolymers have a lower Ca content compared to Portland cement, hence lower CO_2 emissions, and exhibit high early strength development as well as potential for heavy

metal immobilisation (van Jaarsveld and van Deventer, 1999; Zhang Yunsheng et al, 2007). Recent studies have evaluated treatment of APC residues via geopolymerisation.

Lancellotti et al (2010) used metakaolin-based geopolymeric matrices to treat MSWI fly ashes (electro-filter and fabric filter ashes), at additions of 20 wt.%. Geopolymeric products containing fly ash were prepared with Si/Al and Na/Al ratios of 1.9 and 1.0 respectively and immobilisation efficiency was assessed according to the EN12457 compliance leaching test. Problematic heavy metals such as Cr, Cd and Pb were successfully retained and results obtained were below Italian regulatory limits for non-hazardous waste landfills. Chloride release however was high and up to 84% and 51% for fabric filter and electro-filter ash respectively. The authors attributed the difference in chloride release to an increased immobilisation capacity when electro-filter ash is used.

Luna Galiano et al (2011) investigated geopolymerisation of MSWI fly ash using electro-filter fly ash, coal fly ash, kaolin, metakaolin and GGBS as raw materials. Reagents for the activating solutions included sodium or potassium hydroxide and sodium or potassium silicate. Conventional S/S specimens were also prepared using CEM II and/or lime. Immobilisation efficiency was assessed according to four leaching tests, TCLP, EN12457-4, NEN 7345 (tank test) and a Generalised Acid Neutralisation Capacity (GANC) test. Mixes with CEM II and lime achieved the best compressive strength results although all mixes satisfied the adopted threshold of 0.35 MPa. Leaching performance varied depending on the leaching test. Tank test results were similar for both geopolymeric and CEM II products and complied with the Dutch Soil Quality Decree, although CEM II mixes exhibited lower release of Zn. Mo, V and Cr showed the worst results irrespective of the mix while geopolymeric matrices performed better compared to CEM II according to EN12457-4.

Lei Zheng et al (2011) evaluated the effect of water-wash pre-treatment on the S/S of MSWI fly ash via geopolymerisation. Geopolymers were prepared by mixing raw or washed MSWI fly ash with an activating solution comprising NaOH and Na_2SiO_3, and compacted in cylindrical moulds. Metal leaching was evaluated via a static monolithic leaching test using an acid leachant (pH = 4). Washed fly ash geopolymers exhibited higher early strength development and higher compressive strength after 28 days. This was attributed to the removal of Cl-containing compounds, as Cl can retard strength development by causing structural discontinuity in the geopolymeric gel. The total leached fractions of Cr, Cu and Zn

were lower for the washed fly ash. It was suggested that release of Na, K and Cl ions in the fly ash can compromise the structural integrity of the geopolymeric matrix, resulting in cracks, while the precipitation of ettringite in washed fly ash geopolymers during leaching can reduce pore size and result in a denser matrix.

2.4.3 Other Methods

Todorovic et al (2003) investigated solidification of APC residues from a refuse-derived fuel incinerator with water. APC residues were mixed with water and then compacted in layers in cylindrical moulds. Factors investigated were the amount of water added (l/kg), drying temperature and drying time. Solidification with water was studied based on potential cementitious reactions during the process, resulting in a hardened product. Compressive strengths of up to 7.3 MPa were achieved and releases of Pb and Zn lower than 0.5% of total availability. However, Na, K and Cl were weakly bound to the solid matrix with leaching exceeding 88% of the total available. The authors also concluded that release of these elements was not diffusion-controlled. Release of Cr was also high (40% of total availability).

According to Amutha Rani et al (2008a), a stabilisation technique was developed by Shell Bitumen in the early 1990s for the treatment of APC residues based on the asphalt manufacturing process. APC residues were stirred with approximately 50 wt.% addition of hot bitumen for several hours to ensure complete coating. The resultant material was packed into steel drums or poured directly into moulds at a waste storage site. The properties of bitumen (i.e. durability, chemical stability etc.) make it an effective binder for hazardous waste. Volatility in oil prices however, may render application of bitumen encapsulation too expensive for large scale applications.

Yongjie Xue et al (2009) investigated the reuse of MSWI fly ash and basic oxygen furnace slag from steel manufacturing processes, as partial replacements for fine and coarse aggregate respectively, and/or mineral filler in stone matrix asphalt (type of hot mix asphalt with high rutting resistance). Asphalt mixes were prepared according two different mix design procedures, the Marshall method (ASTM D1559) and the Superpave method (AASHTO TP4). MSWI fly ash addition in the mixes tested varied between 8% and 16% and the total amount of solid waste utilised, including the basic furnace oxygen slag, was more than 80%. Products were assessed in terms of pavement performance (i.e. rutting resistance, fatigue performance

etc.) and potential environmental impact using the TCLP test. All mixes satisfied requirements for stone matrix asphalt using the Marshall or Superpave design methods, although Superpave mixes performed better. A progressive (5-step) TCLP test showed relatively poor immobilization of Ni (release up to 30%) and leaching of Zn up to 13%. Better performance was observed for Pb and Cr (release up to 0.27% and 4.3% respectively).

2.5 Modelling of Solidified/Stabilised Waste Forms

Although results from laboratory studies and leaching tests provide an indication of the extent of leaching of contaminants of concern, they are not enough to provide a solid understanding of the underlying release mechanisms and long-term (i.e. >100 years) leaching characteristics. This implies that improving our fundamental understanding of contaminant leaching requires a more rigorous computational approach. Geochemical reaction and transport modelling can form the basis for predicting long-term release behaviour and understanding the mechanisms that govern release of contaminants and species of concern.

Modelling of leaching characteristics of S/S waste forms has been extensively utilised over the last decade in order to improve the fundamental understanding of the mechanisms governing the release of pollutants. In certain occasions both raw and cement stabilised APC residues have been used as a model waste due to the high content of heavy metals and soluble salts. An approach for evaluating the solidified/stabilized wastes involves the combination of a chemical equilibrium model and a leach model (Park and Batchelor, 1999a; Meeussen, 2003).

The chemical equilibrium model describes the speciation of contaminants at equilibrium in the multi-component environment of stabilized/solidified wastes. Such a model should be able to describe equilibrium chemistry of binder components as well as waste components. It should also be able to describe the effect of high ionic strength on equilibrium chemistry and it should be able to incorporate solid phases (pure or solutions) known to exist in these systems. Furthermore it should be flexible so that it can be applied to different systems comprising of different binders and wastes (Batchelor and Wu, 1993). Once the speciation of the system at equilibrium has been described and the mobile fraction of elements established, a transport model can be used to evaluate release of contaminants.

2.5.1 Chemical Equilibrium Modelling

A system's composition at equilibrium can be predicted according to two equivalent thermodynamic formalisms, i) the minimisation of the Gibbs free energy or ii) equilibrium constants. In both cases, knowledge of the systems speciation is required as well as thermodynamic information for the system's standard state and its divergence from the ideal as it will be shown below.

a) Minimisation of the Gibbs Free Energy

The Gibbs free energy is derived from the enthalpy (*H*) and entropy (*S*) of a system according to the following general equation (assuming an isothermal and isobaric system):

$$G = H - TS \qquad (2.1)$$

The Gibbs free energy describes the tendency of a reaction to occur based on changes in enthalpy (heat/energy) and entropy (disorder of the system). Changes in the Gibbs free energy ($\Delta G = \Delta H - T\Delta S$) indicate whether a reaction will occur spontaneously and define its direction as follows:

- $\Delta G < 0$, favoured reaction (reaction occurs spontaneously)
- $\Delta G = 0$, equilibrium
- $\Delta G > 0$, reaction not favoured (non-spontaneous reaction)

The partial Gibbs free energy or chemical potential (μ_i) of a species *i* in an electrolyte solution comprising *N* number of species at constant temperature and pressure is given by the following expression (Balomenos et al, 2006):

$$\left(\frac{\partial G}{\partial n_i}\right)_{T,P} = \mu_i = \Delta G(i)_T^0 + RT \ln a_i \qquad (2.2)$$

Where $\Delta G(i)_T^0$ is the standard Gibbs free energy of formation of species *i* in *T* degree of absolute temperature and a_i is the activity of species *i.* The standard Gibbs free energy of formation is the change in free energy that occurs when a compound is formed from its

elements in their most thermodynamically stable states at standard-state conditions. It can be obtained from thermodynamic tables or can be calculated based on the enthalpies and entropies of formation based on equation (2.1).

Activities are related to concentrations (on any scale) by means of the activity coefficients according to the equation:

$$\boldsymbol{\alpha_i} = \gamma_i \cdot n_i / n_i^0 \equiv \gamma_i \cdot n_i \qquad (2.3)$$

where α is the activity of species A_i (dimensionless), γ is the activity coefficient (dimensionless) and n is its concentration (any scale). In the above equation n_i^0 is the standard state and it is unity for all species. It cancels in the practical enumeration but causes the activity to become dimensionless (Appelo and Postma, 2007). Substituting Eq. (2.2) in Eq. (2.1) the chemical potential of a species *i* is given by:

$$\left(\frac{\partial G}{\partial n_i}\right)_{T,P} = \mu_i = \Delta G(i)_T^0 + RT \ln n_i + RT \ln \gamma_i \qquad (2.4)$$

The last term in Eq. (2.4) is the excess partial Gibbs free energy and is the difference between the real and the ideal partial free energy for species *i.* Considering a system comprising *N* number of chemical species, the system's Gibbs Free Energy can be attained by the summation of the number of (2.4) equations for the individual chemical species in the system. Chemical equilibrium can then be calculated by the minimization of the objective function of the system's Gibbs free energy since equilibrium is attained for $\Delta G = 0$. Constraints that need to be taken into account such as mass (mole) balances constitute this a constrained minimization problem.

b) Law of Mass Action and Equilibrium Constants

The fundamental equation which describes equilibria in aqueous solvents is the law of mass action. Assuming a system of *N* species where *L* reactions occur, reaction *j* involving *i* species can be written according to the generalised type:

$$u_{1j}A_1 + u_{2j}A_2 + \ldots \leftrightarrow u_{kj}A_i + u_{k+1j}A_{k+1} + \ldots$$

the distribution at equilibrium of species in solution is given by:

$$K_j = \frac{[A_i]^{u_{kj}}[A_{k+1}]^{u_{k+1j}} \ldots}{[A_1]^{u_{1j}}[A_2]^{u_{2j}} \ldots} \qquad (2.5)$$

K_j is the equilibrium constant, u_{ij} is the stoichiometric coefficient of species A_i and the quantities in brackets are the effective concentrations (activities) of the reactants/products. As mentioned previously activities are used to account for ion interactions in the solution and the divergence from a *standard-state* i.e. a 1M aqueous solute behaving like in infinite dilution.

Using the activity expression of Eq. (2.3) and substituting for each species in Eq. (2.5) and using properties of logarithms, Eq. (2.5) reduces to:

$$\log K_j = \sum u_{ij} \cdot \log a_i = \sum u_{ij} \cdot \log n_i + \sum u_{ij} \cdot \log \gamma_i \qquad (2.6)$$

The third term in Eq. (2.6) is the conditional or stoichiometric constant K_j^c, describing the standard state of the reaction and the fourth term describes the non-ideality and is a function of ionic strength (*I)* as it will be shown in following sections. Therefore Eq. (2.5) becomes:

$$\log K_j^c = logK_j - f(I) \qquad \text{for } j = 1 \text{ to } L \quad (2.7)$$

Therefore, for the system of *N* species and *L* reactions, a set of equations can be solved including equations for mass and charge balance to determine the system's composition at equilibrium.

Equilibrium constants can be linked to thermodynamic data and found in relevant tables. As mentioned in the previous section, the Gibbs energy of formation can be expressed as:

$$\Delta G_r = \Delta G_r^0 + RT \ln \frac{[\mathrm{A}_i]^{u_{kj}}[\mathrm{A}_{k+1}]^{u_{k+1j}} \ldots}{[\mathrm{A}_1]^{u_{1j}}[\mathrm{A}_2]^{u_{2j}} \ldots} \qquad (2.8)$$

The activity product in the last term is the mass action constant for reaction *j*, K_j. In addition, at equilibrium, $\Delta G_r = 0$ and so Eq. (2.8) reduces to (Appelo and Postma, 2007):

$$\Delta G_r^0 = -RT \ln K_j \qquad (2.9)$$

The practical application of Eq. (2.9) is that equilibrium constants can be calculated based on tabulated thermodynamic data for dissolved substances, minerals or gases. The quality of the data used however, should be checked in order to avoid obtaining erratic values. Alternatively, equilibrium constants can be determined experimentally. An example of an experimental determination of the mass action constant (or solubility product in the case of minerals) can be found in Ziegler and Johnson (2001). The researchers determined the solubility of calcium zincate ($CaZn_2(OH)_6 \cdot H_2O$) by equilibrating laboratory-prepared calcium zincate with a 0.1M NaCl aliquot containing different amounts of acid or base for 28 days.

c) Chemical Equilibrium Models

It is evident that in both the minimisation of the system's free energy and the equilibrium constants, one needs to know the system's speciation, thermodynamic data for the standard state and a description of the system's non-ideality via activity corrections. Several models have been developed focusing on accurate predictions of thermodynamic properties and activity coefficients.

The Debye - Hückel theory of interionic attraction provided the basis for the prediction of activity coefficients in electrolyte solutions. It considers an electrolyte solution where the ions have point charges and equal finite size, characterized by the distance of closest approach (*a)*. These ions interact in a dielectric medium, the solvent, characterized by its dielectric constant (*ε)* (Balomenos, 2006). The derivation of the Debye - Hückel equation is provided in several studies (Zemaitis, 1983; Balomenos, 2006). The equation for the mean molal activity coefficient according the Debye - Hückel theory is:

$$\log \gamma_{\pm} = -A \left| z_{+} z_{-} \right| \sqrt{I} \qquad (2.10)$$

where A is the Debye - Hückel constant and is temperature dependant, z is the number of charges on the ion and I is the ionic strength. The ionic strength describes the number of electrical charges in solution (Appelo and Postma, 2007):

$$I = \frac{1}{2} \sum m_i \cdot z_i^2 \qquad (2.11)$$

where z_i is the charge number of ion i, and m_i is the molality of i. As with the activity in Eq. (2.2) the ionic strength is dimensionless by division with the standard state (m_i^0).

The assumptions made in the Debye - Hückel theory make it valid only when the ions are far apart, effectively for dilute solutions of ionic strength of 0.001M or less. The theory fails in solutions of greater concentrations because it neglects the short-range interactions. When the ions come in short range of one another, the point charge assumption is no longer valid and specific short-range ion-ion interactions create strong repulsive or attractive potentials, which may even lead to the formation of ion pairs immediately reducing the solution's ionic strength (Balomenos, 2006). Debye and Hückel improved the predictive power of their model using modifications such as a regression parameter a (distance of closest approach) which allowed the model to give reasonable results for solutions of ionic strength of up to 0.1M.

Over the last years several semi-empirical models have been proposed as refinements/improvements to the Debye - Hückel for the calculation of activity coefficients at higher ionic strengths. They are called semi-empirical due to the incorporation of regression parameters derived from experimental data. Semi-empirical models are classified into three main categories based on their fundamental logic for activity prediction (Balomenos, 2006):

i) Ion interaction models which describe the system through interaction forces and respective potentials between the different components in the system.
ii) Ion association models which describe the system through chemical interactions and equilibrium constants.
iii) Hybrid model which use concepts from the previous two categories.

Ion interaction models can be further divided into physical and local composition models, whereas ion association models are also characterized as chemical models. A study by Balomenos et al (2006) provides an extensive overview of the development of chemical equilibrium models.

Refinements of the Debye - Hückel theory for the derivation of activity coefficients at ionic strength values greater than 0.1M have been proposed in studies by Guggenheim E.A, Davies C.W, Bromley L.A, Pitzer K.S, Chen C-C and others (Zemaitis, 1986). These refinements include modifications to the Debye - Hückel limiting law by using regression parameters, in order to increase its effectiveness for concentrated electrolyte solutions i.e. for greater ionic strengths. The Davies equation is a function of the ionic strength and is applicable to ionic strengths of up to 0.5M. The Davies equation is also commonly used in commercial geochemical modelling software.

$$\log \gamma_i = -Az_i^2 \left(\frac{\sqrt{I}}{1+\sqrt{I}} - 0.3I \right) \qquad (2.12)$$

where A is temperature dependent coefficient from the Debye - Hückel equation.

Other studies have attempted to predict activity coefficients by accounting separately for the long-range and short-range interactions. Generally, these models are based on the summation of the excess Gibbs free energy (diversion from ideality) of the electrolyte solution coming from the contribution of long-range interactions and short-range interactions (Song, 1990). Long-range interactions are determined based on the Pitzer - Debye - Hückel theory whereas models accounting for the short-range interactions are based on local compositions models (Sadeghi, 2005). Several models have been developed to describe the contribution of short-range interactions. Such models include Pitzer's virial model and Chen's local composition model which was further enhanced by Liu Y. (Song and Larson, 1990), while several subsequent studies have attempted to improve their efficiency (Balomenos et al, 2006; Sadeghi, 2005; Jaretun and Aly, 1999, 2000).

Successful chemical representation of S/S systems and waste/binder interactions requires collection of accurate thermodynamic properties for the individual hydration products as well

as for combinations of such products (i.e. solid solutions). One of the major challenges for modelling chemical equilibrium of S/S wastes is the complexity of hydration of cementitious binders (i.e. variable stoichiometry of CSH, formation of hydration products in the presence of contaminants/impurities) as well as incorporation of the various immobilization (i.e. complexation, sorption etc.) and matrix degradation (i.e. carbonation) mechanisms.

2.5.2 Leaching Models

As mentioned briefly in a previous section chemical speciation models can be coupled with transport models in order to predict release of contaminants from S/S wastes. Although determination of equilibrium chemistry is important in order to establish the species available for leaching, modelling of transport of ions in porous cementitious matrices is also essential for determining release of contaminants. Modelling of the transport mechanisms is typically based on diffusion. Molecular diffusion is the process whereby a concentration difference between two points in a stagnant solution is levelled out in time due to the random Brownian movement of molecules. Movement of molecules by diffusion is described by Fick's laws (Appelo and Postma, 2007). Fick's first law relates the flux of a chemical species to the concentration gradient:

$$F = -D\frac{\partial c}{\partial x} \qquad (2.13)$$

Fick's second law expresses the change in concentration with time according to the following equation:

$$\frac{\partial c}{\partial t} = D_e\frac{\partial^2 c}{\partial x^2} \qquad (2.14)$$

where c is the concentration of the contaminant [M/L^3], and D_e is the effective diffusion coefficient, incorporating tortuosity and porosity of the solidified matrix [L^2/T]. The equation of the effective diffusion coefficient is:

$$D_e = \frac{e}{\tau^2}\, D_d \qquad (2.15)$$

where *e* is the porosity of the matrix, τ is tortuosity and D_d is the diffusion coefficient of the ion in a dilute solution.

Tortuosity is a measurement of physical retardation and gives an indication of the path length that a diffusing ion must cover in a porous matrix. It is a material property and not ion-dependent (NEN 7375:2004). The basic premise behind the bulk diffusion model is that contaminant release is a result of the concentration gradient between the leachant and the bulk concentration within the monolith (Baker and Bishop, 1997). The main assumptions of the model are (Barna et al, 1994):

- the contaminants are distributed uniformly in the monolith at an initial concentration (C_0).
- the monolith remains homogeneous and the effective diffusion coefficient remains constant during leaching.
- no chemical reaction disturbs the physical mass transfer.

The bulk diffusion model is widely used for modelling purposes and forms the basis for leach tests such as the ANS 16.1 and the NEN 7375:2004. Limitations of the bulk diffusion model in describing leachability from S/S wastes have been previously reported. These limitations pertain to the failure of the bulk diffusion model to describe interactions between the leachant and the solids, especially in cases where an acid leachant is used as it will be explained in the following section.

a) Shrinking Unreacted Core Model

According to Baker and Bishop (1997), previous studies on the behaviour of cement in acidic leachants have shown the existence of a calcium depletion zone, with a sharp interface, on the exterior layer of samples leached in acid solution. Depletion of acid-soluble species was also observed in this zone, while an unreacted zone was noted in the interior of the leached specimens. The same authors reported that previous studies on leaching characteristics of S/S wastes leached under acidic conditions observed the following:

- The leached layer was essentially depleted of calcium and soluble contaminants.

- The leached layer consisted of an amorphous silica-rich gel with a much higher porosity than the unreacted specimens.
- A thin zone of calcium-rich re-mineralization was noted at the leach front.
- The specimen beyond the leach front remained unchanged.
- A small pH gradient in the leach shell was noted, followed by a large pH change over the very narrow leaching zone. A constant, high pH was observed in the unreacted core.

The shrinking unreacted core model (SUC) was developed to account for the effects of the diffusion acidic species into the leached specimen. In contrast to the bulk diffusion model, where contaminant leaching is considered to be a result from the diffusion from the specimen into the leachant, the SUC model considers the diffusion of acidic species from the leachant into the specimen as the leaching controlling mechanism. Figure 2.5 presents a schematic illustration of the SUC model.

According to the SUC model acid leachant permeates the pore structure of the cement or pozzolanic-based paste. The acid consumes the calcium hydroxide in the paste lowering the pH of the matrix. Reduction in pH results in metal ions dissolving and diffusing in a direction towards the leachant, or towards the unaltered core of the specimen where they precipitate again due to constant high pH. This zone, where metal ions precipitate again as insoluble hydroxides, is called the remineralisation zone.

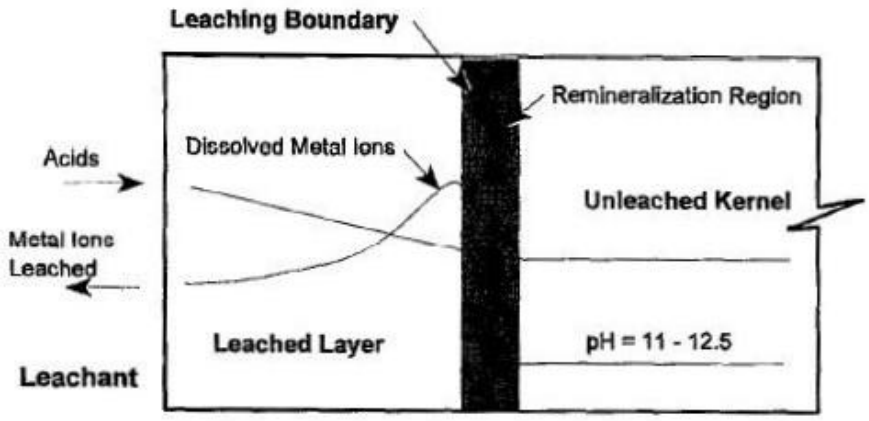

Figure 2.5 Schematic illustration of the shrinking unreacted core leaching model (Baker and Bishop, 1997).

The key elements of the model therefore as shown in Figure 2.5 are the leached shell which is a highly porous structure (Cheng and Bishop, 1990), the leaching front and the unaltered core. Cheng and Bishop (1990) consider two distinct processes in the SUC model. Diffusion across the leached layer can be considered a steady-state process. At the leaching front however, diffusion of hydrogen ions process as if the medium is infinite and dissolution reactions occur at the same time in the pores. The proton reactions in the leaching front have a half-life of less than milliseconds. The system in such a case could be considered as an unsteady-stated diffusion-controlled fast reactions process.

The shrinking unreacted core model follows a similar rationale to decalcification, apart from the fact that in the latter calcium hydroxide is not neutralized under the effect of an acid but it leaches out of the specimen due to the dissolution of portlandite crystals. In both cases the same zones are observed comprising a leached calcium depleted zone, the leaching front and a sound/unreacted zone or core. The physical properties of cement based materials depend on the amount of calcium present. In both cases, matrix alteration may take place leading to changes in its physical properties during leaching, creating a new porosity.

2.6 Recent Waste Modelling Studies and Developments

Modelling efforts have attempted to couple geochemical speciation and reaction with transport to assess release from waste materials. Several modelling codes have been developed by researchers for their own use or have become available either commercially or in the public domain. Examples of the latter include but are not limited to the Leaching Expert System (LeachXS – database of leaching data, including the geochemical speciation and transport framework, ORCHESTRA), PHREEQC, GEMS-Selektor, and MINTEQA2. These codes have been used to model contaminant release during various leaching tests (i.e. batch, pH-dependence, monolithic or percolation) or under field conditions. It is noted that from these codes GEMS-Selektor is the only true Gibbs free energy minimisation algorithm whereas other popular codes such as LeachXS and PHREEQC involve equilibrium constants.

A series of papers (Batchelor and Wu, 1993; Park and Batchelor, 1999a, 1999b, 2002a, 2002b) describes the development of a code to model reactions and transport from solidified wastes. The Pitzer ionic interaction model was initially used to calculate activity coefficients and the thermodynamic database of the program MINTEQA2 was used and extended to

include cement hydration products. CSH variable stoichiometry was described by a set of empirical regression equations (Reardon model, described further in Batchelor and Wu, 1993). The use of the Pitzer ionic interaction model however, led to slow and unreliable convergence and was later replaced by the Davies equation. In addition Reardon's model was replaced with Berner's model for the description of the variable stoichiometry of CSH. Berner's model exhibited better agreement with experimental data at pH > 11. This model assumes that the variable stoichiometry and variable solubility of CSH can be described as a non-ideal mixture of two independent solid phases. This assumption is applied to three discrete regions defined by different values of the molar ratio of calcium to silicate in CSH. The solid phases for each region are:

- SiO_2 and CaH_2SiO_4, $0 < Ca/Si \leq 1.0$
- CaH_2SiO_4 and $Ca(OH)_2$, $1 < Ca/Si \leq 2.5$
- CaH_2SiO_4 and $Ca(OH)_2$, $2.5 < Ca/Si$

Sorption of alkalis (Na, K) was incorporated in the model using a set of regression equations taking into account the water-to-cement ratio and its effect in the surface area of CSH. A linear pH-dependent sorption model was also included to account for sorption of metals through surface complexation according to the reaction:

$$= SOH + M^{2+} \rightarrow \equiv SOM^{+} + H^{+}$$

where ≡ SOH is an available sorption site; M^{2+} the metal ions; and ≡ SOM^{+} a sorption site occupied by ion M^{2+}. Finally the chemical speciation code was coupled with a transport model based on one dimensional Fickian diffusion. The chemical speciation code calculated the mobile fraction of components which was entered as a variable in the diffusion equations. The latter was solved using a Crank-Nicolson finite difference method.

Hamil et al (2005) simulated leaching of Pb, Cd, Cr and As from cementitious waste using PHREEQC. The experimental procedure involved preparation of metal-spiked cement mixes and leaching according to a modified TCLP procedure, using 0.1M or 0.6M acetic acid or a municipal solid waste landfill leachate. Model input included mineral phases assumed to be present in the cementitious waste and their calculated quantities, availability of heavy metals,

complexation reactions with organic ligands, adsorption on hydrous ferric oxides and silica gel and solid solution formation. In addition, dissolution rates were included for cement minerals while equilibrium with their possible equilibrium-controlling species was assumed for most solid compounds. Model output was the total concentration in solution for each element of interest, its speciation at different time steps, SI values of relevant minerals and solution pH. Modelling results showed that precipitation was the dominant solubility-controlling mechanism for Pb and Cd. In the presence of acetic acid and at low pH values Pb and Cd were present as acetates whereas at high pH values hydroxide species dominated. Simulations showed that complexes with organic ligands where the dominant heavy metal species when landfill leachate was used as the leachant. The authors also suggested that at high pH values release of As may be controlled by the competition between calcium carbonate and calcium arsenate competition.

Astrup et al (2006) used LeachXS to perform speciation calculations based on data from a pH-dependence leaching test on APC residues and identified possible solubility-controlling minerals for Al, Ba, Ca, Cr, Pb, S, Si, V, and Zn. The plausibility of each mineral was evaluated by calculating element concentrations in equilibrium with specific minerals obtaining solubility-type curves and comparing with the experimental data. Predicted concentrations for most elements based on solubility control from selected minerals present in the thermodynamic database were within one order of magnitude in the pH range 4.5-12.5. Some data points for Pb, Zn, Cr and V could not be explained solely by solubility control and the authors suggested that processes such as redox, sorption or incorporation in mineral phases may be important at certain pH values.

A similar approach was used by Hyks et al (2007) using ORCHESTRA to identify solubility-controlling phases in washed and raw APC residues varying also the time of the pH-dependence leaching test used. The same controlling phases were suggested for Al, Ca, Mg, Si, S, Mo, Zn, Cd, and Cu regardless of the equilibration period or untreated/washed nature of APC residues, whereas leaching of Ba, Sr was better described by considering a longer equilibration time (kinetic effects). It is also noted that the authors compared the activity coefficients for Ca, S determined with the Davies and Pitzer equation and established that the same solubility-controlling phases are obtained in both cases.

Tiruta-Barna (2008) developed a code in PHREEQC to model dynamic leaching tests with continuous renewal of leachant. In the model system, dissolution/precipitation reactions begin at the solid/liquid interface while additional chemical reactions (acid/base, complexation, redox) occur in the aqueous phase. Soluble chemical species diffuse from the pores of the material towards the leachate and the resulting changes in the pore water composition affect in turn mineral solubility. Surface corrosion (dissolution) is also assumed to occur at the solid surface in contact with the leachant. The main model building blocks were a diffusion compartment (porous block) in contact with a leaching compartment, which was assumed to behave according to an open stirred reactor scheme. Exchange of chemical species occurs between the two compartments. Model predictions for two cases involving i) laboratory leaching tests on a cement S/S material and ii) leaching from a pilot scale water storage pool constructed with a S/S material, were within one order or of the same order of magnitude as the experimental data. In the case of the water storage pool scenario, CO_2 uptake incorporated in the model produced accurate predictions for the evolution of pH. Predictions for non-reactive elements (Na and Cl) however, were not in good agreement with the experimental values which was attributed to an increase in porosity with time.

More recently Martens et al (2010) modelled various extraction leaching tests and a modified Dutch NEN 7345 diffusion test for stabilized/solidified MSWI bottom ash also using PHREEQC. Their approach involved similar steps with previous studies including selection of appropriate mineral phases, experimental measurement and model input of hydrous ferric oxides and amorphous aluminium mineral for heavy metal adsorption, determination of the potential formation solid solutions (i.e. calcite-cerrusite) and in the case of the diffusion test, determination of the effective diffusion coefficient. The main difference in the study is the use of a different thermodynamic database (CEMDATA07.1) for various cement hydrates such as CSH, AFm phases (monosulphoaluminate, strätlingite), AFt (tricarboaluminate, ettringite), hydrogarnet and hydrotalcite. The model gave good prediction for Ca, Na, K and Pb but underestimated release of Al and Mg. Release of Ca was found to be controlled by hydration products such as portlandite, the jennite-like and tobermorite II-like solid solution strätlingite and calcite. In contrast with the study by Halim et al (2005) leaching of Pb was not only controlled by precipitation/dissolution but sorption by surface complexation and solid solution formation adequately described its amphoteric behaviour.

The above studies demonstrate that geochemical and transport modelling is a useful tool for identifying the chemical and transport processes that are involved in the release of contaminants, based on laboratory leaching tests. Moreover, modelling can also be used to model numerous site conditions such as leaching from recycled construction materials, concrete performance and leaching in landfills, where experimental studies are limited by the time required to assess long-term effects (i.e. > 100 years).

De Windt et al, (2007) used a reactive transport code to extrapolate results of batch and dynamic tests to a simplified landfill cell scenario for a Pb-containing waste treated with CEM I and considering a period of 100 years. The researchers used identical chemistry and mineralogy to cubic laboratory specimens. Additional model inputs included the rainfall and effective infiltration rate with the waste assumed fully saturated, while CO_2 penetration was partly incorporated. The effect of fracture or micro-crack development in the matrix was evaluated. Model results showed that Pb leaching from damaged S/S matrices was up to 100 times greater (extreme conditions) compared to undamaged monoliths, but was 0.1% of the total Pb content. Considerations in such models are the complex nature of the field scenario in terms of matrix degradation, carbonation (CO_2) effects, reactions under unsaturated conditions or drying and wetting cycles as well as the effects of landfill liners.

Van der Sloot et al (2007) followed a combined experimental-modelling tiered approach in order to evaluate the potential for environmental impact of stabilised waste. The authors utilised data from laboratory leaching tests (i.e. pH-stat and monolithic) and lysimeter/field studies coupled with modelling (using LeachXS) to assess the long-term effects of stabilized waste disposed in hazardous waste landfills. pH-stat leaching tests and subsequent modelling provided an insight on the solubility controlling phases (geochemical characterisation). Modelling of tank leaching data was then used to validate the geochemical characterization derived from the pH-stat test under diffusion-release, taking into account the physical properties of the matrix (i.e. porosity, tortuosity). The next step involved determining the interactions between the stabilized waste (both in monolithic and crushed form) with the layer of soil simulating landfill conditions (release by diffusion and percolation). This integrated, tiered approach was considered a basis for improving the understanding of the factors affecting release in field conditions and for contributing to improved hazardous waste landfill design. The authors attributed differences between the measured and modelled results to the description of processes such as sorption, complexation to organic matter and kinetic

effects during leaching. They also noted the complexity of processes such as carbonation that can have a marked effect on leaching characteristics.

As it is observed from the above examples, modelling of cementitious waste systems is a complex process. Laboratory leaching tests coupled with geochemical modelling provides a framework for characterising the material of interest/concern and assessing release under different conditions (i.e. leaching test, field scenarios etc.). This can result in improved management decisions pertaining to either treatment or disposal of wastes or landfill design. In the case of stabilized/solidified waste using cementitious binders, it can contribute to improved mixed design and assessment of long-term release which is not feasible with laboratory leaching tests.

One of the basic principles for the success of the model is an accurate formulation of the initial problem as well as identification of the possible solubility-controlling phases and their thermodynamic properties. Furthermore, the immobilization mechanisms considered in the model may play a very important role in the accuracy of the results and the eventual fit with experimental data. This requires knowledge of characteristics of the S/S waste such as plausible solubility-controlling solids and their thermodynamic properties and physical properties of the S/S matrix.

2.7 Summary

This review demonstrates that the chemistry of S/S is complex. The effect of metal-containing waste on cement hydration, and thus the effectiveness of the treatment depends on the nature of the waste. Combination of heavy metals may induce hydration poisoning effects, compared to retardation effects when metals are studied in isolation. APC residues represent a problematic waste since it contains not only combinations of heavy metals, but also high concentrations of chlorides. S/S has been previously used for the treatment of APC residues with the majority of the studies using Portland cement types at additions no greater than 60 wt.%. In addition, the focus in these studies has been on the metal immbolisation capacity of S/S APC residues, whereas the effects and fate of chloride, its most abundant problematic constituent, have been less detailed. Finally, geochemical modelling is increasingly used to provide a deeper understanding of S/S immobilisation processes for elements of concern.

3. RESEARCH OBJECTIVES

The main objective of this research is to assess the effectiveness of S/S of APC residues in high waste/low binder mixes taking into account not only the immolization of heavy metals, but also of chlorides. The goal is to contribute to existing knowledge on S/S of APC residues by determining the effect of all dominant problematic elements on S/S products, and ultimately, to the development of more efficient and sustainable treatment methods for APC residues in the UK.

This research programme was part of the project *Process Envelopes for Cement-based Stabilisation/Solidification* (*PRoCeSS*), sponsored by the UK Department of Innovations, Universities and Skills now merged with the Department for Business, Innovation and Skills. The project objective was to identify a range of operating conditions (operating window/ process envelope) under which the S/S process would operate effectively for different types of hazardous wastes. The underlying project aim was to increase transparency of S/S technology, and support standards for good practice in the S/S industry.

Specific deliverables of the research include:

- **i.** Assessment of the suitability of CEM I and GGBS as potential matrices for the S/S of APC residues, according to regulatory criteria and performance thresholds. Unlike previous studies, GGBS was not activated using an activator (e.g. alkali solution) and the inherent alkalinity of APC residues was used instead.
- **ii.** Characterisation of the S/S matrices and geochemical modelling in order to provide an insight to factors that control release of all dominant contaminants.
- **iii.** A preliminary analysis on the viability and future of S/S as a treatment method for APC residues and proposal of alternative treatment methods, if required.

In order to achieve the aforementioned objectives, the research programme was divided in two parts:

1. *Experimental Study*. This part involves S/S specimen preparation and testing for physical parameters and contaminant leaching according to international standards. S/S samples are prepared and tested on a laboratory scale varying two key recipe

parameters, the waste-to-binder and the water-to-solids ratios. Testing parameters and standards are summarized in Table 3.1. Contaminant immobilization efficiency is evaluated using the Dutch NEN 7375:2004, a dynamic leaching test for monolithic materials. Results obtained are then compared to performance thresholds and regulatory limits to assess the effectiveness of the S/S treatment. Finally, the S/S matrices are characterised using techniques such as XRD and Scanning Electron Microscopy (SEM).

2. *Chemical Speciation and Leaching Modelling*. The second part of the study involves modelling of: i) the monolithic leaching test for S/S APC residues and ii) a combined alkaline/acid leaching procedure for raw APC residues. Modelling of the monolithic leaching test aims to provide an insight on the parameters affecting release from S/S APC residues. Modelling of the pH dependent release from raw APC residues aims to evaluate the potential for extraction of elements from APC residues prior to S/S. The predictive power of the models was evaluated by determining the goodness of fit between the predicted and measured values. Modelling data are expected to contribute to more efficient management of APC residues, aligned with UK waste management policy.

The research framework is also presented visually in Figure 3.1. The materials and methods of the Experimental Study and results obtained are detailed in Chapters 4 and 5 respectively. Chapter 6 is dedicated to the Modelling Study presenting the methodology followed by the results obtained.

Table 3.1 Laboratory testing parameters for S/S products

Testing Parameter	Standard Method
Setting Time	BS EN 196-3:2005
Consistence	BS EN 4551
Unconfined Compressive Strength	BS EN 196-1:2005
Water Content	Drying at 60 C to constant weight
Bulk Density	Environment Canada Method
Specific Gravity	ASTM D5550-94
Porosity	Environment Canada Method
Acid Neutralization Capacity	Environment Canada ANC Method
Monolithic Leaching Test	NEN 7375:2004

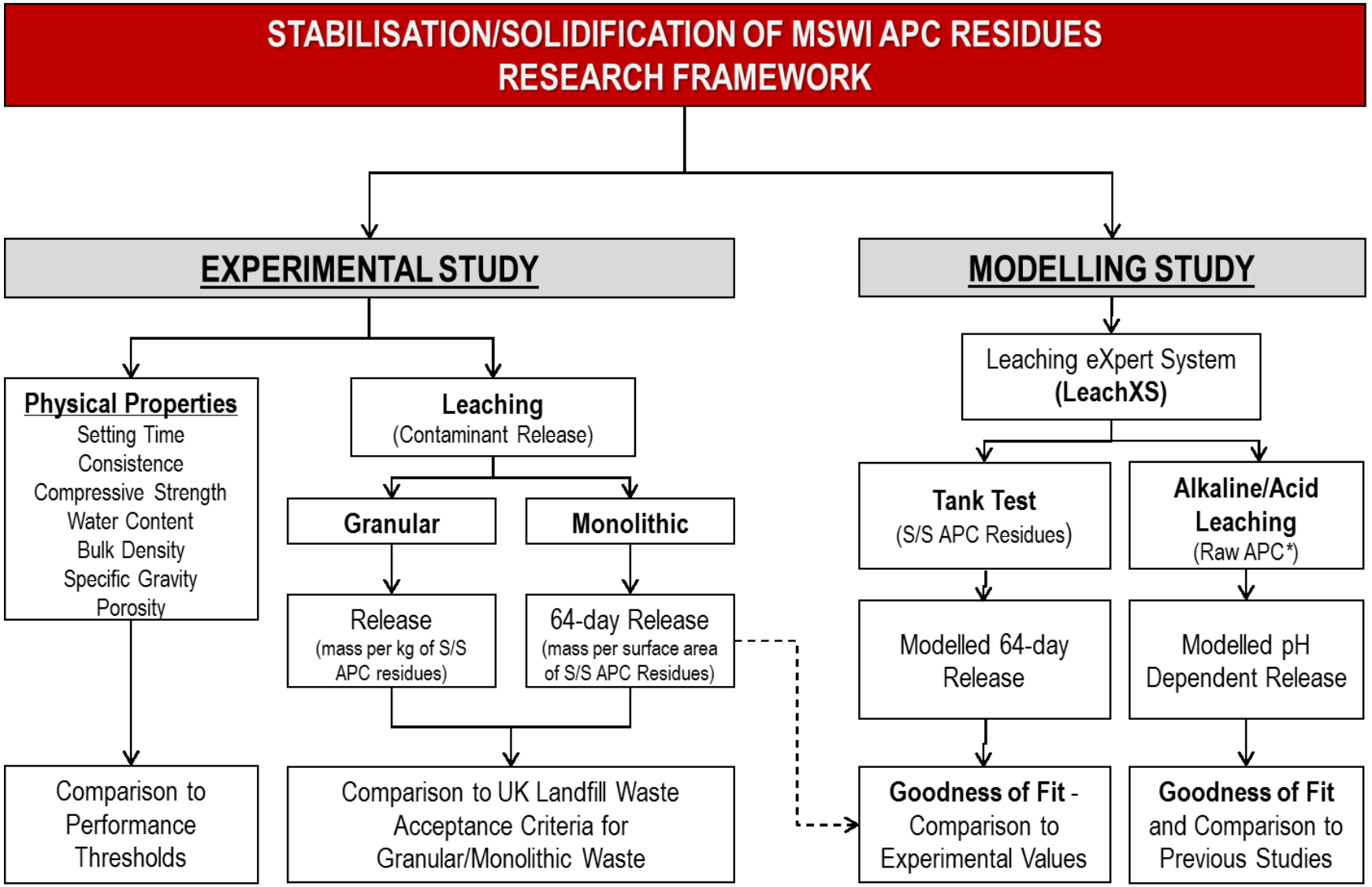

Figure 3.1. Research Framework

4. MATERIALS AND EXPERIMENTAL METHODS

4.1 Materials

APC residues were obtained from the South East London Combined Heat and Power (SELCHP) plant, a major EfW plant in SE England with the capacity to burn 420,000 tonnes per year of MSW. This plant uses conventional mass-burn technology and generates 34 MWh of electricity. Bulk samples (approximately 20kg) of APC residues, obtained directly from the bag house filters, were provided by the EfW plant operator. CEM I (supplied by Lafarge Cement), GGBS (supplied by Civil and Marine Slag Ltd.) and distilled water were used to prepare all S/S APC residue samples. Elemental composition data for both the CEM I and GGBS are shown in Table 4.1.

Table 4.1 CEM I and GGBS elemental composition expressed as oxides

	CaO	SiO_2	Al_2O_3	Na_2O	K_2O	MgO	MnO	Fe_2O_3	SO_3	TiO_2
CEM I	61.57	23.6	4.24	0.27	0.88	2.59	0.06	2.4	1.37	0.32
GGBS	38.8	34.7	13.9	0.25	0.28	9.2	0.37	0.5	0.05	1.01

The as-received APC residues were examined by scanning electron microscopy (JEOL-JSM-840A) and a typical image is shown Figure 4.1. This indicates APC residues consist of agglomerated spherical particles with a mean particle size of approximately 25μm.

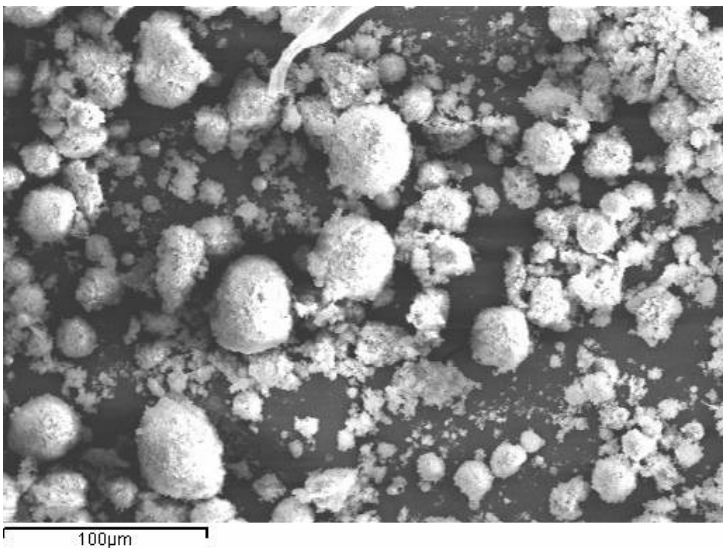

Figure 4.1 SEM image of as-received APC residues

Crystalline phase analysis of as-received APC residues was determined using X-Ray Diffraction (XRD, Philips PW1700 series) with Cu Kα radiation and a secondary graphite crystal as mono-chromator. XRD data, typical elemental composition and leaching data (liquid-to-solid, L/S, ratio of 2-10 determined according to EN12457-3) for APC residues are presented in the following sections. Additional XRD and XRF analysis provided by the EfW plant operator is included in Appendix I.

4.2 Isothermal Conduction Calorimetry

The interaction between APC residues and CEM I was investigated using isothermal conduction calorimetry (Wexham Developments, JAF calorimeter). This gives the rate of heat evolution from hydration reactions with curing time. In these experiments mixes have been prepared with high CEM I/low APC residue additions (0, 10 and 30 wt % of total dry mass) and low CEM I/high APC residue additions (100, 70 and 50 wt %). For both sets of samples, the CEM I was thoroughly mixed with the APC residues using a water/solids (w/s) ratio of 0.5, and 25g of the paste transferred to a polyethylene bag for testing. This was carefully placed around the heat sensor of the calorimeter and the chamber then placed in a water bath set at 20 ºC. Temperature differences between the sample and the water bath were measured immediately. Hydration was monitored for 98 hours. At the end of the experiment, the set-up was calibrated using the integral heater in the calorimeter, so that measured voltages could be converted to rate of heat evolution data.

4.3 Stabilised/Solidified Product Preparation

The main variables affecting the performance and properties of the S/S products were expected to be the APC residue/binder ratio and the water content (water/solids or w/s ratio). Samples were prepared with CEM I or GGBS additions of 0, 10, 20 and 50 wt. % of total dry mass and w/s ratios between 0.35 and 1.0. The ranges for binder addition and w/s ratios were based on industrial applicability considerations for commercial viability (i.e. cost of binder) and workability respectively, as well as performance of the S/S matrices. CEM I or another alkali activator was not used with GGBS because the free lime and alkalis in the APC residues can activate the GGBS and initiate pozzolanic hydration reactions. It is also noted

that zero binder addition aims to investigate s/s of APC residues by adding only water, based on the study by Todorovic et al (2003).

The binder was thoroughly mixed with the APC residues prior to water addition using a 5L capacity mortar mixer (ELE, UK). Distilled water was then added to achieve the desired water/solids ratio. Mixing for 3 minutes produced a homogenous paste that was formed into 50mm cube samples using a vibrating table (Controls, Italy) to remove air voids from the mix. Specimens were de-moulded after 24 hours and transferred to polyethylene re-sealable plastic bags containing a damp tissue to maintain a high humidity environment. This also minimised carbonation that could alter the properties and leaching characteristics of the S/S wastes. Specimens were prepared and cured in a laboratory environment at room temperature (20-24 ^{o}C) and pressure.

The experimental schedule is presented in Table 4.2. No binder addition refers to the investigation of S/S of APC residues by using only water. The experimental schedule was compiled based on preliminary experiments on a laboratory scale that aimed to obtain an indication of the mixing behaviour of APC residues, coupled with a review of existing data from mixes investigated in previous studies. The literature review determined that mixes with waste additions greater than 60 wt.% are not commonly observed and therefore data are relatively thin. Formulations with low binder addition (i.e. 10 and 20 wt.%) were selected not only for evaluating the performance of low binder S/S mixes, but also with the economics of a commercial process in mind. An assessment of the economics of the S/S process for APC residues, however, was outside the scope of the study. Finally, the ranges for the w/s ratios selected were based on preliminary experiments, where water additions resulting in mixes that would not set in 24 hours or that could not be cast were not considered further.

Table 4.2 Experimental Schedule

Binder	**Binder Addition (% of dry mass)**	**Waste-to-Binder Ratio (g/g)**	**Water-to-Solids Ratio (ml/g)**			
CEM I	50	1	0.40	0.50	0.55	0.6
	20	4	0.45	0.50	0.60	-
	10	9	0.50	0.55	0.60	0.65
GGBS	50	1	0.35	0.40	0.50	-
	20	4	0.40	0.50	0.60	0.7
	10	9	0.50	0.60	0.70	0.8
No Binder	NA	NA	0.60	0.70	0.80	1.0

4.4 Stabilised/Solidified Product Testing

4.4.1 Physical Tests

S/S products were tested for physical parameters that may determine a successful process on a commercial scale taking into account workability and the structural integrity of the S/S monolithic matrix. Physical tests conducted on S/S APC residues include:

i. **Consistence** (based on **BS EN 4551**). Consistence was determined using a flow table with a disc diameter of 255 mm and a 100 mm diameter conical mould. The test involves removing the conical mould from the mixed slurry sample, applying 15 rapid vertical displacements (jolts) to the disc and measuring the diameter of the spread of the sample.

ii. **Setting time (BS EN 196-3:2005).** Initial and final setting times were determined using a manual Vicat apparatus. This test involves determination of the time at which a needle of a specific weight and shape penetrates a cement paste to a given depth (initial setting time) or when it leaves no mark on the paste's surface (final setting time).

iii. **Bulk density.** Bulk density was calculated using the equation:

$$\text{Bulk density (BD in g/cm}^3\text{)} = \frac{m_s}{V_s}$$

Where m_s is the mass (g) of the cube specimen determined by weighing on electronic balances (Sartorius and Oertling) and V_s is the volume (cm^3) calculated by measuring the specimen dimensions using Vernier callipers.

iv. **Water content**. Water content was determined by drying samples at 60°C to constant weight after immersing samples in acetone to prevent further hydration, and the results were calculated on a wet mass basis.

v. **Specific gravity**. The specific gravity of samples was determined using a He gas volume expansion meter (Robertson Research, ASTM D5550-94).

vi. **Unconfined compressive strength**. S/S products were tested in triplicate at 7 and 28 days for unconfined compressive strength (UCS, Automax 5) using a loading rate of 300 N/s. Water-saturated 28-day UCS data was obtained by curing samples for 21 days as described above and then immersing them in water for 7 days before measurement of UCS.

vii. Porosity. Specimen porosity (p) was calculated from the bulk density, water content and specific gravity using the equation (Stegemann et al, 1991):

$$\text{Porosity (p)} = 1 - \left[\frac{BD \times (1 - WC)}{SG \times d} \right]$$

where BD = bulk density (g/cm^3), WC = water content (w/ww), SG = specific gravity (dimensionless) and d = density of water (1 g/cm^3).

The effect of the main experimental variables (i.e. waste-to-binder and water-to-solids ratios) on the physical properties of the S/S matrices was further evaluated via statistical techniques such as hypothesis tests and analysis of variance (ANOVA) using commercial software STATA version 9.2.

4.4.2 Acid Neutralisation Capacity (ANC)

The acid neutralisation capacity of the S/S products was determined using a three-point ANC test at, 1 and 2 meq/g and no acid addition using 1M HNO_3. Samples cured for 28 days were dried at 60ºC, crushed using a mortar and pestle and sieved to <150µm. The crushed sample was then placed in 100ml plastic bottles and distilled water and HNO_3 were added to give a liquid-to-solid ratio of 10 and the desired acid addition. The bottles were sealed and rotated end over end for 48 hours. Leachate was extracted, centrifuged at 10,500 rpm for 10 minutes (Sorvall RC6 centrifuge) and the pH determined.

Part of the leachate from no acid addition (0 meq/g) samples was filtered through a 0.45µm cellulose nitrate membrane filters (Whatman International Ltd.) and analysed for chloride using the argentometric method (APHA, 2005). This involves titrations using silver nitrate ($AgNO_3$) as the titrant and potassium chromate (K_2CrO_4) as indicator. It should be noted that the sample without acid addition was leached at the same liquid-to-solid ratio as is applied in the regulatory granular leaching test, BS EN12457-3. Since a smaller particle size and longer contact time were applied, the leaching results for no acid addition can be considered to be a conservative estimate of the results of BS EN12457-3.

4.4.3 Tank Leaching Test (NEN 7375:2004)

The monolithic (tank) leaching test (NEN 7345:2004) is a dynamic test for assessing diffusion-controlled leaching and has been used as the basis for developing the UK monolithic Waste Acceptance Criteria (monWAC) (Hall et al, 2005). The test involves leaching of monolithic specimens in sealed containers, using distilled water as the leachant to assess surface area related release. The leachant is renewed at 8 different times (fractions) over a period of 64 days and results are expressed in terms of emission of mass per unit surface area (mg/m^2).

Products that had a UCS after water immersion > 1MPa were tested for diffusion-controlled leaching from the monolith. The mixes subjected to the tank test are shown in Table 4.3.

Table 4.3 Mixes subjected to the monolithic (tank) leaching test

Binder	Binder Addition (% of dry mass)	Water-to-Solids Ratio (ml/g)			
CEM I	50	0.40	0.50	0.55	0.6
	20	0.45	0.50	0.60	
	10	0.50			
GGBS	50	0.35	0.40	0.50	

50mm cube specimens cured for 28 days were immersed in distilled water at $V_L/V_S = 4.0$, where V_L is the volume of distilled water and V_S is the volume of the specimen, with renewal of the leachant at 0.25, 1, 2.25, 4, 9, 16, 36 and 64 days. The long duration of the tank test coupled with time constraints for the experimental study allowed for only replicate to be tested for each mix.

At each fraction the pH was measured using a pH meter (accuracy ±0.05 pH units), calibrated using standard buffer solutions before each measurement. An aliquot of leachate was filtered through 0.45µm cellulose nitrate membrane filters (Whatman International Ltd.) for chloride analysis by the argentometric method which involves titration using $AgNO_3$. Liquid samples for metal analysis were preserved and matrix-matched to the ICP calibration by adding 1ml of concentrated HCl (ARISTAR Grade, VWR UK) to 9ml of sample. These samples were stored in capped, 12 ml polystyrene test tubes, prior to analysis. Metal analysis was conducted by via Inductively Couple Plasma – Optical Emission Spectroscopy (Optima 4300

DV - Severn Trent Laboratories, UK ICP-OES). The methods used for analysis are presented in the Appendix II.

It is noted that samples were tested by ICP-OES for sulphur (S). However, due to the nature of the mixes it is assumed that the major sulphur species in the system is sulphate (SO_4^{2-}) and reference is made only to $SO4^{2-}$ hereafter. S emissions were adjusted accordingly for the mass of SO_4^{2-}. Speciation of sulphur in commercial GGBS for use in concrete may comprise both sulphides and sulphates with maximum permissible contents of 2.0% and 2.5% by mass respectively, according to BS EN 15167-1:2006. A study by Roy (2009) however, has shown that in activated slags it is likely that sulphides will be transformed to sulphates. Sulphur content (as SO_3) in the GGBS used in this study was 0.05%.

As with the physical properties, statistical techniques were used to evaluate the effect of the main experimental variables on the leaching characteristics of the S/S matrices subjected to the tank test.

4.5 Process Performance Criteria and Thresholds

Although previous studies on APC residues have investigated the potential for reuse, the main management route in the UK is pre-treatment, as required by the Landfill Directive, followed by disposal in hazardous waste landfills. Therefore, performance thresholds adopted in this study pertain mainly to disposal in UK landfills and are presented in Table 4.4. However, reference is also made in following sections to criteria for re-use (i.e. construction), as included in international standards.

Table 4.4 Performance values and thresholds for S/S products

PARAMETER	PERFORMANCE THRESHOLD
S/S Matrix Properties	
Consistence	175±10 mm
Initial Setting Time	2< initial setting time < 8 hours
Final Setting Time	< 24 hours
28-day Compressive Strength	> 1.0 MPa
Contaminant Leaching Properties	
Pb, Zn, Cr, Cu, Cl, SO_4	Compliance with UK monWAC

Success criteria for properties of the S/S matrices were chosen based on a previous study by Stegemann and Zhou (2009). The authors proposed a set of screening tests that would provide confidence for a full-scale application of the S/S process. In the present study, success criteria pertain to the freshly mixed and hardened S/S product characteristics, as well as contaminant leaching properties. Freshly mixed product characteristics include mix consistence (i.e. flow table spread) and setting time (initial and final). Hardened product characteristics include UCS, including strength after water immersion.

Setting times and rheology of the mixes are connected to the amount of water in the mix. It is desirable to limit water content to an amount sufficient for complete hydration. Excess water can increase the amount of water-filled pores in the matrices with detrimental effects both on their physical integrity and leaching properties. This however should be balanced with workability considerations for the processing and handling of the freshly mixed products. Stegemann and Zhou suggest that a flow greater than 175 mm is used as a guideline for flowable mixes, which was also measured as the flow of a cement paste of standard consistence according to BS EN196-3:2005. In addition an initial setting time greater than two (2) but less than eight (8) hours will facilitate handling, while a final setting time of less than twenty-four (24) hours is adequate for practical operational considerations of a landfill such as vehicle traffic.

UCS is a measure of the structural integrity of the matrix and according to Stegemann and Zhou it can also act as surrogate parameter of the degree of hydration reactions. This means

that assuming satisfactory hydration conditions, compressive strength should increase with age (e.g. $UCS_{(28d)} > UCS_{(7d)}$). UCS after water immersion is also important to determine deleterious effects such as swelling or matrix dissolution that can compromise the structural integrity of the matrix. This is particularly important for APC residues due to the amount of soluble salts in the waste. Ideally, and similarly with cement pastes, strength after immersion should be greater or equal to the strength of specimens cured in a humid environment. Guidance from the USEPA requires an immersed UCS of 350 kPa at 28 days to support overburden and equipment, whereas the UK Environment Agency requires a minimum UCS of 1 MPa at 28 days (Environment Agency, 2006).

Finally, performance of the S/S matrices in terms of contaminant release is assessed by comparing results from the NEN7375:2004 against regulatory standards, the UK Landfill Waste Acceptance Criteria for monolithic wastes (monWAC). The monWAC will be presented in the following chapter along with the presentation of the leaching results to allow for easier comparison.

4.6 Stabilised/Solidified Product Characterisation

S/S products were characterised in terms of mineralogy and microstructure by means of XRD and Scanning Electron Microscopy-Energy Dispersive Spectrometry (SEM-EDS) respectively. Crystalline phases in the S/S products were determined by XRD using a PANalytical X-Pert Pro MPD diffractometer with a Cu X-ray source. Samples cured for 7 and 28 days were dried at 60°C and crushed to a fine powder. These were loaded onto a zero background silicon holder, and analysed from 5 to 60° 2θ using 0.04° 2θ step size and 30 seconds count time per step. Phase identification was carried out using the software X'Pert Highscore Plus.

The microstructure of the S/S products was investigated by SEM-EDS (LEO 1525 FEG). Fractured surfaces were dried, mounted on 0.1-inch stabs and gold-coated prior to placement in the microscope. EDS spectra were obtained by examining the fractured, instead of polished surfaces and should be considered as approximations only.

4.7 Geochemical Release Modelling

The modelling tools and methodology are described in more detail in Chapter 6, which is dedicated solely to the modelling study. A brief summary however is presented here for completeness.

Geochemical release was modelled using the commercial software LeachXS. LeachXS was developed by collaboration between the Energy Centre Netherlands (ECN), Vanderbilt University and DHI, an independent, international consulting and research organisation. It is a database/expert decision support system for characterisation and environmental impact assessment based on estimated contaminant release as derived from leaching tests. LeachXS allows for easy data representation and comparison, as well as geochemical release modelling. It combines a database of various leaching results (lysimeter results, laboratory and field leaching data for various materials and wastes), a regulatory database, and the geochemical modelling and transport capabilities of the code ORCHESTRA. ORCHESTRA (**O**bjects **R**epresenting **CHE**mical **S**peciation and **TRA**nsport models) is a computer program for modelling (geo)chemical speciation and mass transport processes, similar to programs such as PHREEQC and MINTEQ. An overview of the structure of LeachXS is presented in Figure 4.2.

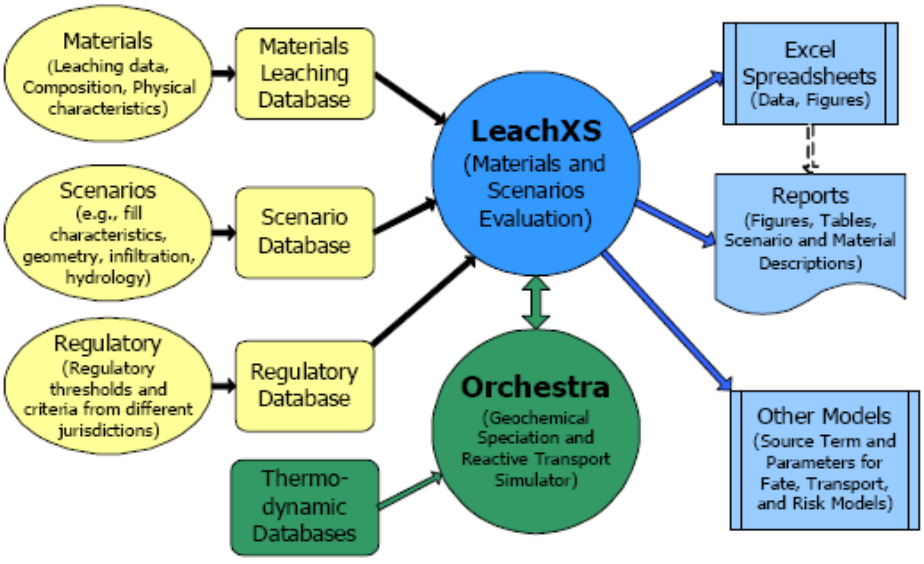

Figure 4.2 Overview of the structure of the LeachXS framework

The modelling study involves modelling of the monolithic leaching test for S/S APC residues as well as a combined alkaline/acid leaching test for raw (untreated) APC residues:

- The monolithic leaching test forms the bulk of the modelling study. Monolithic leaching data obtained from the present study were incorporated in the LeachXS database. Modelling of the monolithic leaching test using LeachXS requires utilisation of pH dependent release data, which would provide an insight to the solubility controlling minerals in S/S APC residues and assist with an improved initial material description (or model definition). Due to the fact that a pH-dependence leaching test was not conducted for the S/S products however, release data for S/S MSWI fly ash included in the LeachXS database were used as a surrogate. The aim of modelling the monolithic leaching test is to contribute to an improved understanding of the parameters affecting leaching from S/S APC residues.
- pH dependence release data for the SELCHP APC residues have been previously obtained by Rouchotas (2001) who used a combined alkaline/acid leaching procedure. The data were entered in the LeachXS database and were modelled in order to determine solubility-controlling minerals and associated release of elements of concern over varying pH conditions. This approach aims to evaluate the potential for extraction of salts and metals from APC residues prior to S/S.

5. EXPERIMENTAL RESULTS

5.1 Characterization of APC residues

Characterisation of APC residues involved identification of the major crystalline phases via XRD, as well as chemical composition and leaching characteristics. Chemical composition data were provided by SELCHP, the producer of the APC residues investigated in this study, and selected data are presented in Table 5.1. The full suite of characterisation data from SELCHP are presented in Appendix I. Additional data were obtained from the Water Research Centre (WRc), which provided ranges for each element based on the composition of various residues (Table 5.2) and were used to validate the data provided by SELCHP. Data in bold in both tables indicate problematic elements based on UK WAC for hazardous waste landfills.

5.1.1 Crystalline Phases

The major Ca containing phases identified through XRD were calcium chloride hydroxide (CaClOH), $Ca(OH)_2$ and $CaCO_3$. Furthermore, soluble salts such as KCl and NaCl were also present as major phases.

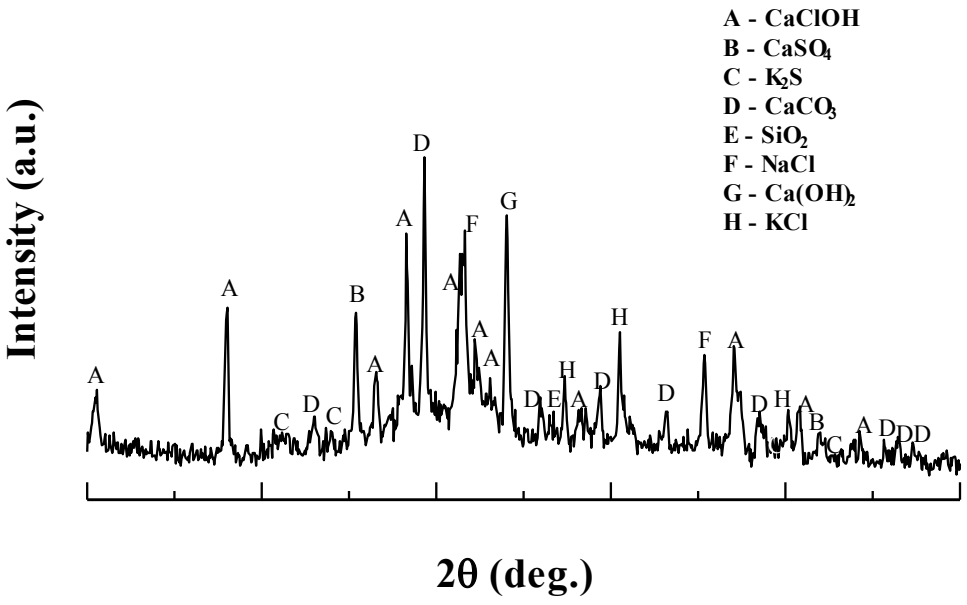

Figure 5.1 XRD data for as-received APC residues

Table 5.1 Total elemental concentrations and granular leaching data provided by SELCHP. All concentrations are in mg/kg. Leachability in water at L/S 2-10 cumulative was determined according to EN123457-3.

	Total Concentrations	**Potential Availability for Leaching**	**Leachability in water at L/S 2-10 cumulative**
Al	14000	9.89	0.65
As	9.1	1.61	0.22
Ba	340	130	33.35
Ca	290000	269575	68936
Cd	110	101.1	0.006
Co	14	1.0	0.017
Cr (total)	70	14.14	0.2
Cu	410	98.09	1.04
Fe	3200	25.83	2.28
K	23000	23677	19104
Mg	4100	1845	4
Mn	340	69.39	<0.16
Na	20000	20807	18861
Ni	23	6.41	0.17
P	4100	51.25	<1
Pb	**2800**	**72.98**	**686**
Si	510	15067	135
Sn	310	10.25	<0.002
Zn[2]	**7200**	**4069**	**36.8**
		Water extractable ions	
Br	2020	1055	1656
Cl	**n/a**	**165025**	**77275**
SO_4	11200	61192	3285
CO_3	21300	13120	<985

5.1.2 Chemical Composition and Leaching data

The mineral and elemental composition data indicate that APC residues contain a high level of soluble salts. The limit values for compliance leach testing using this procedure are shown in Table 5.1. It can be observed that the concentrations of Pb and Zn leaching from the APC residues are greater than the WAC limits for inert waste landfill and those for Pb are higher than the limits for hazardous waste landfills. The total amount of chloride present is typically around 16% and the leachable chloride of 140,000 - 170,000 $mgkg^{-1}$ is much greater than the WAC limits.

[2] Although results for Zn do not exceed UK granular WAC for hazardous waste landfills, it was highlighted in this study as an element of concern based on its high concentration compared to other heavy metals. This in turn warrants investigation as part of the monolithic leaching test.

Table 5.2 Granular waste UK WAC limits and APC residue composition data and range of concentrations typically leached using the L/S=10 EU compliance leaching test for granular wastes BS EN 12457-3. Units in mg kg-1 unless specified. (Environment Agency, 2006; Resource Recovery Forum, 2004)

APC Composition Data	Aqua regia total metals/water soluble ions	Leachable metals/ions at L/S10	WAC Limits		
			Inert Waste Landfill	Non-reactive waste at non hazardous waste landfill	Hazardous Waste Landfill
Total organic carbon (w/w %)	1 – 2.5	130 mg/kg DOC as C	3%	5%	6% *
LOI (%)	1.5 – 3.0	n/d			10% *
free lime %w/w CaO	15 - 20	n/d			
pH	12.0-12.6	11.6-12.8		> 6	
Al	10000-24000	<5			
As	10-210	<0.0005 – 4	0.5	2	25
Ba	70-400	10 – 45	20	100	300
Ca	250000-300000	50000 - 90000			
Cd	100-260	<0.5	0.04	1	5
Co	9-18	<0.05 - 0.15			
Cr	12-200	0.5 - 2.5	0.5	10	70
Cu	350-920	1.3 - 3	2	50	100
Fe	3000-7200	0.5 - 2.5			
Hg	<1-34	0.04 - 0.5	0.01	0.2	2
K	9000-24000	16000 - 22000			
Mg	4000-6000	0.3 - 1.5			
Mn	350-560	0.01 - 0.25			
Mo	2-16	<1 - 4	0.5	10	30
Na	13500-22500	11000 - 18000			
Ni	**15-45**	**0.2 - 45**	**0.4**	**10**	**40**
P	1500-3000	<5			
Pb	**2500-5500**	**300 - 700**	**0.5**	**10**	**50**
Sb	200-500	<0.0001 - 0.2	0.06	0.7	5
Se	0.1-6	<0.0005 - 9	0.1	0.5	7
Sn	200-800	<4			
Ti	900-4000	<0.9			
Tl	0.5-0.8	<0.06			
V	<30	0.09 - 0.6			
Zn	4000-18500	40-85	4	50	200
Water extractions					
Br	1000-2000	900 - 1700			
F	100-1500	1 - 45	10	150	500
Cl	**130000-220000**	**140000 - 170000**	**800**	**15,000**	**25,000**
water soluble SO_4 #	8000-38000	7000 - 12000	1000	20,000	50,000
CO_3 as $CaCO_3$	10000 - 45000	1500 - 8500			
water soluble alkalinity as $CaCO_3$	-	23000 - 32000			
TDS +			4,000	60,000	100,000
*Trace Organics (*ug/kg = ng/kg*)*					
Total phenols (9)	< 1-30	n/d			
Total PCBs (7)	<=20	n/d	1		
Total PAHs (16)	70-300	n/d	100		
PCDD/DF (ITEQ)	0.5 – 2.6	n/d			

* Either TOC or LOI must be used for hazardous wastes

\+ The values for TDS can be used instead of the values for Cl and SO_4

\# If an inert waste does not meet the SO_4 L/S 10 limit, alternative limit values of 1500 mg l^{-1} SO_4 at C_2 (initial eluate from the percolation test (prCEN/TS 14405:2003)) and 6000 mgkg^{-1} SO_4 at L/S10 (either from percolation test or batch test BS EN 12457 -3), can be used to demonstrate compliance with the acceptance criteria for inert wastes

5.2 Isothermal Conduction Calorimetry (Heat of Hydration)

Figure 5.2 shows the results for high CEM I/low APC residue additions (0, 10 and 30 wt % of total dry mass) whereas Figure 5.3 shows the effect on the heat of hydration for low CEM I/high APC residue addition (50, 70 and 100 wt.% of total dry mass) samples. Table 5.2 gives quantitative data from the conduction calorimetry experiments.

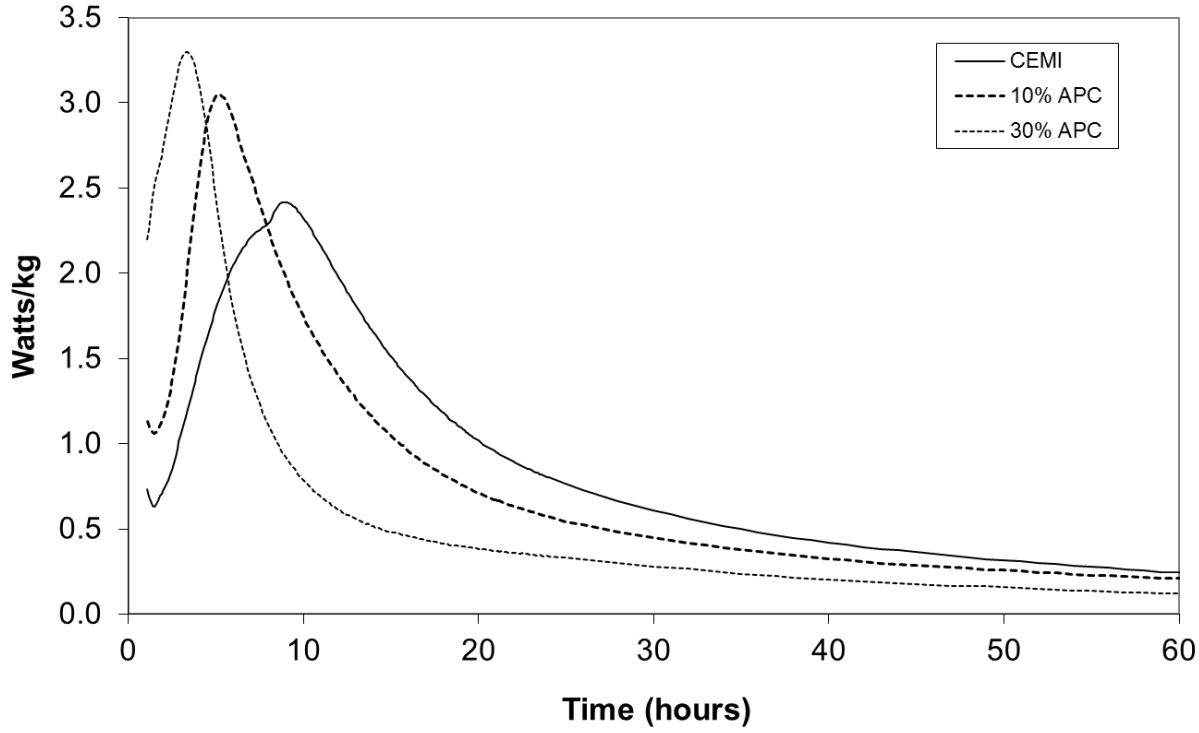

Figure 5.2 Heat evolution during hydration of high CEM I/low APC residue mixes

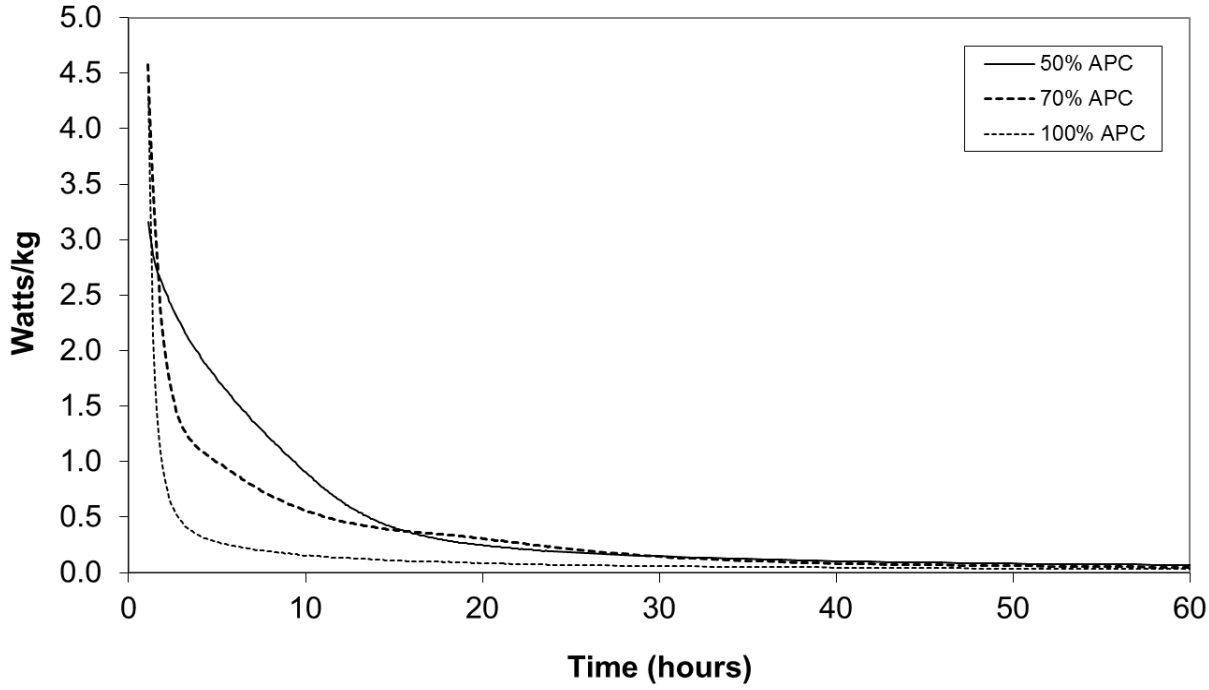

Figure 5.3 Heat evolution during hydration of low CEM I/high APC residue mixes

For APC residue additions up to 30 wt %, the main CEM I hydration peak occurs earlier than for 100% CEM I and the maximum rate of heat evolution increases. However, the total energy evolved is reduced with increasing APC residue addition. The total predicted heat evolution calculated based on the amounts of APC residues and CEM I in each mix, is also greater than actually evolved, indicating retardation of cement hydration. The hydration curves for samples containing 50%, 70% and 100% APC residues show no peak associated with CEM I hydration and the total heat evolved is much lower than for 100% CEM I samples.

Conduction calorimetry demonstrates that APC residues have a significant effect on CEMI hydration. A 10% APC residue addition to CEMI caused the main CEMI hydration peak to occur after 5.2 hours compared to 8.9 hours, while the total heat evolved during the 98 hour monitoring period was reduced. This level of APC residue addition is equivalent to the addition of ~ 2.4 wt % Cl ion to the CEMI and this is in the range of Cl ion additions used to accelerate CEMI hydration (1.0 % - 3.0 wt %) (Hewlett, 1998). Similar observations apply to samples prepared with 30 wt % CEMI additions.

Table 5.3 Conduction calorimetry data for CEMI/APC mixes.

Sample (w/s = 0.5)	Max. rate of heat evolution (W/kg)	Time of max. rate of heat evolution (hours)	Total heat evolved during 98 hour test (kJ/kg)	Total heat expected* (kJ/kg)
CEMI	2.42	8.9	205.4	N/A
10% APC	3.05	5.2	186.2	189.6
30% APC	3.30	3.3	132.5	157.8
50% APC	4.56	0.6	103.5	126.1
70% APC	8.05	0.6	85.5	94.0
100% APC	13.69	0.6	46.7	N/A

* Expected heat was calculated based on the heat evolved from the 100% APC and CEMI mixes and the relative amounts of each component in the different mixes.

The main CEMI hydration peak was no longer observed in S/S mixes containing low CEMI/high APC residue, although there was significant heat evolved during at least the initial 10 hours after mixing. There is also no evidence of hydration reactions occurring for the 100% APC residue samples and the early heat evolved can be attributed to the exothermic reaction of free lime with water.

5.3 Physical Properties of S/S products

This section presents results on the physical properties of the S/S products, namely setting time and consistence, porosity, bulk density, water content and unconfined compressive strength. Results were compared against the performance thresholds previously presented in Table 4.2.

5.3.1 Setting Time and Consistence

Setting time and consistence results for CEM I and GGBS mixes are presented in Figures 5.4a-d and 5.5a-c respectively and raw raw data are presented in Appendix VII. Both parameters are highly correlated with water addition. Correlation coefficients (r^2) for a fitted exponential curve ranged between 0.97-0.99 for consistence, 0.88-0.97 for initial setting time and 0.94-0.99 for final setting time for CEM I mixes. Similar values were obtained for GGBS mixes ranging from 0.76-0.98 for consistence, 0.88-0.99 for initial setting time and 0.90-0.99 for final setting time. Achievement of a target consistence of 175 ± 10 mm was desired, to provide a mix that was sufficiently flowable to allow compaction. However, the water demand of the APC residue was high, and this target could not easily be achieved for the 0% CEM I mixes, even with high water additions. The consistence criterion could be satisfied for

CEM I and GGBS-containing mixes, but the water additions are higher than typical water/solids ratios used for concrete. Increasing water addition could improve consistence but it could affect other properties such as setting time, compressive strength and porosity. The effect of water addition on other parameters is presented in sections to follow. Increasing the amount of APC residues in the mix resulted in a decrease in consistence values for the same water addition. It is noted that a 50 wt.% GGBS sample at a w/s ratio of 0.6 did not set in 24 hours.

The hygroscopic nature of soluble salts present combined with the fineness of APC residues means that high levels of water are required to obtain workable mixes containing high APC residue additions. A hygroscopic substance is one that readily attracts water from its surrounding environment through either absorption or adsorption. The extent to which a particular material or compound is affected by ambient moisture may be considered its coefficient of hygroscopic expansion (CHE) or coefficient of hygroscopic contraction (CHC), the difference between the two terms being a difference in sign convention and a difference in point of view as to whether the difference in moisture leads to contraction or expansion. For example calcium chloride is so hygroscopic that it eventually dissolves in the water it absorbs: this property is called deliquescence.

Deliquescent materials are materials (mostly salts), which have a strong affinity for moisture and will readily attract large amounts of water from the atmosphere if exposed to it and eventually form a liquid solution. In order for deliquescence to occur the vapour pressure of the ambient air must be greater than the vapour pressure in the saturated solution. When water vapour is collected by the pure solid compound, a mixture of the solid and liquid or an aqueous solution of the compound forms until the substance is dissolved and is in equilibrium with its environment; at this time the vapour pressure of water over the aqueous solution will equal the partial pressure of water in the atmosphere in contact with it. A crystalline salt aerosol particle will deliquesce in the atmosphere when the relative humidity surpasses a characteristic value, the so-called deliquescence point (IUPAC, 1997). Examples of deliquescent materials are NaCl and KCl, which are major constituents in APC residues. The assumption of the high water requirement of APC residues due to their hygroscopic nature was validated by curing specimens in a high humidity environment. Under curing conditions of 98% RH water beads appeared on the surface of the cube specimens. This effect was augmented for high APC residues and low water additions.

a. No Binder Addition

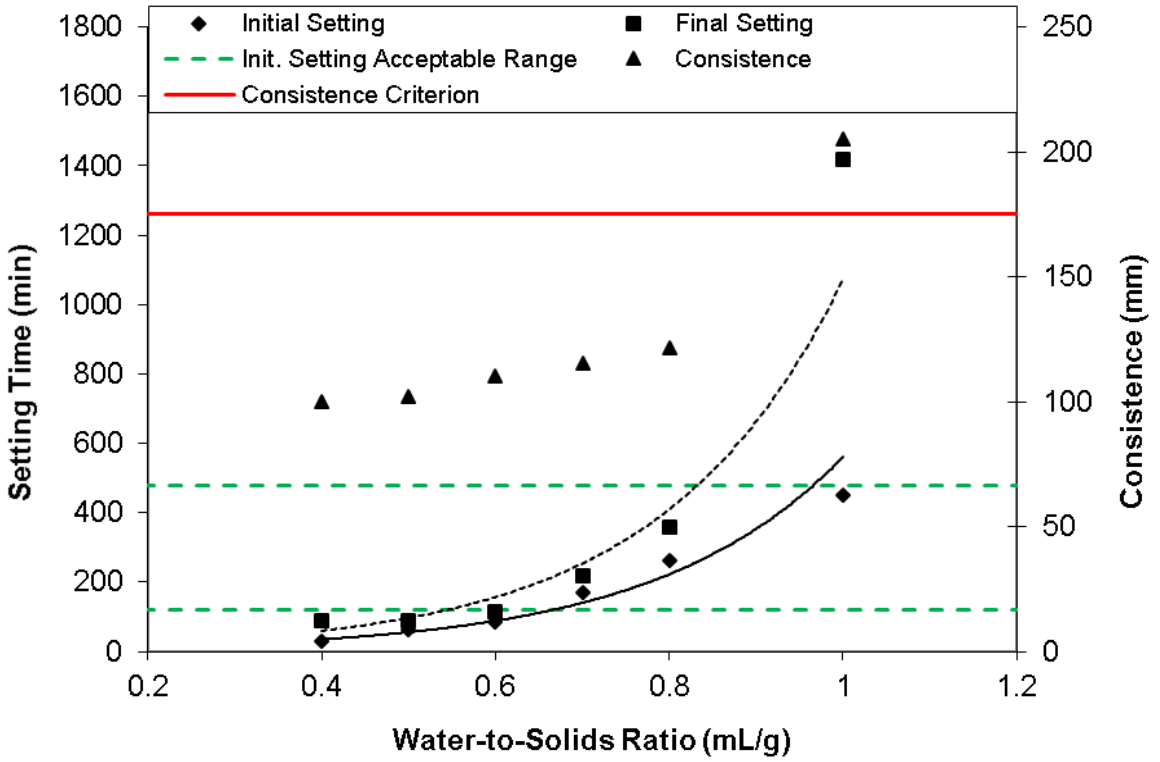

b. 10% CEM I Addition

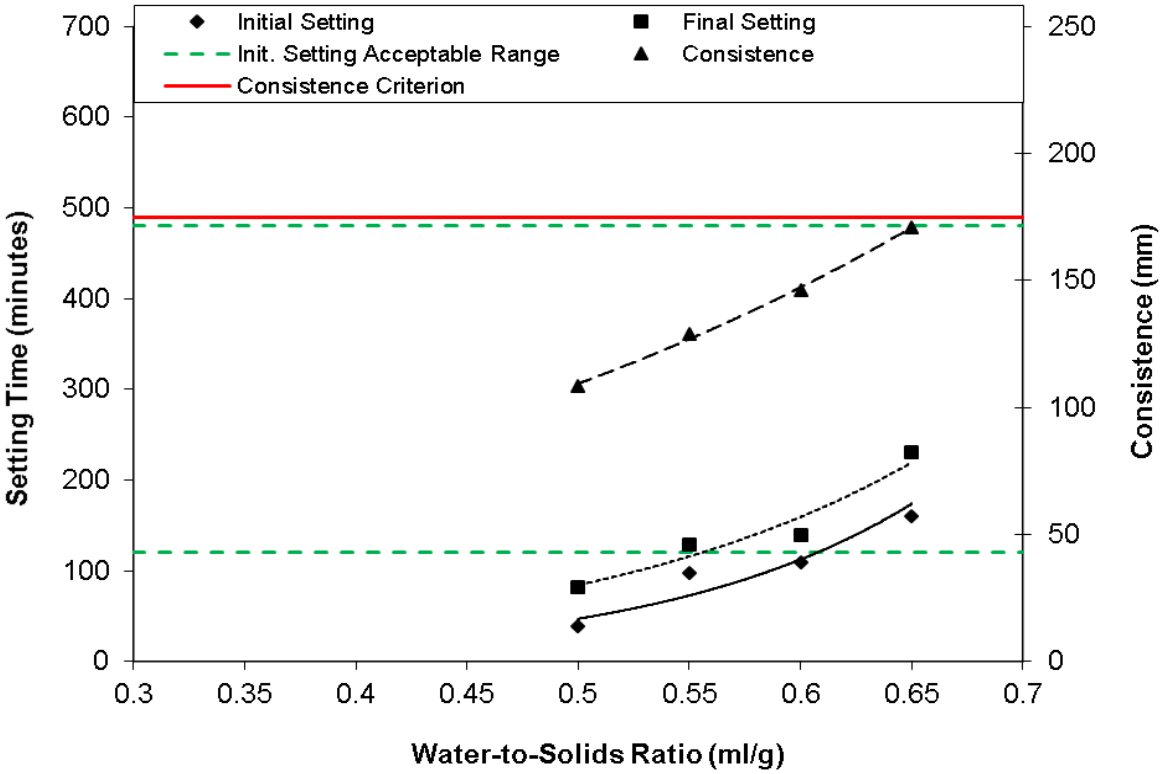

c. 20% CEM I Addition

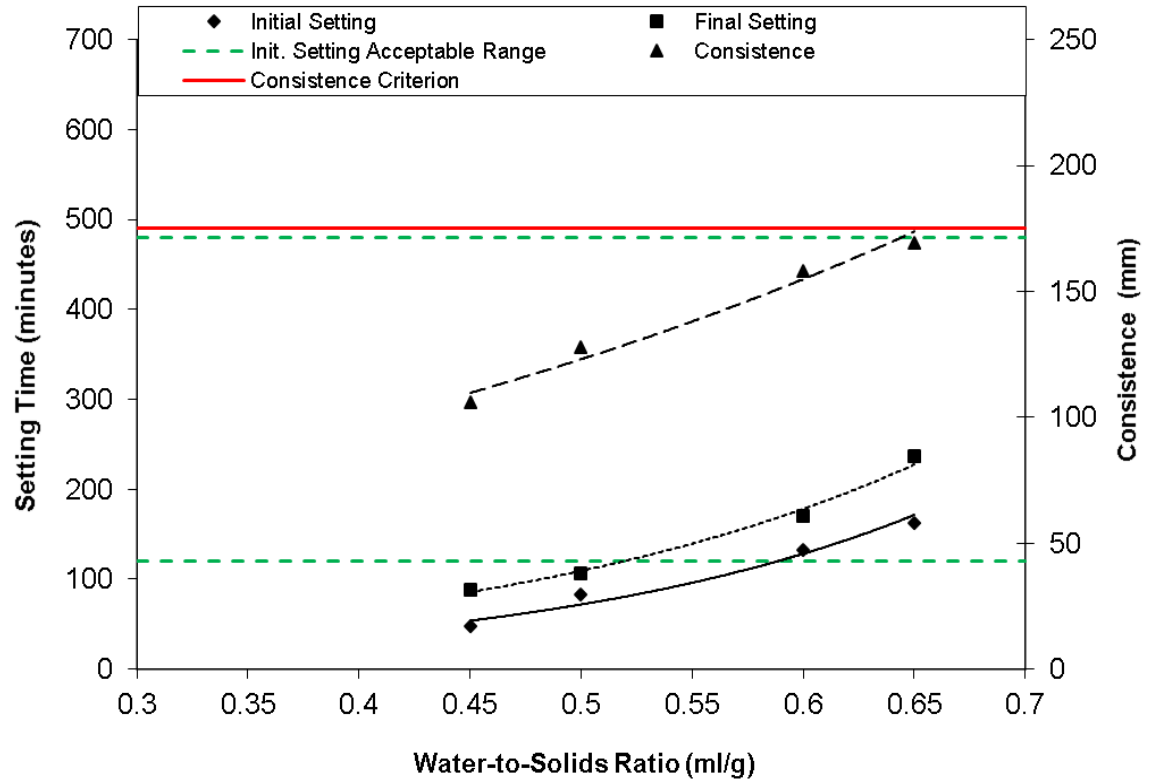

d. 50% CEM I Addition

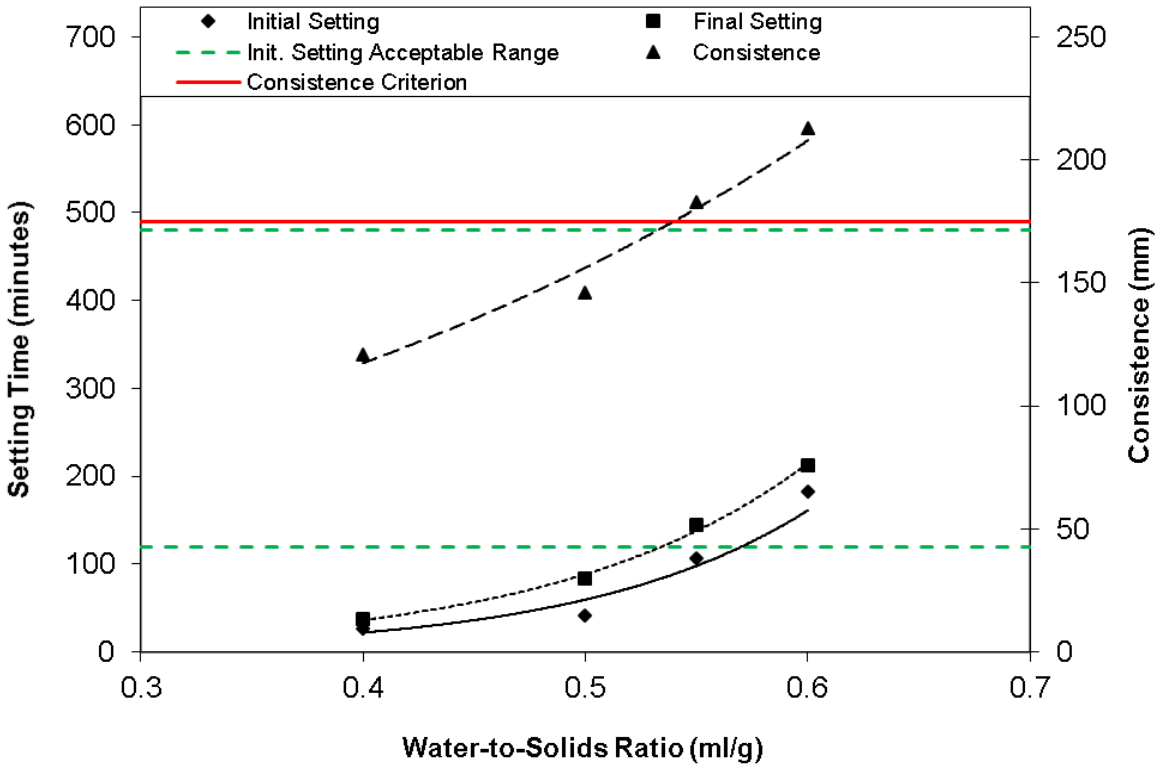

Figure 5.4 Setting time and consistence of CEM I S/S APC residues with: **a)** no binder addition, **b)** 10% CEM I addition, **c)** 20% CEM I addition and **d)** 50% CEM I addition

a. 10% GGBS Addition

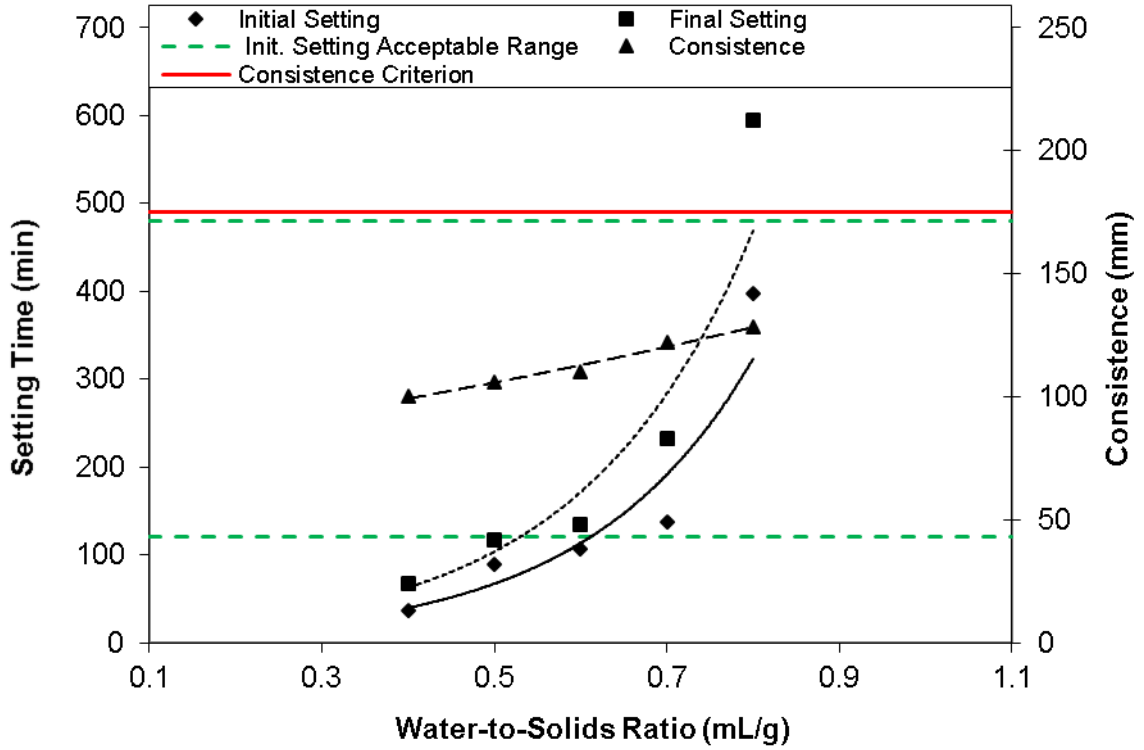

b. 20% GGBS Addition

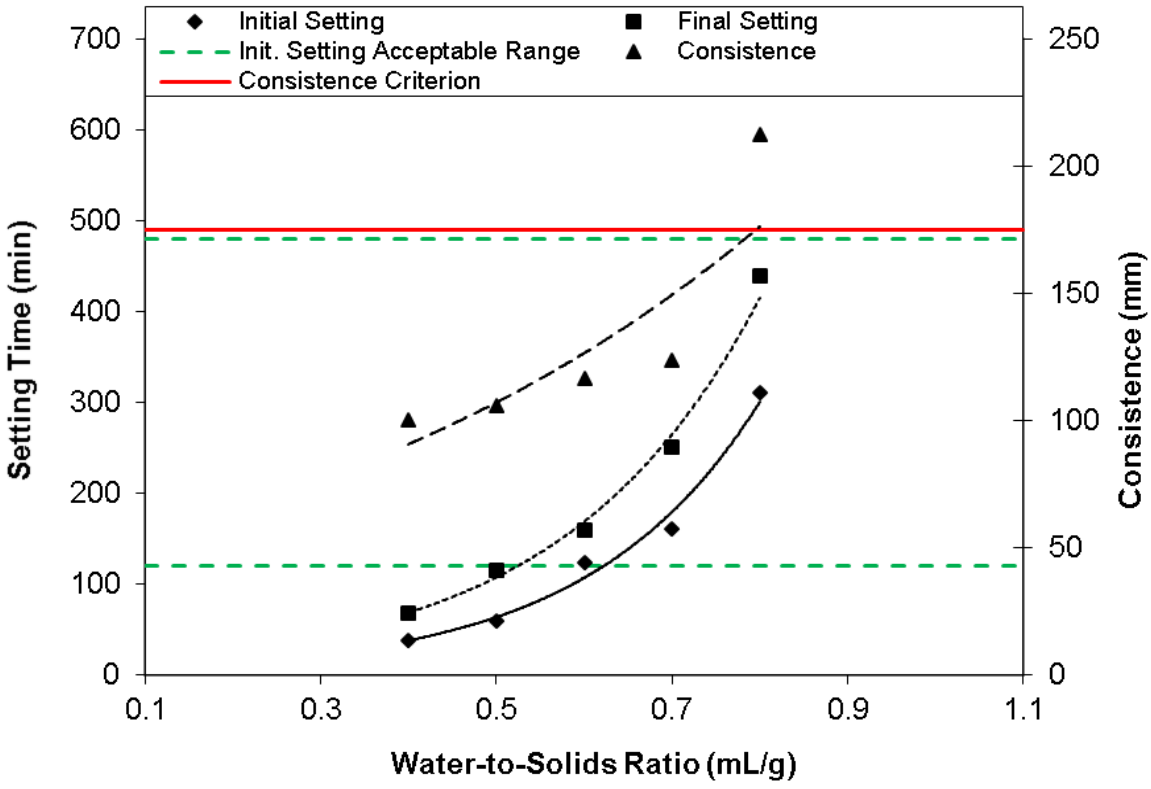

c. 50% GGBS Addition

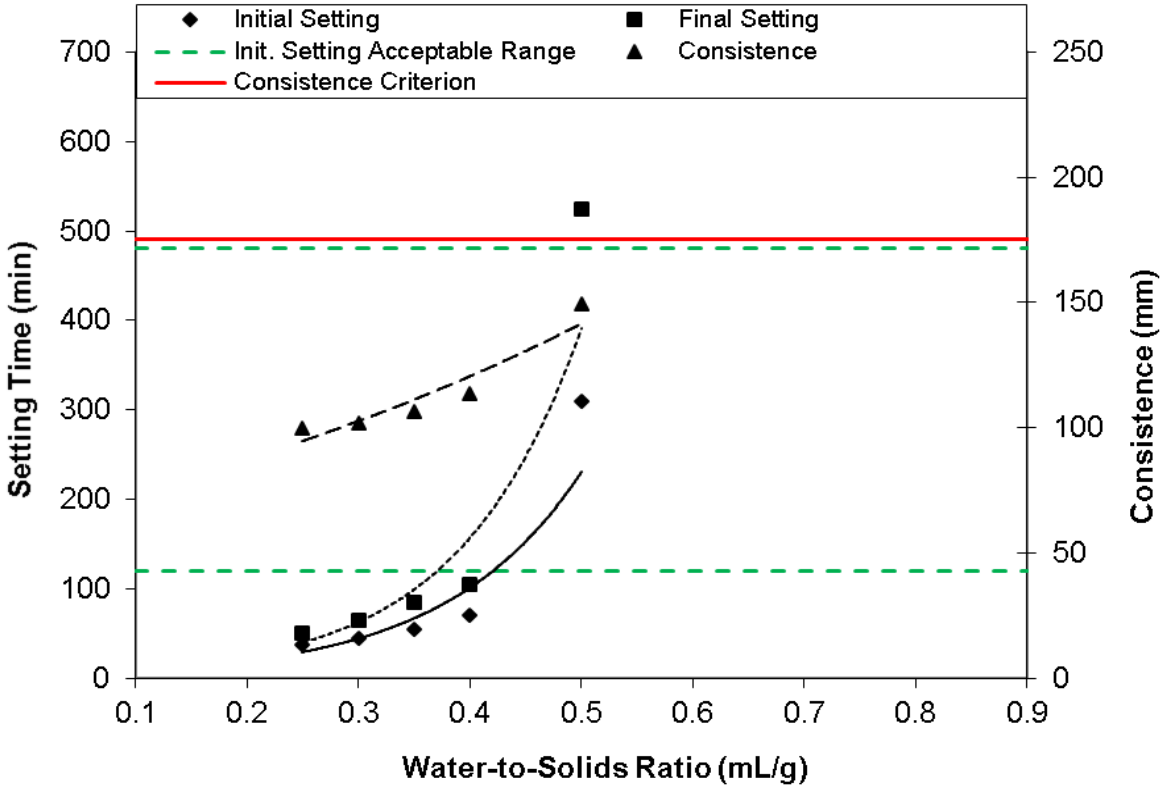

Figure 5.5 Setting time and consistence of GGBS S/S APC residues with: a) 10% GGBS addition, c) 20% GGBS addition and d) 50% GGBS addition

5.3.2 Porosity, Bulk Density, Water Content and Specific Gravity

Results for water content, bulk density and specific gravity of the S/S products cured for 7 and 28 days for CEM I and GGBS mixes are presented in Table 5.3. Calculated porosities are presented in Figures 5.6 a-b. Porosity increases linearly with increasing water addition for both CEM I and GGBS. Porosities ranged from ~30 volume % for 50 wt % CEM I at w/s = 0.4, to ~60 volume % for 0 wt % CEM I at w/s = 0.8 w/s. Porosities for GGBS mixes ranged from ~34 volume % for 50 wt.% GGBS, 0.35 w/s ratio samples to ~60 volume % for 10 wt.% GGBS, 0.8 w/s ratio samples. As expected, porosity and water addition are highly correlated with correlation coefficients ranging between 0.89 and 0.99 for CEM I mixes and 0.98, 0.99 and 0.99 for 10%, 20% and 50% GGBS mixes respectively.

In hardened cement paste the volume and continuity of the water-filled pores increases with increasing w/c ratio and decreases with the progress of hydration as a result of the deposition of hydration products in these pores. The remnants of water-filled pores present in cement

pastes which have not been filled with the hydration products form the capillary porosity. These types of pores play an important role in controlling the permeability and strength of hardened cement pastes (Glasser, 1993; Asavapisit, 1998). When the water-to-cement ratio is greater than the optimum required for complete hydration the amount of hydration products formed will be insufficient to fill the voids occupied by the mixing water (Asavapisit, 1998).

Table 5.4 Bulk density, water content and specific gravity results of S/S APC residues

Binder Addition	Water-to-solids (mL/g)	Bulk Density 7 days (g/cm^3)	Bulk Density 28 days (g/cm^3)	Water Content 7 days (%)	Water Content 28 days (%)	Specific Gravity 7 days	Specific Gravity 28 days
No Binder	0.40	1.56	1.66	33.0	31.5	2.15	2.09
	0.60	1.49	1.50	38.8	39.0	2.13	2.10
	0.70	1.49	1.48	41.9	41.0	2.13	2.05
	0.80	1.47	1.43	44.1	45.2	2.13	2.04
10% CEM I	0.50	1.68	1.64	30.2	31.1	2.07	2.08
	0.55	1.65	1.63	33.2	32.3	2.07	2.08
	0.60	1.62	1.62	34.2	33.5	2.06	2.08
	0.65	1.62	1.59	36.3	37.6	2.06	2.09
20% CEM I	0.45	1.74	1.75	27.1	27.5	2.08	2.08
	0.50	1.71	1.72	29.2	29.0	2.06	2.09
	0.60	1.64	1.62	33.4	34.0	2.08	2.07
	0.65	1.61	1.58	34.3	35.5	2.06	2.07
50% CEM I	0.40	1.85	1.84	21.3	20.9	2.15	2.10
	0.50	1.69	1.73	25.9	24.9	2.12	2.08
	0.55	1.72	1.71	28.3	26.6	2.12	2.07
	0.60	1.68	1.68	29.7	27.0	2.11	2.07
10% GGBS	0.50	1.60	1.55	32.6	38.6	2.15	2.05
	0.60	1.55	1.48	34.5	40.1	2.15	2.04
	0.70	1.45	1.49	41.8	40.9	2.13	2.01
	0.80	1.49	1.49	42.7	45.0	2.13	2.04
20% GGBS	0.40	1.68	1.59	29.8	31.4	2.17	2.05
	0.50	1.59	1.57	35.1	36.1	2.16	2.04
	0.60	1.54	1.52	36.2	38.7	2.13	2.04
	0.70	1.54	1.49	39.1	41.5	2.15	2.04
50% GGBS	0.35	1.80	1.74	23.7	22.7	2.24	2.03
	0.40	1.68	1.72	26.4	24.8	2.21	2.02
	0.50	1.66	1.67	29.3	27.9	2.17	2.02

a. Porosity CEM I S/S APC Residues

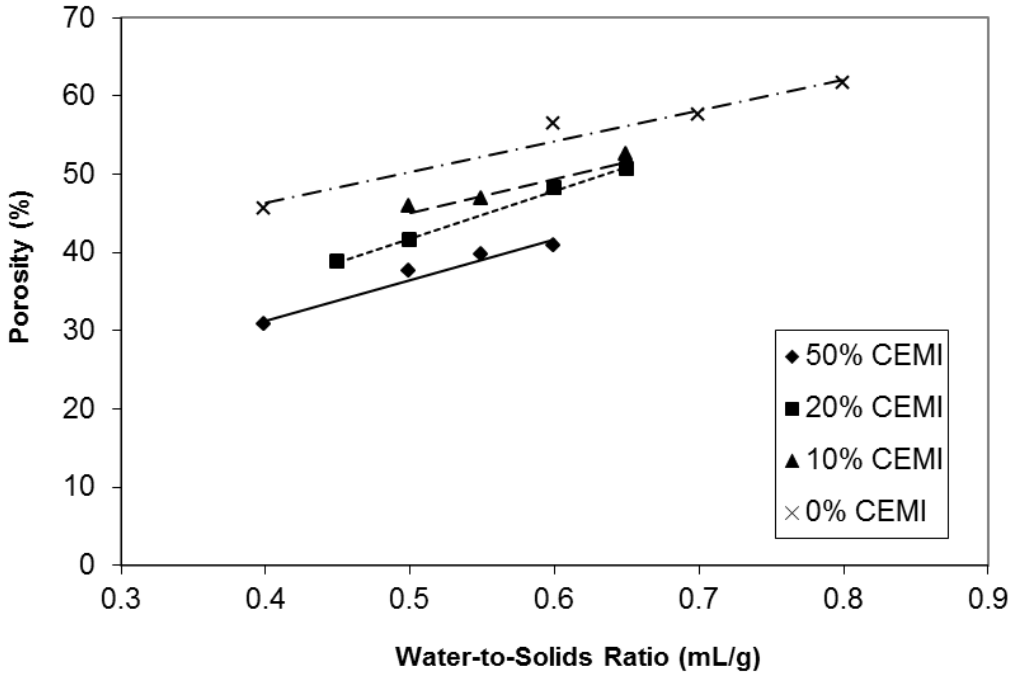

b. Porosity of GGBS S/S APC Residues

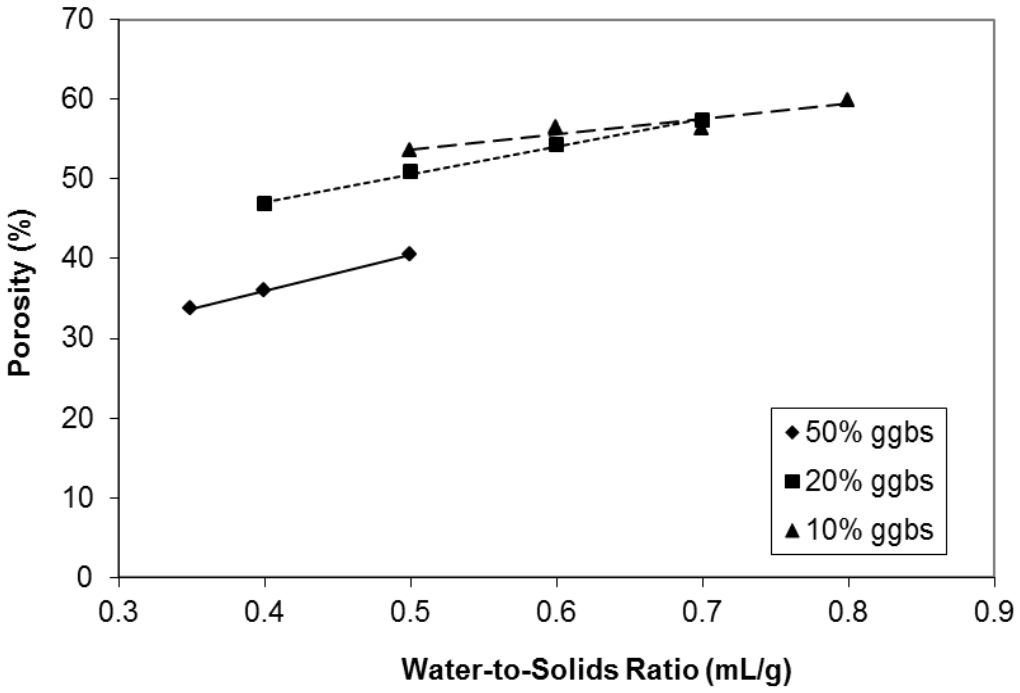

Figure 5.6 Porosity of a) CEM I and b) GGBS S/S APC residues

5.3.3 Unconfined Compressive Strength (UCS)

UCS data are presented in Figure 5.7 a-d and Figure 5.8 a-c for CEM I and GGBS mixes respectively. Values reported are the average of three replicates. Increasing water or reducing the binder content resulted in reduced compressive strengths. 50 wt. % CEM I mixes achieved average 28 day UCS values ranging from 8.0 to 17.0 MPa depending on the w/s. GGBS 28 day UCS values ranged from 10.0 to 21.0 MPa for the same binder addition. Maximum values were reduced to 10.4 at 20% and 5.5 MPa at 10% for CEM I mixes whereas maximum values for GGBS at the same binder additions were 1.7 and 0.4 MPa respectively. The significance of these results for CEM I mixes as indicators of hydration is questionable, considering that no hydration peak was observed for these mixes by calorimetry. On the other hand, the marked change in compressive strength between 7 and 28 days for 50 wt.% GGBS mixes indicates that hydration reactions start contributing to significant strength gain after the first week of curing. Solidified products without any binder addition (0% CEM I) exhibited very low strength, with a maximum 28 day UCS of ~1 MPa exhibited by the mix with w/s = 0.4 and no strength increase between 7 and 28 days curing. This observation, combined with the conduction calorimetry data and the low amounts of Si and Al present in the APC residues, indicate that pozzolanic reactions are not a major contributor to strength development when no binder is added.

The percentage reduction in UCS after water immersion increased with increasing APC residue and water addition and was ~80% for 10% CEM I samples with low water content (w/s of 0.50 or 0.55). Specimens with low CEM I content (0 and 10%) and high water additions (w/s of 0.60 or 0.65) disintegrated during 7 days water immersion. 10% and 20% GGBS samples could not be tested for wet UCS value because they suffered from poor structural integrity as dry UCS values indicate. The strength of S/S products containing 50% CEM I or GGBS did not decrease after immersion and the data actually show a marginal increase in UCS. The marginal strength increase after immersion for 50 wt.% binder mixes may be due to the inherent variability in compressive strength measurement rather than a real effect. Strengths after water immersion indicate that it is difficult for specimens with high APC residue addition to maintain structural integrity when exposed to water. Dissolution of salts present in APC residues severely affects matrix durability. The target of 1.0 MPa for dry UCS was satisfied by all CEM I-containing mixes at both 7 and 28 days. Mixes containing 10 and 20 wt.% GGBS exhibited very low compressive strengths both at 7 and 28 days and the

majority failed to meet the target of 1.0 MPa. The effect of certain heavy metal oxides as inhibitors of hydration reactions has been studied extensively (Asavapisit, 1998; Fernandez, 2001). Zinc hydroxy anions present at pH values between 12 and 13 may form metal-containing calcium phases, such as calcium hydroxyzincate [$CaZn_2(OH)_6.H_2O$], which coat CEM I grains and inhibit further hydration, resulting in products with poor mechanical properties.

The effect of heavy metals on and potential associated mineral phases on cement hydration has been described in more detail in Chapter 2 of the study. The theoretical framework will be placed in the context of this study in the following sections, taking into account monolithic leaching results as well as geochemical speciation and transport modelling.

a. No Binder Addition

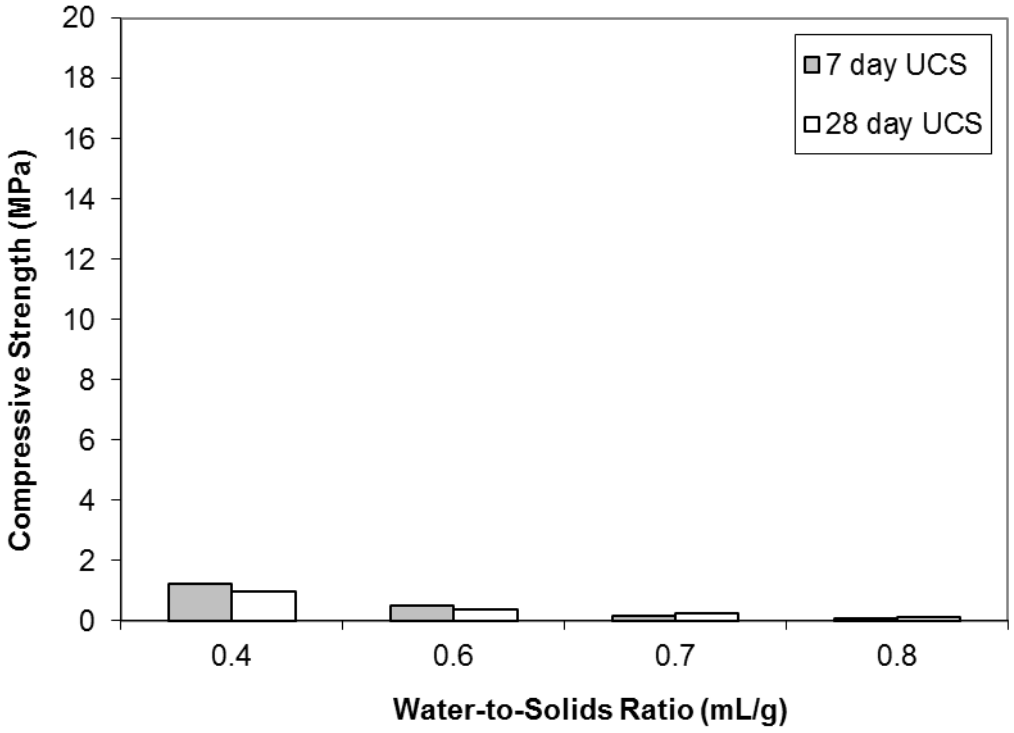

b. 10% CEM I Addition

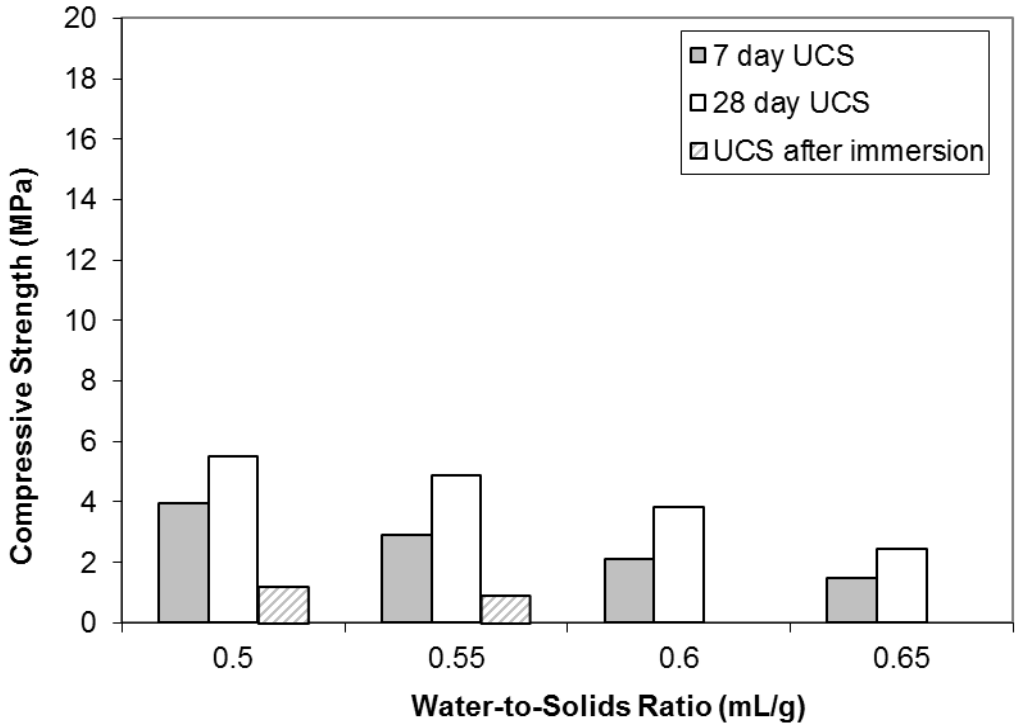

c. 20% CEM I Addition

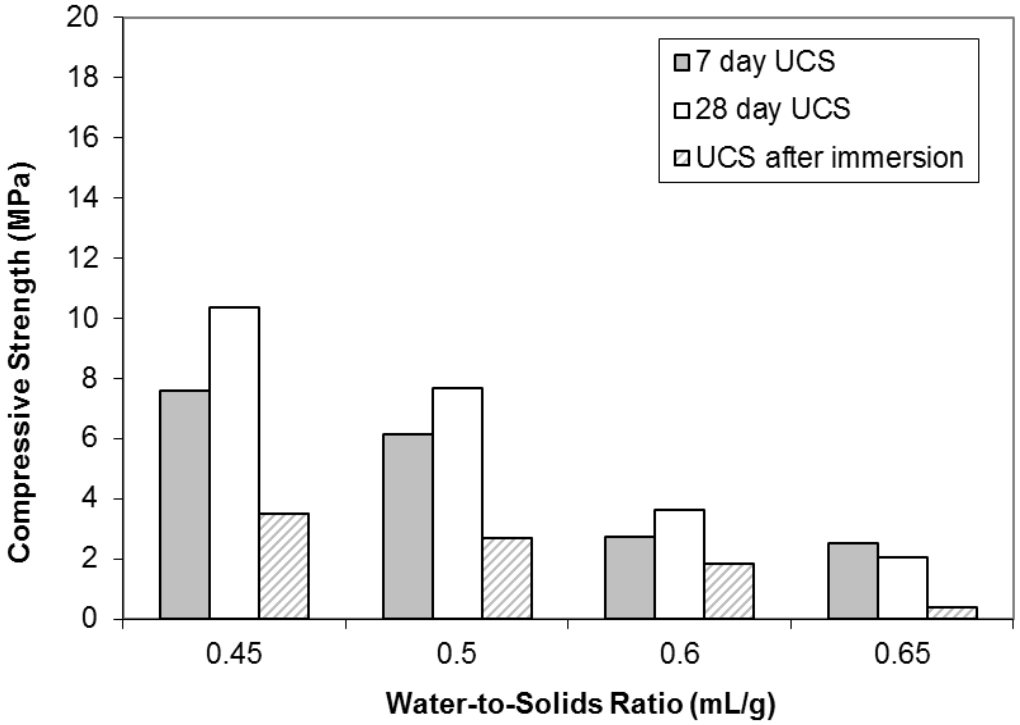

d. 50% CEM I Addition

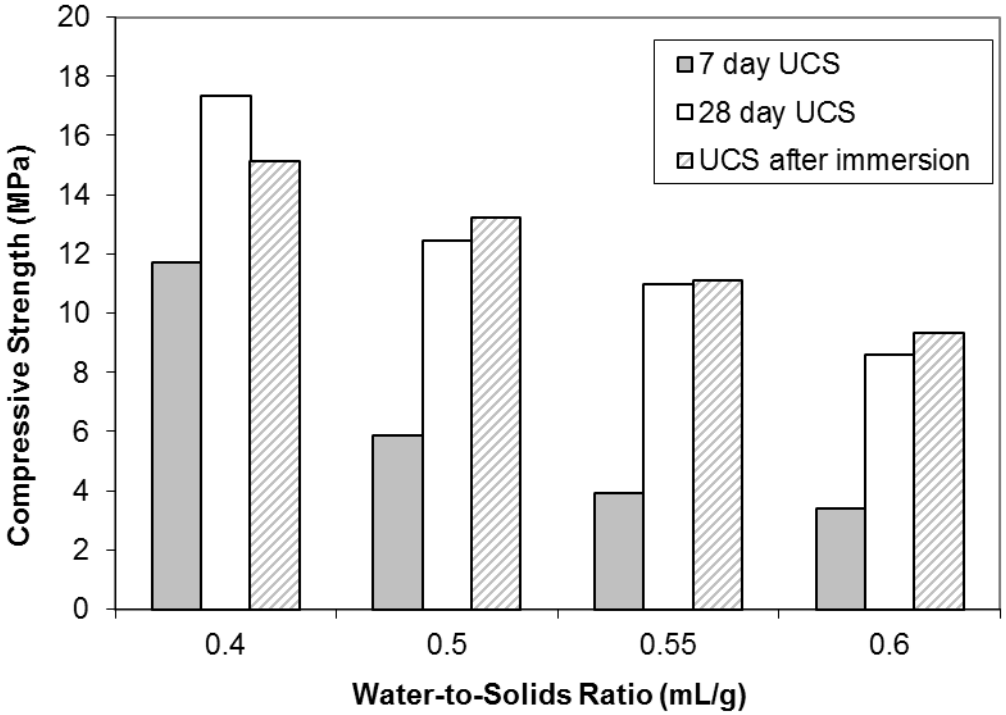

Figure 5.7 Compressive strength of CEM I S/S APC residues: **a)** No binder addition, **b)** 10% CEM I addition, **c)** 20% CEM I addition and **d)** 50% CEM I addition

a. 10% GGBS Addition

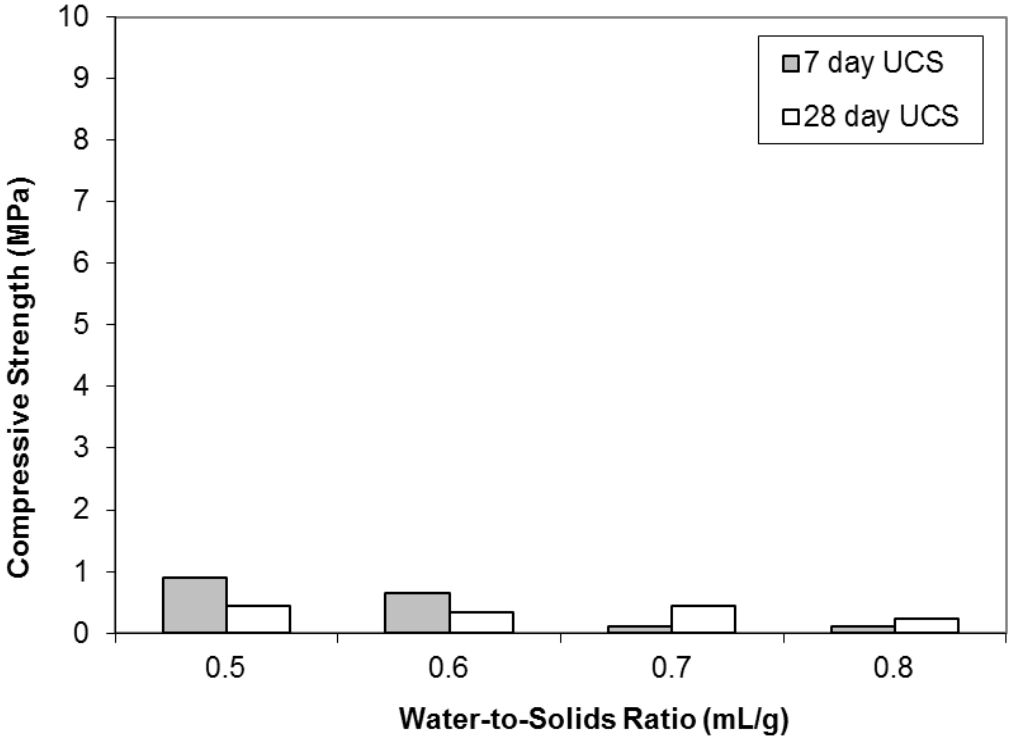

b. 20% GGBS Addition

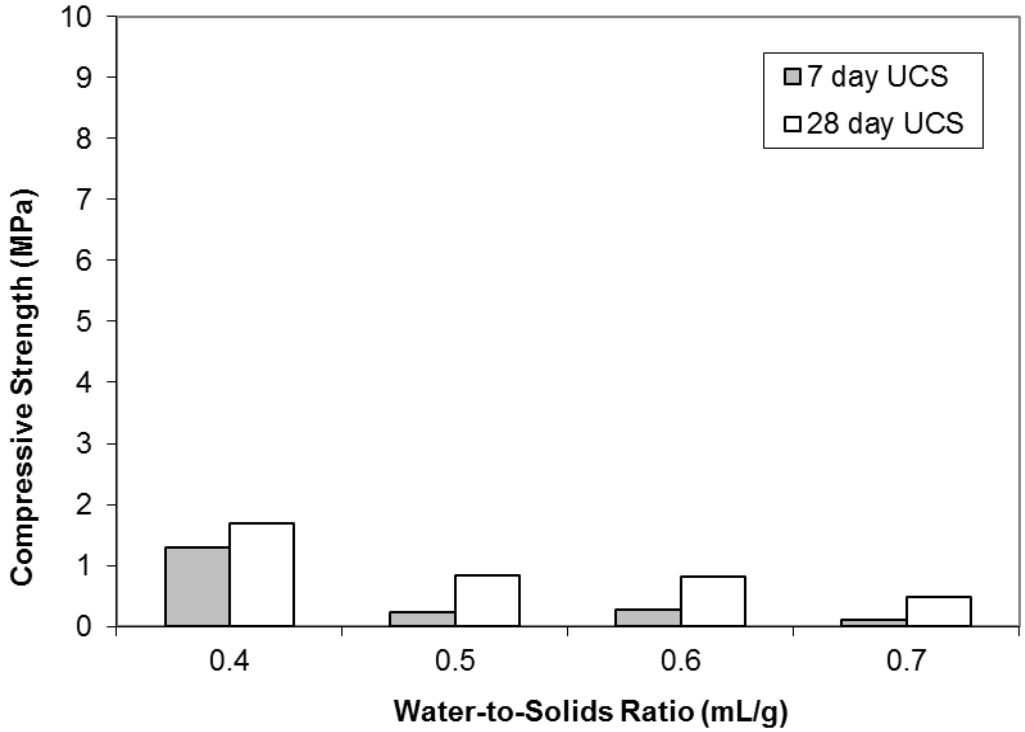

c. 50% GGBS Addition

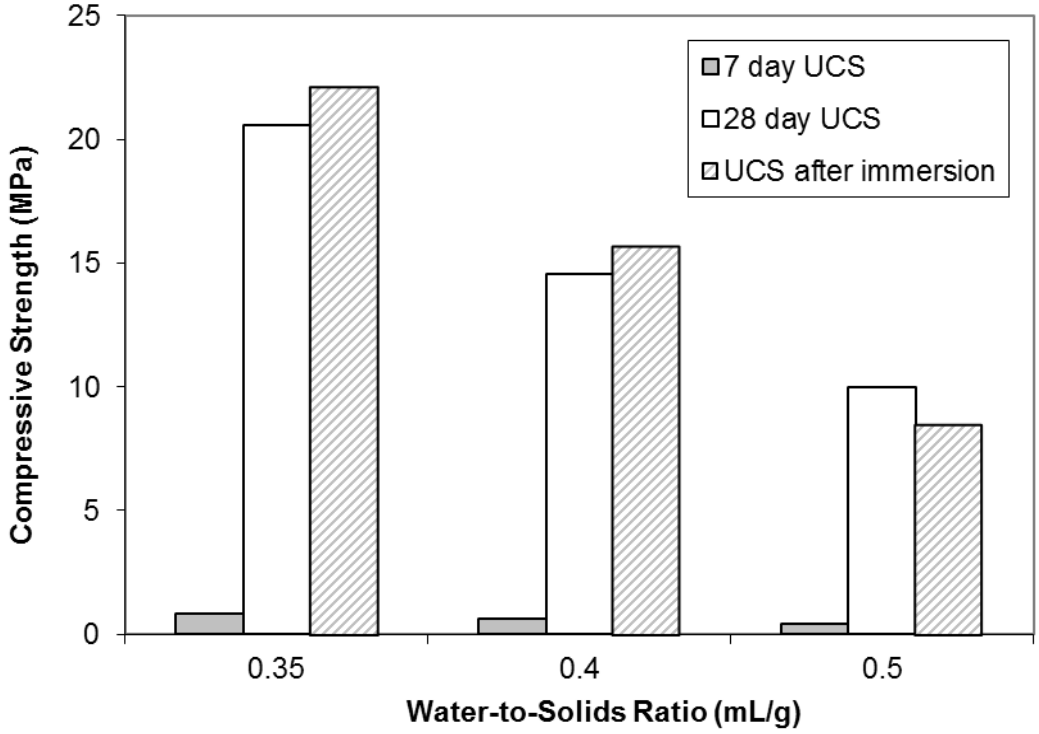

Figure 5.8 Compressive strength of GGBS S/S APC residues: **a)** 10% GGBS addition, **b)** 20% GGBS addition and **c)** 50% GGBS addition

5.4 Acid Neutralization Capacity and Granular Leaching

5.4.1 Acid Neutralisation Capacity (ANC)

Leachate pH results and chloride granular leaching data (conservative estimate of BS EN12457-3 – See Section 4.4.2) for CEM I and GGBS mixes are presented in Table 5.4. The leachate pH of all the products was high, typically ~ 11.5-12.6 and this is a range where many metal hydroxides such as zinc and lead exhibit relatively high solubility. Up to 2 meq/g of acid addition had no effect on the leachate pH of the 0% CEM I mixes. A greater effect is observed for the 10%, 20% and 50% CEM I mixes, which exhibited a higher pH initially, although pH reduced by less than 0.6 units. No difference in pH was observed between 1 meq/g and 2 meq/g acid additions for all CEM I mixes.

Table 5.5 ANC and chloride granular leaching data for S/S APC residues

Binder Addition	Liquid-to-solids (mL/g)	$[Cl^-]$ (mg/kg)	pH - 0 meq/g acid addition	pH - 1 meq/g acid addition	pH - 2 meq/g acid addition
No Binder	0.4	144,500	12.2	12.3	12.2
	0.6	143,500	12.1	12.2	12.2
	0.7	137,000	12.1	12.2	12.2
	0.8	137,000	12.1	12.2	12.2
10% CEM I	0.5	113,200	12.3	12.1	11.9
	0.55	121,200	12.3	12.1	12.0
	0.6	113,500	12.3	12.0	11.9
	0.65	119,000	12.3	12.1	11.9
20% CEM I	0.45	93,500	12.4	12.0	12.1
	0.5	93,700	12.3	12.1	12.0
	0.6	90,700	12.4	12.0	12.0
	0.65	88,000	12.4	12.1	12.1
50% CEM I	0.4	55,700	12.6	12.3	12.1
	0.5	47,500	12.6	12.2	12.2
	0.55	46,500	12.6	12.2	12.0
	0.6	52,700	12.6	12.1	12.1
10% GGBS	0.50	125,500	12.1	12.2	11.7
	0.60	128,000	12.1	12.2	11.7
	0.70	121,000	12.1	12.1	11.7
	0.80	123,000	12.1	12.0	11.6
20% GGBS	0.40	107,500	12.0	11.9	11.4
	0.50	106,000	11.9	11.6	11.2
	0.60	105,500	11.9	11.6	11.2
	0.70	106,500	11.9	11.6	11.1
50% GGBS	0.35	63,500	11.5	11.3	11.0
	0.40	65,500	11.5	11.3	11.0
	0.50	59,500	11.5	11.3	11.0

The leachate pH for 50% GGBS samples was reduced by ~ 0.2 and 0.5 units at 1 and 2meq/g acid additions respectively. The same effect was observed for 20% GGBS mixes with the leachate pH being lowered by ~ 0.3 and 0.7 units. Up to 1 meq/g of acid addition had no effect on the leachate pH of the 10% GGBS mixes, while 2 meq/g additions lowered the pH by ~ 0.4 units.

5.4.2 Granular Leaching – Results for Chloride

Leaching of the finely crushed solidified products in the ANC test is indicative of the level of chemical stabilisation and the data show that most of the chloride remained soluble. 0% CEM I mixes leached high levels of chloride, which are within the range of the amounts potentially available for leaching given in Table 5.1, demonstrating that curing of APC residues mixed with water has no significant effect on chloride solubility. Chloride amounts leached from all mixes were two (2) to approximately six (6) times greater than the UK WAC for granular waste for hazardous waste landfills (25,000 mg/kg – See Table 5.1).

5.5 Monolithic Leaching (Tank Test)

The results of the monolithic leaching (tank) test were analysed according to standard NEN7375:2004. Cumulative measured leaching was calculated according to the formula:

$$\varepsilon_n^* = \sum_{i=1}^{n} E_i \qquad \text{for } n = 1 \text{ to N} \qquad (5.1)$$

where ε_n^* is the measured cumulative leaching of a component for period n comprising fractions i=1 to n, in mg/m^2 of sample surface area, E_i is the measured leaching of the component in fraction i in mg/m^2 and N is the total number of leachant renewal periods. Results for measured cumulative leaching vs. time are presented on a double log scale. A similar presentation of results is also included in the draft prEN 15863 dynamic monolithic leaching test standard.

Leaching data are also presented as log-log plots of cumulative derived leaching (ε_n) vs. time. Cumulative derived leaching was calculated according to the formula:

$$\varepsilon_n = E_i \times \frac{\sqrt{t_i}}{\sqrt{t_i} - \sqrt{t_{i-1}}} \qquad (5.2)$$

where ε_n is the derived cumulative leaching for a component for period *n* comprising fraction i = 1 to *n* in mg/m^2, E_i is the measured leaching of the component in fraction *i*, in mg/m^2, t_i is the replenishment time of fraction *i* in s and t_{i-1} is the replenishment time of fraction *i*-1.

According to NEN 7375:2004, the gradient of leaching intervals on a log-log plot of cumulative derived leaching vs. time indicates the predominant leaching mechanism as shown in Table 5.5. Gradients below 0.35 indicate either surface wash-off or depletion. Gradients between 0.35 and 0.65 indicate diffusion-controlled release, whereas gradients greater than 0.65 indicate dissolution.

Table 5.6 Significance of slopes of different leaching increments according to NEN 7375:2004

Leaching Increment	**Slope**		
	≤ 0.35	**> 0.35 and ≤ 0.65**	**> 0.65**
2-7	Surface wash-off	Diffusion	Dissolution
5-8	Depletion	Diffusion	Dissolution
4-7	Depletion	Diffusion	Dissolution
3-6	Depletion	Diffusion	Dissolution
2-5	Depletion	Diffusion	Dissolution
1-4	Surface wash-off	Diffusion	Delayed diffusion or dissolution

It is noted that for the GGBS mix with 50 wt.% binder addition at a w/s ratio of 0.5 and for the third fraction of the tank leaching test in particular (2.25 days), loss occurred during transport of the sample to the laboratory. This prevented ICP-OES analysis for that fraction of the test and therefore experimental results were obtained only for the release of Cl. The metal release values for the third fraction for that particular mix were estimated using a 6th order polynomial regression. The order of the equation was chosen based on the resulting correlation coefficient (r^2); i.e the 6th order polynomial produced a correlation coefficient of one (r^2 = 1.0) and was considered appropriate for the estimation of the missing values.

The values for the different elements estimated via polynomial regression should be considered as approximations that serve the purpose of completing the data set for the tank leaching test. The regression is limited by the small number of values obtained from the monolithic leaching test (8 points) as well as the large concentration of small x (time) values, which may introduce a bias in the regression.[3] However, as the missing values are for an early leaching interval (i.e. small x value), the regression was expected to produce reasonable estimates. This was also verified by comparing the regression estimated values with the values for the same leaching interval for the other GGBS mixes with the same binder addition. It is noted that the results for the 50 wt.% mix are not presented in this section but are predominantly used for the modelling study.

Finally, the effectiveness of the S/S process was evaluated by comparing the cumulative measured leaching (Eq. 5.1) with the UK Waste Acceptance Criteria for monolithic waste (monWAC) for contaminants of concern as shown in Table 5.6. A full list of the parameters in the UK monWAC is provided in Appendix III.

Table 5.7 UK monWAC for contaminants of concern in APC residues

Parameter	**Stable non-reactive hazardous waste in non-hazardous landfill and non-hazardous waste in same cell**		**Hazardous Waste Landfill**	
	Cumulative limit values (mg/m^2)			
	Compliance*	**Characterisation****	**Compliance**	**Characterisation**
Lead(Pb)	1.5	6.0	5.0	20.0
Zinc (Zn)	7.5	30.0	25.0	100.0
Chloride (Cl^-)	2,500	10,000	5,000	20,000
Sulphate (SO_4^{2-})	2,500	10,000	5,000	20,000

* 4-day cumulative leaching
** 64-day cumulative leaching

[3] Five (5) of the sampling fractions of the tank test involve a contact time of less than 10 days whereas only three (3) fractions involve a greater contact time which is also not equally distributed

5.5.1 Interpretation of the Monolithic Leaching Test Resuls

Sections 5.5.2 to 5.5.9 provide the results from the monolitc leaching test for S/S APC residues in graphical format. Intrepretation of results is based on the following:

- Leaching results for each element include both the cumulative leaching calculated as per equation 5.1, as well as the cumulative derived leaching as per equation 5.2. Graphs on the left hand side of each figure present leaching results pertaining to cumulative leaching, whilst graphs on the right hand side pertain to cumulative derived leaching.
- Cumulative derived leaching versus time expressed on a log-log scale provides an indication of the dominant leaching mechanism according to NEN 7375:2004. The dominant release controlling mechanism can be determined by the slopes of the individual leaching intervals as described in Section 5.5, as well as visually based on Annex E of NEN 7375:2004. Tables with the slopes for each leaching interval for each element, as well as Annex E of NEN 7375:2004 are provided in Appendix IV.
- A line with a slope of 0.5 has been plotted as a dashed black line on the cumulative measured leaching vs. time plots according to the presentation included in Annex E of NEN 7375:2004. This provides an additional visual aid to identify diffusion-controlled leaching. Cumulative leaching curves with a slope of 0.5 indicate diffusion as the dominant mechanism controlling release of a given element.
- Where applicable (Pb, Zn, Cl and SO_4), UK monWAC limits for disposal in hazardous waste landfills are presented in the cumulative measured leaching graphs as a solid red lines.

5.5.2 pH Results

The pH values determined for the different fractions of the tank leaching test for the S/S products are presented in Figure 5.9. All CEM I mixes exhibited pH values ranging between 11.5 and 12.1, while GGBS mixes had lower pH values ranging between 10.7 and 11.2.

The leachate pH values remained above 11.5 for all leachate fractions from the monolithic leaching test for CEM I mixes. Lower pH values were exhibited by the GGBS mixes, and this can be attributed to the consumption of free lime present in the mix resulting from slag activation. The values obtained are similar to those for a pure $CaO\text{-}SiO_2\text{-}H_2O$ system where Na and K are present, according to data presented by Polettini et al (2001). The high pH values for CEM I mixes are conducive to the release of amphoteric metals such as Pb and Zn whose solubility is pH dependent. It is noteworthy that the pH generally increases with the length of the leaching interval.

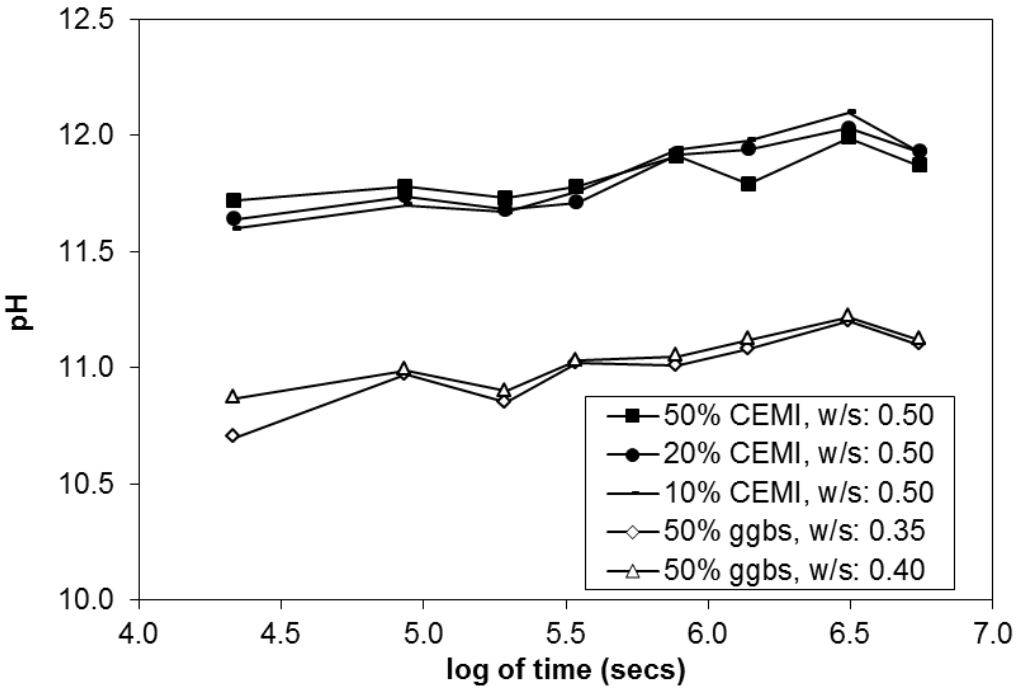

Figure 5.9 pH values for the different fractions of the tank leaching test

5.5.3 Calcium, Aluminium and Silicon

Cumulative measured and derived leaching for Ca, Al and Si is presented in Figure 5.10. These elements are expected to be building blocks for the mixes due to cementitious nature of the S/S specimens. As detailed in Chapter 2, leaching of calcium in particular, through the mechanism termed as decalcification can have a significant long-term effect on the structural integrity and porosity of the cementitious specimens.

a) Calcium

It is observed that high amounts of Ca are released from all mixes. GGBS mixes release lower amounts compared to CEM I mixes with the same binder addition which can be attributed to the consumption of free lime in APC residues for the activation of GGBS. It is noted that the inherent alkalinity in APC residues was used to activate the GGBS without the use of additional activators.

Comparing the curves for the different binder additions for CEM I mixes, it is observed that mixes with lower binder addition (i.e. 10 and 20 wt.% CEM I mixes) release higher amounts of Ca compared to the mixes with higher binder addition. Ca release for the different CEM I additions in increasing order is 50 wt.% < 20 wt.% < 10 wt.%. It is noted that Ca release from 10 and 20 wt.% CEM I mixes (at a w/s of 0.5) is similar at 844,000 and 884,000 mg/m^2 respectively. In contrast, release from the 50 wt.% mix was approximately 474,000 mg/m^2, which is approximately 54% and 56% lower compared to the 10 and 20 wt.% CEM I mixes respectively.

The slopes of the log-log plots for Ca indicate surface wash-off and depletion or a change in chemical form and release conditions for CEM I mixes. However, this does not necessarily imply that calcium is being depleted. Calcium loss may occur due to leaching of soluble Ca-containing compounds such as CaClOH. Once Ca derived from such compounds is removed, Ca leaching may continue from other sources such as $Ca(OH)_2$ and CSH at a much lower rate and based on solubility-control. Leaching of Ca from portlandite and CSH leading to decalcification may result in a degradation of the s/s matrix as discussed in Chapter 2. In contrast release of Ca from GGBS mixes appears to be controlled by diffusion.

The effect of water addition can be determined by examining release from mixes with the same binder but varying water content. The 64-day release from 50 wt.% CEM I mixes with

water addition varying between 0.4 and 0.6 ranged between 419,000 and 498,000 mg/m^2 with a mean of 469,753 mg/m^2 and a standard deviation of 35,137 mg/m^2. Ca release from these mixes increased with increasing water addition. The 64-day release from 20 wt.% CEM I mixes was higher and ranged between 583,000 and 908,000 mg/m^2 with a mean of 778,055 mg/m^2 and a standard deviation of 172,183 mg/m^2 but in this case release decreased with increasing water addition.

Ca release from 50 wt.% GGBS mixes with water addition varying between 0.35 and 0.5 ranged between 159,000 and 234,500 mg/m^2 with a mean of 209,000 mg/m^2 and a standard deviation of 42,930 mg/m^2. The 50 wt.% GGBS mixes at w/s of 0.35 and 0.4 exhibited similar releases of Ca of 234,500 and 233,000 mg/m^2 respectively. In contrast the 50 wt.% GGBS mix at a w/s of 0.5 exhibited a lower release of 163,000 mg/m^2.

b) Silicon

Release of Si was lower compared to Ca by 2-3 orders of magnitude depending on the mix characteristics. In contrast to Ca, release of Si was approximately five (5) times greater for GGBS mixes compared to CEM I mixes. Comparison of the release from CEM I mixes with varying binder addition, shows that mixes with lower binder addition (i.e. 10 and 20 wt.%) release lower amounts of Si compared to the mixes with higher binder addition. Si release for the different CEM I additions in increasing order is 10 wt.% < 20 wt.% < 50 wt.%. Release of Si from 50 wt.% CEM I mixes in particular was approximately one and a half (1.5) and two (2) times greater compared to 20 and 10 wt.% CEM I mixes respectively.

Examination of the log-log plots shows that depletion of Si is occurring from all mixes during the later stages of the tank test. As with Ca, this can be attributed to the release of Si from soluble Si-containing compounds in early stages of the test and release thereafter from less soluble compounds based on solubility control at a lower rate.

The 64-day release from 50 wt.% CEM I mixes with water addition varying between 0.4 and 0.6 ranged between 121 and 253 mg/m^2 with a mean of 160 mg/m^2 and a standard deviation of 63 mg/m^2. The 64-day release for 20 wt.% CEM I mixes was lower and ranged between 65 and 81 mg/m^2 with a mean of 73 mg/m^2 and a standard deviation of 8.0 mg/m^2. Si release from 50 wt.% GGBS mixes with water addition varying between 0.35 and 0.5 ranged

between 551 and 648 mg/m^2 with a mean of 608 mg/m^2 and a standard deviation of 50.3 mg/m^2.

c) Aluminium

Al release from GGBS mixes was approximately five (5) times greater compared to CEM I mixes. Comparing the curves for the different binder additions for CEM I mixes, it is observed that mixes with lower binder addition (i.e. 10 and 20 wt.% CEM I mixes) release lower amounts of Al compared to the mixes with higher binder addition. Al release for the different CEM I additions in increasing order is 10 wt.% < 20 wt.% < 50 wt.%. It is noted that Al release from 10 and 20 wt.% CEM I mixes (at a w/s of 0.5) is similar at 33 and 38 mg/m^2 respectively. In contrast, release from the 50 wt.% CEM I mix at the same water addition was approximately four (4) times greater at 129 mg/m^2.

Examination of the log-log plots shows that surface wash-off of Al is occurring for CEM I mixes whereas release from GGBS mixes is controlled by diffusion. It is also observed that higher amounts of Al are released from 50 wt.% CEM I mixes compared to mixes with lower binder addition, i.e. 20 and 10 wt.%. It is noted that for certain fractions of the tank test for CEM I mixes with 20 and 10 wt.% binder addition ICP-OES results were below the detection limit (10 μg/L). In this case the detection limit was used for the analysis.

64-day release from 50 wt.% CEM I mixes with water addition varying between 0.5 and 0.6 ranged between 92 and 323 mg/m^2 with a mean of 165 mg/m^2 and a standard deviation of 107 mg/m^2. The wide release range for the 50 wt.% CEM I mixes is due to a potential analytical error for the first leaching interval of the mix at a w/s of 0.4. In that case Al release was higher by an order of magnitude compared to the other 50wt.% mixes and therefore this data point may be an outlier. The 64-day release from 20 wt.% CEM I mixes was lower and ranged between 35 and 38 mg/m^2 with a mean of 36.5 mg/m^2 and a standard deviation of 1.5 mg/m^2. Al release from 50 wt.% GGBS mixes with water addition varying between 0.35 and 0.5 ranged between 639 and 783 mg/m^2 with a mean of 722 mg/m^2 and a standard deviation of 74 mg/m^2.

a) Ca Leaching

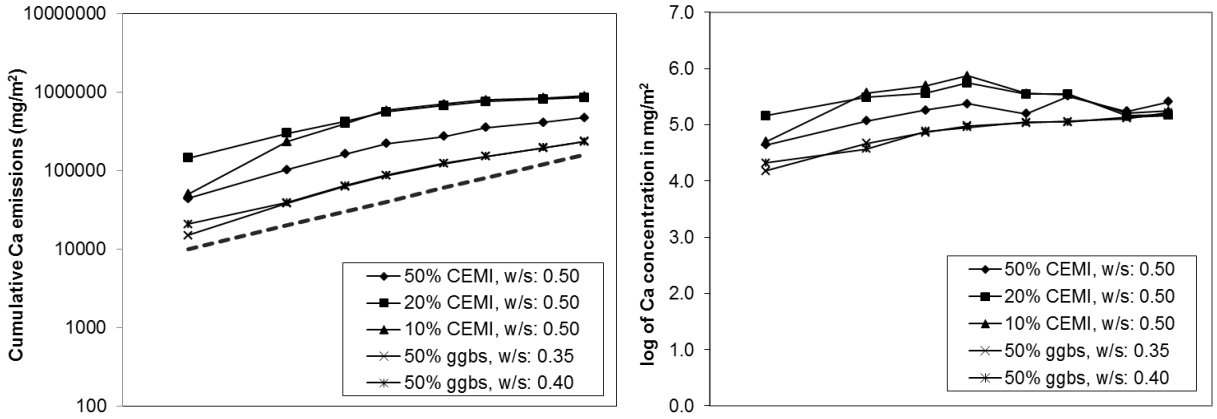

b) Si Leaching

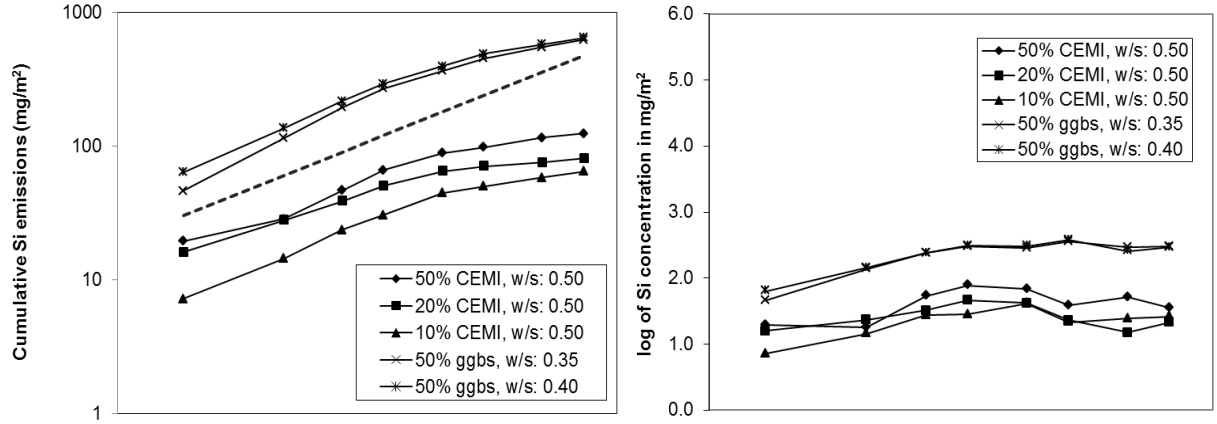

c) Al Leaching

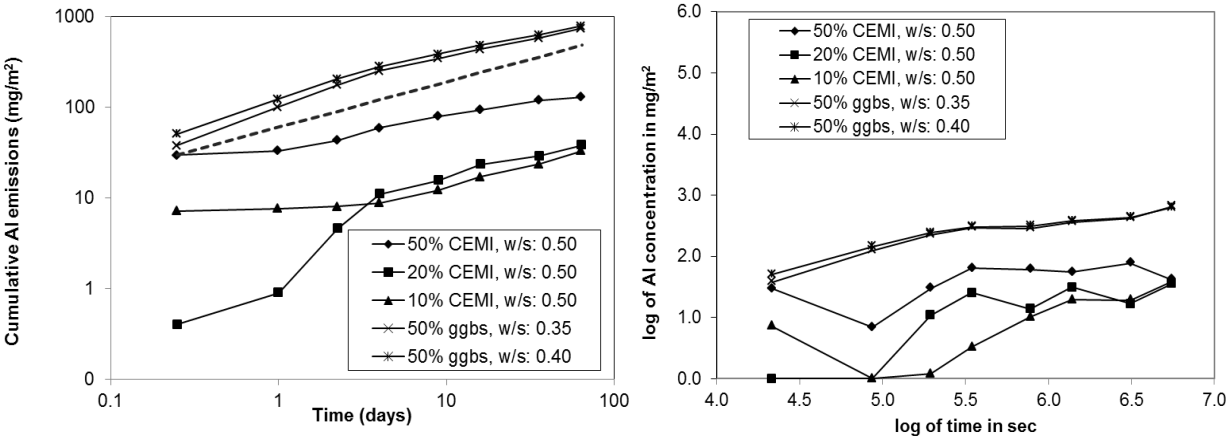

Figure 5.10 Cumulative measured and derived leaching for a) Ca, b) Si and c) Al

5.5.4 Alkali Metals (Na, K, Li)

a) Sodium (Na) and Potassium (K)

Cumulative measured and derived leaching for Na and K is presented in Figures 5.11a-b. It is observed that high amounts of Na and K are released from all S/S mixes. The high release and rapid loss of Na and K is associated with the presence of soluble salts in APC residues. As demonstrated in previous sections, NaCl and KCl salts are major constituents of APC residues. There are no requirements in the monWAC for leaching of Na and K and therefore a comparison with regulatory standards is not applicable.

Examination of the slopes of the log-log plots for cumulative derived leaching demonstrates that there is depletion of Na and K occurring at later leaching intervals for all mixes. In addition, for CEM I mixes at 50 and 10 wt.% binder addition dissolution is observed at the early leaching intervals. It is also interesting to note for these two mixes the lower release (by an order of magnitude compared to the remaining mixes) for both Na and K during the first interval of the test.

Release of Na and K from CEM I mixes was lower compared to GGBS mixes with the same binder addition. In particular, the 64-day release for Na from CEM I mixes with 50 wt.% binder addition at a w/s ratio of 0.5 was 125,000 mg/m^2 whereas release from the GGBS mix at the same binder and w/s ratio was 129,000 mg/m^2. However, this difference of approximately 3.2% is not considered practically significant taking also into account the potential analytical error. A more pronounced difference was observed for Na for the same binder addition but a w/s ratio of 0.4. Release from the CEM I mix in this case was 112,000 mg/m^2 whereas release from the GGBS mix was 136,000 mg/m^2, a percentage difference of approximately 21%.

In the case of Na, the 64-day release from 50 wt.% CEM I mixes with water addition varying between 0.4 and 0.6 ranged between 112,000 and 127,000 mg/m^2 with a mean of 121,500 mg/m^2 and a standard deviation of 7,003 mg/m^2. The 64-day release for 20 wt.% CEM I mixes was greater and ranged between 133,000 and 197,000 mg/m^2 with a mean of 175,500 mg/m^2 and a standard deviation of 37,255 mg/m^2. Na release from 50 wt.% GGBS mixes with water addition varying between 0.35 and 0.5 ranged between 131,000 and 139,000 mg/m^2 with a mean of 135,200 mg/m^2 standard deviation of 4,064 mg/m^2.

In the case of K, release from 50 wt.% CEM I mixes with water addition varying between 0.4 and 0.6 ranged between 116,000 and 125,500 mg/m^2 with a mean of 119,400 mg/m^2 and standard deviation of 4,294 mg/m^2. The 64-day release from 20 wt.% CEM I mixes with water addition varying between 0.45 and 0.6 ranged between 32,200 and 168,600 mg/m^2 respectively with a mean of 120,400 mg/m^2 and standard deviation of 76,440 mg/m^2. As with Al, results for the 20 wt.% CEM I, w/s of 0.6 mix were erratic resulting in the broad K release range and high standard deviation. Release from 50 wt.% GGBS mixes with water addition varying between 0.35 and 0.5 ranged between 126,000 and 139,000 mg/m^2 with a mean of 132,500 mg/m^2 standard deviation of 6,500 mg/m^2.

b) Lithium (Li)

Cumulative measured and derived leaching for Li is presented in Figure 5.11c. Amounts of Li released are lower by 2-3 orders of magnitude compared to Na and K which is attributed to the lower amounts initially present in the raw APC residues. However, release patterns are similar to Na and K. Release is diffusion-controlled at early leaching intervals with depletion occurring at later leaching intervals as defined by the slope of the plots in Figure 5.11c. As with Na and K there are no applicable regulatory requirements for the leaching of Li.

GGBS specimens with 50 wt.% binder addition released greater amounts of lithium compared to CEM I specimens with the same binder addition. The 64-day release for the GGBS mix containing 50 wt.% binder addition at a w/s ratio of 0.5 was 218 mg/m^2, whereas release for the CEM I mix with the same binder and water addition was approximately 166 mg/m^2. A similar percentage difference of approximately 31-32% was observed for mixes with a different water addition (i.e. 50 wt.% binder addition at a w/s ratio of 0.4).

Mixes with the same binder but varying water content release similar amounts of Li. The 64-day release from 50 wt.% CEM I mixes with water addition varying between 0.4 and 0.6 varied between 156 and 173 mg/m^2 with a mean of 163 mg/m^2 and a standard deviation of 7.5 mg/m^2. The 64-day release for 20 wt.% CEM I mixes was lower and ranged between 122 and 139 mg/m^2 with a mean of 133 mg/m^2 and a standard deviation of 9.7 mg/m^2. Release from 50 wt.% GGBS mixes with water addition varying between 0.35 and 0.5 ranged between 208 and 230 mg/m^2, with a mean of 219 mg/m^2 and a standard deviation of 10.9 mg/m^2.

a. Na Leaching

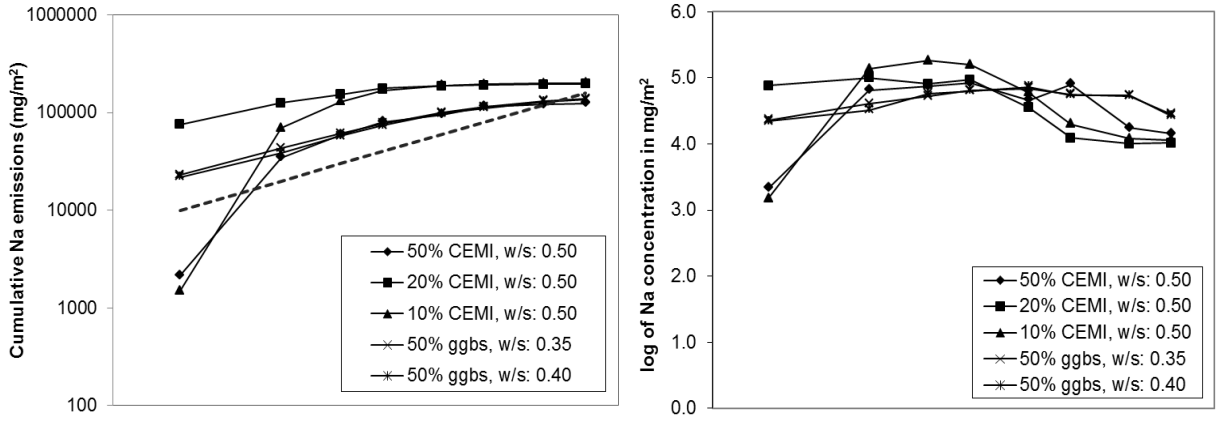

b. K Leaching

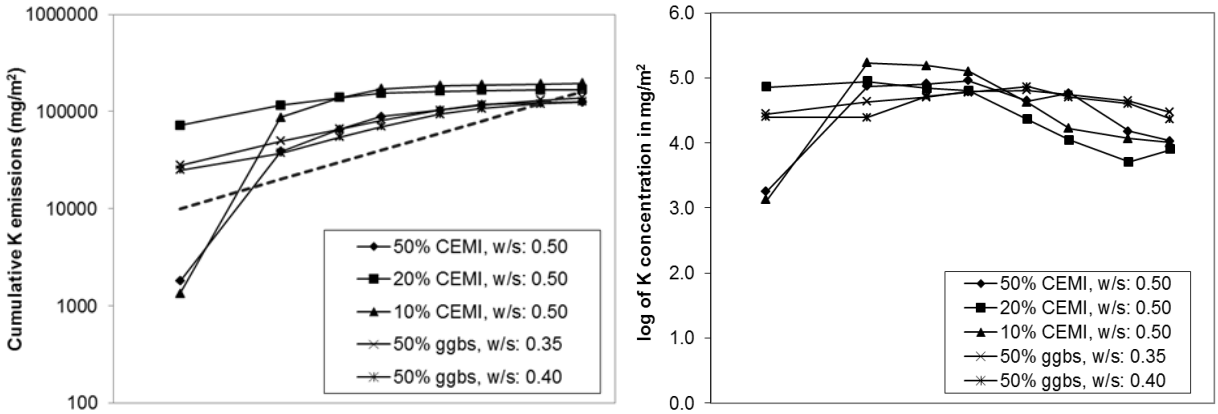

c. Li Leaching

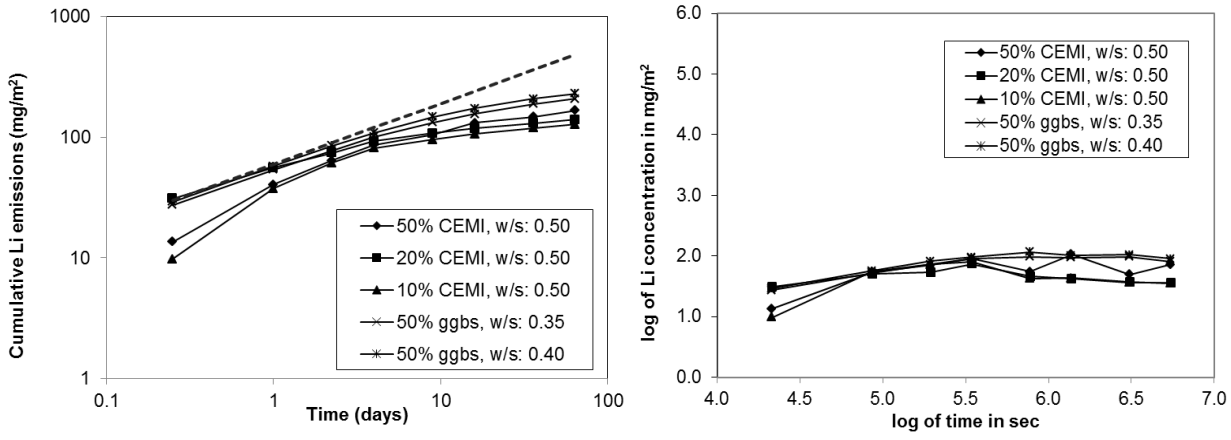

Figure 5.11 Cumulative measured and derived leaching of a) Na, b) K and c) Li

5.5.5 Chloride (Cl)

Cumulative measured and derived leaching for Cl is presented in Figure 5.12. Comparing the measured and estimated leaching values with the monolithic WAC limit for 64 day release of 20 x 10^3 mg/m2 suggests that chloride mobility was high for both CEM I and GGBS systems investigated, as all mixes surpassed the WAC limit within the first 2 days of the test.

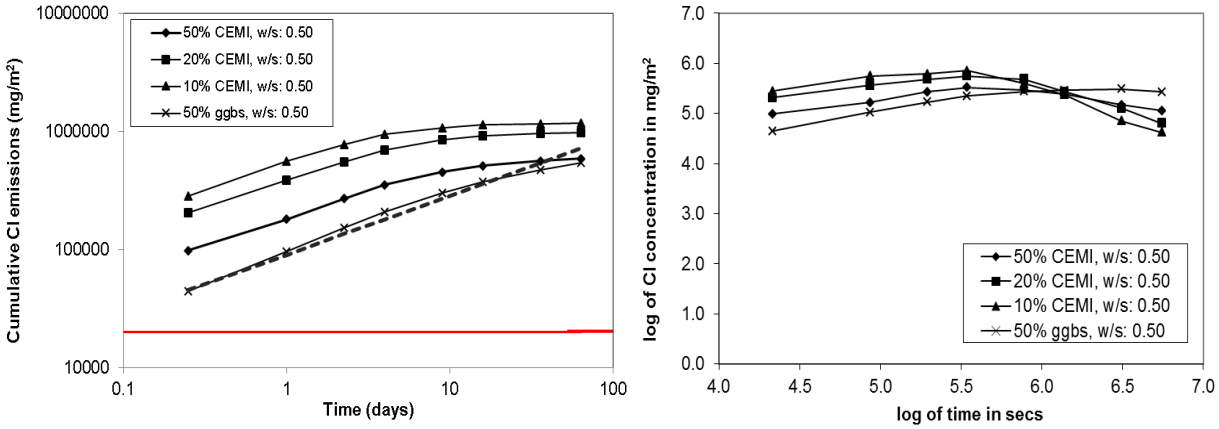

Figure 5.12 Cumulative measured and derived leaching of Cl

Examination of the slopes for different leaching intervals in Figure 5.12 shows diffusion control for CEM I mixes in early leaching intervals (e.g. 1-4), with depletion of chloride from the specimens in later leaching intervals. On the other hand diffusion control is observed throughout most of the test (intervals 1-7) for GGBS samples, with depletion of chloride in the final increment intervals (7-8).

The results for the diffusion-controlled interval were used to calculate estimated 64 day emissions, which are shown in Table 5.7. Estimated emissions were calculated according to the formula in the NEN 7375:2004 standard:

$$\varepsilon_{64} = \sqrt{64}\left\{\prod_{i=a}^{b}\frac{E_i^*}{\sqrt{t_i}-\sqrt{t_{i-1}}}\right\}^{\frac{1}{1+b-a}}$$

where

ε_{64} is the derived cumulative leaching for a component over 64 days, in mg/m^2;

E_i^* is the measured leaching of the component in fraction i in mg/m2;

t_i is the end time of fraction *i* for which diffusion has been established, measured from the start of the test, in days;

t_{i-1} is the start time of fraction *i* for which diffusion has been established, measured from the start of the test, in days; and

a, b are dimensionless indices by which an increment *a-b* is indicated for which a diffusion mechanism is established.

It should be noted that this approach is a deviation from the standard NEN method, which was carried out to obtain an indication of probable emissions, despite the rapid depletion of chloride from the specimen. Therefore, the results should be considered as approximations only.

Table 5.7 also includes estimated 64-day emissions from similar studies on chloride leaching from CEM I S/S APC residues. Stegemann et al (2005) studied the influence of aggregates on the leaching of chloride from CEM I S/S APC residues. Release values for 50% APC addition were from specimens without aggregate addition, and are similar to the values obtained in this study for the same waste addition (i.e. 50 wt.%). In the study by Stegemann et al, it is also interesting to note that estimated 64-day Cl release was similar for all mixes regardless of the content of APC residues and the use of aggregates in the mix.

Table 5.8 Estimated 64-day release for CEM I mixes based on diffusion-controlled interval

Study	% w/w APC	Estimated 64 day chloride emission (mg/m^2)
Present work	**50.0**	**1,420,000**
	80.0	3,100,000
	90.0	4,310,000
Stegemann et al (2005)	15.5	1,500,000
	20.1	1,200,000
	25.1	1,500,000
	30.6	1,900,000
	36.5	1,900,000
	50.0	**1,800,000**
Hall et al (2005)	0.25-5	2,044

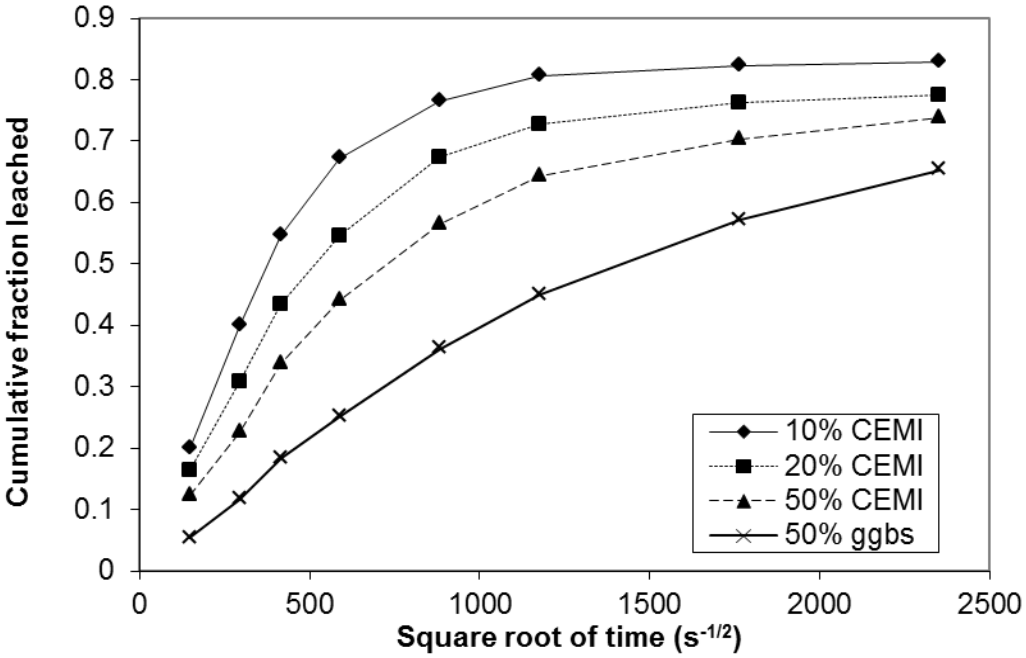

Figure 5.13 Cumulative fraction leached for Cl (all mixes at w/s: 0.5)

The 64-day release from 50 wt.% CEM I mixes with water addition varying between 0.4 and 0.6 ranged between 573,000 and 615,000 mg/m^2 with a mean of 589,452 mg/m^2 and a standard deviation of 18,284 mg/m^2. The 64-day release for 20 wt.% CEM I mixes was higher and ranged between 875,000 and 1,027,000 mg/m^2 with a mean of 959,600 mg/m^2 and a standard deviation of 77,611 mg/m^2. Cl release from 50 wt.% GGBS mixes with water addition varying between 0.35 and 0.5 ranged between 542,000 and 592,000 mg/m^2 with a mean of 566,021 mg/m^2 and a standard deviation of 25,171 mg/m^2.

The cumulative fraction of chloride leached from S/S APC residues is presented in Figure 5.13 as a function of the square root of time, for specimens containing 10%, 20%, 50% of total dry mass CEM I and 50% of total dry mass GGBS, all at a w/s of 0.5. The cumulative fraction leached for 50 wt.% GGBS was 0.65, compared to 0.74 for 50 wt.% CEM I, indicating that the GGBS mix retained approximately 9% more chloride compared to CEM I.

The potential mechanism for immobilisation of chloride in CEMI is the binding to the C_3A phases in the form of the chloro-complex Friedel's salt ($3CaO.Al_2O_3.CaCl_2.10H_2O$) (Suryavanshi et al, 1996). This depends on the amount of C_3A and also the presence of other anions such as SO_4^{2-} which affect the immobilisation efficiency (Dehwah, 2006). Further discussion on the immobilisation of Cl is provided in following sections.

5.5.6 Sulphate

Cumulative measured and derived leaching results for SO_4^{2-} are presented in Figure 5.14. As detailed in Section 4.4.3 the eluates from the leaching test were tested for sulphur (S) via ICP-OES. Taking into account the nature of the specimens however, it is assumed that sulphur will be mainly present as SO_4^{2-} and therefore sulphur concentrations were adjusted accordingly.

It is observed that all CEM I mixes met the monWAC limits for SO_4^{2-} for both hazardous waste (20,000 mg/m^2) landfills and for stable non-reactive hazardous waste in non-hazardous landfill (5,000 mg/m^2). GGBS mixes released greater quantities of SO_4^{2-} compared to CEM I and met the monWAC limits only for hazardous waste landfills. In particular, SO_4^{2-} released from GGBS mixes at 50 wt.% binder addition was up to ten (10) times or an order of magnitude greater compared to CEM I mixes at the same binder addition.

Examination of the log-log plots shows that depletion of SO_4^{2-} is occurring for all CEM I mixes, whereas release from GGBS mixes is controlled by diffusion. It is noteworthy that for the 10 wt.% CEM I mix, 87% of the total release occurred during the first five fractions or 9 days of the test.

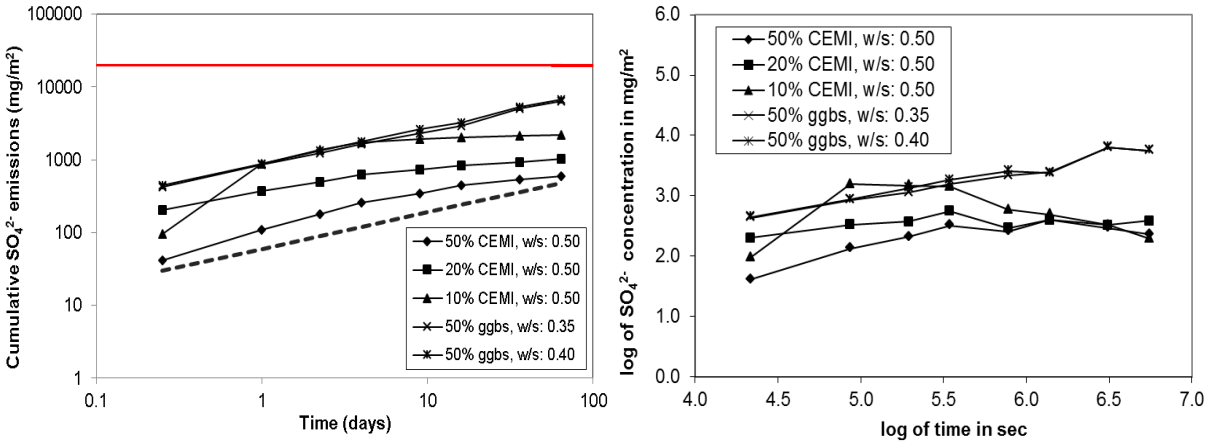

Figure 5.14 Cumulative measured and derived leaching of SO_4^{2-}

The 64-day release from 50 wt.% CEM I mixes with water addition varying between 0.5 and 0.6 ranged between 600 and 1,730 mg/m^2 with a mean of 952 mg/m^2 and a standard deviation of 524 mg/m^2. In this case, erratic results were obtained for the mix at a w/s of 0.4

for the first fraction of the tank test resulting in the broad release range and high standard deviation. The 64-day release for 20 wt.% CEM I mixes was higher and ranged between 660 and 1,108 mg/m^2 with a mean of 947 mg/m^2 and a standard deviation of 219.4 mg/m^2. SO_4^{2-} release from 50 wt.% GGBS mixes with water addition varying between 0.35 and 0.5 ranged between 4,240 and 6,780 mg/m^2 with a mean of 5,820 and a standard deviation of 1,380 mg/m^2.

5.5.7 Zinc

Cumulative measured and derived leaching results for Zn are presented in Figure 5.15. It is observed that all mixes met the monWAC limits for Zn for hazardous waste landfills (100 mg/m^2) In addition, both 50 wt.% CEM I and GGBS mixes also met the monWAC values for stable non-reactive hazardous waste in non-hazardous landfill (30 mg/m^2).

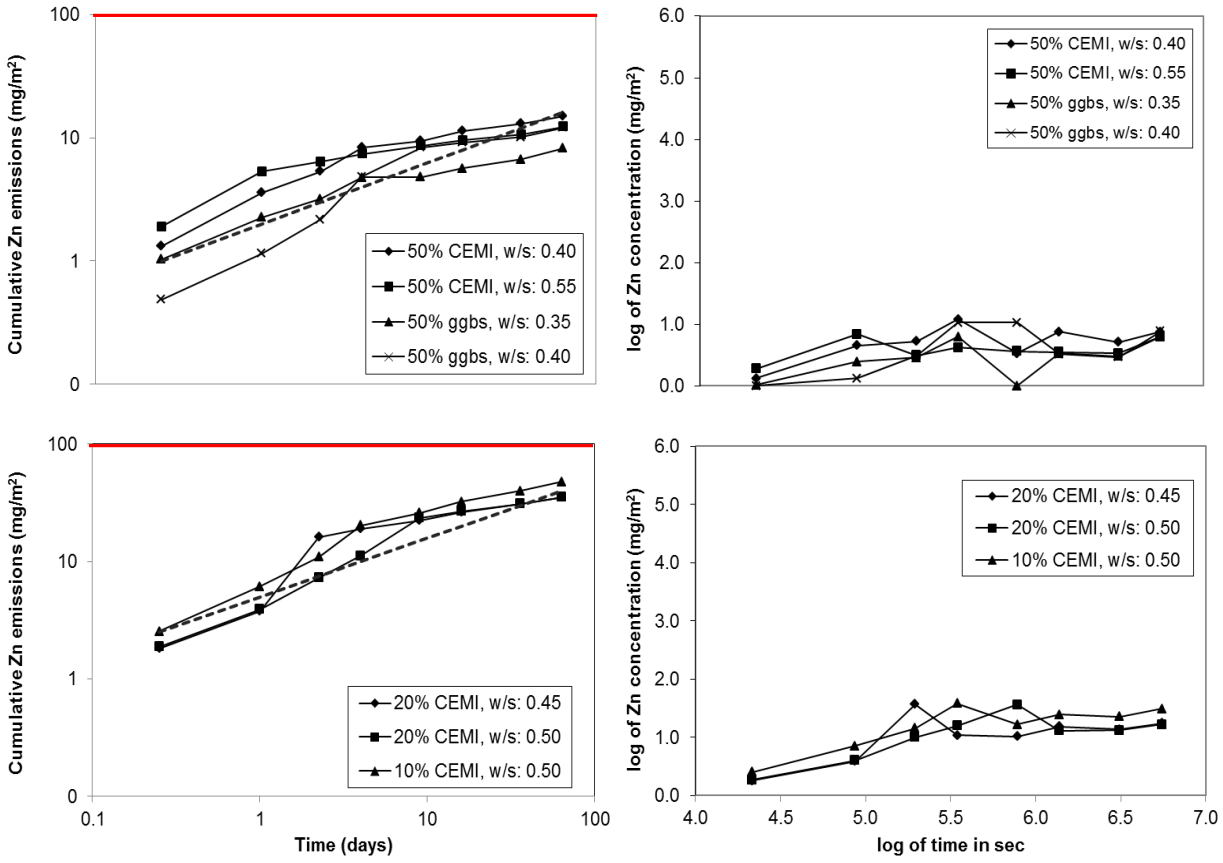

Figure 5.15 Cumulative measured and derived leaching of Zn

Examination of the log-log plots shows diffusion at early stages and changes in the release mechanism or chemical for later stages of the tank test for all mixes. Similar release

behaviour for Zn from monolithic stabilised waste has been previously reported by Van der Sloot et al (2007).

The 64-day release from 50 wt.% CEM I mixes with water addition varying between 0.4 and 0.6 ranged between 12 and 24 mg/m^2 with a mean of 16.7 mg/m^2 and a standard deviation of 5.2 mg/m^2 . The 64-day release for 20 wt.% CEM I mixes was greater and ranged between 18 and 35 mg/m^2 with a mean of 29.6 mg/m^2 and a standard deviation of 9.8 mg/m^2. Zn release from 50 wt.% GGBS mixes with water addition varying between 0.35 and 0.5 ranged between 7.3 and 12 mg/m^2 with a mean of 9.2 mg/m^2 and a standard deviation of 2.5 mg/m^2.

Although both binders effectively reduced mobility of Zn to meet the monWAC for stable non-reactive hazardous waste in non-hazardous landfill at 50 wt.% binder addition, GGBS exhibited lower release compared to CEM I mixes.

5.5.8 Lead

Cumulative measured and derived leaching results for Pb are presented in Figure 5.16. It is observed that 50 wt.% mixes met the monWAC limits for Pb for hazardous waste (20 mg/m^2). In contrast, 10 and 20 wt.% CEM I exceeded the monWAC values with the former exhibiting a 64-day release of 72 mg/m^2 and the latter exhibiting a release of up to 46 mg/m^2 depending on water addition.

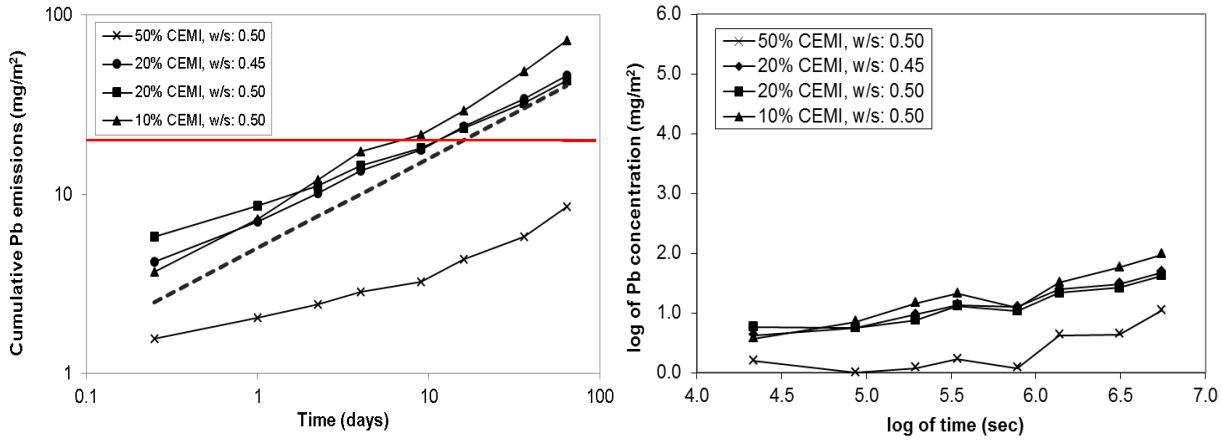

Figure 5.16 Cumulative measured and derived leaching of Pb

Examination of the log-log plots shows that Pb release from 10 and 20 wt.% CEM I addition is controlled by diffusion. The slope of the curve for the 50 wt.% CEM I mix indicates

surface-wash or potentially a change in the release mechanisms throughout the test. However, it is noted that ICP-OES results were lower than the laboratory detection limit for fractions 3 (2.25 days) and 4 (4 days) of the tank test and therefore the detection limit (10 µg/L) was used for the analysis. As this may skew the analysis it is believed that release of Pb from 50 wt.% CEM I mixes is also controlled by diffusion with the potential of surface wash-off during the early stages (1-2) of the tank test.

The 64-day release from 50 wt.% CEM I mixes with water addition varying between 0.4 and 0.6 ranged between 5.5 and 12.3 mg/m^2 with a mean of 9.5 mg/m^2 and a standard deviation of 3.1 mg/m^2. Pb release was found to increase with increasing water addition for these mixes. The 64-day release for 20 wt.% CEM I mixes was greater and ranged between 28.4 and 46 mg/m^2 with a mean of 39.1 mg/m^2 and a standard deviation of 9.4 mg/m^2 although a pattern was not observed for this binder addition.

Pb release for all 50 wt.% GGBS mixes was lower than the laboratory detection limit (10 µg/L) for all fractions of the tank test and therefore was lower compared to CEM I mixes with the same binder addition. The range of the release in terms mass per surface area can be approximated, as described above, by assigning either the detection limit or half the detection limit as the value of the release for all test fractions. If the value of the detection is assumed then the release from 50 wt.% GGBS mixes is 2.8 mg/m^2. If half the detection limit is assumed then the release is approximately 1.5 mg/m^2.

Although release from GGBS mixes was lower compared to CEM I mixes at 50 wt.% binder addition both binders were effective at reducing Pb mobility and met the pertinent monWAC limit of 20 mg/m^2 for hazardous waste landfills. However, 50 wt.% GGBS mixes also met the monWAC value for stable non-reactive hazardous waste in non-hazardous landfill (6 mg/m^2).

5.5.9 Other Metals

a) Iron (Fe)

Cumulative measured and derived leaching results for Fe are presented in Figure 5.17. Release of Fe, is similar for GGBS and CEM I at the same binder addition. Comparison to monWAC is not applicable to Fe as there are no pertinent limits in place.

Comparing the curves for the different binder additions, it is observed that mixes with lower binder addition (i.e. 10 and 20 wt.% CEM I mixes) release lower amounts of Fe compared to the mixes with higher binder addition. Fe release for the different CEM I additions in increasing order is 20 wt.% < 10 wt.% < 50 wt.%.

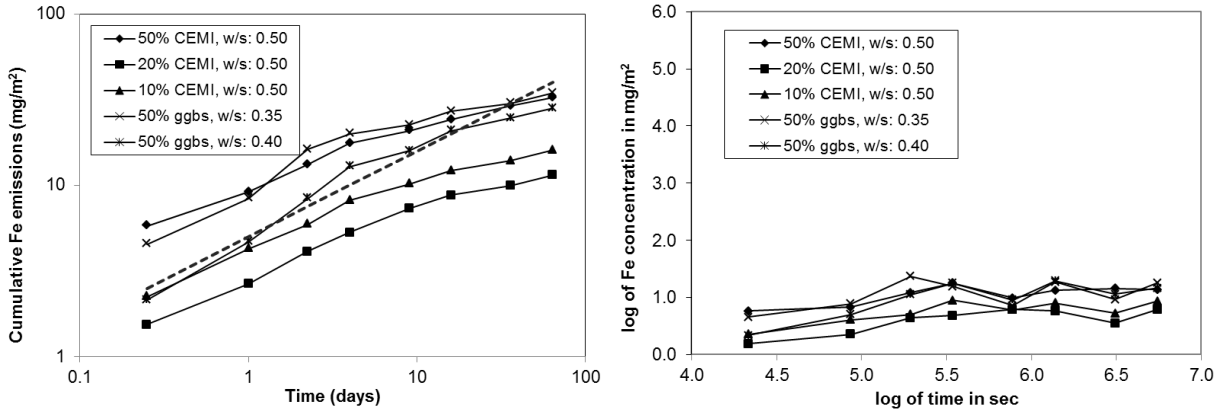

Figure 5.17 Cumulative measured and derived leaching of Fe

Examination of the log-log plots shows that release of Fe is similar to the release of Zn with diffusion at early stages and change in the release mechanisms or chemical forms in later stages of the test for mixes with a binder addition of 50 wt.%. The curves for 10 and 20 wt.% CEM I addition show that depletion of Fe is occurring at later stages of the test for these mixes. As with Ca and Si however, this may imply that at later stages of the test Fe release continues based on solubility control from less soluble Fe-containing phases.

The 64-day release from 50 wt.% CEM I mixes with water addition varying between 0.4 and 0.6 ranged between 26.8 and 32.4 mg/m^2 with a mean of 29.7 mg/m^2 and a standard deviation of 2.3 mg/m^2. The 64-day release for 20 wt.% CEM I mixes was lower and ranged between 7.6 and 12.3 mg/m^2 with a mean of 10.4 mg/m^2 and a standard deviation of 2.5 mg/m^2. Fe release from 50 wt.% GGBS mixes with water addition varying between 0.35 and 0.5 ranged

between 28.2 and 34.6 mg/m^2 with a mean of 30.6 mg/m^2 and a standard deviation of 3.5 mg/m^2.

b) Strontium (Sr)

Cumulative measured and derived leaching results for Sr are presented in Figure 5.18. Sr release was lower for GGBS mixes. As with Fe, there are not any applicable monWAC limits for Sr. Sr release in increasing order for the different CEM I additions is 10 wt.% < 50 wt.% < 20 wt.%. It is interesting to note that 20 and 50 wt.% CEM I mixes released similar amounts of Sr. The 50 wt.% CEM Imix in particular exhibited the same Sr release pattern as the 10 wt.% mix up to the 5th fraction of the tank test (9 days) after which a hump was observed resulting in a cumulative release similar to the 20 wt.% CEM I mix.

Examination of the log-log plots shows that release of Sr is controlled by diffusion at early stages of the tank while depletion is occurring at later stages for mixes investigated. This effect appears to be more pronounced for CEM I mixes.

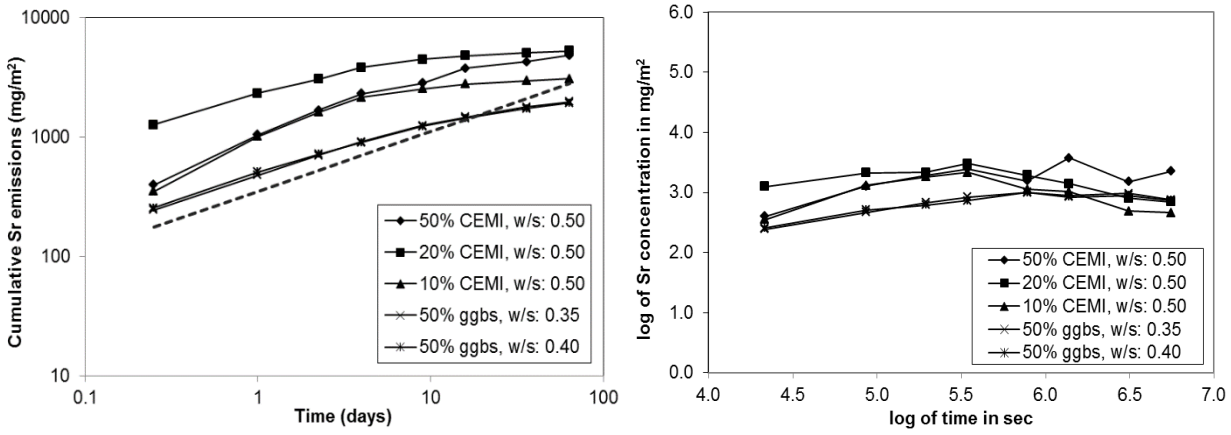

Figure 5.18 Cumulative measured and derived leaching of Sr

The 64-day release from 50 wt.% CEM I mixes with water addition varying between 0.4 and 0.6 ranged between 4,817 and 5,479 mg/m^2 with a mean of 5,011 mg/m^2 and a standard deviation of 313.6 mg/m^2. The 64-day release for 20 wt.% CEM I mixes was similar and ranged between 3,909 and 5,229 mg/m^2 with a mean of 4,379 mg/m^2 and a standard deviation of 737.9 mg/m^2. Sr release from 50 wt.% GGBS mixes with water addition varying between 0.35 and 0.5 was lower and ranged between 1,884 and 1,973 mg/m^2 with a mean of 1924.9 mg/m^2 and a standard deviation of 45.1 mg/m^2.

5.6 Mineralogy of S/S Products

Crystalline phases identified in the s/s products are presented in Figures 5.19-5.21. Figure 5.19 shows the mineralogical composition of APC residues with 50% CEM I addition after 7 and 28 days. Major crystalline phases are $Ca(OH)_2$, $CaCO_3$ (calcite) and the chloro-complex Friedel's salt, $Ca_2Al(OH)_6Cl{\cdot}2H_2O$ and $Ca_2Al(OH)_7{\cdot}2H_2O$. Friedel's salt forms by the reaction between calcium aluminates and chloride compounds such as NaCl and $CaCl_2$. The absence in the diffraction pattern of peaks related to the CaClOH previously found in the untreated APC residue indicates that this has been transformed into less soluble chloro-complex salts, but NaCl and KCl remain present.

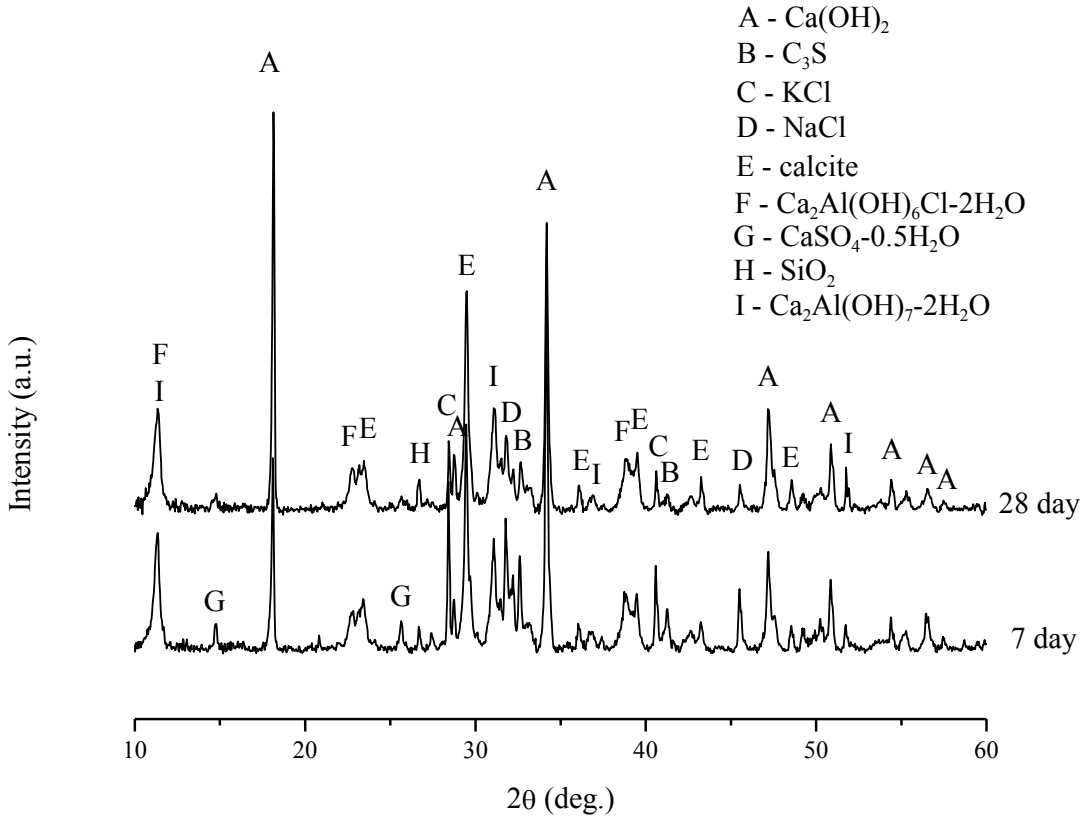

Figure 5.19 X-Ray diffractograms for 50 wt.% mixes at different curing age

Figure 5.20 shows the XRD analysis of APC residues with 50% GGBS addition. During the hydration of GGBS, the $Ca(OH)_2$ supplied by the APC residue is completely consumed, while CaClOH reacts to form Friedel's salt. The broad hump between 20° and 36° 2θ represents the poorly-crystalline forms of the highly reactive phases present in GGBS.

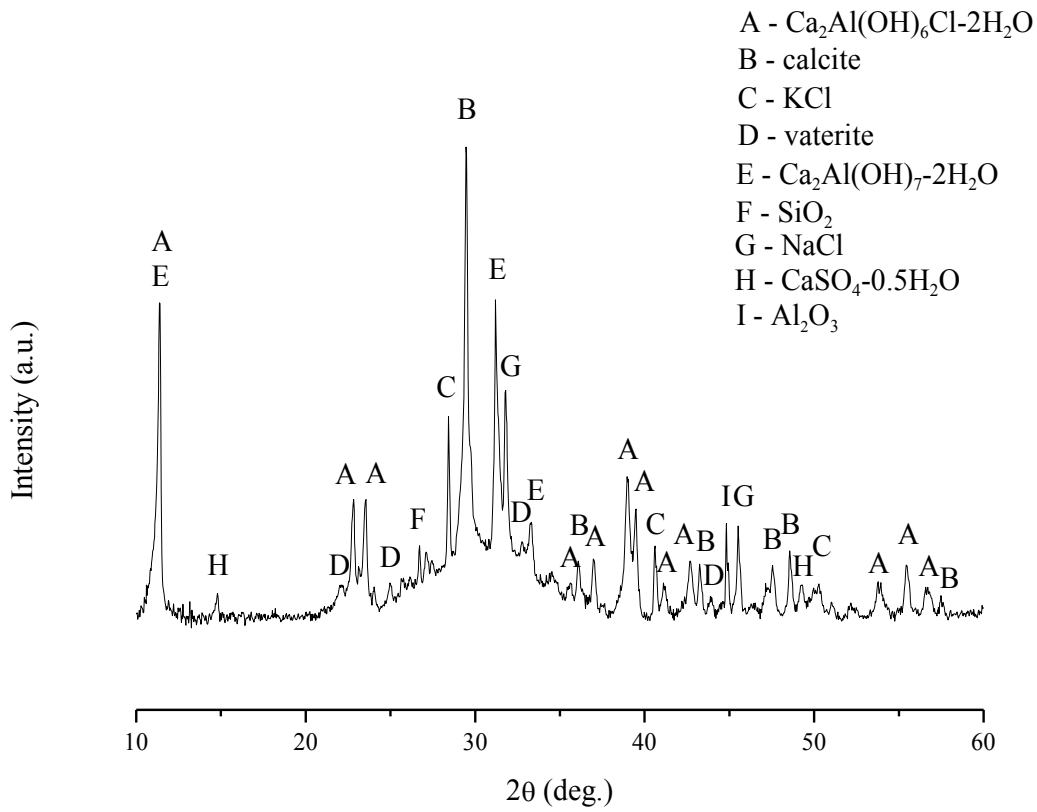

Figure 5.20 X-Ray diffractograms for 50 wt.% GGBS mix (w/s: 0.5)

The effect of CEM I addition on the mineralogical composition of APC residues at varying binder addition is presented in Figure 5.21. The comparison of the three solidified products shows the extent of the interaction between APC residues and CEM I. In S/S products with 10 and 20 wt. % CEM I, residual CaClOH was identified. It is also evident that tricalcium aluminate (C_3A in cement chemist's notation) reacted to form chloro-complex salts. Neither ettringite ($Ca_6Al_2(SO_4)_3(OH)_{12}$•$26H_2O$) nor monosulphate ($Ca_4Al_2SO_4(OH)_{12}$•$26H_2O$) were detected in the S/S products prepared with CEM I, while several calcium sulphates, anhydrite ($CaSO_4$), bassanite ($CaSO_4$·$0.5H_2O$) and gypsum ($CaSO_4$·$2H_2O$) were identified for 10 and 20% CEM I addition. It seems that C_3A may react preferably with the chloride-bearing phases to produce chlorocomplexes and for this reason the sulphate phases remained unreacted.

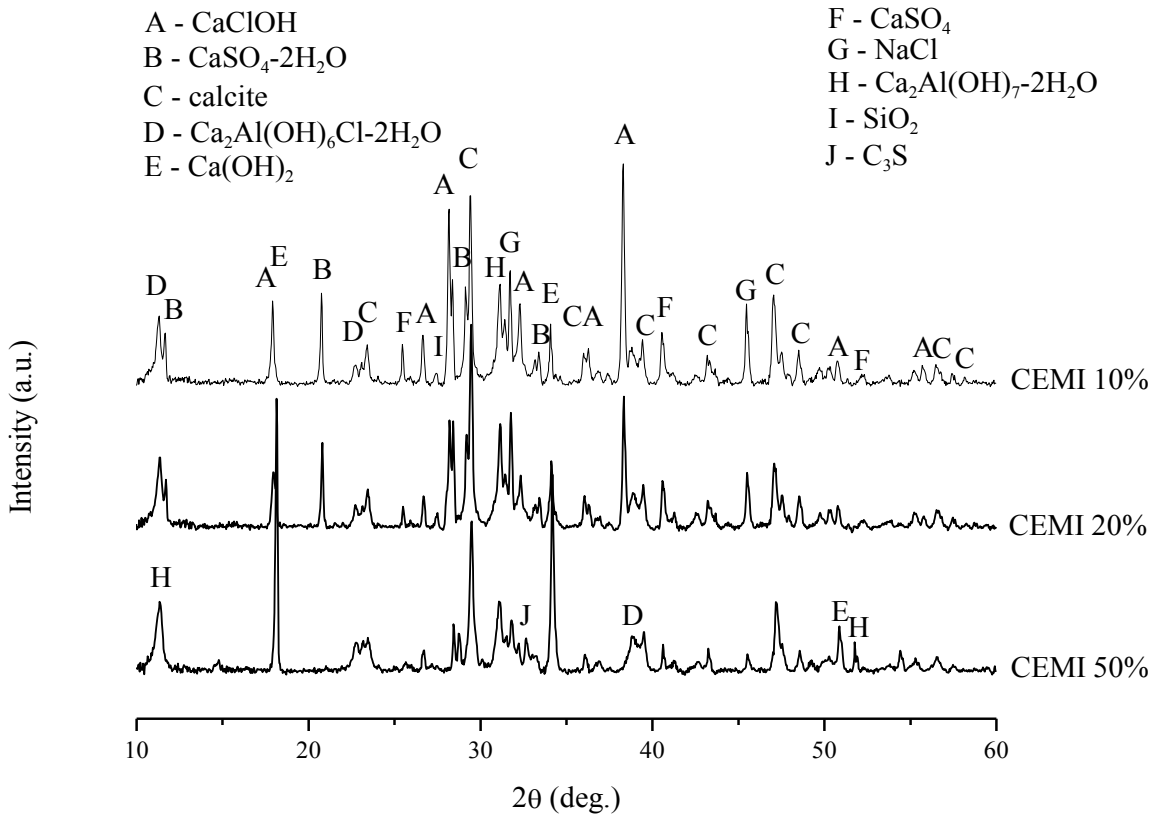

Figure 5.21 X-Ray diffractograms for CEM I mixes with varying binder addition

5.7 Microstructural Characterisation

The microstructure of selected S/S APC specimens was investigated by examining fracture surfaces using SEM. This section presents the results of the microstructural characterisation of these specimens. Energy Dispersive Spectrometry (EDS) spectra were also obtained as part of the characterisation. However, the surfaces of the specimens were not polished and therefore the quantification of elements was not taken into consideration. In addition, the heterogeneity of the specimens is an additional parameter than hampers quantification of elements during the microstructural analysis.

Figure 5.22 shows the micrographs for the 50 wt.% GGBS mix at a w/s of 0.35 at different magnification levels. The structure appears to be dense with relatively low porosity.

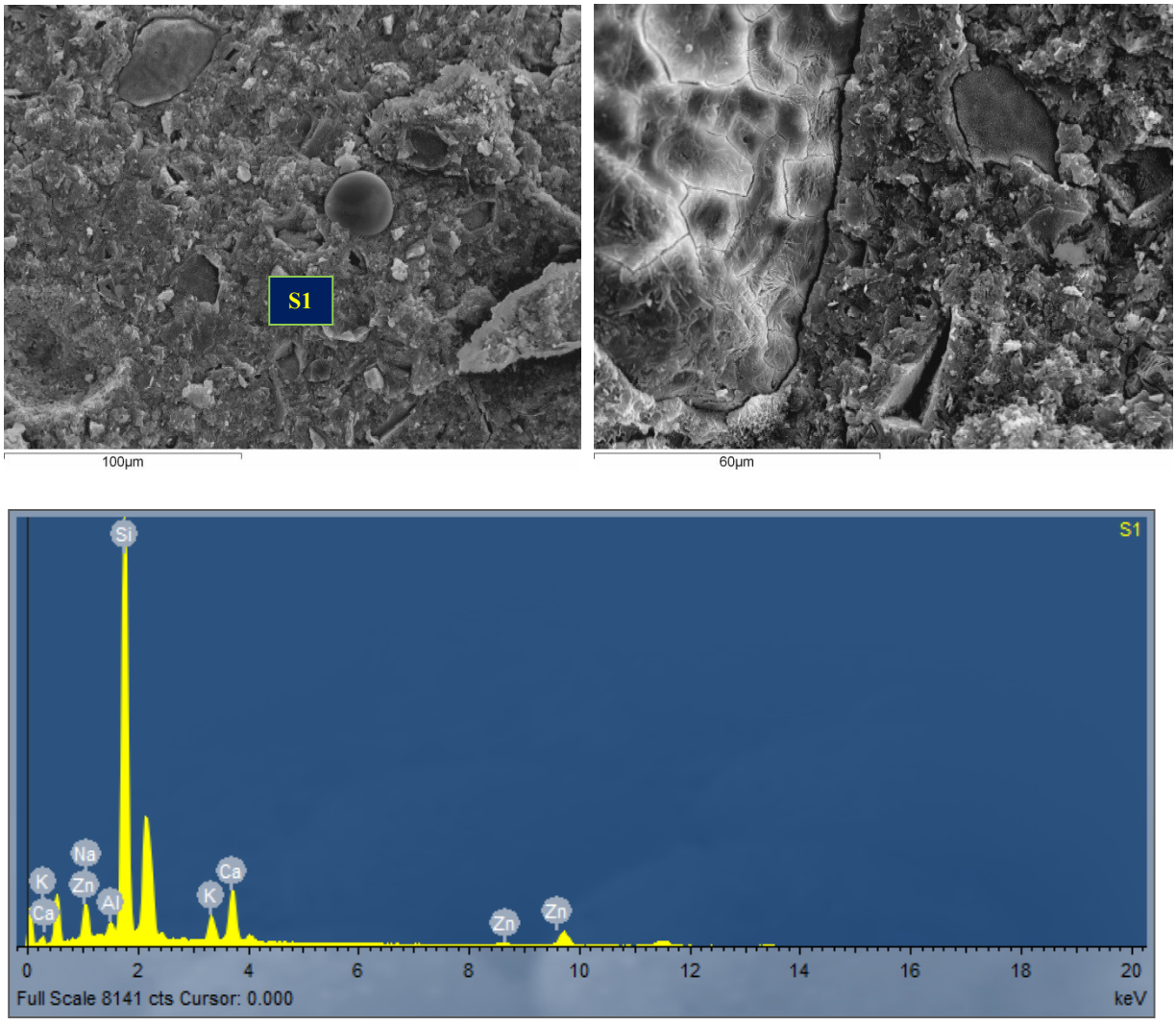

Figure 5.22 SEM micrograph of 50 wt.% GGBS mix at w/s of 0.35

It is interesting to note the unreacted spherical particle marked on Figure 5.22. Although the specimen was not polished, the investigation attempted to obtain EDS spectra and thus an approximation of the composition of the unreacted particle. The EDS spectra show that the sphere is mainly aluminosilicate including also elements such as Ca, Na and K. In addition, Zn was detected in the composition of the spherical particle. Young-Sook Shim et al (2003) have previously suggested that such unreacted aluminosilicate particles can act as surfaces for the absorption of metals in MSWI ashes in a similar manner to zeolites.

Figure 5.23 shows the micrographs for the 20 wt.% CEM I mix at a w/s of 0.50 at different magnification levels. As expected, the structure appears to be less dense and with larger pores compared to the GGBS mix with 50 wt.% binder addition. As in the 50 wt.% GGBS mix, similar unreacted spherical particles were also observed in the 20 wt.% CEM I mix. The EDS

spectra for these particles are also presented in Figure 5.23 and show that the spheres observed in the 20 wt.% CEM I mix have similar composition with the spheres in the 50 wt.% GGBS mix in Figure 5.22.

An approximation of the percentage elemental composition of these spherical particles is presented in Table 5.8. As the specimens were not polished the percentages presented should be considered as approximations only. The spheres appear to be predominantly aluminosilicate in nature with other major elements including Ca, K and Na. The variance in the content of the different elements can be attributed to the fact that samples were not polished.

Table 5.9 Percentage elemental composition of unreacted spheres as obtained by SEM-EDS

Sample	Si	Al	Ca	K	Na	Mg	Fe	Ti	Zn
50 wt.% GGBS (S1)	65.22	1.89	15.11	6.68	7.83	-	-	-	3.26
20 wt.% CEM I (S1)	48.75	11.98	10.12	6.07	6.13	1.10	8.87	1.70	5.29
20 wt.% CEM I (S2)	39.61	26.24	10.59	11.04	6.66	-	-	5.86	-
Mean	51.19	13.37	11.94	7.93	6.87	-	-	-	-
Std. Deviation	12.98	12.23	2.75	2.71	0.87				

The amount and exact composition of the unreacted spherical particles in APC residues warrant further investigation due to their heavy metal immobilisation potential. Moreover unreacted low density (0.4-0.8 g/cm^3) hollow aluminosilicate spherical particles produced during combustion process (and especially during coal combustion) have commercial value. These particles are typically termed cenospheres and are used in a variety of applications ranging from production of low density concrete to conductive paints for antistatic coatings.

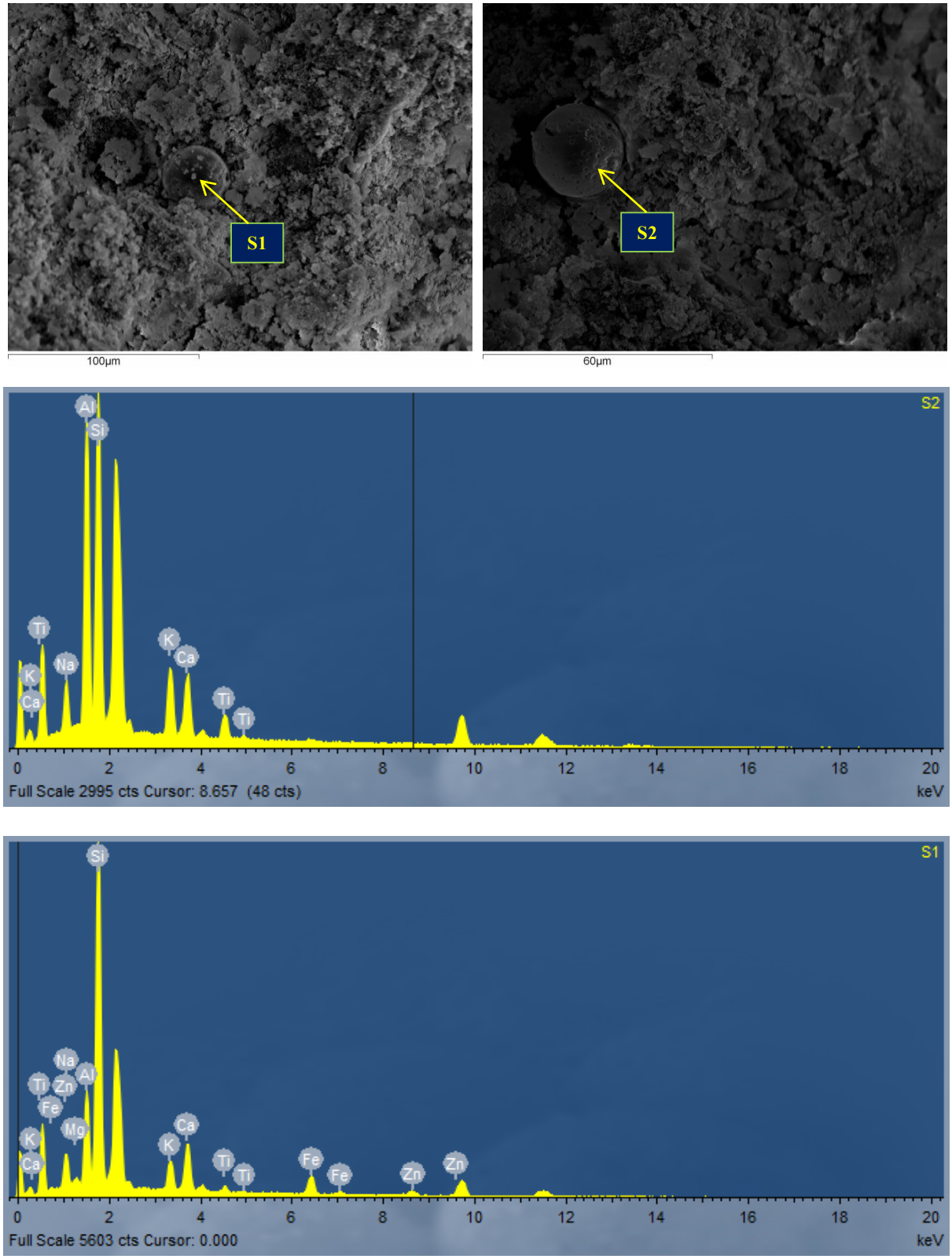

Figure 5.23 SEM micrograph of 20 wt.% CEM I mix at w/s of 0.5

Figure 5.24 shows the micrographs for the 90 wt.% CEM I mix at a w/s of 0.50 at different magnification levels. As expected, the structure appears to be less dense and flake-like, with larger pores compared to the GGBS mix with 50 wt.% binder addition.

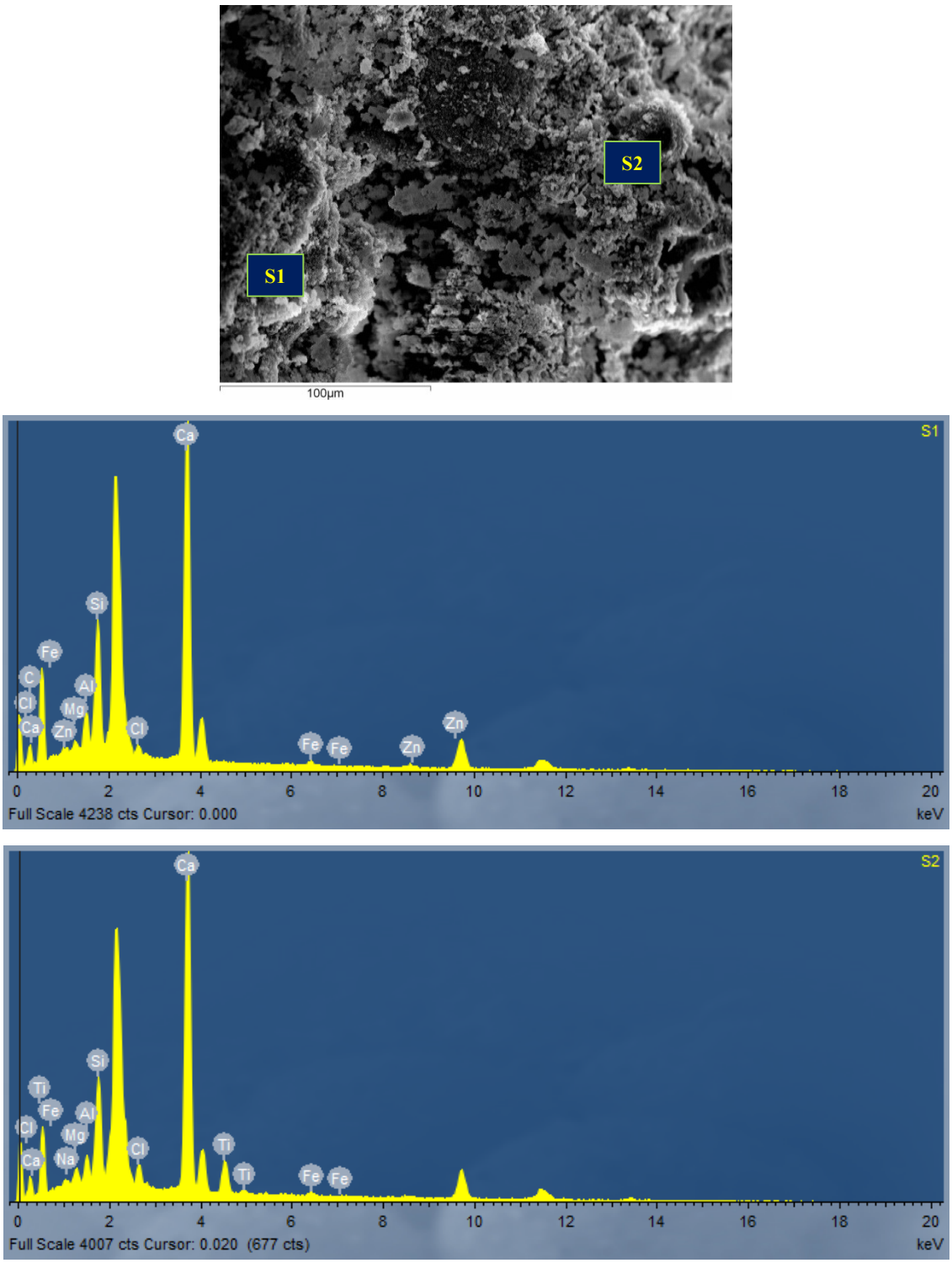

Figure 5.24 SEM micrograph of 90 wt.% CEM I mix at w/s of 0.5

In contrast to the previous specimens examined, unreacted spherical particles were not observed in the 90 wt.% CEM I mix. EDS spectra were also obtained for this specimen in the areas marked on Figure 5.24 as S1 and S2. The differences in the EDS spectra on the surface of the same specimen are indicative of both the unpolished nature of the specimens as well as the inherent heterogeneity of the mixes. The effect and significance of each of these factors cannot be determined or quantified based on the current dataset and therefore the results presented should be considered as approximations only.

The results of the microstructural characterisation validate the results of the physical properties analysis and in particular UCS and porosity, where structural integrity diminishes with decreasing binder addition. Although the results of the EDS spectra are approximations, there are two interesting observations that could be further investigated:

1) The exact composition and quantities of unreacted spherical particles in APC residues. As noted above these particles may have an effect on the heavy metal immobilisation capacity of the S/S matrices. Moreover, these spheres may have commercial value if their composition (predominantly aluminosilicate) and physical properties (i.e. low density) classify them as cenospheres.
2) Among the heavy metals of concern in APC residues (i.e. Pb and Zn) only Zn was identified in the EDS spectra. However, distribution of Zn was not even across the surface and Zn detection varied among sites on the same specimen. The varying distribution of Zn across the specimen may imply a certain affinity of zinc for specific compounds or sites on S/S APC residues. Therefore the factors affecting this affinity and the mechanisms involved (i.e. precipitation, sorption etc.) require further investigation.

6. GEOCHEMICAL MODELLING

6.1 Introduction

The background and the importance of geochemical modelling in the field of hazardous waste management as well as its increasing utilisation over the past year has been described in detail in Chapter 2. Geochemical modelling was utilised as part of this study in order to obtain an improved understanding of:

a. the underlying mechanisms that control release of contaminants from S/S APC residues.
b. the potential for extracting contaminants and/or elements of interest from raw APC residues prior to treatment via S/S.

An improved understanding is deemed important in order to assist efforts for more efficient treatment of APC residues as part of the DEFRA UK strategy for the treatment of hazardous wastes focusing on reuse and recycling instead of disposal.

The first sections of this chapter describe the methodology and tools used for the modelling study test as well as the assumptions made. The modelling results for different constituents of concern in APC residues are presented in the following sections.

6.2 Modelling Scope

The modelling study comprised two distinct parts which involve two different leaching tests for S/S and raw APC residues respectively. The first part and the bulk of the modelling work involved modelling of the monolithic leaching test for S/S APC residues and is described in this chapter. The second part involved modelling of a combined alkaline (water-wash) and acid leaching procedure for raw APC residues. Chapter 8 is dedicated to the results and discussion associated with this work.

LeachXS was utilised for both parts of the modelling study due to the tools (algorithms) already built-in for modelling of the two tests. Modelling of the two different tests serves a twofold purpose:

- Modelling of the monolithic leaching test aims to provide an insight into processes and/or minerals controlling release of elements of concern from S/S APC residues. Previous chapters demonstrated that elements such as Cl, Pb and Zn are problematic and depending on the binder addition, S/S APC residues do not meet UK monWAC (i.e. landfill acceptance criteria for monolithic waste) for all or a combination of these elements. Knowledge of release-controlling processes and minerals can be utilised for improved s/s mix design and overall management of APC residues in line with the UK DEFRA strategy.
- Modelling of a combined water-wash (alkaline leaching) and acid leaching procedure aims to evaluate the potential of extracting elements of concern from APC residues as a pre-treatment step prior to S/S or other potential treatment processes. The rationale behind the two-step leaching procedure is as follows:
    - Water washing can be used as a first step to remove easily soluble compounds from raw APC residues such as chlorides. It was demonstrated in previous sections that chlorides constitute one of the most problematic compounds within raw APC residues. The water-wash step is termed as alkaline leaching due to the alkaline nature of raw APC residues which results in a pH > 12 during leaching, without the requirement of a base.
    - As APC residues contain amphoteric metals the water-wash step may not effectively remove all elements of concern due to the high natural pH of APC residues. Having removed the greatest fraction of easily soluble compounds during the water-wash step, a pH dependence (or acid leaching) test on the washed APC residues can provide an indication of the pH conditions that could maximise the yield of other elements of interest.

  Modelling results, coupled with the geochemical footprint obtained by identifying probable mineral phases in APC residues, can be utilised to optimise the extraction of elements during washing of APC residues. These elements could be thereafter be recovered through hydrometallurgical processes, although an extensive review of these is not included in this study.

The following sections detail the methodology and process followed to model both the monolithic and pH dependence leaching tests.

6.3 Geochemical Modelling Tools

Geochemical modelling was conducted using commercial and public domain software, namely LeachXS and PHREEQC. The former was developed by ECN, whereas the latter was developed by the US Geological Survey. LeachXS was utilised extensively due to its built-in algorithms for the modelling of a variety of leaching tests including pH dependence and the monolithic leaching test. In contrast PHREEQC was used to a lesser extent to perform simpler speciation calculations (e.g. single mineral pH-dependent solubility calculations).

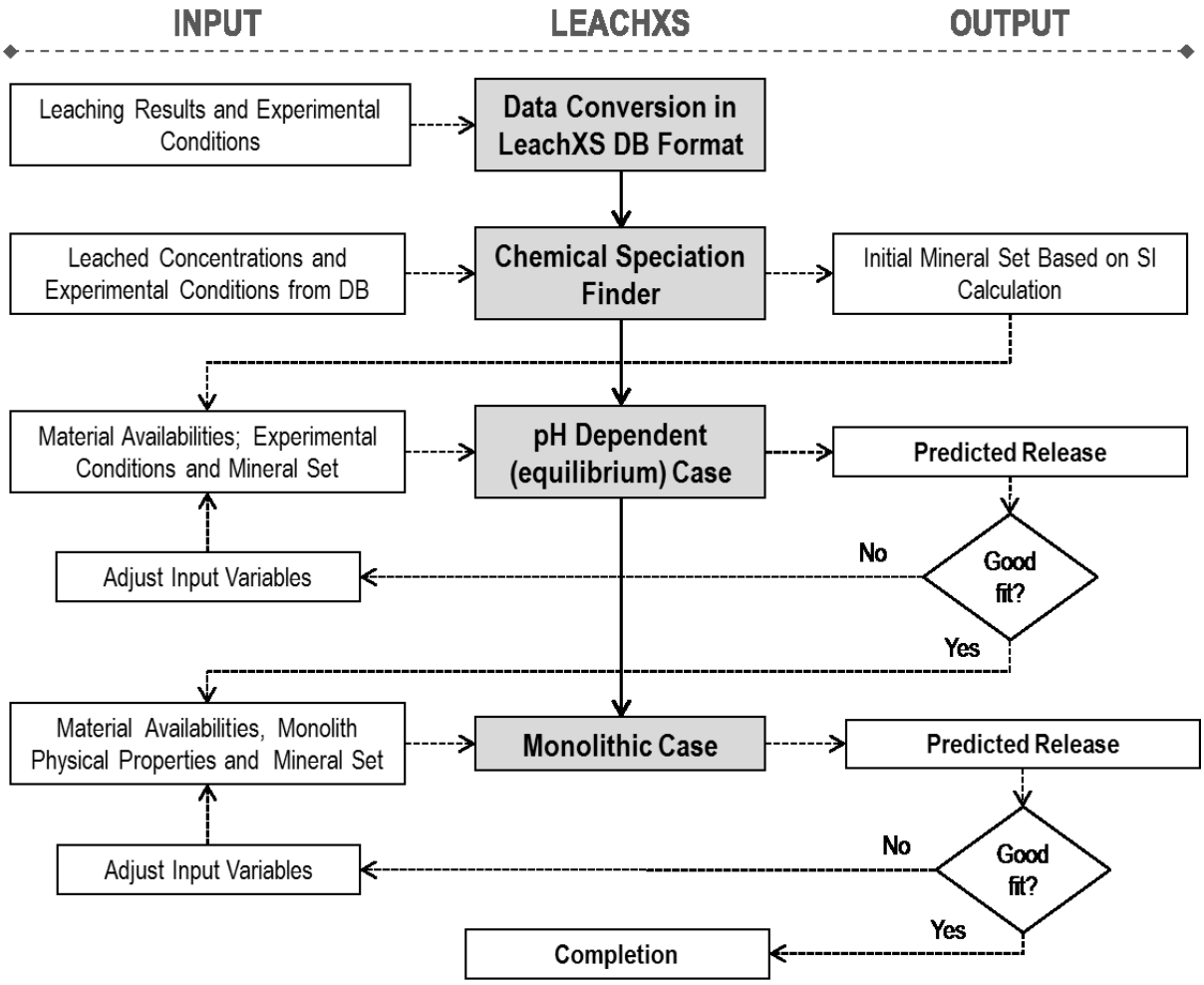

Figure 6.1 LeachXS modelling process (DB: database; SI: Saturation Indices)

LeachXS has been described briefly in Chapter 4. It includes a database of leaching data for a variety of materials and leaching tests (i.e. batch, pH dependence, monolithic etc.) and allows for easy presentation of data and comparison between different data sets and regulatory limits.

The database is also coupled with the ORCHESTRA geochemical speciation and transport code which is written in the Java programming language.

A number of leaching procedures can be modelled with LeachXS using its built-in algorithms for coupled chemical speciation, reaction and transport processes. Although different laboratory leaching tests and field studies can be modelled with LeachXS, this section will focus on the description of the tests modelled in this study i.e. the pH-dependent and monolithic leaching test. An overview of the process for modelling these leaching tests with LeachXS is presented in Figure 6.1. Chemical speciation and transport calculations are conducted within LeachXS using the ORCHESTRA framework. Reference to modelling procedures within LeachXS thereafter will imply use of the ORCHESTRA framework coupled with the LeachXS database.

Figure 6.1 shows that there are 3 to 4 process steps required depending on the leaching test that is to be modelled. Obviously if only a pH dependence case is modelled there is no subsequent monolithic case model and completion is achieved when a good model fit has been obtained. Assessment of goodness of fit is described in more detail in Section 6.6 but in essence it is a measure of how well the mathematical model describes the natural phenomena. The boxes shaded in grey represent LeachXS functions/capabilities. These will be described in more detail in the following sections, including also the input parameters and key assumptions made for the modelling of the two leaching tests assessed in this study.

6.4 Modelling of Leaching Test Procedures

The focus of this study was the monolithic leaching test which is a dynamic leaching test involving immersion of a monolithic specimen (e.g. cube, cylinder etc.) in water (leachant) and renewal of the leachant at eight (8) different time periods (fractions). The high level process followed for modelling the monolithic leaching test using LeachXS follows the structure depicted in Figure 6.1. There are four (4) key steps involved in modelling the monolithic leaching test with LeachXS:

1. Data conversion to the LeachXS database format;
2. Chemical Speciation Finder;
3. pH dependence (equilibrium) run; and

4. Modelling of the monolithic leaching test.

The first three (3) steps also apply to the modelling of pH dependence or batch extraction tests and therefore the modelling methodology for these tests will be detailed in this section. Additional information, such as input parameters used to model the combined alkaline/acid leaching procedure will be described in separate sections.

6.4.1 Data Conversion to the LeachXS Database Format

Any manipulation and analysis of data with LeachXS requires that the data are in a format that the software can access/read. Leaching data already in the LeachXS database is in the format of a Microsoft (MS) Access database. New leaching data can be imported to LeachXS by converting to the same MS Access format.

ECN has developed a tool called 'Material Exchanger' that can convert spread-sheets (i.e. Excel files) into MS Access databases. The new leaching data that are to be imported to LeachXS are first transferred to a template spread-sheet that is provided along with the Material Exchanger. Material Exchanger then converts the spread-sheet in an MS Access database format. The newly created database can be merged with an existing LeachXS database or it can exist as a stand-alone database. The specifics of the 'Material Exchanger' are outside the scope of this study and will not be discussed. More information is provided in the manual of Material Exchanger.

Monolithic leaching data entered in the database include sample geometry, dimensions and weight (g.), moisture content (% wet. weight), the type and volume of leachant (ml), the contact time (h), the measured pH at each fraction of the test as well as leached concentrations of elements (μg/L). LeachXS uses these values in order to calculate release in mg/m^2 (emission of mass per surface area).

6.4.2 Chemical Speciation Finder

All the steps that follow conversion of the leaching data to the LeachXS DB format take place in a graphical user interface (GUI). The second step in the LeachXS modelling process is the calculation of chemical speciation based on measured leaching data.

Determination of chemical speciation (i.e. amounts or concentrations of chemical components in all phases present in equilibrium state) in the monolithic samples is based on calculation of saturation indices (SI) for all minerals in the LeachXS thermodynamic database for all fractions of the test. DOC interaction can also be taken into account through the NICA Donnan model. The SI results (0 indicates equilibrium, negative values represent undersaturation and positive values represent oversaturation) can be used to select a set of minerals that can be used in subsequent chemical speciation, pH prediction and monolithic leaching modelling runs. The Chemical Speciation Finder allows for the entry of multiple leaching data under the same run. For example, data for the pH dependent test and the monolithic leaching test can be present in the same run for chemical speciation. This has the benefit of identifying minerals of relevance which may not appear significant for both data sets due to the different test conditions.

Modelling with LeachXS requires a Chemical Speciation run prior to modelling of any leaching procedure. The Chemical Speciation Finder assists in identifying a possible set of relevant minerals for the material(s) of interest. The preliminary mineral set can be adjusted if required during subsequent modelling of leaching procedure i.e. monolithic leaching. Preliminary mineral sets for the different mixes in the present study were selected based on the results of the Chemical Speciation Finder as well as a review of relevant literature. As the chemical speciation run returns SI for all minerals in the database, only minerals with SI in the range [-0.2, +0.2] were considered for inclusion in the preliminary mineral sets.

It is noted that LeachXS also includes a method to weight the SI results obtained and provide a calculated figure called Figure of Merit (FOM). The FOM is used as an alternative method to sort and select minerals of relevance. The FOM was used as an indication of the relevance of a mineral. Selection of relevant minerals in this study was not only based on the FOM as calculated by LeachXS, but also on the review recent studies involving characterisation of raw and treated APC residues. This resulted in including minerals which had saturation indices outside the range noted above and with low FOM values.

6.4.3 pH-Dependence (Equilibrium) Case

Following the selection of a preliminary set of minerals relevant to the material to be studied, the next step involves running a pH-dependent leaching case. Modelling of pH-dependent tests in LeachXS involves calculating the concentration of different elements of concern at equilibrium state over a pH range from 2 to 14. Key input parameters for the model include the bulk material composition in the form of element availabilities, the set of relevant minerals as determined in the Chemical Speciation run, as well as the L/S ratio. Additional parameters pertaining to the waste material include solid and dissolved humic acid (DHA) concentrations, concentrations of hydrous ferric oxides (HFO) in the waste material, as well as concentrations of dissolved organic carbon (DOC). Finally, the chemical composition of the leachant can also be defined by the user.

This step is a requirement in the LeachXS modelling framework for the monolithic leaching test and therefore requires measured values for pH dependent release. Modelling of the pH-dependent release aims to establish the geochemical footprint of the materials which will subsequently serve as input for the monolithic leaching test model. Monolithic samples in this study however were not subjected to a pH-dependent leaching test and therefore such experimental data were not available.

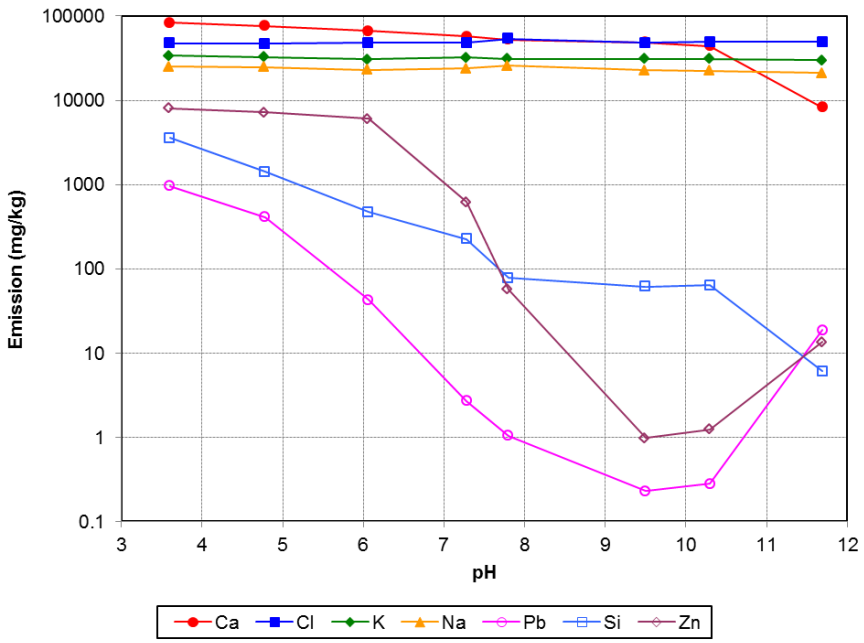

Figure 6.2 Release of selected constituents from surrogate S/S waste

Apart from modelling capabilities, LeachXS also includes a database of leaching data for various materials. One of the materials included in the LeachXS database is a cement S/S metal-containing waste[4] that was subjected to the ANC 14429 procedure. This leaching procedure involves parallel extractions of the material at an L/S of 10 for 48 hours at a series of pre-set pH values.

Given the LeachXS requirement to perform a pH-dependent modelling run before using the monolithic leaching model, as well as the lack of experimental pH-dependent release data for the S/S APC residue samples investigated in this study, the S/S waste material in the LeachXS database was used as a surrogate. All parameters and data required to model the pH-dependent release for the surrogate waste material were obtained from the LeachXS database, as well as from van der Sloot et al (2007) and Meeussen et al (2010). The measured release of selected constituents from the surrogate material over a pH range from 3.6 to 11.7 is shown in Figure 6.2, whereas a detailed report is included in Appendix IV. High release of Na, K and Cl irrespective of pH is observed for the surrogate material, which is consistent with release patterns for S/S APC residues in the present study. In addition, the surrogate material exhibits high release of Pb, Zn and Ca consistent with release behaviour of S/S APC residues investigated in this study as shown in Chapter 5.

Undoubtedly the use of a surrogate material may introduce additional uncertainties and significant deviation in composition from S/S APC residues investigated in this study may render modelling results invalid. It was considered appropriate, however, in this study for the following reasons:

- The surrogate material in the LeachXS database is of similar nature to the S/S APC residues investigated in this study, and includes similar elements of concern. As demonstrated above this includes high potential release of Pb and Zn, as well as soluble salts and Ca.
- It satisfies the LeachXS requirement for conducting a pH-dependent run prior to proceeding with modelling of the monolithic leaching test.
- As stated above, the pH-dependent run aims to establish the geochemical footprint of a given material which can then serve as input for the monolithic leaching test model. Therefore, the use of the surrogate materials aims to provide a preliminary set of

[4] LeachXS code is *Stabilised Waste NL (P,6,1)*

plausible solubility-controlling minerals, which only serves as a starting point for modelling of the monolithic leaching test which is the main focus of this study. This preliminary set was further refined during modelling of the monolithic leaching test based on actual experimental leaching data obtained for the S/S APC residues investigated in this study, coupled with existing observations in relevant literature on solubility-controlling minerals present in S/S APC residues.

It is noted that the use of a surrogate S/S material was only required for modelling of monolithic leaching test. Modelling of the alkaline/acid washing (leaching) procedures which is futher described in Chapter 8 did not require use of a surrogate materials as pH-dependent release data were available.

6.4.4 Monolithic Leaching Test

Modelling the monolithic leaching test is a complex task that involves both chemical reactions as well as contaminant transport. A number of parameters and/or variables are taken into consideration namely:

- Sample Geometry;
- Material Properties;
- Element Availability Concentrations;
- DHA and DOC concentrations; and
- Mineral Set.

a) Sample Geometry

One of the challenges in modelling the monolithic leaching test is the fact that in a real-life scenario release from the monolith is three-dimensional with all the surfaces of the specimen exposed to the leachant. LeachXS represents the real-life scenario by creating a grid comprising 24 cells. The allocation of the cells is as follows:

- Cell 0 represents the aggressive leaching solution (leachant);
- Cells 1-21 represent the solid phase layer;
- Cell 22 is the solution used for refreshing the aqueous phase (leachant); and

- Cell 23 is a "waste bucket" which is used only in the case of advection.

Assuming that the specimen to be tested is a cube, LeachXS creates the model grid by dividing the solid phase (specimen subjected to the leaching test) into 20 hollow cubes called cells. The geometry of each cell is derived as shown in Figure 6.3. The outer cell (cell 1) in contact with the leachant has a surface area of $A_1 = 6 \times L^2$ and a volume of $V_1 = A_1 \times dx$. The next cell (2) has a surface area of $A_2 = 6 \times (L-2dx)^2$ and a volume of $V_2 = A_2 \times dx$. The geometry of the subsequent 18 cells is derived in the same manner.

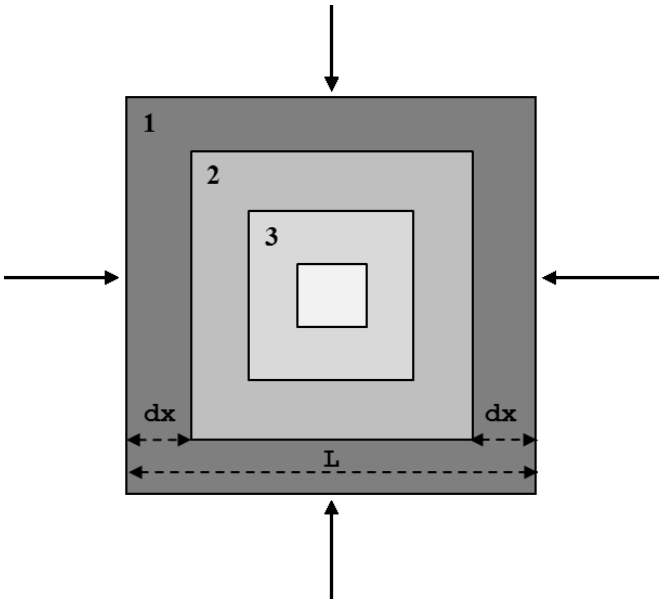

Figure 6.3 Idealisation of three-dimensional release in LeachXS

The geometry and dimensions of the specimen can be defined by the user. The distance *dx* is also a variable in LeachXS called 'Factor to increase size of successive grid cells'. This can be adjusted by the user in order to vary the geometry of the model cells. Transport is then calculated based on diffusion and concentration gradients between the compartments of the idealised structure in Figure 6.3. The specimens in this study were 50mm cubes. The distance *dx* was set between 1.25 and 1.28 based on data provided by ECN.

b) Material Properties

Material properties that can be adjusted in the model include bulk density, available porosity, tortuosity and pH. Bulk density values were calculated automatically by LeachXS based on the experimental (observed) data entered in the database. Values for material pH and porosity

were obtained from the experimental data and were entered manually using the LeachXS GUI. In particular, pH values were obtained from the ANC test at no acid (0 meq/g) addition. It is noted that this pH value refers to the natural pH of the material to be tested (i.e. S/S APC residues) and not the pH of the eluate at fractions of the leaching test.

Tortuosity was not determined experimentally for the samples tested in this study. Tortuosity was determined by varying its value in the model and assessing its effect on species with low retardation coefficients such as soluble salts (i.e. Na and Cl). The tortuosity value that resulted in the best fit with leaching data for such elements was selected for subsequent modelling runs.

c) Element Availability, DHA and DOC Concentrations

Input of element availabilities, DHA and DOC concentrations has been described as part of the pH-dependence run. The majority of availability concentrations, as well as DHA and DOC concentrations were obtained from the surrogate material in the LeachXS database and previous modelling studies on stabilised waste conducted by ECN. These parameters are summarised in the following sections for each mix modelled.

d) Mineral Set

The mineral set is one of the key variables in the model. The initial mineral set was based on the Chemical Speciation Finder and pH-dependence runs for the surrogate material. The mineral set was adjusted after each modelling run until a good fit with the measured values was obtained. The mineral set was adjusted based on previous studies in the literature as well as other probable minerals according to LeachXS SI calculations.

In general, due to the lack of data for tortuosity and element availability concentrations the modelling framework for the monolithic leaching test consisted of the following steps:

1. Adjustment of tortuosity values until a good fit is obtained for release of soluble salts;
2. Adjustment of mineral set and/or availabilities until a good fit is obtained for pH and the release of major elements such as Ca, Al, SO_4^{2-} etc.
3. Adjustment of mineral set and/or availabilities until a good fit is obtained for trace elements of concern such as Pb and Zn.

6.5 Data Analysis

A number of runs were conducted for each modelling case varying the different input parameters of the model (problem definition). Modelling cases investigated as part of the present study include the following mixes:

- 50 wt.% CEM I, w/s: 0.5
- 50 wt.% GGBS, w/s: 0.5
- 20 wt.% CEM I, w/s: 0.5
- 10 wt.% CEM I, w/s: 0.5

As the w/s ratio is the same for each of the mixes investigated, the modelling study evaluated the effect of binder type and content on the leaching characteristics of the S/S APC residues. Water content was not investigated in the modelling study due to the fact that varying the w/s ratio (for the same binder addition) did not result in statistically significant results in terms of monolithic leaching as it will be explained in the Discussion chapter.

Modelling results for each element were compared to the observed values by calculating the residuals, i.e. difference between observed and predicted value. Different statistical methods exist for determining the goodness of fit. In the present study due to the low number of data points (8 values for the tank test and 9 fractions for the pH-dependence test), the sum of the squared residuals from all test fractions was used to determine goodness of fit for each element as well as pH. In summary, the problem definition with the best fit for each element and pH was determined according to the following equation:

$$m_X = min\left[\sum_{i=1}^{z}(y_i^{obs} - y_i^{pred})^2\right] \quad (6.1)$$

where,

m_X, is problem definition with the best goodness of fit for the elements of concern as well as pH;

z, is the total number of fractions of the leaching test modelled. z = 8 for the monolithic leaching test and z = 9 for the pH dependence test;

y_i^{obs}, is the measured value (element concentration or pH) determined experimentally for leaching fraction *i*.

y_i^{pred}, is the model predicted value (element concentration or pH) for leaching fraction *i*.

The overall goodness of fit obtained from the different mineral sets was then assessed based on the goodness of fit of individual elements and pH as shown in Equation 6.2. The sums of the squared residuals for each element and pH were added to obtain a single number for each problem definition. In addition, weights were applied to the different elements in order to avoid skewed results due to large residual values for elements with high leached concentrations (e.g. Ca).

$$M_X = min\left[\sum_1^n m_X\right] \quad (6.2)$$

The M_X value was then used as an indicator of goodness of fit, and the problem definitions (set of parameters) from the different modelling runs were compared based on these values as well as existing literature to improve the problem definition for subsequent runs. The same methodology for assessing goodness of fit was used for both the monolithic and the pH-dependence test. The comparison between measured and predicted values for the monolithic leaching test was performed on the concentrations (mg/l) for each leaching fraction whereas for the pH-dependence test it was based on the measured release (mg/kg) for each batch extraction.

In addition, the effect of varying the model input parameters was evaluated using statistical techniques such as paired t-tests and analysis of variance (ANOVA). The commercial statistical software package STATA (v. 9.2) was used for all statistical analyses.

6.6 Results

This section presents the results from the modelling study for both the monolithic leaching test and the alkaline/acid leaching procedure. The section for the monolithic leaching test is further subdivided based on the different elements of concern. It is noted that although many modelling runs were conducted in order to assess the significance of individual model parameters, the results presented below pertain to the set of parameters that yielded the best fit for the majority of the elements.

6.6.1 General Observations

a) Model Complexity

In summary, the input to the model comprises fixed element availabilities, a set of possible solubility-controlling minerals, active Fe- and Al-oxide sites (where Fe- and Al-oxides are summed and used as input for hydrous ferric oxides), clay content to quantify clay interaction, particulate organic matter, and a description of the DOC concentration as a function of pH (using a polynomial curve fitting procedure) (Meeussen et al, 2010).

The speciation of all elements and transport of ions is calculated in LeachXS based on a single problem definition (i.e. one set of parameters). Moreover, the numerous possible combinations of relevant minerals, significantly increases the complexity in forming the problem definition. This limits the degrees of freedom in selecting parameters, as improvement of the model for one element may worsen the outcome for other elements.

As element availabilities were not measured for the S/S APC residues investigated in this study, data from previous similar studies (van der Sloot et al, 2007; Meeussen et al, 2010) were used as a starting point for certain elements. These studies used the maximum release value as obtained in the pH-dependence leaching test (between pH 3 and 13) as the available concentration. Lack of measured availability concentrations, constitutes an additional level of uncertainty. Therefore sensitivity analysis was conducted using availability concentrations of the raw APC residues (as provided by the EfW plant operator) in cases where availability data were found to be significantly influencing model predictions (i.e. sulphur, carbonate, calcium).

b) Dissolved Inorganic Carbon (DIC)

As with previous modelling studies using LeachXS (Meeussen et al, 2010), it was found that total (available for leaching) carbonate concentration can significantly affect the model results. This parameter was not measured either in the present study or the studies from which element availability data was obtained. Leachable carbonate concentration was estimated by Meeussen et al (2010) based on the total inorganic carbon content. In their study, the concentration was adjusted until the major elements (mainly Ca as calcite) showed a reasonably good match with the observed leaching data, as this is the main phase for carbonate in the cementitious systems investigated. A similar approach was also followed in the present study.

c) Soluble Salts

Constituents of soluble salts such as Na, K, Li and Cl were not found to be affected by the set of relevant minerals for all mixes investigated in the modelling study. It was observed that differences in predicted concentrations were not statistically significant ($p < 0.05$) and in fact there was no difference observed for the majority of the fractions of the leaching test. Predicted concentrations were only affected by changes in porosity (ε) and tortuosity (τ) (i.e. the "obstruction" factor ε/τ). This result also justifies the approach of the modelling study to determine the tortuosity value based on the best fit for elements such as Na and Cl, since porosity values were determined experimentally.

In addition, since Na, K, Cl and Li were not affected by differences in the mineral set (parameter of the problem definition) they were not taken into account in the set of elements when determining goodness of fit for the different mineral sets evaluated.

6.6.2 Monolithic Leaching Test

a) Portland Cement (CEMI)

The set of parameters (problem definition) that resulted in the best fit for the majority of the elements of each of the CEM I mixes investigated is presented in Table 6.1.

Table 6.1 Problem definitions for CEM I mixes modelled in the study

CEM I Mix	50 wt.%	20 wt.%	10 wt.%
Mineral Set	AA_CaO_Al2O3_8H20[s] AA_CaO_Al2O3_SiO2_8H20[s] AA_CaO_Al2O3_CaCO3_11H20[s] AA_CaO_Fe2O3_CaSO4_12H20[s] AA_Brucite AA_Calcite AA_Gypsum AA_Jennite AA_Portlandite AA_Tobermorite-I CaZincate Cd[OH]2[A] Celestite Cu[OH]2[s] Ettringite_ECN Ferrihydrite Manganite Ni[OH]2[s] Pb[OH]2[C] P-Wollstanite Willemite	AA_CaO_Al2O3_8H20[s] AA_CaO_Al2O3_SiO2_8H20[s] AA_CaO_Fe2O3_SiO2_8H20[s] AA_CaO_Fe2O3_CaSO4_12H20[s] AA_Brucite AA_Calcite AA_Fe[OH]3[microcr] AA_Gypsum AA_Jennite AA_Tobermorite-I AA-Tricarboaluminate CaZincate Cd[OH]2[A] Cu[OH]2[s] Ferrihydrite Lime Manganite Ni[OH]2[s] Plattnerite P-Wollstanite Strontianite	AA_CaO_Al2O3_8H20[s] AA_CaO_Al2O3_SiO2_8H20[s] AA_CaO_Fe2O3_SiO2_8H20[s] AA_CaO_Fe2O3_CaSO4_12H20[s] AA_Brucite AA_Calcite AA_Fe[OH]3[microcr] AA_Gypsum AA_Jennite AA_Tobermorite-I AA-Tricarboaluminate CaZincate Cd[OH]2[A] Cu[OH]2[s] Ferrihydrite Lime Manganite Ni[OH]2[s] Plattnerite P-Wollstanite Strontianite
Availability Concentrations (mg/kg)			
Ca	83,600	150,000	160,000
Al	4,456	4,450	4,450
Si	3,560	3,556	3,000
H_2CO_3	8,000	13,500	16,500
SO_4	10,600	23,350	23,400
Fe	73.9	73.9	73.9
Na	10,000	17,000	18,000
K	10,000	19,000	19,000
Cl	53,500	91,450	96,000
Li	17.5	15.0	12.5
Mg	3,903	3,903	3,903
Mn	174.8	174.8	174.8
Pb	956	1,600	1,800
Zn	1,330	3,700	4,320
V	0.58	0.58	0.58
Cd	17.8	17.8	17.8
Cr	4.5	9.7	9.7
Ni	9.3	9.3	9.3
Sr	206	206	206
Ba	19.3	19.3	19.3
pH (*natural)*	12.56	12.30	12.30
HFO (kg/kg)	0.0001	0.0001	0.0001
SHA (kg/kg)	0.0001	0.0001	0.0001
Physical Properties			
Porosity	0.38	0.40	0.46
Tortuosity	1.7	1.5	1.2

As shown by the results of the experimental study there are no significant differences in the leaching results and mineralogy between the 20 wt.% and 10 wt.% CEM I mixes. The modelling study shows that a very similar problem definition describes release from these mixes for the majority of the elements of concern. The main differences in the problem definition for the 10 and 20 wt.% CEM I mixes are predominantly in the availabilities of elements of concern and the physical properties of the two matrices.

pH

Accurate prediction of pH is important in order to assess the potential release of elements of concern such as Pb and Zn, whose solubility depends predominantly on pH. As shown in Figure 6.4, the model predicts the pH of the mixes investigated within a 0.03-0.4 unit range. Carbonation effects were not taken into account in the model which may explain over-prediction of pH for the 50 wt.% CEM I mix for the late fractions of the leaching test with the long duration intervals (i.e. 36 and 64 days).

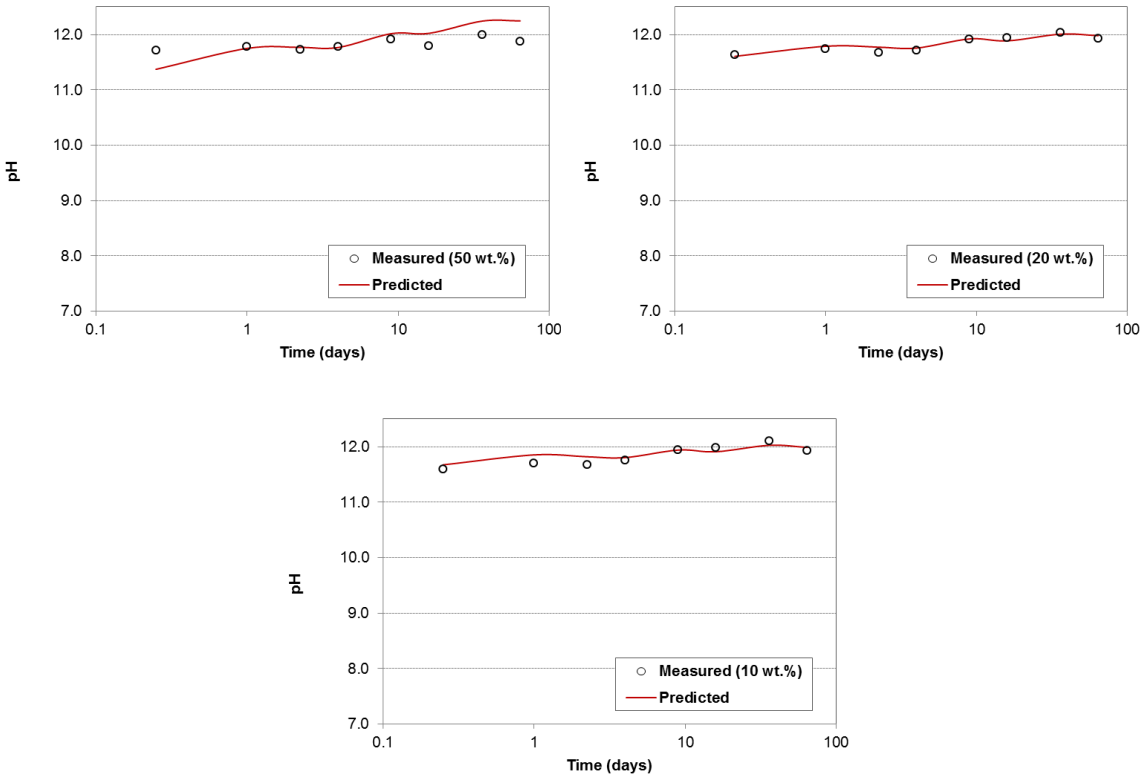

Figure 6.4 Measured and predicted pH for CEM I mixes

The model predictions agree relatively well with the measured values for all mixes but differences of up to 0.4 units are observed for later fractions of the leaching test. Under-prediction of pH may result in under-prediction of elements of concern such as Pb and Zn as discussed below. As expected, the natural pH of the material affects the model predictions which is evident when comparing the results for CEM I and GGBS (see separate section). It is noted that the study considered as natural, the pH values obtained from the ANC test at no (0 meq/g) acid addition.

Ca, Al and Si

Given the cementitious nature of the S/S specimens, calcium, aluminium and silicon are considered structural elements for the S/S matrix. As discussed in section 2.3.1, leaching of Ca (decalcification) can have long term detrimental effects on the structural stability of the cementitious matrices resulting in higher porosity and loss in compressive strength. The results for the predicted cumulative release for Ca, Al and Si for each of the CEM I mixes investigated are shown in Figures 6.5a-c.

Predicted release of Ca was found to depend predominantly on the presence of portlandite, calcite, as well as the availability of carbonate. As noted in the previous section, due to the lack of available data the availability of carbonate was adjusted until a good fit was observed for leaching Ca. In addition, Ca availabilities used by Meeussen et al, (2010) and van der Sloot et al, (2007) were used only for the 50 wt.% CEM I mix and were adjusted for the 10 and 20 wt.% mixes to account for the higher availability of calcium in these mixes. As calcium in raw APC residues is mainly present in soluble minerals (lime, CaClOH and anhydrite) and the extent of hydration is questionable[5] it is expected that these mixes would exhibit greater availability of Ca (i.e. CaClOH is more soluble than CSH). The availability for Ca for these mixes was adjusted based on total concentration and availability data provided by the EfW plant operator and producer of APC residues. This data indicates that the total concentration of Ca in APC residues is 290 g/kg and the availability for leaching for Ca is approximately 270 g/kg. This shows that the majority (>90%) of Ca present in raw APC residues is soluble.

[5] Hydration calorimetry in the experimental section showed severe retardation of hydration for mixes with low binder content.

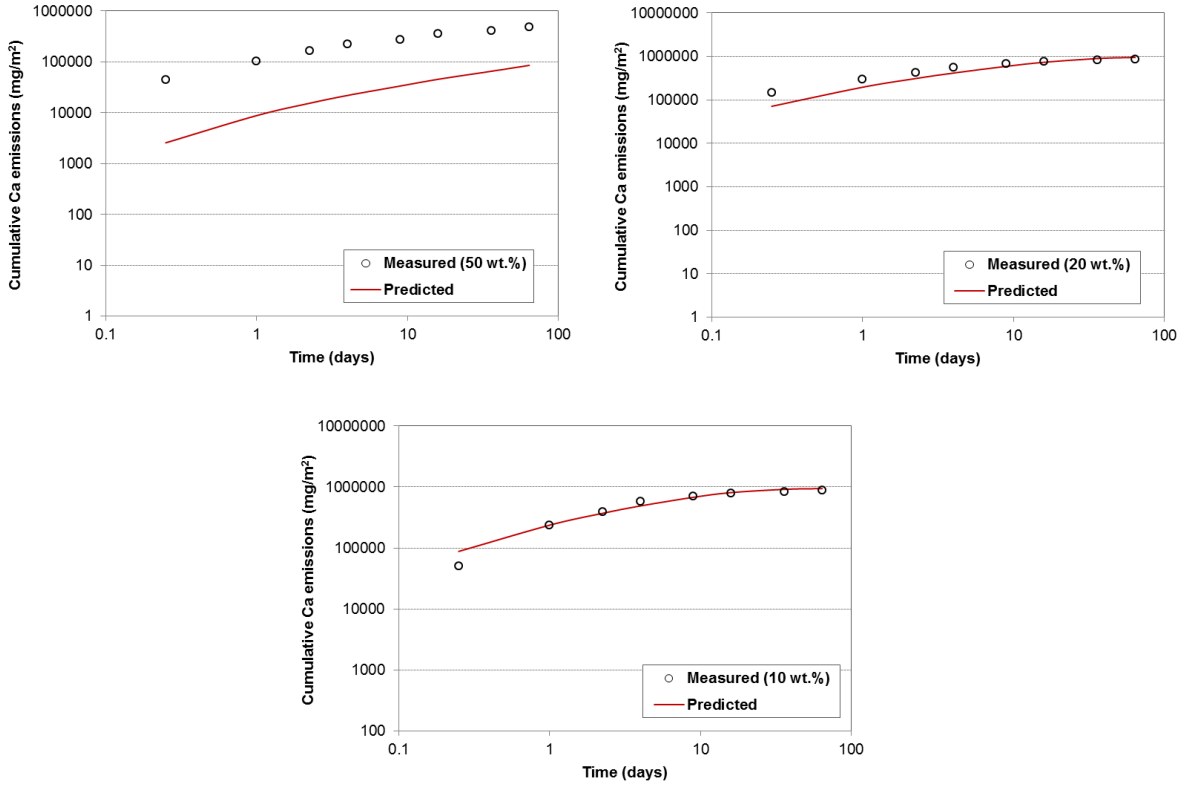

Figure 6.5a Cumulative measured and predicted Ca release for CEM I mixes

Fairly accurate predictions for the release of calcium were obtained for the majority of the mixes after adjusting for carbonate and in the cases of 10 and 20 wt.% CEM I, calcium availability. The problem definitions including the set of Ca-containing relevant minerals coupled with the selected availabilities for each mix, describe well the differences in release by increasing the content of APC residues in the S/S matrix. Portlandite and calcite were found to have the most significant effect on the predicted release of Ca for 50 wt.% CEM I mixes. Model predictions for the 50 wt.% mix were underestimated by an order of magnitude despite adjustments to the carbonate availability. Inclusion of calcite in the mineral set was found to suppress leaching of Ca, whereas better agreement was obtained in the absence of the mineral. Chemical speciation calculations showed under-saturation of calcite (SI < 0) for all fractions of the test. However, the mineral was selected based on the results of the X-ray diffractograms and previous studies investigating cementitious matrices and S/S waste. Model predictions for 10 and 20 wt.% mixes agree well with measured values. Lime and predominantly calcite were found to control release of Ca for these mixes. Lime was selected instead of portlandite to account for soluble minerals such as CaClOH which are not present in the thermodynamic database of LeachXS.

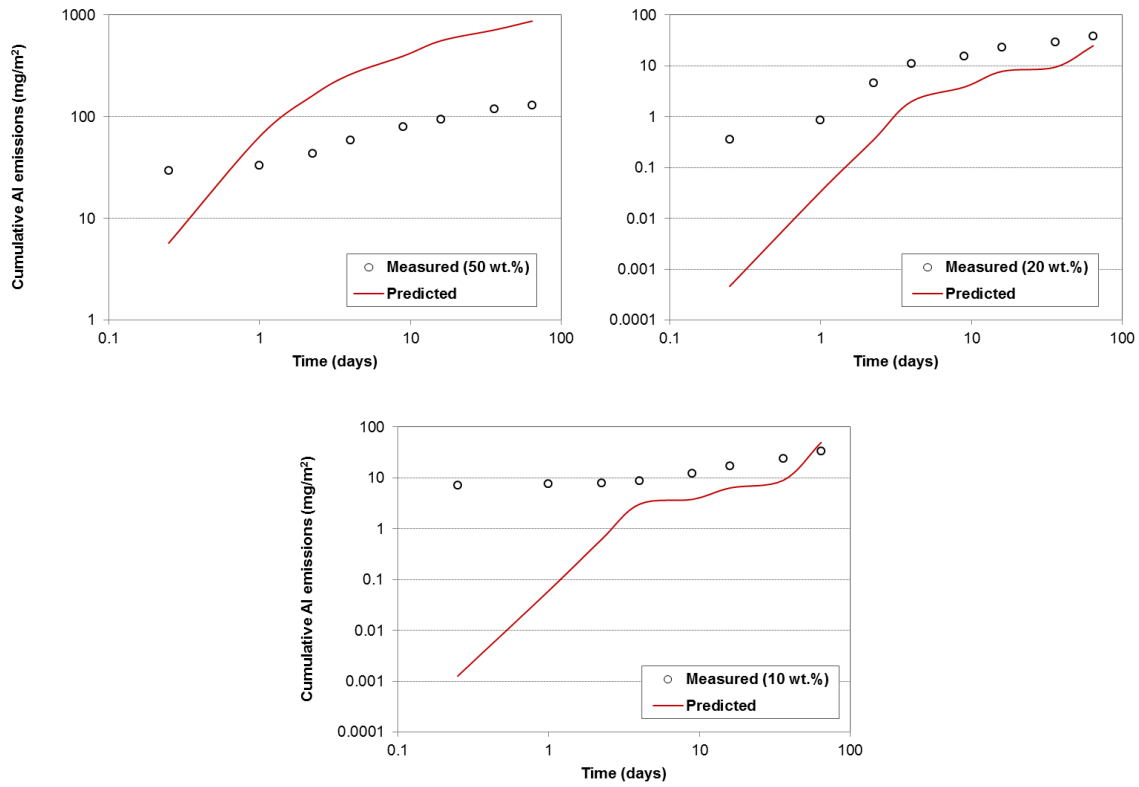

Figure 6.5b Cumulative measured and predicted Al release for CEM I mixes

The model over-predicts release of Al for the 50 wt.% CEM I mix by an order of magnitude for the majority of the test fractions. In contrast, the 64-day model predictions for Al for 20 and 10 wt.% CEM I mixes agree reasonably well with the measured values, although the 64-day release is underestimated for the 20 wt.% CEM I mix. It is observed that the model under-predicts release of Al for early leaching intervals for 20 and 10 wt.% CEM I mixes. It is noted however that results obtained for these fractions of the leaching test for these mixes were below the laboratory detection limit and the latter was selected for the presentation of results. The actual Al concentrations released may be lower than the measured concentrations presented here and therefore model predictions are considered representative of Al emissions during early fractions of the monolithic leaching test.

In general, obtaining good predictions for the release of Al was challenging. Attempts to modify the problem definition to improve predictions for Al resulted in hampering predictions for other constituents, such as SO_4^{2-}. This is attributed to the complexity of the Al-containing hydrates such as AFm with varying end members such as OH, SO_4, Cl and CO_3^{2-} or their solid solutions (Matschei, 2007). Moreover, although availability concentrations by Meeussen et al, (2010) and van der Sloot et al, (2007) were used for all

mixes, these values may not be entirely representative, especially for mixes with low binder addition. Therefore, availabilities for these mixes would need to be determined to confirm the results of this study.

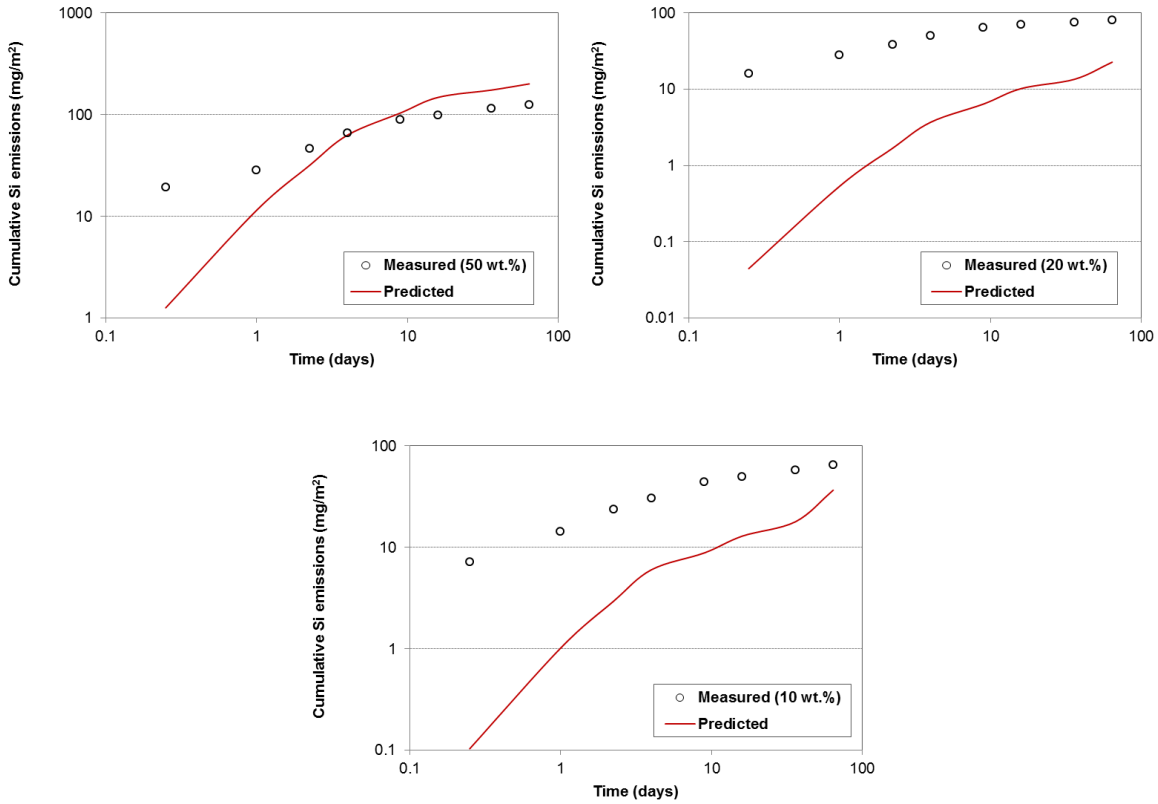

Figure 6.5c Cumulative measured and predicted Si release for CEM I mixes

Similar observations to Al also pertain to Si. Si was shown to exhibit solubility controlled release for the majority of the CEM I mixes. Release patterns agree reasonably well with measured values and the 64-day predicted release is in the same order of magnitude for the majority of the mixes, although the model under-predicts release for 10 and 20 wt.% CEM I mixes. Release of Si appears to be controlled by diffusion at early leaching intervals with easily soluble Si compounds in the matrix providing the driving force for diffusion. As hydration reactions proceed however, release of Si continues from less soluble Si hydration products based on solubility-control. It should be noted that the minerals selected to describe the CSH gel were Jennite and Tobermorite-I. Although CSH exists as a separate mineral in the LeachXS thermodynamic database the selection of Jennite and Tobermorite-I type gel was selected based on previous similar studies (Meeussen et al, 2010; Lothenback and Winnefeld, 2007). Differences in the results obtained by using the CSH mineral in the database however, were not statistically significant ($p < 0.05$).

Alkali Metals (Na, K, Li)

The results for the predicted cumulative release for Na, K and Li for each of the CEM I mixes investigated are shown in Figures 6.6a-c. It is noted that the availability of Na and K was adjusted based on known data for their availability in raw APC residues, assuming that they will be present in the form of soluble salts (i.e. NaCl, KCl).

As these elements are constituents of soluble salts present in APC residues, the predicted release was not affected by changes in the mineral set as part of the problem definition. Additions of possible solubility-controlling minerals did not result in statistically significant differences between the predictions. In contrast, release of these elements was only affected by changes in physical properties, namely porosity and tortuosity. Previous studies have identified incorporation of alkalis in CSH or other hydration products (Lothenbach and Winnefeld, 2007; Sung-Yoon Hong and Glasser, 1999). In the present study, release of alkali metals based predominantly on the physical properties of the matrix was found to provide an accurate indication of potential release without accounting for incorporation in any hydration phases. Nevertheless, this may be attributed to the large concentration of these metals (mainly Na and K) which may overshadow any smaller fractions incorporated in hydration phases.

It is observed that predicted 64-day release is in the same order of magnitude for all mixes. The cumulative release for Na and K is under-predicted for early test fractions (1-4) but agrees well with measured values for later test fractions (5-8). Initial problem definitions over-predicted release of Li for the majority of the test fractions for all CEM I mixes. This was attributed to an over-estimated availability for Li for mixes in the problem definition. Release of Li was found to be availability-controlled and was found to increase with increasing binder content as shown in the experimental section. This suggests that Li is present in lesser amounts in mixes with lower binder content and therefore has lower availability. Hence, availability concentrations for Li in the model were adjusted to fit measured values and the results are shown in Figure 6.6c.

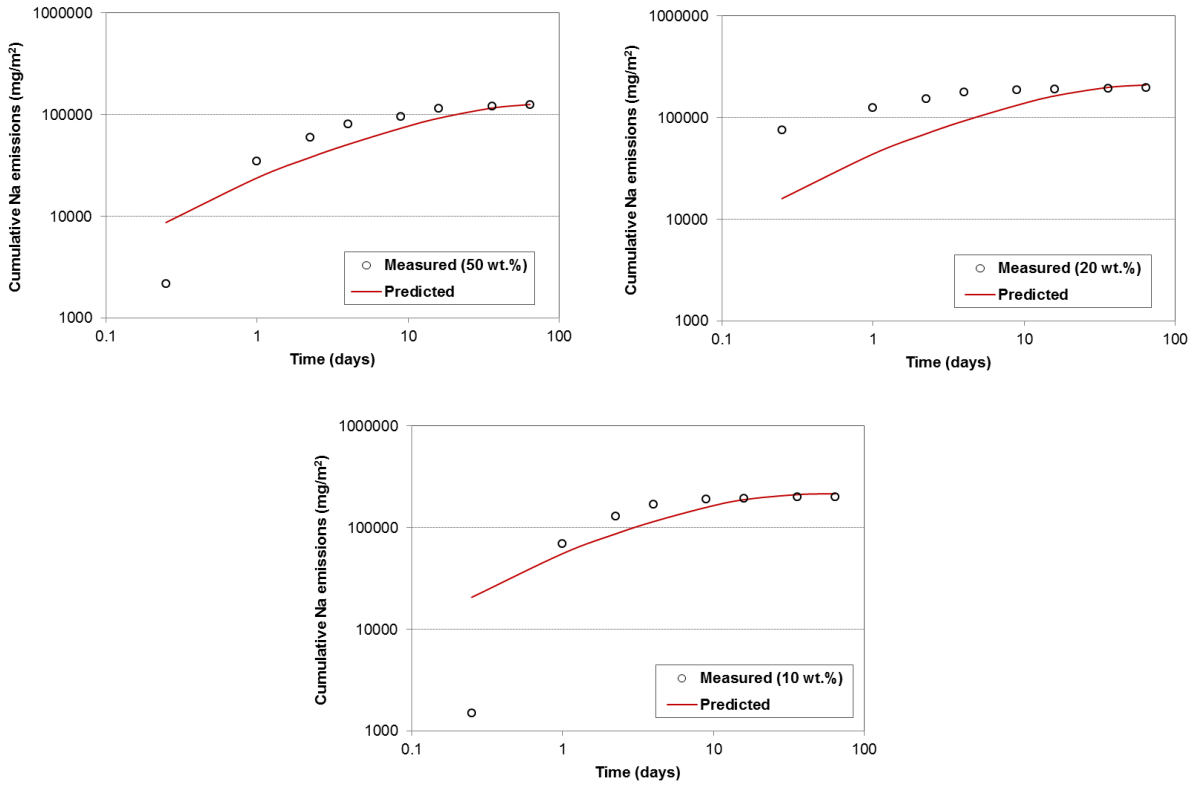

Figure 6.6a Cumulative measured and predicted Na release for CEM I mixes

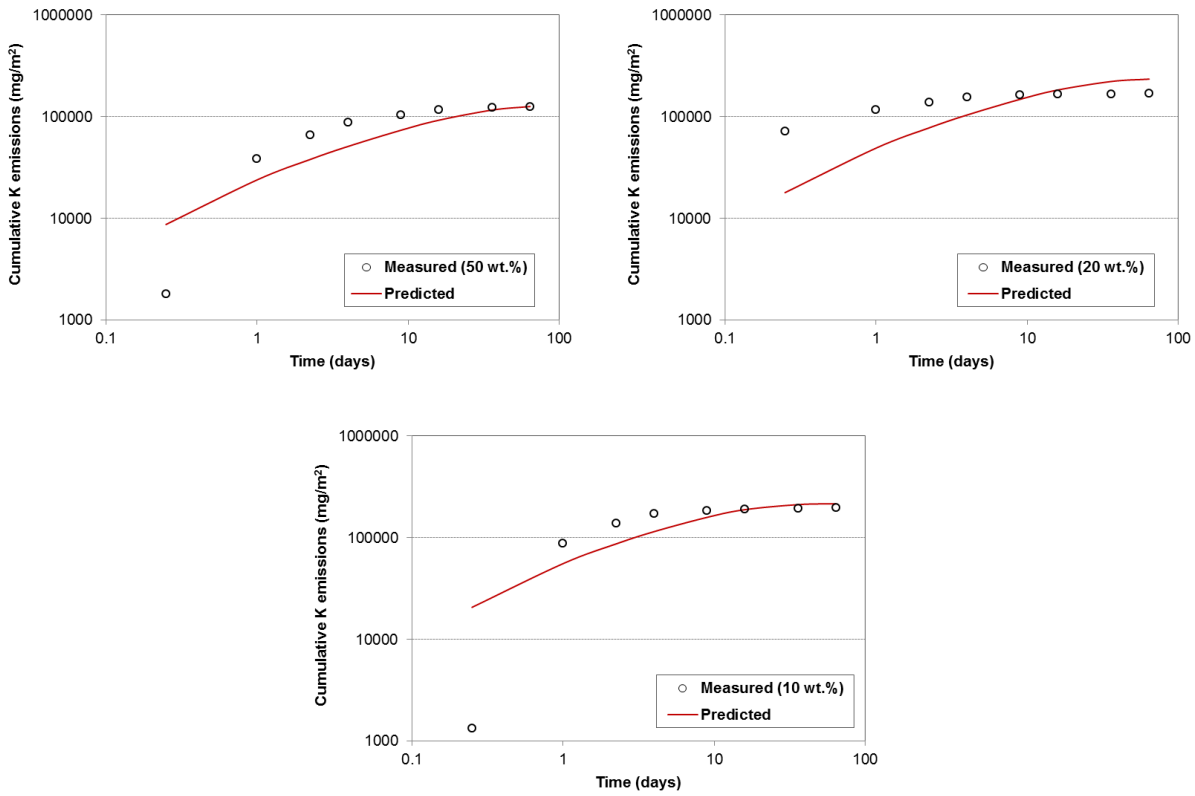

Figure 6.6b Cumulative measured and predicted K release for CEM I mixes

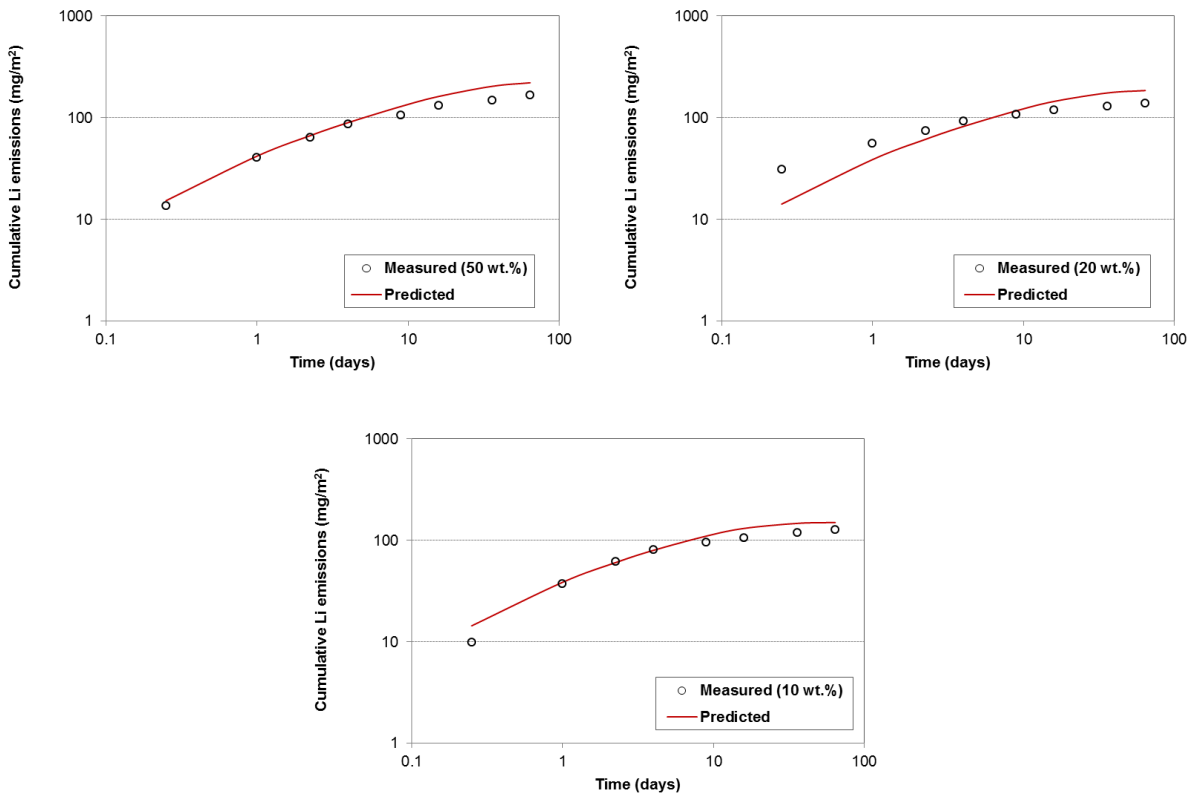

Figure 6.6c Cumulative measured and predicted Li release for CEM I mixes

The effect of tortuosity on the release of soluble salts is demonstrated below by conducting a sensitivity analysis on the release of Cl. Since release of Na, K and Cl is associated with the presence of soluble salts, these elements are affected in a similar manner by changes in tortuosity. Therefore sensitivity analysis is presented only for Cl.

Finally as release of these elements is availability-controlled, an additional parameter that affects the predicted release is the availability for leaching as part of the problem definition. The availability of these elements was adjusted based on their availability for leaching in raw APC residues. The effect of the availability is observed by comparing the predicted release for Na, K and Li for each of the mixes. Figures 6.6a-c show that high availability concentrations in the problem definition result in greater predicted release.

Chloride

The results for the predicted cumulative chloride release for each of the CEM I mixes investigated is shown in Figure 6.7. It is observed that the model predictions agree reasonably well with measured chloride release for the majority of the leaching test fractions. Predicted release was not affected by changes in the set of relevant minerals, but as Na and K, it was affected by changes in physical properties of the S/S matrix, namely, porosity and tortuosity. It is noted again that porosity was measured experimentally, whereas tortuosity was determined based on the best fit for soluble salts.

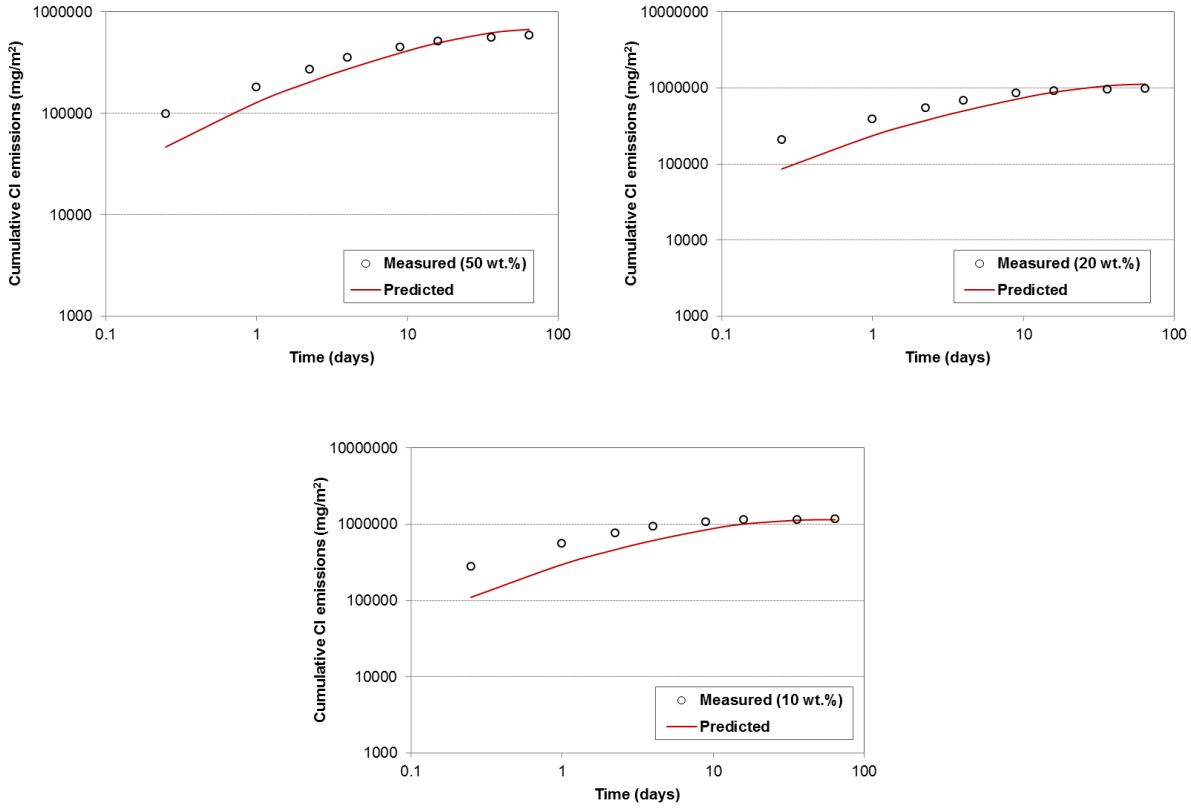

Figure 6.7 Cumulative measured and predicted Cl release for CEM I mixes

Sensitivity analysis was conducted to assess the effect of tortuosity on leaching of Cl. Figure 6.8 presents results obtained by varying the tortuosity of the specimen for the 50 wt.% CEM I mix at w/s: 0.5. As expected increasing tortuosity results in a decrease in the predicted chloride release. Similar results were obtained for the rest of the CEM I and GGBS mixes that were investigated.

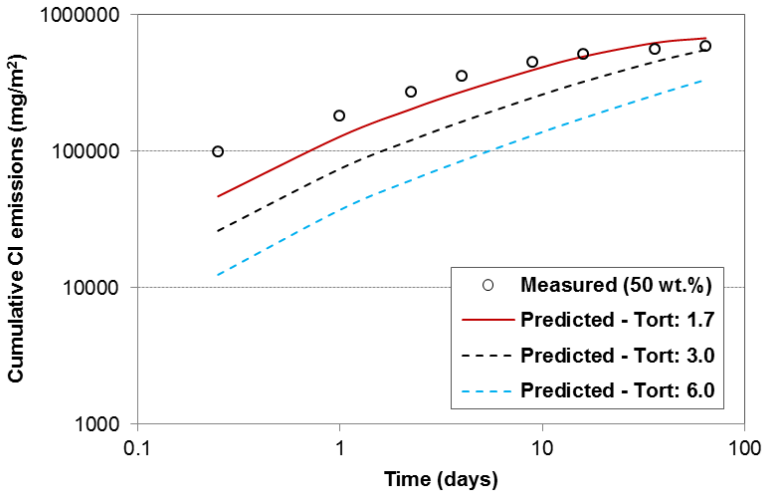

Figure 6.8 Effect of tortuosity on the release of Cl

Mineralogical analysis as part of the experimental study identified the presence of a chloride-containing calcium aluminate hydrate. Data for hydrates such as Friedel's salt or hydrocalumite-Cl are not present in the default LeachXS database. A recent study by Balonis et al, (2010) provided thermodynamic data for hydration products formed in the presence of chlorides and sulphates such as Friedel's salt and Kuzel's salt. The data obtained are shown below and were entered in the LeachXS database in order to assess the effect of these hydration products on the release of Cl. In addition, thermodynamic data for hydrocalumite-Cl were provided by ECN and were also included in the mineral set to assess immobilisation of chloride in hydration products.

Friedel's Salt: $Ca_4Al_2(OH)_{12.05}(Cl)_{1.95}.4H_2O = 4Ca^{2+} + 2AlO_2^- + 1.95Cl^- + 4.05OH^- + 8H_2O$; $logK_{sp}$: -27.69

Kuzel's Salt: $Ca_4Al_2\ (SO_4)_{0.5}(Cl)(OH)_{12}.6H_2O = 4Ca^{2+} + 2AlO_2^- + Cl^- + 0.5SO_4^{2-} + 4OH^- + 10H_2O$; $logK_{sp}$: -28.53

It was observed that Friedel's or Kuzel's salt are under-saturated for all test fractions (SI < 0) and had no effect on the release of Cl in model prediction. Hydrocalumite-Cl was found to form in later leaching fractions which may reflect the formation of a polytype of Friedel's salt (Renaudin et al, 2005). The effect of the addition of hydrocalumite-Cl on the release of Cl is shown in Figure 6.9. The model including hydrocalumite-Cl resulted in a difference of +14% compared to the measured 64-day release whereas the model without hydrocalumite-Cl resulted in a difference of +3%. Although inclusion of hydrocalumite-Cl improved prediction for Cl, it significantly worsened prediction for Al and SO_4. Given the marginal improvement in the prediction for Cl, hydrocalumite-Cl was not considered for subsequent model runs.

Nevertheless, this study confirmed that Cl-containing AFm phases can act a sink for free Cl^- ions and can play an important role in Cl fixation at lower Cl concentrations or in cases of external Cl ingress.

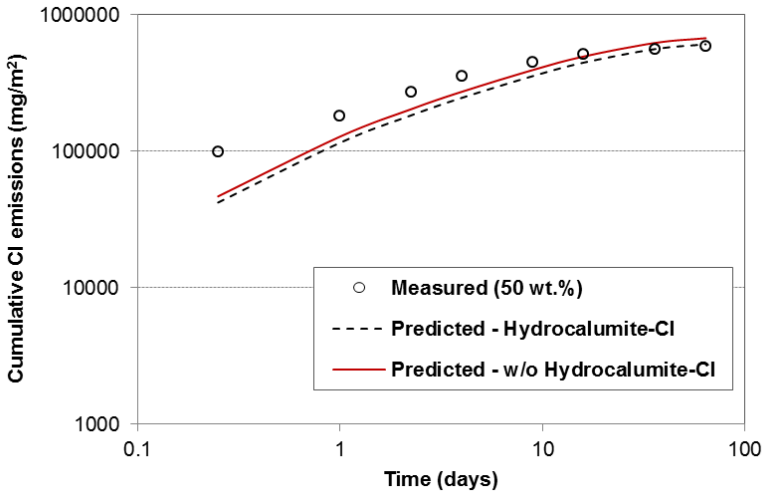

Figure 6.9 Effect of chloride-containing hydrates on the release of Cl from 50 wt.% CEM I mixes

Sulphate

The results for the predicted cumulative sulphate release for each of the CEM I mixes investigated are shown in Figure 6.10. Availability concentrations for the 50 wt.% mixes were as for the rest of the elements from the literature. Availabilities for the 10 and 20 wt.% mixes were adjusted in a similar manner to Ca, based on the availability of SO_4 in raw APC residues as provided by the operator of the EfW plant. This was meant to account for the higher amount of water soluble sulphate in mixes with low binder content. It is noted that the availability of SO_4 reported by the EfW plant operator is approximately 61 g/kg.

Predictions agree fairly well with the measured data for all mixes as shown in Figure 6.10, although the model over-predicts release for the 50 wt.% CEM I mix . Gypsum was found to control release for the 50 wt.% mix, whereas anhydrite was also investigated as a potential release-controlling mineral for mixes with lower binder addition. However, choosing between gypsum and anhydrite did not result in statistically significant differences in the model predictions. Model prediction for the 50 wt.% CEM I mix using the availability obtained from the literature (approximately 10,000 mg/kg), typically resulted in over-prediction

compared to the measured release. SO_4 availability for the 50 wt.% CEM I mix was adjusted to approximately 2,500 mg/kg as part of sensitivity analysis. As expected, adjusting the availability of SO_4 resulted in improved model predictions as shown in Figure 6.11. The fate of SO_4 in CEM I mixes with high binder addition requires further investigation.

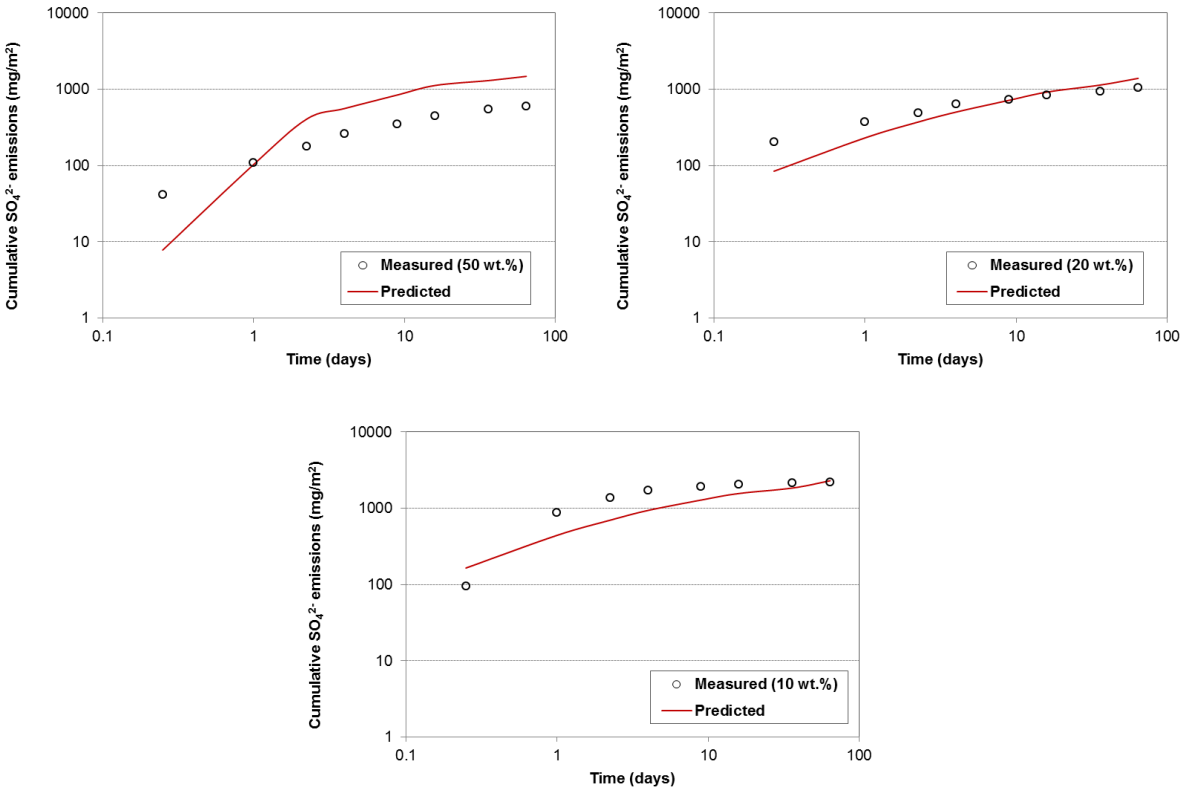

Figure 6.10 Cumulative measured and predicted SO_4^{2-} release for CEM I mixes

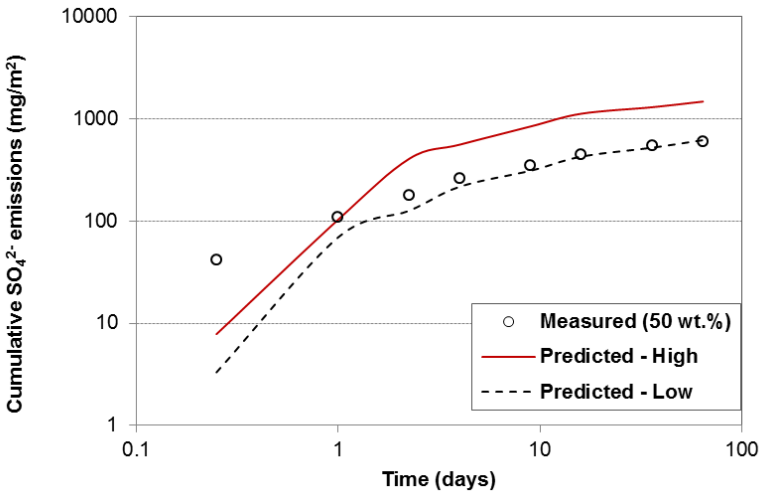

Figure 6.11 Effect of availability on the release of SO_4^{2-} for 50 wt.% CEM I mixes (High: 10600 mg/kg; Low: 2500 mg/kg)

Zinc

The results for the predicted cumulative zinc release for each of the CEM I mixes investigated are shown in Figure 6.12. In the case of 50 wt.% CEM I mixes all Zn-containing minerals investigated resulted in an over-prediction of the 64-day release by an order of magnitude. This indicates that availability of Zn might be overestimated in the problem definition of the 50 wt.% mix. In contrast, there is better agreement with measured emissions for the release of Zn from 10 and 20 wt.% CEM I mixes. Zn release for these mixes was found to be controlled by calcium zincate. Calcium zincate has been previously reported (Asavapisit et al, 1998) to precipitate on unreacted cement grains, preventing contact with water and inhibiting further hydration.

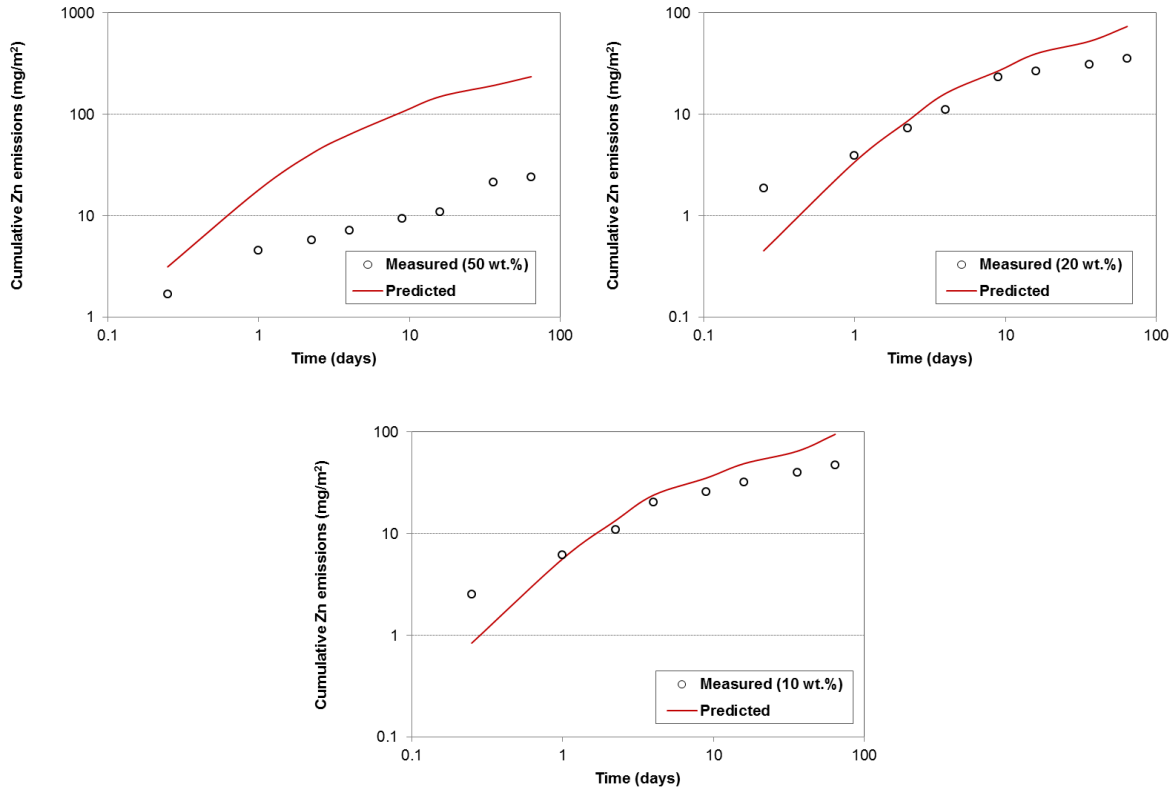

Figure 6.12 Cumulative measured and predicted Zn release for CEM I mixes

The model results agree with the measured values indicating that release of Zn is not fully diffusion-controlled. The results indicate that there may be changes in the release mechanisms starting with diffusion-controlled release (concentrations increase with leaching duration for each fraction) whereas solubility-controlled release is observed for later leaching fractions. This is particularly evident for mixes with lower binder additions.

It is noted that availability concentrations for Zn for mixes with lower binder addition were adjusted based on total concentrations provided by the EfW operator (see Appendix I). Admittedly this may result in an overestimation of the available concentrations for leaching it was taken into consideration as a worst case scenario. However, as release of Zn was found to be predominantly controlled by the solubility of calcium zincate, varying availability concentration did not result in significant differences in the model predictions.

Lead

The results for the predicted cumulative lead release for each of the CEM I mixes investigated are shown in Figure 6.13. The selection of $Pb(OH)_2$ as the relevant mineral for Pb was found to adequately describe its emission for 50 wt.% CEM I mixes. Although model predictions do not agree well with the measured values for early leaching intervals for the 50 wt.% CEM I mix, good agreement is observed for 64-day release.

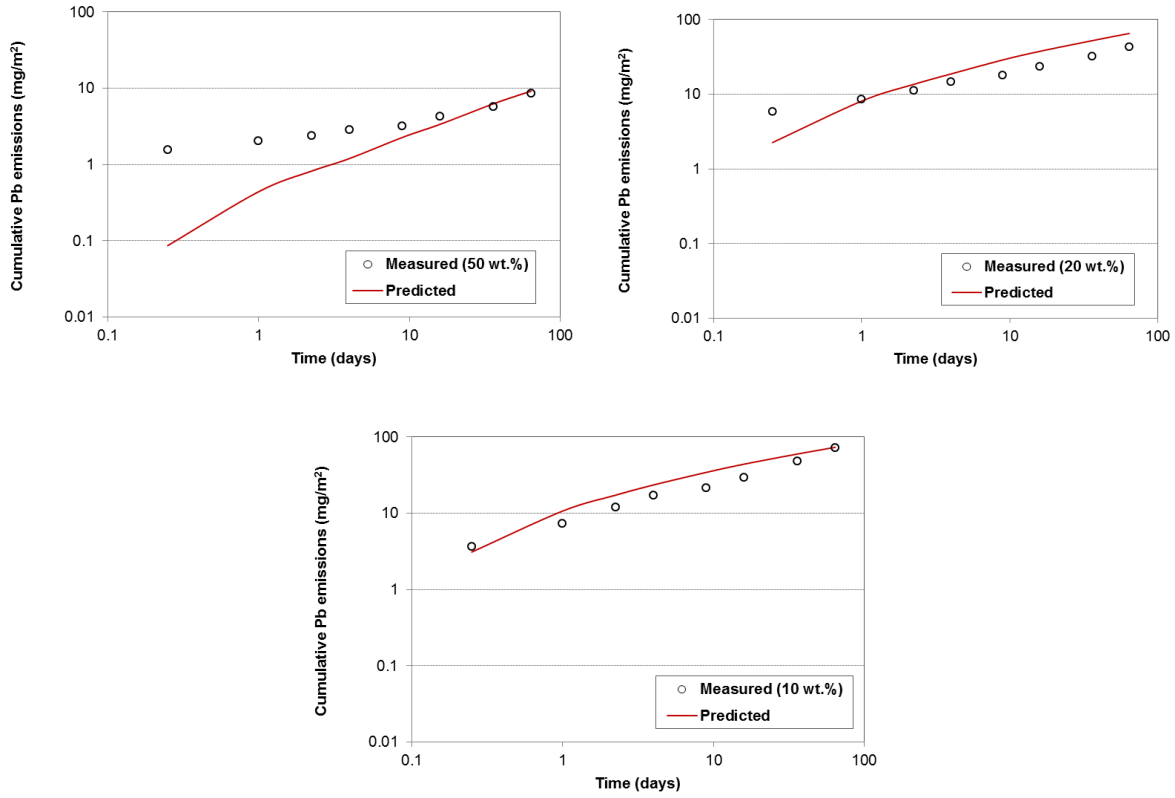

Figure 6.13 Cumulative measured and predicted Pb release for CEM I mixes

Pb availability concentrations were adjusted based on the total concentration of Pb in APC residues as in the case of Zn. Data provided by the EfW operator (Appendix I) show that Pb

availability in raw APC residues is approximately 70 mg/kg, which is two orders of magnitude less than what was assumed in this study. Plattnerite (PbO) was found to be the main mineral controlling release at low CEM I additions as demonstrated by the agreement of the model results with the measured values for the 10 and 20 wt.% mixes. Based on the presence of oxyanions such as VO^{2+}, other possible minerals include $Pb_2V_2O_7$ or $Pb_3(VO_4)_2$. Pb phosphate salts may also play a role in controlling release but given the high pH during the test, the role of oxides/hydroxides is likely to be more significant. Inclusion of such compounds in the mineral set did not result in statistically significant differences in the predicted results.

Other Metals (Fe and Sr)[6]

The results for the predicted cumulative release for Fe, and Sr for each of the CEM I mixes investigated are shown in Figures 6.14a-b. Release patterns for Fe suggest solubility-control for most of the leaching test fractions. Solubility of Fe was found to be controlled by minerals similar to $Fe(OH)_3$ and ferrihydrite. In addition, the calcium hydrate containing Fe and SO_4^{2-} may also play a role in controlling release of Fe with increasing CEM I addition. Model predictions agree well with the measured values for the 50 wt.% CEM I mix. In contrast, model prediction underestimate release of Fe for the 10 and 20 wt.% mixes However, the difference between the measured and predicted 64-day release for both 10 and 20 wt.% mixes is approximately 8 mg/m^2. This difference is mainly attributed to under-prediction (by 1-2 orders of magnitude) for the first fraction of the leaching test during, which release may be controlled by readily soluble Fe compounds not included in the mineral set.

Release of Sr was under-predicted for all CEM I mixes. Strontianite, celestite ($SrSO_4$) and $BaSrSO_4$[50% Ba] were investigated as relevant minerals for Sr. Although the model under-predicts Sr release, the predicted release was within the same order of magnitude as the measured release for the 10 and 20 wt.% CEM I mixes. In contrast, the model under-predicted release of Sr for the 50 wt.% mix by one order of magnitude. This may be attributed to underestimation of the availability of Sr in CEM I mixes.

[6] Results for Mg were observed only for the 50 wt.% CEM I mixes and therefore are not presented as they cannot be compared to the other CEM I mixes.

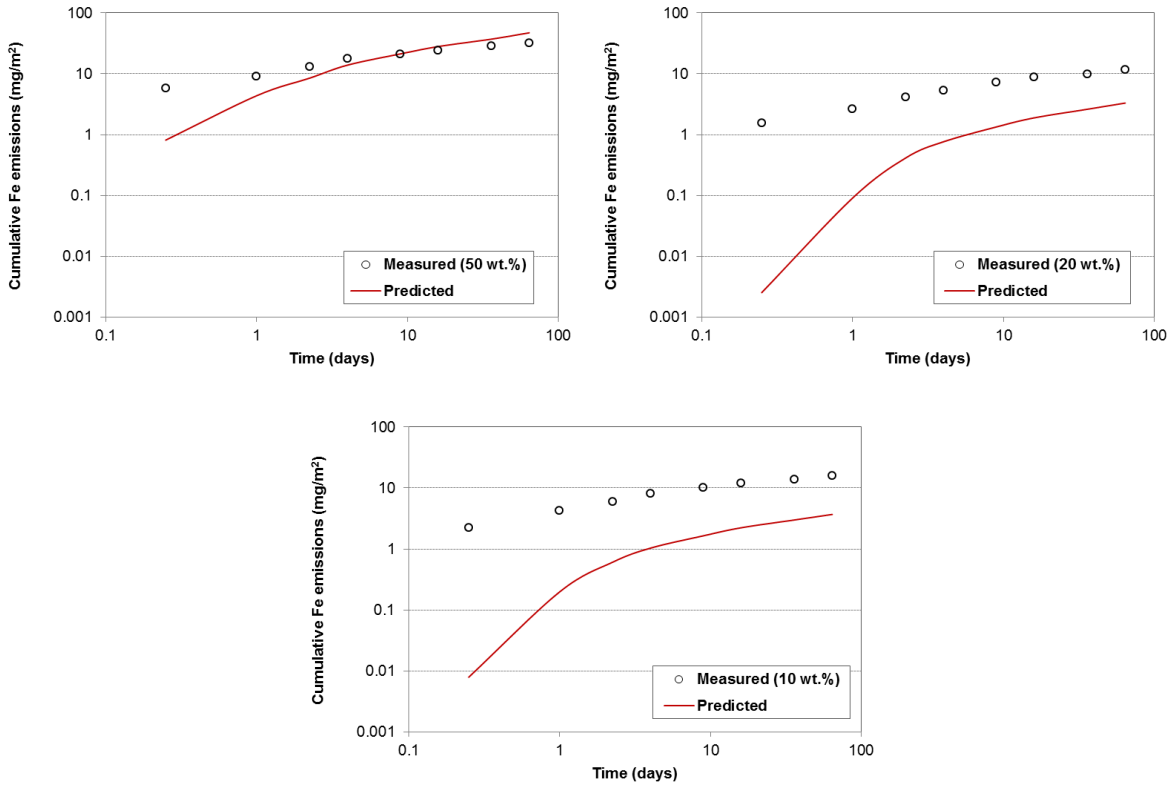

Figure 6.14a Cumulative measured and predicted Fe release for CEM I mixes

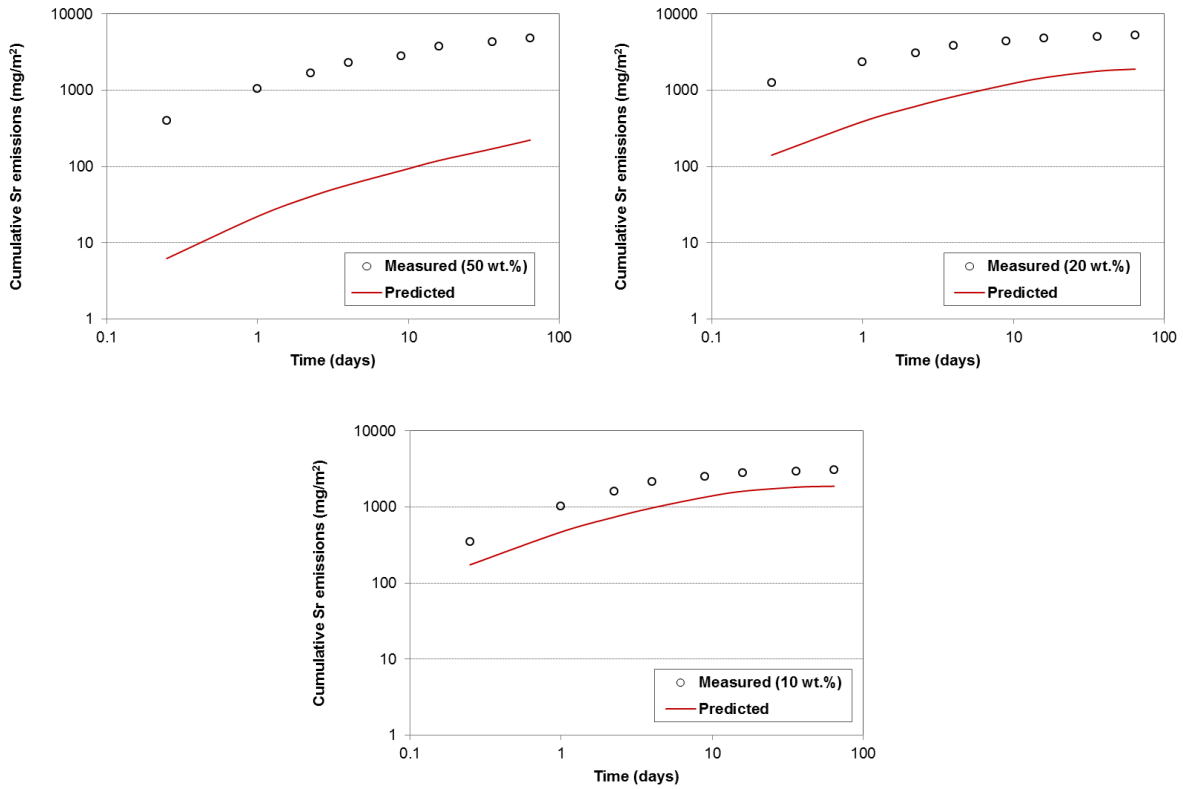

Figure 6.14b Cumulative measured and predicted Sr release for CEM I mixes

b) Ground Granulated Blast Furnace Slag

The set of parameters (problem definition) that yielded the best fit for the 50 wt.% GGBS mix is shown in Table 6.2.

Table 6.2 Problem definition for the 50 wt.% GGBS mix modelled in the study

Mineral Set	***Availability Concentrations (mg/kg)***			
AA_CaO_Al2O3_SiO2_8H20[s] AA_CaO_Al2O3[Ca[OH]2]0_5_[CaCO3]0_5_11_5H20[s] AA_CaO_Al2O3_CaCO3_11H20[s] AA_CaO_Fe2O3_CaSO4_12H20[s] AA_Brucite AA_Calcite AA_CO3-hydrotalcite AA_Gypsum AA_Jennite AA_Portlandite AA_Tobermorite-I AA_Tricarboaluminate CaZincate Cd[OH]2[A] Celestite Cu[OH]2[s] Ettringite_ECN Ferrihydrite Manganite Ni[OH]2[s] Pb[OH]2[C] P-Wollstanite Willemite	Ca	83,600	Mg	3,903
	Al	4,456	Mn	174.8
	Si	3,356	Pb	956
	H_2CO_3	16,500	Zn	1,330
	SO_4	10,600	V	0.58
	Fe	73.9	Cd	17.8
	Na	10,000	Cr	4.5
	K	10,000	Ni	9.29
	Cl	53,500	Sr	206
	Li	15.0	Ba	19.33
	HFO (kg/kg)	0.0001	SHA (kg/kg)	0.0001
	pH (*natural*)		11.4	
	Physical Properties			
	Porosity		0.40	
	Tortuosity		1.7	

pH

The majority of sets of relevant minerals evaluated for the GGBS S/S matrix provided good predictions for pH for the majority of the fractions of the monolithic leaching test. All sets yielded results that varied between 0.02 and 0.7 units from the measured values depending on the fraction of the leaching test. The pH prediction for the optimised set of parameters (problem definition) is shown in Figure 6.15. It is noted that only the values which correspond to the different leachant renewal periods are presented and not the output at each time step of the model.

It is observed that the model predicted values agree relatively well with the measured pH for early leaching intervals but over-predicts pH by 0.4 to 0.6 units for later leaching intervals with a longer contact period. This may be attributed to carbonation effects which cannot be easily avoided during the leaching test (especially for leaching fractions with long duration i.e. 64 days) and which are not accounted for in the model.

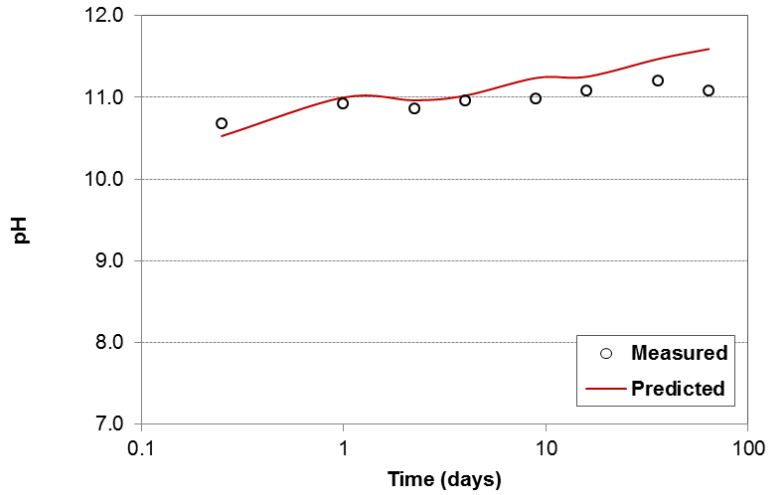

Figure 6.15 Measured and predicted pH for the 50 wt.% GGBS mix

Ca, Al and Si

The model predictions for the 50 wt.% GGBS mix for Ca, Al and Si are shown in Figure 6.16. Release of these elements is predicted reasonably well by the model, although release of Al is under-predicted. The selection of cement hydrates in the mineral set as part of the problem definition is representative of the cementitious system and the release of these elements.

Release of Ca for the GGBS mix was dependent on the carbonate availability of the system. As details for availability of carbonate were not determined in the present study, sensitivity analysis was conducted to assess its effect on the release of Ca. In addition, portlandite and calcite were found to be minerals that control release of Ca. Although cement hydrates were included in the set of relevant minerals they did not have a significant effect on the release of Ca. This suggests DIC could be an important parameter affecting release of Ca (through precipitation as calcite) given that CO_3^{2-} would be its dominant form in the pH region of cementitious systems

a. Ca release

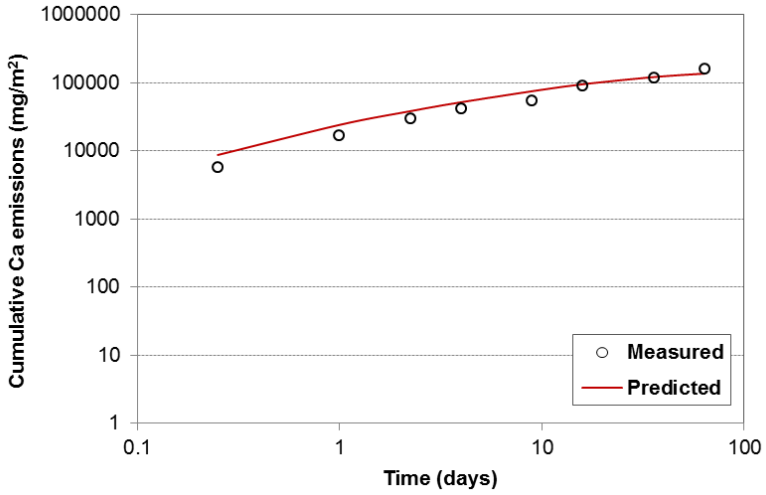

b. Al release

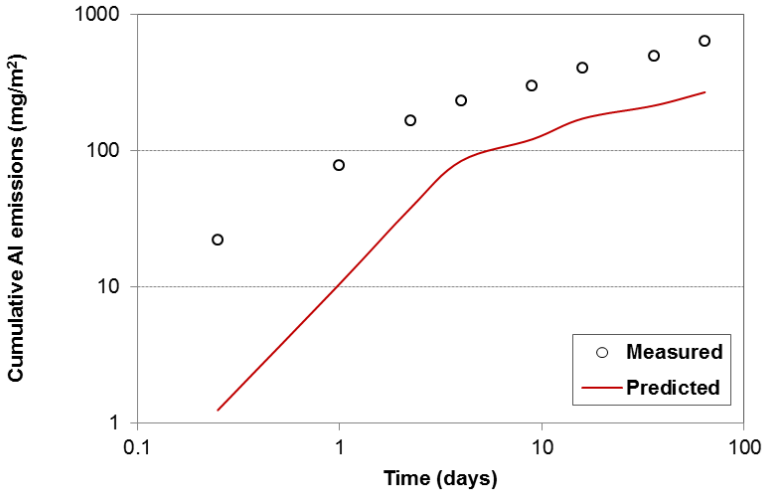

c. Si release

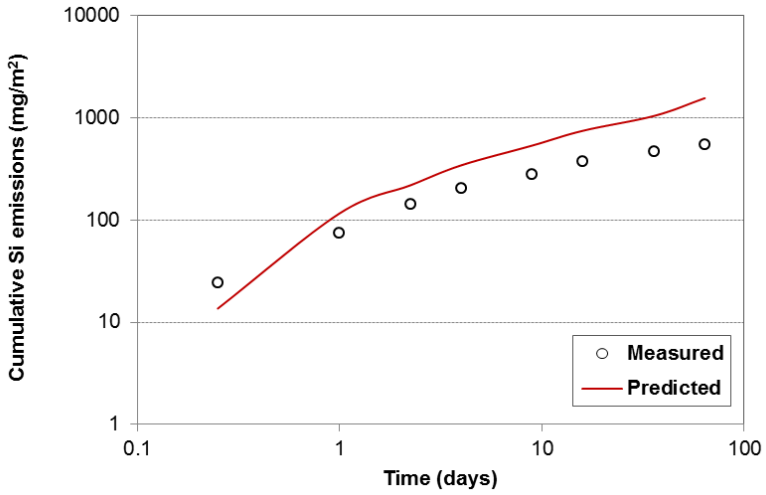

Figure 6.16 Cumulative measured and predicted release for the 50 wt.% GGBS mix: a) Ca, b) Al and c) Si

DIC availability in this study was determined based on the value that resulted in the best fit in terms of release of Ca. Results from sensitivity analysis in the release of Ca by assigning different DIC availability values are shown in Figure 6.17. It is shown that increasing availability of DIC results in reduced release of Ca.

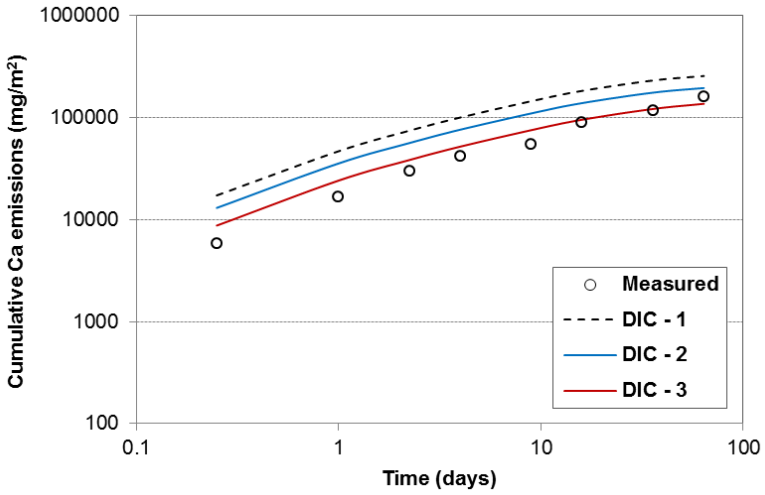

Figure 6.17 Effect of DIC availability on the predicted release of Ca (DIC-1 = 12,500mg/kg, DIC-2 = 15,000 mg/kg, DIC-3 = 16,500 mg/kg)

The model under-predicted release of Al but the predicted release was still in the same order of magnitude as the measured values for the majority of the fractions of the leaching test. As with CEM I, release of Al for the GGBS model was sensitive to changes in the availabilities of Al and SO_4, carbonate as well as pH. This can affect the formation of different hydration products as it was be explained for CEM I.

In contrast to Al, release of Si was over-predicted by the model but the predicted values were similar to the measured release. The problem definition for the 50 wt.% GGBS mix also used Jennite and Tobermorite-I to describe the CSH gel. As with CEM I, using the CSH mineral present in the LeachXS database resulted in similar release values as with the combination of Jennite and Tobermorite.

a. Na release

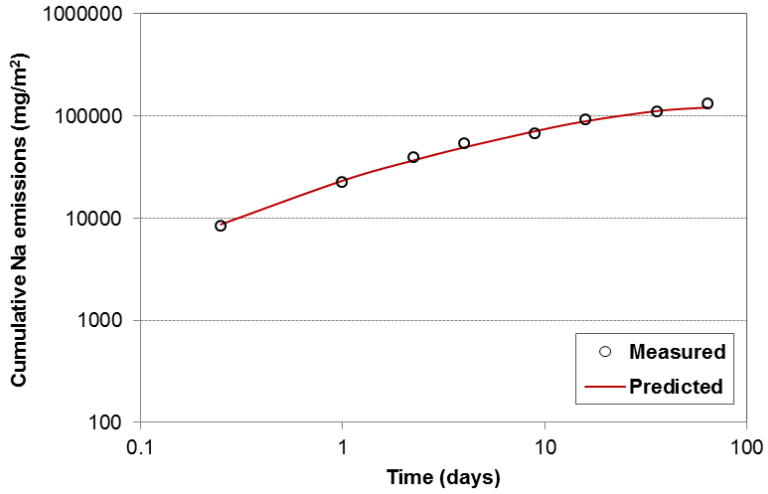

b. K release

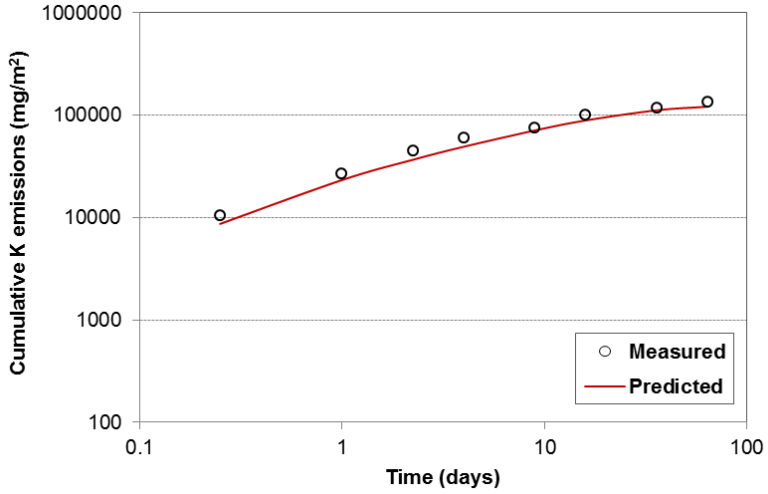

c. Li release

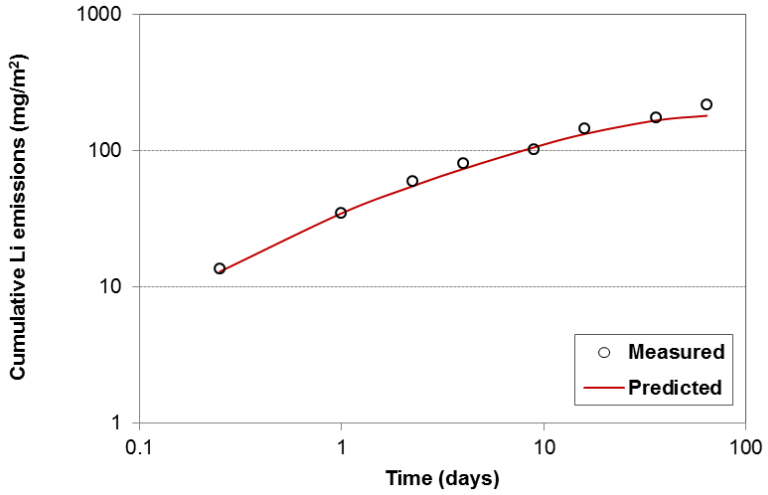

Figure 6.18 Cumulative measured and predicted release for the 50 wt.% GGBS mix: a) Na, b) K and c) Li

Alkali Metals (Na, K, Li)

The results for the predicted cumulative release for Na, K and Li for the 50 wt.% GGBS mix are shown in Figure 6.18. As with CEMI, the modelling study showed that release of Na, K and Li for the GGBS mix was not affected by differences in the set of relevant minerals but only by differences in the physical properties of the S/S matrix. The differences in the predicted release values for these elements by adding or removing possible solubility-controlling were not statistically significant. Good agreement with measured values is observed for Na and K. Leaching of Li is under-predicted by the model but is still in the same order of magnitude with the measured values which is attributed to an underestimation of the availability concentration in the problem definition.

Chloride

The results for the predicted cumulative chloride release for the 50 wt.% GGBS mix are shown in Figure 6.19.

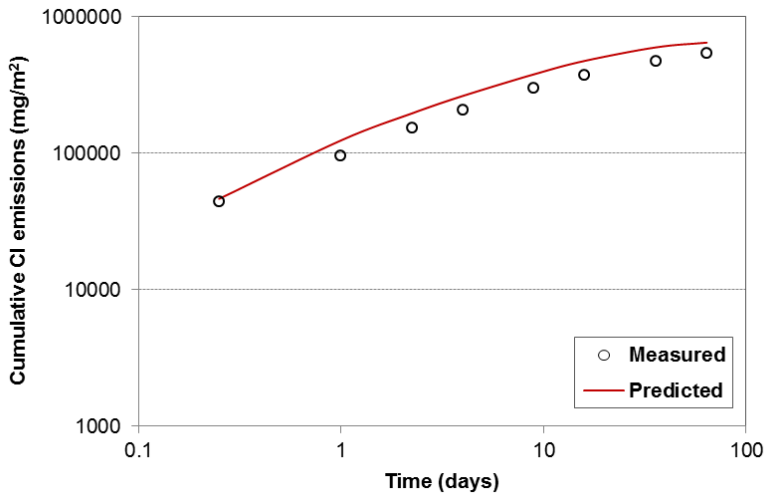

Figure 6.19 Cumulative measured and predicted Cl leaching for the 50 wt.% GGBS mix

It is observed that the model predictions agree well with measured values for chloride release for the majority of the fractions of the monolithic leaching test. As with CEM I, release of chloride was affected predominantly by the physical properties of the matrix such as tortuosity and to a lesser extent by the selection of minerals. The differences in the predicted chloride release for the different mineral sets investigated were not statistically significant.

Although well within the same order of magnitude, the model over-predicts leaching of Cl for the majority of the fractions of the leaching test by approximately 20% on average. Given that good agreement is observed for Na and K with the same problem definition, this may imply partial immobilisation in minerals which were not included in any of the mineral sets investigated.

Inclusion of layered double hydroxides to assess potential immobilisation of Cl was also assessed for the 50 wt.% GGBS mix. The same potential phases were considered as for CEM I, comprising Friedel's salt, Kuzel's salt and hydrocalumite-Cl. Inclusion of Friedel's and/or Kuzel's salt did not result in improvement in the predicted release of chloride. In contrast, inclusion of hydrocalumite-Cl improved the predicted release for chloride as shown in Figure 6.20. The model including hydrocalumite-Cl resulted in a difference of 6.5% compared to the measured 64-day release whereas the model without hydrocalumite-Cl resulted in a difference of 19.5%. At the same time inclusion of hydrocalumite-Cl significantly worsened the outcome for Al^{3+}, Ca^{2+} and SO_4^{2-}.

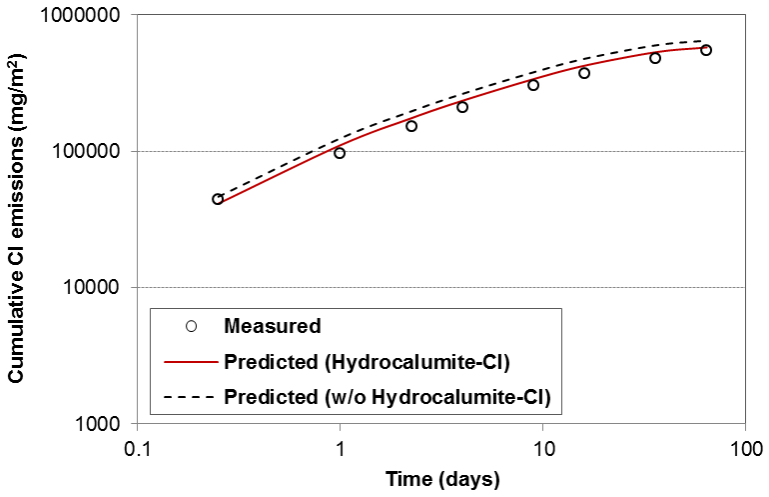

Figure 6.20. Effect of chloride-containing hydrates on the release of Cl from 50 wt.% GGBS mixes

This is again indicative of the complexity of the mineralogy and changes that occur in the S/S matrix in the presence of large intermixed concentrations of chlorides and sulphates. It was also observed that varying the availabilities of CO_3^{2-}, Al^{3+} and SO_4^{2-} in the problem definition for the 50 wt.% GGBS mix can significantly affect model predictions in the presence of Cl-containing AFm phases. This is aligned with previous research which identified stability

windows for different AFm phases depending on the ratios Cl^-, SO_4^{2-} and CO_3^{2-} to Al^{3+} (Matschei, 2007). However, this study did not attempt to determine such stability windows due to the lack of available experimental data on availabilities of these elements.

Sulphate

The results for the estimated cumulative sulphate release are shown in Figure 6.21 for each of the mixes investigated. It is observed that the model gives good model predictions for sulphate release for the majority of the fractions but under-predicts release for early fractions of the test which may be associated with surface wash-off. As with CEM I, sulphates may compete with Cl^-, OH^-, and CO_3^{2-} ions for incorporation in the different cement hydration phases (Matschei et al, 2007). Although ettringite was not detected in the X-ray diffractograms of 50 wt.% GGBS mix, it was included in the modelling study to account for incorporation of SO_4^{2-} ions in AFt phases or similar solid solutions. Results from the model however agreed with the mineralogical analysis and did not show precipitation of ettringite.

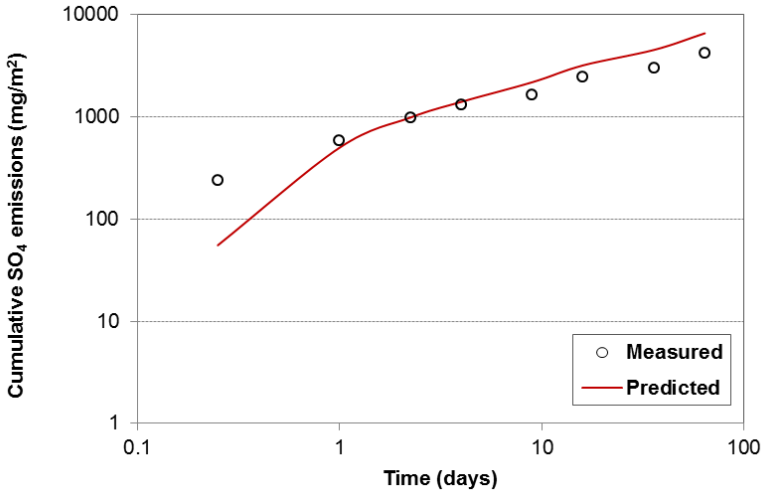

Figure 6.21 Cumulative measured and predicted SO_4^{2-} leaching for the 50 wt.% GGBS mix

Predicted release of SO_4^{2-} was dependent on the availability of Al^{3+} and SO_4^{2-} as part of the problem definition as well as the availability of carbonate. As in the case of Cl^-, varying the ratios of these elements had a significant impact on model predictions in presence of CO_3^{2-}, Cl^- and/or SO_4^{2-} containing phases. Further investigation on the respective amounts of Cl^-, SO_4^{2-}, OH^- and CO_3^{2-} compared to Al in the pore solution of S/S APC residues, is required to better understand the stability of SO_4-containing compounds.

Zinc

The results for the predicted cumulative zinc release for the 50 wt.% GGBS mix are shown in Figure 6.22. It is observed that the model represents release of zinc fairly well based on the selection of the Zn-containing minerals calcium zincate and willemite (Zn_2SiO_4). Although the model over-predicts the 64-day release, the predicted values are similar to the measured release for the majority of the leaching intervals. Over-prediction at late leaching intervals with longer contact durations (i.e greater than 16 days) may be attributed to the over-prediction of pH, resulting in higher solubility for Zn. In addition, under-prediction in the early leaching intervals may be associated with surface wash-off which is not accounted for in the model.

It is noted that that SI values for willemite ($ZnSiO_4$) from chemical speciation calculations showed undersaturation (SI < 0) for all fractions of the tank test but the mineral was selected based on results of previous relevant studies. Calcium zincate on the other hand exhibited calculated SI values closer to equilibrium (SI = 0). Selection of this mineral alone however, over-predicted release of Zn by an order of magnitude.

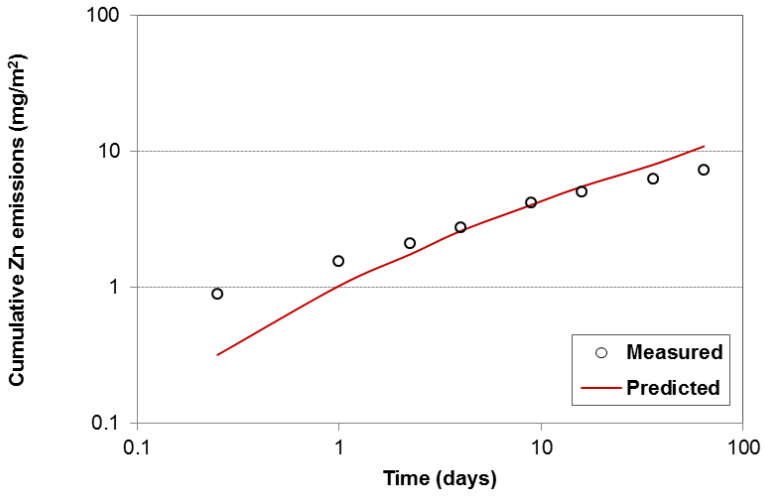

Figure 6.22 Cumulative measured and predicted Zn leaching for the 50 wt.% GGBS mix

Lead

Figure 6.23 shows the model predictions for the release of Pb. It is observed that the model under-predicts release of Pb for the 50 wt.% GGBS mix. It is noted however, that the measured release was estimated using the laboratory detection limit, since Pb concentrations for all fractions of the test were below the detection limit for the 50 wt.% GGBS mix. Actual release may therefore be closer to the model predictions, given the inherent uncertainty with using the laboratory detection limit.

As the same mineral, $Pb(OH)_2$, was found to best describe release of Pb for both CEMI and GGBS at 50 wt.% binder addition, the difference in measured and predicted release between CEMI and GGBS is attributed to the lower pH of the latter.

Similarly to the CEM I mix other Pb-containing minerals such as $Pb_2V_2O_7$ or $PbCrO_4$ may play a role in the release of the metals included in these compounds. This was not investigated for the GGBS mix due to lack of relevant data. Inclusion of these metals in the problem definition however did not result in statistically significant results for the release of Pb.

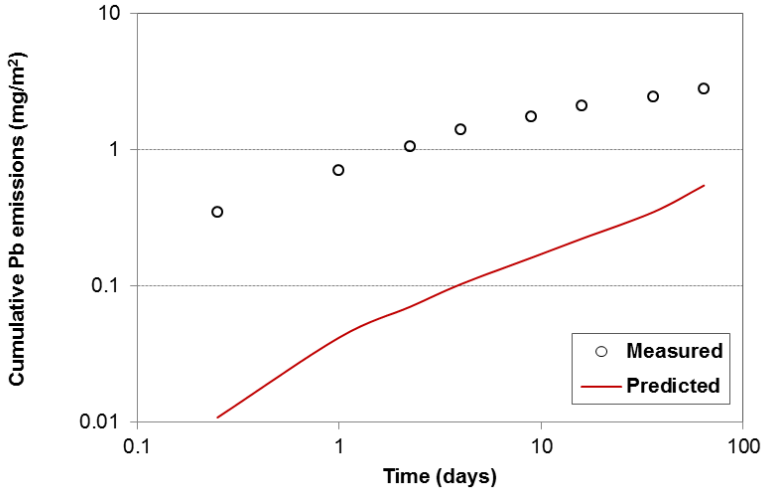

Figure 6.23 Cumulative measured and predicted lead leaching for the 50 wt.% GGBS mix

Other Metals (Fe, Mg and Sr)

The results for the predicted cumulative release for Fe, Mg and Sr for the 50 wt.% GGBS mix are shown in Figure 6.24. It is observed that the model for GGBS over-predicts release for Fe for the majority of the fractions of the leaching test but under-predicts release of Mg and Sr. The release patterns for Fe suggests that the solubility of the Fe-containing minerals are determining release. The 64-day release is over-predicted but is still in the same order of magnitude as the measured values. This suggests that different minerals, solid solutions or processes may be controlling release of Fe than the ones chosen in Table 6.3. It is noted however that different minerals were examined and although predicted release for Fe was improved, predictions for other elements such as Si and Al were hampered. The complexity of the S/S APC residue system and the dynamic nature of the tank test are challenges for the determination of a single problem definition that accurately predicts release for all elements.

The predicted release pattern for Mg is similar to the measured release exhibiting a plateau at later leaching intervals suggesting the diffusion may be determining release without solubility constraints. The under-prediction compared to the measured values suggests that the availability for Mg may have been underestimated in the original problem definition. Release of Mg may also be suppressed in the model due to the inclusion of carbonates and subsequent precipitation of CO_3-hydrotalcite.

As with Fe, the release patterns for Sr suggest solubility-control. The 64-day release was affected by the carbonate content in the problem definition. In addition, and as with Mg, release may be under-predicted due to under-estimation of its availability in the problem definition.

a. Fe release

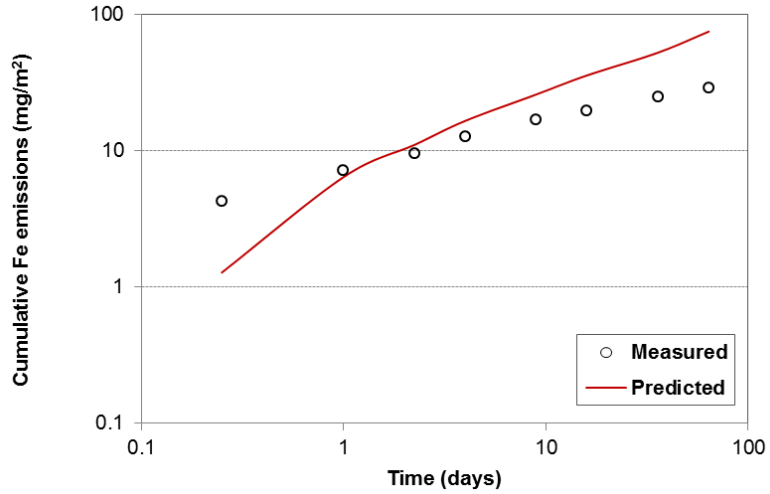

b. Mg release

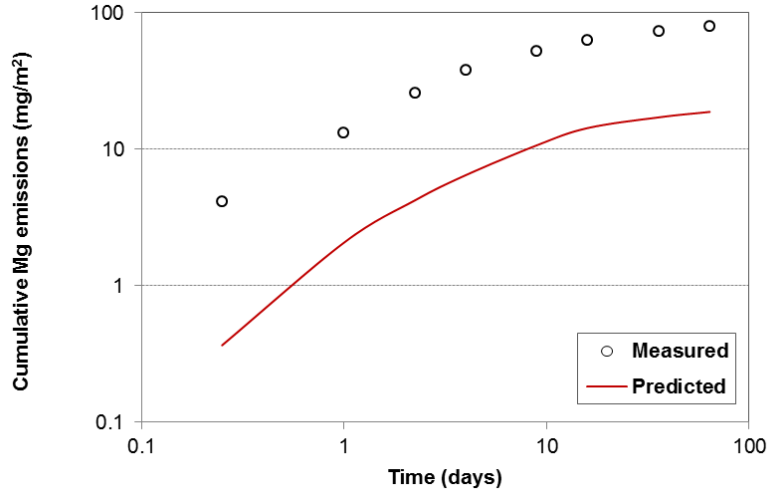

c. Sr release

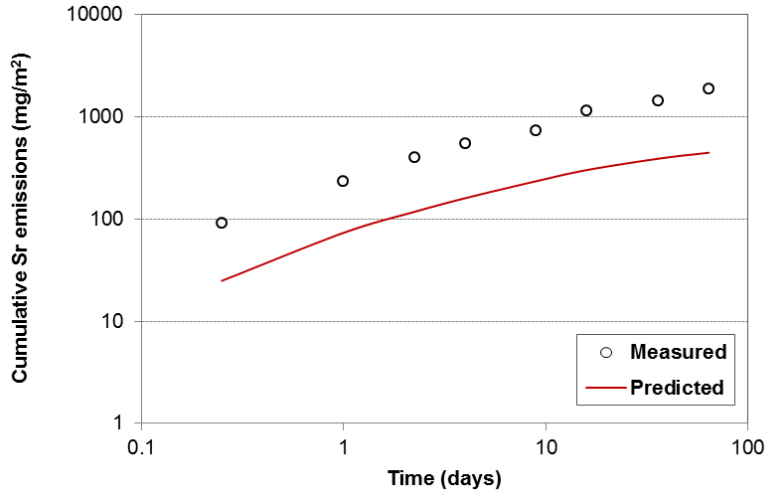

Figure 6.24 Cumulative measured and predicted leaching for the 50 wt.% GGBS mix: a) Fe, b) Mg and c) Sr

7. STATISTICAL ANALYSIS AND DISCUSSION

7.1 Introduction

The present section provides a discussion on the experimental and modelling results presented in the previous two chapters. It is divided in 3 separate subsections covering the influence of APC residues on hydration reactions, physical properties (e.g. setting time, compressive strength etc.) and chemical and leaching properties.

The discussion is supported by literature and previous studies as well as statistical analysis conducted using the commercially available statistical software package STATA (version 9.2). In particular, hypothesis tests (i.e. *t*-tests), analysis of variance (ANOVA) and multivariate regression are utilised in order to make inferences about the observed results. Although a thorough review of the statistical tests is not the scope of this study, fundamentals are presented here pertaining mainly to the interpretation of the results of these tests.

ANOVA and *t*-tests were used to assess statistical significance of the differences in the physical properties and leaching characteristics of the different mixes. The *t*-test compares the differences in the means of two samples. The two opposing hypotheses were H_o (null hypothesis): $\mu_1 - \mu_2 = 0$ and H_1 (alternative hypothesis): $\mu_1 - \mu_2 \neq 0$. The test produces a *p*-value which is compared to a predetermined significance level (a). If the *p*-value is less or equal to the predetermined significance level the initial hypothesis is rejected and the alternative hypothesis can be supported (statistically significant difference). The significance level chosen for this study was 0.05.

Similarly to the t-test, ANOVA is used to assess statistical significance. ANOVA can test for statistically significant differences among a group of samples whereas the *t*-test is limited to two samples. ANOVA utilises the *F* test (distribution) to assess differences among the groups. The output of ANOVA is the *F* statistic and an associated *p*-value. The greater the *F* statistic is the greater is the significance of the difference among the groups. The interpretation of the associated *p*-value follows the same rationale as the *t*-test. Similarly to the *t*-test the significance level selected was 0.05. If the null hypothesis is rejected in an ANOVA test then

we know that there are statistically significant differences in at least two of the groups compared in the test. In summary the interpretation of the *p*-values from the ANOVA and *t*-tests is as follows:

- If $p < 0.05$ then we reject the null hypothesis i.e. the difference in the means is statistically significant
- If $p \geq 0.05$ then we accept the null hypothesis i.e. the difference in the means is not statistically significant

Finally, multivariate regression was used to assess the contribution of mix parameters to the development of physical parameters, namely UCS and porosity. Ordinary least squares (OLS) or linear regression was used to obtain linear models with the dependent variable being UCS or porosity and the independent variables being the mix parameters such as the binder type and content and the w/s ratio. Key output statistics from the OLS regression include:

- The correlation coefficient R^2 which shows how much of the variance is explained by the model. This coefficient ranges from zero to one, one meaning that the model explains perfectly the variance within the observations.
- The *RMSE* which describes the difference between the predicted and the observed values. It is a measure of how close the model fits the observed data. Low *RMSE* values indicate a good fit.
- The coefficients for the independent variables which are indicative of the marginal effect on the dependent variable and associated *t* values. The *t* values are indicative of the significance of these variables with *t* value suggesting greater significance. In addition, the coefficients indicate the direction of the effect of the independent variables. For example negative coefficients indicate a negative correlation whereas positive coefficients indicate a positive correlation.

The body of the text includes only key statistics from these tests whereas the output from STATA is included in Appendix V. In the case of *t*-tests the key statistic is the *p*-value whereas for ANOVA the key statistics are the *F* and *p*-values. Statistics reported for multivariate regression model include the coefficients for each independent variable, the associated *t* statistics, as well as the R^2 and *RMSE*.

Statistical analysis is limited by the low number of observations (i.e. sample size) for certain experimental tests such as compressive strength where each mix is represented by 3 results/specimens. Small sample sizes and violations of assumptions of statistical tests (e.g. deviations from the normal distribution) can render the results of parametric tests as approximations (Kanjii, 1999). In cases where the results of parametric tests are ambiguous (e.g. close to the pre-selected significance level) non-parametric tests such as the Wilcoxon-Mann-Whitney were used to evaluate the result obtained. It is noted however that the nature of cementitious specimens is such that there should not be significant variance in the physical properties among the population of samples for a particular mix. The mean of the three replicates for UCS for example should be a fairly accurate representation of the population mean.

7.2 Influence of APC Residues on Hydration Reactions

Conduction calorimetry indicates that APC residues have a significant effect on CEM I hydration. A 10% APC residue addition to CEM I caused the main CEM I hydration peak to occur after 5.2 hours compared to 8.9 hours for the control mix, while the total heat evolved during the 98 hour monitoring period was reduced. APC residue addition between 10 and 30 wt.% is equivalent to the addition of ~ 2.0 wt.% Cl^- ion to the CEM I and this is in the range of Cl^- ion additions used to accelerate CEM I hydration (1.0 % - 3.0 wt.%) (Hewlett, 1998).

The main CEM I hydration peak was no longer observed in S/S mixes containing low CEM I/high APC residue, although there was significant heat evolved during at least the initial 10 hours after mixing. There is no evidence of hydration reactions occurring for the 100% APC residue samples and the early heat evolved can be attributed to the exothermic reaction of free lime with water.

7.3 Physical Properties

7.3.1 Setting Time and Consistence

Setting time and consistence were affected both by the amount of binder in the mix and the amount of water. The correlation coefficients of exponential fitting for both CEM I and

GGBS show that, as expected, setting times and consistence are positively correlated to water addition with the former increasing with increasing water addition.

Less flowable mixes were obtained for high APC residue additions. The presence of soluble salts combined with the fineness of APC residues means that high levels of water are required to obtain workable mixes containing high APC residue additions. Salts such as NaCl and KCl are deliquescent and readily adsorb large amounts of moisture from the environment. As a result the consistence criterion of 175±10 mm chosen for this experimental work and therefore a workable mix could not be obtained with low water additions. The mixes that achieved the consistence criterion were:

- 50 wt.% CEM I, w/s: 0.55;
- 20 wt.% CEM I, w/s: 0.65; and
- 10 wt.% CEM I, w/s: 0.65.

It is observed that none of the GGBS mixes achieved the consistence criterion. Although the consistence criterion can be achieved with greater water additions, this is not desirable due to detrimental effects to other physical properties such as UCS and porosity. This will be discussed as part of following sections. In general, the trade-off between S/S matrix performance and commercial applicability should be ideally evaluated as part of a scaled-up pilot plant.

CEM I mixes seem to yield more workable mixes compared to GGBS. A comparison of consistence values between CEM I and GGBS mixes with the same binder and water addition is presented in Table 7.1. Both binders exhibit similar consistence values at 50 wt.% binder addition. However, the results demonstrate that the difference increases with decreasing binder addition.

Table 7.1 Comparison of consistence values between CEM I and GGBS mixes

Binder Addition	Water-to-Solids (ml/g)	CEM I (mm)	GGBS (mm)	Delta (mm)
50 wt.%	0.4	121	114	7
	0.5	146	149	-3
20 wt.%	0.5	128	106	22
	0.6	158	117	41
10 wt.%	0.6	146	110	36

All mixes investigated satisfied the requirements of maximum initial (< 8 hours or 480 minutes) and final setting time (< 24 hours or 1440 minutes). Although all mixes satisfied these requirements, mixes with short setting times (e.g., less than 2 hours or 120 minutes) could cause operational difficulties in a full-scale facility.

A comparison between the setting times of CEM I and GGBS mixes with the same binder and water addition is presented in Table 7.2. GGBS exhibited longer setting times compared to CEM I mixes for 50 wt.% binder addition. This is consistent with literature results which show that GGBS mixes have greater setting times compared to CEM I. In particular, the UK Cementitious Slag Makers Association (2012) states that replacement of CEM I with GGBS can extend setting time by approximately 30 minutes and this effect becomes more pronounced with increasing CEM I replacement.

It is noted again that the GGBS mix with 50 wt.% binder addition and w/s of 0.6 failed to set, even after 24 hours and therefore this mix was not considered for further testing.

Table 7.2 Comparison of initial and final setting times between CEM I and GGBS mixes

Binder Addition	**Water-to-Solids (ml/g)**	**CEM I (min)**		**GGBS (min)**		**Delta (min)**	
		Initial	Final	Initial	Final	Initial	Final
50 wt.%	0.4	26	37	70	105	-44	-68
	0.5	41	84	310	525	-269	-441
20 wt.%	0.5	83	107	60	115	23	-8
	0.6	132	170	123	159	9	11
10 wt.%	0.6	110	140	107	135	3	5

It is noted that typically comparison of setting times is conducted on mixes with similar rheological characteristics i.e. mixes with standard consistence. The comparison presented in Table 7.2 is based purely on the setting times observed for the different mixes. Although this deviates for standard tests for cementitious specimens, it provides an indication of the effect of the different mix parameters on workability

Shirley and Black (2011a) investigated the effect of APC residue addition to alkali-activated PFA and obtained similar results in their effect on workability for mixes with similar

characteristics. In their study workability decreased with increasing APC residue addition or decreasing w/s ratio. Setting times also increased with increasing APC residue addition and this was attributed to the retarding effect of cations such as Pb^{2+} and Zn^{2+} on hydration reactions.

Hui-Sheng Shi and Li-Li Khan (2009c) investigated MSWI fly ash – cement matrices and the effect of different pozzolanic materials such as GGBS, PFA and metakaolin. Substitution of cement with MSWI fly ash was found to increases the water demand for normal consistency. When the amount of MSWI fly ash is less than 30%, both initial and final of setting time are earlier than control specimen. This was attributed to the presence of anions such as Cl^-. This is also aligned with results from hydration calorimetry in the present study where it was suggested that acceleration of hydration reactions occurs due to the concentrations of Cl. The researchers also observed that when the amount of MSWI fly ash is greater than 30%, the initial of setting time is slightly retarded, whereas the final of setting time is still shorter. As with Shirley and Black (2011a) retardation effects were attributed to the presence of metal cations and the poisoning of hydration reactions.

Polettini et al, (2001) investigated the effect of Portland cement substitution with various types of MSWI fly ash and obtained similar results with regards to the effect of binder content to setting times. In particular, the authors found that for the majority of MSWI fly ash types, cement replacement levels higher than 20% always delayed the initial setting time beyond 24 h.

Workability and setting times are important for the technical and economic viability commercial S/S applications. The above demonstrate that APC residues have similar adverse effects on the physical properties of cementitious matrices regardless of the mix characteristics. It is noted that the maximum binder substitution in the studies above was not greater than 60%[7] and therefore results may not be directly comparable with mixes with low binder addition in this study. However, the effects are directionally comparable.

[7] In the study by Polletini et al (2001) binder substitutions reached 80% depending on type of MSWI fly ash. However, for comparison purposes, only one type of MSWI fly ash (FF3) was considered which had composition similar to the APC residues investigated in this study. The replacement level for this type of MSWI fly was up to 30%.

7.3.2 Compressive Strength

100% APC residue specimens exhibited no strength increase between 7 and 28 days curing. This observation, combined with the conduction calorimetry data and the low amounts of Si and Al present in raw (untreated) APC residues, indicate that pozzolanic reactions are not a major contributor to strength development when no binder is added. The 1MPa strength of the 100% APC sample with a w/s ratio of 0.4 is attributed to the hydration of lime, i.e., essentially due to drying, without formation of a durable matrix. These observations, coupled with low workability, indicate that S/S with water and without binder addition is not a suitable technique for the treatment of APC residues.

In contrast, the target of 1MPa for dry UCS was satisfied by all CEM I-containing mixes at both 7 and 28 days. S/S specimens containing 50% CEM I had maximum compressive strengths of 17.3MPa. These were reduced to 10.4 MPa at 20% and 5.5MPa at 10% CEM I additions. The significance of compressive strength development for low binder addition as an indication of hydration is questionable, considering that no hydration peak was observed for these mixes by calorimetry. Certain heavy metal oxides are known to inhibit CEM I hydration reactions and this produces poor mechanical properties (Fernandez, 2001; Asavapisit et al, 1997). Zinc hydroxy anions present at pH values between 12 and 13 form calcium hydroxyzincate [$CaZn_2(OH)_6.H_2O$], which coat CEM I grains and inhibit further hydration.

Strengths after water immersion indicate that it is difficult for specimens with high APC residue addition to maintain structural integrity when exposed to water. Dissolution of salts present in APC residues severely affects matrix durability. Specimens prepared with high APC/low CEM I additions had significant strength loss or totally disintegrated when immersed in water. Higher water content samples had inferior mechanical properties, due to their increased porosities which will also be discussed in following sections. High porosity and high water content can also result in increased leaching from S/S products.

CEM I mixes with 50 wt.% binder addition exhibited a marginal strength increase after water immersion. This may be due to the inherent variability in compressive strength measurement rather than a real effect, but does indicate that addition of 50 wt.% of CEM I by total dry mass produced specimens that retain compressive strength when tested after immersion.

However, conventional cement and concrete specimens for UCS testing are cured under water, and their UCS values are greater than those of specimens cured in a humid environment.

The majority of GGBS samples had very low strengths at 7 days and did not meet the strength criterion of 1MPa. Only the sample with 20 wt.% GGBS addition at a w/s of 0.4 met the UCS criterion at 7 days achieving and average compressive strength of 1.3 MPa. However, this is not considered as a sufficient indication of hydration when taking into account the marginal average strength increase of 0.5 MPa at 28 days of curing.

S/S APC residues using 50% GGBS had relatively high compressive strengths (~ 20.0 MPa) after 28 days. Corresponding 28 days strengths were just 1.7 MPa for 20 wt.% and 0.4 MPa for 10 wt.% GGBS additions, exhibiting a marginal strength increase between 7 and 28 days. The increase in compressive strength ranged between 0.1 and 0.7 MPa for these mixes depending on water addition. It is noted that 10 wt.% GGBS mixes at w/s of 0.5 and 0.6 exhibited lower strengths at 28 days compared to strengths at 7 days.

Statistical tests on the means between the GGBS compressive strength values at 7 and 28 days for 20 and 10 wt.% GGBS mixes indicate that there is a statistically significant difference (p-values < 0.05) between the two mixes. These differences can be attributed to the effect of the varying water addition but are not deemed of practical significance in terms of the adequacy of GGBS to effectively treat APC residues at low binder additions.

As with CEM I, the heavy metals present in APC residues may be poisoning hydration reactions and reducing mechanical property development. The substantial increase in compressive strength between 7 and 28 days for 50 wt.% GGBS mixes indicates that hydration reactions start contributing to significant strength gain after the first week of curing. This is consistent with the longer setting times for GGBS mixes compared to CEM I. Moreover these results are positive as they demonstrate that the inherent alkalinity in APC residues can successfully activate pozzolans and initiate hydration reactions. If rapid strength development is desired then this could possibly be achieved by using an additional activator or accelerator.

10% and 20% total dry mass GGBS samples could not be tested for UCS after immersion because they suffered from poor structural integrity, as the UCS without immersion indicates. The hygroscopic nature of the soluble salts present in the APC residues may severely affect the S/S waste matrix durability and result in leaching of soluble salts from these samples when immersed in water.

In contrast, 50 wt.% GGBS samples retained their compressive strength when tested wet after water immersion. As with CEM I mixes, the marginal strength increase observed after water immersion of some 50% GGBS mixes may be due to the inherent variability in compressive strength measurement rather than a real effect. This conclusion is also supported by statistical tests indicating that there is not a statistically significant difference between the strengths at 28 days before and after water immersion for 50 wt.% GGBS mixes. In particular the *p*-values (H_o: μ_{UCS28}-μ_{UCS28W} = 0, α = 0.05) for 50 wt.% mixes at w/s of 0.35, 0.4 and 0.5 were 0.47, 0.36 and 0.17 respectively.

a) Effect of mix parameters on compressive strength

CEM I and GGBS had similar performance at 50 wt.% binder addition as previously mentioned. The *t*-test for mixes a w/s ratio of 0.4 shows that the difference in compressive strength between CEM I and GGBS is not statistically significant (*p*-value: 0.09). It is noted that among the three GGBS specimens tested, one specimen had significantly lower compressive strength (8.6 MPa) compared to the remaining two specimens (average strength of 14.6 MPa). This may be attributed to experimental error and may be influencing the result obtained from the *t*-test. In contrast, the *p*-value for the same test for 50 wt.% mixes at a w/s of 0.5 resulted in a *p*-value of 0.04 which is lower than the pre-selected significance level of 0.05. Results from non-parametric tests result in a *p*-value < 0.05 for both w/s of 0.4 and 0.5. The results from the non-parametric tests allow us to reject the null hypothesis and conclude that the UCS difference between 50 wt.% CEM I and GGBS mixes is statistically significant. However, the practical significance of the difference in the UCS obtained for both binders at 50 wt.% binder addition will depend on the management option for the end product. For example a difference of 2 MPa (as observed for a w/s ratio of 0.5) may not be of practical significance when both binder achieve UCS values greater than 10 MPa and the product will be disposed of at a landfill.

At lower binder additions the difference in compressive strength between CEM I and GGBS mixes is more pronounced. The majority of 20 and 10 wt.% GGBS mixes failed to achieve the criterion of 1MPa even after 28 days of curing. The contribution of binder type and content to UCS development will be further discussed in following paragraphs.

The w/s ratio can also have a significant effect on compressive strength development. ANOVA tests for both 50 wt.% CEM I and GGBS mixes at varying water addition show that the w/s has a statistically significant (p-values < 0.05) effect on strength developemtn. This confirms that increasing water addition can have a significant adverse effect on strength development. The trade-off between workability and compressive strength would ultimately depend on the end use of the S/S products.

A linear model for UCS for CEM I based on the individual mix parameters is presented in Eq. (4.1). The model was obtained using multivariate regression (See Appendix V). Multivariate regression was not used for predictive purposes but for assessing the significance of the contribution of each of the mix parameters to strength development.

$$\boldsymbol{UCS_{28CEM\,I}} = 0.15 \times CEMI\_wt.\% - 37.3 \times (w/s) + 23.8 \qquad (4.1)$$

The model presented for strength development at 28 days for CEM I mixes based on binder and water content has a good fit as demonstrated by the correlation coefficient of 0.96 and the root mean squared error (*RMSE*) of 0.9. The coefficients of the independent variables and the associated t values (the larger the t value the greater the effect) are indicative of the effect of each variable on strength development. In addition, the sign of the coefficients denotes the positive or negative effect on strength development. In the case of CEM I mixes, the w/s ratio has the most significant effect (t = *-17.5*) and is negatively correlated with strength development. In particular, an increase in the w/s by 0.1 units can result in a decrease in compressive strength by approximately 3.7 MPa. The CEM I content is undoubted a key contributor to strength development but was found to have slightly less significant effect (t = *16.1*) compared to the w/s ratio.

Similar results are obtained for the same regression for GGBS mixes, however the effect of the binder content becomes more pronounced as also indicated by the experimental results. The extent of hydrations reactions is questionable at low binder additions with implications for strength development.

A generalised linear model for UCS for all (both CEM I and GGBS) mixes based on multivariate regression is also presented below (Eq. 4.2). The dependent variable is again UCS at 28 days and the independent variables are binder type (a binary variable with 0 and 1 representing GGBS and CEMI respectively), binder content (wt.%) and the w/s ratio as follows:

$$\boldsymbol{UCS_{28}} = = 2.55 \times binder + 0.22 \times binder\_wt.\% - 19.4 \times (w/s) + 9.8 \qquad (4.2)$$

The results revealed that binder content ((*t = 9.8*) and the w/s ratio (*t = -5.8*) are the most significant parameters for strength development. Results for the binder type indicate that CEM I mixes exhibit a compressive strength which is approximately 2.6 MPa greater compared to GGBS mixes for the same binder content and w/s ratio. Although the practical significance of this difference seems negligible, this result is more pertinent for high binder additions where GGBS does not perform as well as CEM I. In cases where the binder content is less than 20 wt.% this difference is of practical significance in terms of compliance with UCS thresholds and WAC for landfill disposal (> 1 MPa).

The binder content has a greater significance in this model compared to the model assessing only CEM I mixes. This is attributed possibly to the large variance in UCS results for GGBS and poor performance for binder additions less than 20 wt.%. The effect of the w/s ratio is significant as expected and in line with the model for CEM I mixes only. Finally the linear model exhibits relatively good fit as demonstrated by the correlation coefficient of 0.81, however *the RMSE* is relatively high (2.62).

7.3.3 Porosity and Water Content

Table 7.3 summarises the comparison between GGBS and CEM I mixes with the same mix characteristics i.e. binder and water content. It is observed that CEM I mixes achieve lower porosities compared to GGBS mixes with the same binder and water addition.

Table 7.3 Comparison of porosity between CEM I and GGBS mixes

Binder Addition	Water-to-Solids (ml/g)	CEM I (%)		GGBS (%)		Delta (%)	
		7-d	28-d	7-d	28-d	7-d	28-d
50 wt.%	0.4	32.4	30.7	43.9	36.1	-11.5	-5.4
	0.5	41.0	37.5	45.9	40.5	-4.9	-3.0
20 wt.%	0.5	41.3	41.6	52.2	50.8	-10.9	-9.2
	0.6	47.4	48.2	53.8	54.2	-6.4	-6.0
10 wt.%	0.6	48.3	48.2	52.6	56.5	-4.3	-8.3

The difference in porosity (delta) between GGBS and CEM I is similar for all mixes at both 7 and 28 days of curing apart from the mixes with 50 wt.% binder addition. In the case of 50 wt.% GGBS mixes, this observation is aligned with compressive strength development for GGBS during the first week of curing and after 28 days. As noted previously, it is postulated that for 50 wt.% GGBS mixes, hydration reactions start contributing to the development of mechanical properties after the first week of curing.

As expected, porosity is also highly correlated with the water content of the specimens. The correlation coefficients from the linear regression between porosity and water content are 0.92 and 0.99 for porosity at 7 and 28 days respectively.

A generalised linear model for porosity for mixes evaluated in this study is presented below (Eq. 4.3). As with UCS the purpose of the model is to assess to the effect of the different mix parameters on porosity. The dependent variable is porosity at 28 days and the independent variables are binder type (a binary variable with 0 and 1 representing GGBS and CEMI respectively), binder content (wt.%) and the w/s ratio as follows:

$$\boldsymbol{por_{28}} = -5.5 \times binder - 0.25 \times binder\_wt.\% + 38.7 \times (w/s) + 34.4 \qquad (4.3)$$

The binder content (t = -9.2) and w/s ratio (t = -9.4) were found to be the most significant parameters (see Appendix V). As expected binder content is negatively correlated with porosity whereas water content shows a positive correlation. According the linear model, increasing the binder addition by 10 wt.% can result in a reduction in porosity of approximately 2.5%. The w/s ratio has the most significant effect on porosity among the parameters included in the model. Increasing water addition can increase the amount of water-filled pores with an adverse effect on other properties also such as compressive strength as well as leaching. This will be further discussed in following sections.

Although not as significant compared to binder and water content, the type of binder (t = -7.1) also has a significant effect on porosity. According to the regression, CEM I mixes exhibit a lower porosity compared to GGBS mixes (an average difference of approximately 5.5 percentage units) when holding the binder and water content constant. In practical terms, a difference of 5.5 percentage units could also be considered significant and could have implications in terms of the leaching characteristics of monolithic specimens.

7.3.4 Compliance with Performance Thresholds

When considering compliance with the performance thresholds for physical properties only, the following mixes satisfied all requirements for physical properties.

- 50 wt.% CEM I, w/s: 0.55;
- 20 wt.% CEM I, w/s: 0.65; and
- 10 wt.% CEM I, w/s: 0.65.

None of the GGBS mixes satisfied all three criteria for compressive strength, setting time and consistence. However, and as previously mentioned, GGBS was successfully activated by APC residues at 50 wt.% binder addition and achieved mechanical properties comparable to CEM I mixes. Its use therefore should not be dismissed until a scale-up study is conducted. Such a study would also take into account the economics of such a process where two waste materials or by-products are used. Workability is of concern especially for commercial applications and the use of GGBS will be constrained by the type of equipment used in an APC residue S/S facility as well as associated cost. Other S/S methods such as alkali-activation (Shirley and Black, 2011a; Shirley and Black, 2011b) utilising other pozzolanic

by-products have also shown promising results in terms of their use for the S/S for APC residues when cost is concerned.

The development of mechanical properties for CEM I mixes especially at low binder additions is interesting when the results of hydration calorimetry are considered. Mixes with CEM I addition greater than 50 wt.% did not exhibit a hydration peak implying a severe retardation of hydration due to the addition of APC residues. However, the mixes compliant with performance thresholds exhibited high UCS values, which were marginally affected after water immersion. Workability criteria were achieved with water additions that are greater than what would normally be used for pure cement mixes and this affects other properties such as porosity as established above. Shirley and Black (2011) studied the S/S of APC residues using alkali-activated matrices. Their study also identified that achieving the consistence criterion of 175±10 for mixes containing 40 wt.% APC residues, would require liquids-to-solids ratios greater than 1.0 with associated negative effects on the durability and structural stability of the S/S matrix.

7.4 Chemical Properties and Leaching Characteristics

7.4.1 Acid Neutralisation Capacity and Granular Leaching

Acid neutralisation capacity and granular leaching are discussed under the same section as they were part of the same test. As described in previous chapters, granular leaching for chloride was assessed as part of the ANC test without (0 meq/g) acid addition. The test is similar to BS EN 12457-3 with the exception of the smaller particle size (<150 μm) and greater leachant exposure (48 hours). Although this approach deviates from the standard method, it constitutes a more conservative for assessing chloride leaching from APC residues in granular form.

The pH values of raw APC residues (i.e. S/S with water) without acid addition were high and greater than 12.1. No difference in pH was observed for different w/s ratios between 0.4 and 0.8. The pH of raw APC residues remained unaffected even after an acid addition of 2 meq/g. A previous study by Quina et al (2009) examined APC residues from 5 different incinerators in Portugal. It was found that raw APC residues have a high acid neutralisation capacity and exhibit a pH plateau at acid additions between 0 meq/q and 4 meq/g. The same study showed

that an acid addition of approximately 6.5 meq/g would be required to achieve a neutral (7) pH for APC residues. The alkaline nature of APC residues coupled with the solubility of amphoteric heavy metals in the waste such can increase the pore water concentration of the latter and therefore increase leaching.

The pH values for CEM I mixes in the ANC fraction without acid addition were greater than 12.1, which is equal or greater to the natural pH of APC residues. This result was expected taking into account the alkaline nature of both the hydration products as well as APC residues. In particular, the pH for that fraction increased with increasing binder addition (12.6 for 50 wt.% CEM I mixes vs. 12.3 for 10 wt.% CEM I mixes). This is attributed to the greater extend of hydration reactions and formation of hydration products as the binder content increases. The pH value of hardened cement is greater than 12.5 depending on composition and presence of alkalis (Polettini et al, 2001; Caijun Shi, 2004). This observation is also confirmed by results from hydration calorimetry where the maximum heat evolved decreases with decreasing binder. However, the pH of all CEM I mixes remained high (>11.9) even after acid addition of 2 meq/g. The pH reduction following an acid addition of 2 meq/g ranged between 0.1 and 0.4 units. As in the case of raw APC residues, high pH values may affect environmental leaching of heavy metals.

In contrast, pH values of ~11.5-12.1 were observed in the fraction of the ANC without acid addition for GGBS mixes and were lower when compared to CEM I mixes. This is attributed to the consumption of free lime present in APC residues by the pozzolanic reaction. While still in a range where many metal hydroxides, such as Zn and Pb, exhibit high solubility, this reduced pH is expected to decrease pore water concentrations of these metals, though it is not clear to what degree this would affect environmental leaching. This will be further discussed as part of the monolithic leaching section of this chapter. It is interesting to note that the pH of the mix containing 50% total dry mass GGBS, at 11.5, was lower than that usually associated with the formation of stable calcium silicate hydrate without silica gel (Stegemann and Côté, 1991), although strength development has clearly taken place. In addition this mix was not affected by water immersion, as silica gel would be. However, this observation is consistent with an even lower matrix pH, as has been previously observed for a metal sludge S/S with sodium silicate-activated GGBS (Stegemann et al, 1997).

Granular leaching (i.e., for the ANC fraction without acid addition) results indicate minimal fixation of chloride for all mixes regardless of binder type or content. The reduction in the amount leached is mainly attributed to a dilution effect based on the amount of binder added rather than effects of chloride fixation. The leaching values observed were far greater than the EU WAC limits for chloride (20,000 mg/kg for hazardous waste landfills) and would prohibit disposal to hazardous waste landfill without the use of the three times (3x) limit derogation for total dissolved solids (TDS), as is currently operating in the UK (Department of Environment, Food and Rural Affairs, 2002). The DEFRA strategy (2010) for the management of hazardous waste however, may end the application of the limit derogation and therefore impact current S/S processes in the UK.

The highly mobile nature of chloride ions and lack of chemical fixation implies that the primary route for chloride immobilisation is physical encapsulation. Physical encapsulation depends on parameters such as the permeability and tortuosity of the S/S waste. APC residues however are chloride-rich (16 wt.%) and this coupled with the mobile nature of chloride (*Rd* close to 1), implies that it is highly unlikely that other cementitious binders would be more effective for the waste additions investigated in this research.

7.4.2 Monolithic Leaching Test

a) pH

The leachate pH values remained above 11.5 for all leachate fractions from the monolithic leaching test for CEM I mixes. Lower pH values were exhibited by the GGBS mixes, and this, as in the case of granular leaching, can be attributed to the consumption of free lime present in the mix resulting from slag activation. The values obtained are similar to those for a pure $CaO\text{-}SiO_2\text{-}H_2O$ system where Na and K are present, according to data presented by Polettini et al, (2001). The high pH values for CEM I mixes are conducive to the release of amphoteric metals such as Pb and Zn whose solubility is pH dependent. This is also supported by the Pb leaching results for 50 wt.% binder addition, where all GGBS mixes had concentrations lower than the detection limit for all fractions of the tank test. Assuming that the leached concentration is half the detection limit (5 μg/L) then the leached concentration is approximately 1.5 mg/m^2. In contrast 50 wt.% CEM I mixes exhibited Pb concentrations ranging between 5.5 and 12.3 mg/m^2. The same effect was also observed for Zn with GGBS

achieving lower leaching compared to CEM I mixes for the same binder addition. It is noteworthy that the pH generally increases with the length of the leaching interval; this phenomenon may influence the test results.

ANOVA tests on the effect of the w/s ratio on pH show that varying the w/s ratio does not result in statistically significant differences for the same binder addition. For example and for 50 wt.% CEM I addition the result was (F: 1.56, $Prob > F$: 0.22). Similar results were observed for GGBS (F: 0.45, $Prob > F$: 0.64).

Modelling results also showed that pH has a marked effect on the leaching of amphoteric heavy metals such as Pb and Zn. This effect is evident when comparing results for the predicted release of Pb between CEM I and GGBS mixes with the same binder addition. This will be discussed in more detail in following sections.

b) Soluble Salts

One of the greatest barriers by far for the treatment and reuse of APC residues is the presence of chloride. A previous literature review by Quina et al, (2008) showed that the chloride content of APC residues in other studies was up to 34 wt.% depending on type of incinerator and APC technology. The content of APC residues in this study was 16 wt.% and although lower compared to the study by Quina et al, (2008), it still poses a significant barrier for the treatment and/or reuse of the waste.

Comparison of chloride leaching determined using the monolithic leach test with the monolithic WAC limits for hazardous waste (64-day release of 20,000 mg/m^2) indicates that the limit is surpassed within the first 2 days of the test for all mixes and therefore there is insufficient chloride retention by physical encapsulation or fixation. Moreover, the log-log plots of release vs. time show release of chloride is not diffusion-controlled. In contrast, release of chloride and other ions associated with soluble salts such as Na and K is availability-controlled. The results of this study indicate that binder additions greater than 50 wt.% would be required in order to effectively immobilise chloride. Similar results for the leaching of chloride were also obtained by Shirley and Black (2011a) who investigated APC residue additions in alkali-activated matrices of up to 40 wt.%.

Relatively high amounts of Na and K were also released during the leaching test. A diffusion-controlled increment could not be identified for CEM I mixes and the slopes of the log-log plots indicate surface wash-off and dissolution mechanisms. It is clear that the major release of Na and K results mainly from the surface wash-off and dissolution at early stages and later depletion of the highly soluble salts present such as NaCl and KCl. However, the ratio of the sum of the molar amounts of Na and K to Cl ((Na + K)/Cl) ranged between 0.4 and 0.6, indicating that NaCl and KCl are not the only sources of chloride in the S/S products. Chloro-complexes that have formed may also be unstable and eventually lead to chloride leaching. Previous studies have shown that alkalis can affect the physical properties of mixes such as compressive strength, setting time and rheology. Alkalis can be incorporated in calcium silicate hydrate (CSH) gel, affecting the Ca:Si ratio (Sung-Yoon Hong and Glasser, 1999) and subsequently the properties of the cement paste. Alkalis have also been reported to increase the solubility of Friedel's salt (a Cl-containing calcium aluminate hydrate) and decrease the solubility of $Ca(OH)_2$ (Rémond et al, 2002; Duchesne and Reardon, 1995).

The modelling study showed that release of soluble salts is affected by physical properties of the S/S matrix such as porosity and tortuosity. Porosity in turn exhibits a positive linear relationship with water addition. This was observed by previous studies (Loser et al, 2010) and it was expected to have an effect on the release of soluble salts such as Na, K and Cl. The effect of water addition on the release of these elements was assessed using ANOVA and the results for chloride for 50 wt.% CEM I and GGBS mixes showed that water addition does not have a statistically significant effect on the release of these elements as indicated by the low *F* values of the test (0.04 and 0.25 for CEM I and GGBS respectively). Similar results were also obtained for Na and K not only for the 50 wt.% CEM I but also for mixes with higher CEM I addition. Loser et al, (2010) investigated the resistance of concrete to external chloride ingress and also observed that the chloride binding capacity was independent of the water-to-binder ratio.

The use of GGBS or CEM I at 50 wt.% addition does not appear to significantly affect the release of soluble salts. The differences in the mean release of Cl per leaching fraction were not found to be statistically significant (*p*-value = 0.6) for 50 wt.% binder addition and a w/s ratio of 0.5. Results for *t*-tests for the same binder addition but w/s: 0.4 were similar, resulting in a *p*-value of 0.749. Although GGBS achieved lower 64-day Cl release compared to CEM I (3.7% and 8.2% for w/s of 0.4 and 0.5 respectively), the differences are not considered of

practical significance in terms of compliance with UK monWAC limits as both binders exceed the limit by more than 20 times. However, the differences in Cl release are important in terms of the geochemical mechanisms for Cl immobilisation and this is discussed further in following paragraphs.

Similar statistical results were also obtained for the release of Na and K. The resulting *p*-values from *t*-tests on means for the release of Na between 50 wt.% CEM I and GGBS mixes were 0.36 and 0.86 for w/s of 0.4 and 0.5 respectively. The *p*-values for K for the same tests were 0.74 and 0.86 respectively. This also demonstrates that CEM I and GGBS matrices have similar performance in statistical terms for immobilising soluble salts.

Increasing binder addition resulted in lower release of Cl, Na and K but given the low fixation capacity of the matrices this is attributed to a dilution effect, rather than immobilisation. This becomes more obvious when comparing the cumulative Cl fractions leached as shown in Table 7.4 which were similar regardless of binder content.

Table 7.4 Comparison of Cl cumulative fraction leached (w/s: 0.5)

Binder	Binder Content (wt.%)	Cumulative Cl Fraction Leached
CEM I	50	0.74
	20	0.77
	10	0.83
GGBS	50	0.65

One of the key routes for chloride fixation in S/S matrices is incorporation in hydration products. XRD analysis identified the presence of Friedel's salt, a hydrated chloride-containing calcium aluminate, analogous to monosulphate in hydrated ordinary Portland cement. It forms from the reaction of chloride with aluminate phases, and is stable over a wide range of chloride concentrations (Glasser et al, 2008). The chloride binding capacity of cements through the formation of chlorocomplexes such as Friedel's salt has been previously investigated (Dehwah, 2006; Suryavanshi et al, 1996). It was observed that for 50 wt.% binder additions, chlorocomplexes form and the peak of CaClOH disappears. Residual CaClOH peaks remain for 10 and 20 wt.% CEM I additions and this may be due to the reduced amount of C_3A present and the increased amount of CaClOH resulting from the

greater waste addition. Friedel's salt formation is also observed for GGBS mixes and this supports the view that such chloro-complexes can form in the presence of Ca, Al and Cl without requiring initial addition of C_3A phases to the binder. This research however shows that amounts of chloride leached from S/S APC residues are high, despite partial immobilisation in chlorocomplexes like Friedel's salt.

Taking into account the lower porosities achieved with CEM I mixes compared to GGBS, the greater retention of chloride achieved with GGBS mixes is attributed to the greater retention of Cl in hydration products. The higher amount of Al in the GGBS products may also contribute to the higher Friedel's salt diffractogram peaks, relative to the CEM I products, though this was not quantitatively investigated (Dhir et al, 1996; Rui Luo et al, 2003). Loser et al, (2010) reported that matrices with a higher Al_2O_3/SO_3 ratio will lead to the formation of more AFm phases and less Aft phases which in turn increases the potential to form Friedel's salt. Rui Luo et al, (2003) studied the chloride binding capacity of GGBS mortars and observed that bound chloride in a GGBS mortar (30% CEM I and 70% GGBS) was 91% of total chloride. In contrast bound chloride in a CEM I paste with the same mix characteristics was 80% of total chloride.[8] The observed difference in retention between the two binders is consistent with the results of this study.

It is noted however, that it is only the available Al that can react to form Friedel's salt or other Cl-containing calcium aluminate hydrates. This in turn depends on the extent that the mineral admixture has reacted, releasing adequate amounts of Al available to react (Loser et al, 2010). In addition, Loser et al, (2010) and showed that high external concentrations of Cl can destabilise hydration products such as CSH, ettringite and portlandite in favour of Friedel's salt. The same research also showed that if total Cl concentrations are high enough then even Friedel's salt is destabilised and leached and the Cl binding capacity of the matrix is reduced.

Balonis et al, (2010) showed that formation of Cl-containing hydrates depends on the constituents of the system, the competition between SO_4^{2-}, Cl^-, CO_3^{2-}, and OH^- ions and their interaction with structural elements such as Al. Rui Luo et al (2003) reported that increased alkalinity can reduce the Cl binding capacity of cementitious binders due to the competition

[8] Both results are based on an addition of NaCl of 1.0% by weight of binder during mixing (Rui Luo et al., 2003)

between the Cl and OH ions. The lower pH of GGBS for all fractions of the leaching test may therefore contribute to the increased retention of chloride compared to CEM I.

Geochemical modelling was to obtain an understanding of the extent of formation of chloro-complexes for both CEM I and GGBS. The LeachXS database was modified to include Friedel's salt, Kuzel's salt and hydrocalumite-Cl. Formation reactions and solubility products for Friedel's and Kuzel's salts were obtained from Balonis et al, (2010), whereas data for hydrocalumite-Cl were obtained by ECN, as described in previous chapters. Model results showed that hydrocalumite-Cl forms at later fractions of the test binding fraction of the chloride. Formation at later stages is attributed to physico-chemical changes in the S/S matrix and changes in the ratios of the different ions competing for substitution in AFm phases.

Cementitious matrices at binder additions evaluated in this study, have limited capacity for chemical fixation of soluble salts given the high concentrations of the latter. Although XRD results show the formation of chloride-containing compounds, the amount of carboaluminates and double-layer hydroxides is not sufficient to immobilise the high amounts of chlorides in APC residues. Furthermore, the presence of competing compounds such as sulphates can further inhibit the fixation of chloride in these compounds. Although physical encapsulation is expected to play an important role in controlling leaching of soluble salts, its role is overshadowed by the large concentrations of soluble salts in APC residues.

c) Lead and Zinc

The next most significant elements in APC residues in terms of environmental impact potential were Pb and Zn. Previous studies (Quina et al, 2008) have identified other elements with the potential for environmental pollution such as Cr and Cu. These elements however were not either detected in granular leaching tests conducted on raw APC residues or in the monolithic test conducted on S/S APC residues.

Zn was effectively contained in the matrices and its leaching was below the monWAC of 100 mg/m^2 for hazardous waste landfill. Diffusion-controlled release was observed in the early stages and changes in the chemical form or release conditions at later stages. Similar release behaviour for Zn has been reported by Van der Sloot et al, (2007). Pb or Zn bearing minerals were not identified in the XRD data for the S/S products or the untreated APC residues. The

metals may remain with the phases of the APC residue itself, or may be taken up into crystalline hydration products by isomorphic substitution, or present in amorphous materials not detected by XRD. Pb has been found to replace Ca^{2+} in CSH, inhibiting gel formation (Evans, 2008). Zn has been reported to be retained by CSH without the replacement of Ca or Si in the gel but by the linkage of tetrahedral Zn to CSH tetrahedral silicate chains (Evans, 2008; Ziegler and Johnson, 2001). Pb and Zn have previously been reported to adversely affect the hydration of Portland cement and impair its physical properties. At high pH values $Pb(OH)_4^{-2}$ and $Zn(OH)_4^{-2}$ can form Ca-complexes which precipitate and coat cement grains (Asavapisit et al, 1997).

The w/s ratio does not appear to have a significant effect on the release of Zn. ANOVA tests for Zn release resulted in *p*-values of 0.32 (F = 1.22) and 0.26 (F = 1.45) for 50 wt.% and 20 wt.% CEM I mixes respectively whereas the *p*-value for the 50 wt.% GGBS mix was 0.23 (F = 1.60).

It is interesting to note that although release of Zn increased with increasing binder addition for CEM I mixes, (for the same w/s ratio) the differences among the amounts released were not statistically significant (*p*-value: 0.16, F = 1.97). However these results are of practical significance as in contrast to the 50 wt.% mix, the 10 and 20 wt.% CEM I mixes did not meet the monWAC for stable non-reactive hazardous waste in non-hazardous landfill (30 mg/m^2) but only the monWAC for hazardous waste landfills (100 mg/m^2).

Geochemical modelling confirmed that the fate of Zn in S/S systems is complex and several mechanisms probably occur simultaneously, all competing for the available Zn species. Calcium zincate, $Zn(OH)_2$ and willemite were considered in the model as the minerals controlling the release of Zn. Calcium zincate alone was found to accurately describe release of Zn (along with the parameters of the optimum problem definition) for low (10 and 20 wt.%) CEM I additions. In contrast, and for both CEM I and GGBS at 50 wt.% binder addition, calcium zincate and willemite were found to be controlling release of Zn. However, release for the 50 wt.% mix was overestimated by an order of magnitude suggesting that more complex processes may control release of Zn may in the 50 wt.% CEM I mix. In addition, as neither calcium zincate nor willemite were not identified in the mineralogy of these matrices, it is postulated that formation of similar phases or solid solutions may be controlling release of Zn. In addition, adsorption on CSH may also be taking place. It is

therefore concluded that although the model describes release of Zn well with calcium zincate and/or willemite being the solubility-controlling minerals, the experimental data indicate that the fate of Zn is not straightforward and different processes may be competing for available Zn ions.

The leaching results for Pb showed that the monWAC limit of 20 mg/m^2 for hazardous waste landfills was exceeded for mixes with 10 and 20% CEM I addition, but was met for 50 wt.% CEM I. Pb release for 50 wt.% GGBS mixes was below the laboratory detection limit[9] and therefore lower compared to CEM I mixes with the same binder addition. This may be partially attributed to the lower pH values for all fractions of the leaching tests for the 50 wt.% GGBS mix, which reflects lower pore water pH, and therefore a reduced dissolution of Pb ions. $Pb(OH)_2$ was found to adequately represent release of Pb for both CEM I and GGBS matrices with 50 wt.% binder addition. The key difference between these matrices is the lower pH exhibited by GGBS which contributed to the lower release of Pb. Figure 7.1 shows the solubility of $Pb(OH)_2$ over a pH range of 4 to 14 calculated using PHREEQC. It shows that Pb exhibits lower solubility at a pH of approximately 10 compared to a pH of 12.0.

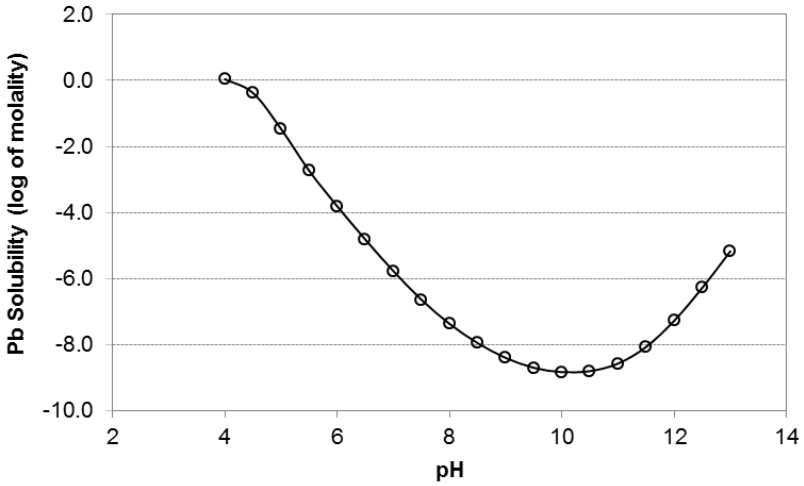

Figure 7.1 Solubility of $Pb(OH)_2$ as a function of pH

[9] A statistical comparison to CEM I was not conducted as release of Pb was below the laboratory detection limit.

The w/s ratio does not appear to have a significant effect on the release of Pb. ANOVA tests for Pb release resulted in *p*-values of 0.35 ($F = 1.13$) and 0.37 ($F = 1.04$) for 50 wt.% and 20 wt.% CEM I mixes respectively. In addition, release from all 50 wt.% GGBS mixes was below the laboratory detection limit regardless of w/s ratio.

In contrast to Zn, differences in Pb release from varying binder content for CEM I mixes were found to be statistically significant (*p*-value: 0.01, $F = 5.31$). These results are also of practical significance as 10 and 20 wt.% CEM I mixes failed to meet monWAC for hazardous waste landfills (20 mg/m^2).

d) Calcium

The absence of a $Ca(OH)_2$ peak in the 50 wt.% GGBS mixes was attributed to consumption of the lime by reaction with the pozzolan. Leaching of Ca from GGBS mixes was also significantly lower compared to CEM I mixes, as CSH is less soluble than lime (Stegemann et al, 1997). The resulting *p*-values of *t*-tests on means between CEM I and GGBS for 50 wt.% mixes at w/s: 0.4 and w/s: 0.5 were both 0.0.

The w/s ratio did not appear to have a significant effect on the release of Ca. ANOVA tests resulted in *p*-values of 0.20 ($F = 1.66$), 0.17 ($F = 1.93$), and 0.1 ($F = 2.67$), for 50 wt.% CEM I, 50 wt.% GGBS and 20 wt.% CEM I mixes respectively.

In contrast, binder addition for CEM I mixes has a more significant effect. The resulting *p*-value of a *t*-test on means between 50 and 20 wt.% CEM I mixes at w/s: 0.5 was 0.01. A similar result (*p*-value of 0.03) was obtained from the same test between 50 and 10 wt.% CEM I mixes at w/s: 0.5. This was attributed to the greater amount of soluble Ca-containing compounds (e.g. lime, calcium hydroxychloride) in mixes with lower binder addition, coupled with the lower formation of less soluble hydration products (e.g. CSH) due to the inhibited hydration reactions, as established from hydration calorimetry. It is noted that the difference in the release of Ca between 10 and 20 wt.% CEM I mixes was not found to be statistically significant (*p*-value of 0.85).

The slopes of the log-log plots for Ca indicate that depletion or a change in chemical form and release conditions may have occurred during the tank test, especially at low binder

additions. However, this does not necessarily imply that calcium is being depleted. Calcium loss may occur due to leaching of soluble Ca-containing compounds such as CaClOH, a major phase in APC residues also detected in the 10 and 20 wt.% CEM I S/S products. Once Ca derived from such compounds is removed, Ca leaching may continue from other sources such as $Ca(OH)_2$ and CSH at a much lower rate. Leaching of Ca from portlandite and CSH leading to decalcification may result in a degradation of the S/S matrix. Decalcification of CSH is a slow process which results in a reduction in compressive strength and increased porosity (Chen et al, 2006; Jain and Neithalath, 2009). Rapid leaching of soluble salts coupled with long-term decalcification may lead to an alteration in the physical properties of the matrix, deleterious to the behaviour of the product, as well as changes in the effective diffusion coefficients of all species over time.

It is interesting to note that calcite was found under-saturated in chemical speciation calculations but was detected in XRD analysis for the S/S products. Calcite, portlandite and DIC had a significant effect on the predicted release of Ca during thermodynamic modelling.

e) Silicon and Aluminium

The experimental study showed that higher amounts of Al and Si are released from GGBS mixes compared to CEM I mixes with the same binder and water addition. Resulting *p*-values from *t*-tests on the mean Al release per leaching fraction for 50 wt.% mixes were 0.02 and 0.00 for w/s of 0.4 and 0.5 respectively. The *p*-values for the same tests for Si were 0.00 for both w/s of 0.4 and 0.5 indicating that the differences are statistically significant.

The higher release values for Si are attributed to the difference in pH between the CEM I and GGBS mixes. Data from previous research indicate that concentrations of Si in aqueous phases with SiO_2 and CaO in equilibrium with tobermorite-like gel are higher when the pH is approximately 11.7 compared to a pH of 12.3. In addition, the concentrations of Si in the aqueous phases were shown to increase with decreasing concentration of Ca. Therefore the higher leaching of Si for the 50 wt.% mix in this study is attributed to both the lower pH in the GGBS matrix as well as the lower released concentration of Ca compared to the 50 wt.% CEM I mix. The higher release of Al for the GGBS mix can be attributed partly to the difference in pH but also to the higher concentrations of Al in the GGBS matrix compared to CEM I.

The w/s ratio does not appear to have a significant effect on the release of Al and Si. ANOVA tests for Al release resulted in *p*-values of 0.15 ($F = 1.92$) and 0.97 ($F = 0.03$) for 50 wt.% and 20 wt.% CEM I mixes respectively whereas the *p*-value for the 50 wt.% GGBS mix was 0.63 ($F = 0.47$). Similar results were obtained for Si with where *p*-values for the 50 wt.% and 20 wt.% CEM I were 0.10 ($F = 2.25$).and 0.50 ($F = 0.73$) respectively, whereas the *p*-value for the 50 wt.% GGBS mix was 0.40 ($F = 0.95$).

Binder addition has a more significant effect for CEM I mixes compared to the w/s ratio for Al and Si. ANOVA tests for varying binder additions with the same w/s ratio resulted in *p*-values of 0.00 ($F = 11.3$) and 0.01 ($F = 6.5$) for Al and Si respectively. Release for both elements was found to increase with increasing binder addition which is attributed to the greater content of these elements in CEM I compared to raw APC residues.

f) Sulphate

Leaching of sulphate is significantly greater from 50 wt.% GGBS compared to all CEM I mixes tested (even 10 and 20 wt.% CEM I mixes), although both binders met the monWAC for SO_4^{2-} for hazardous waste landfills (20,000 mg/m^2). The resulting *p*-value from a *t*-test on the means of 50 wt.% CEM I and GGBS mixes at w/s: 0.5 was 0.002, demonstrating that the difference in the release of SO_4 from the two matrices is statistically significant. Similar results were obtained for the same test for w/s: 0.4 (*p*-value: 0.028).

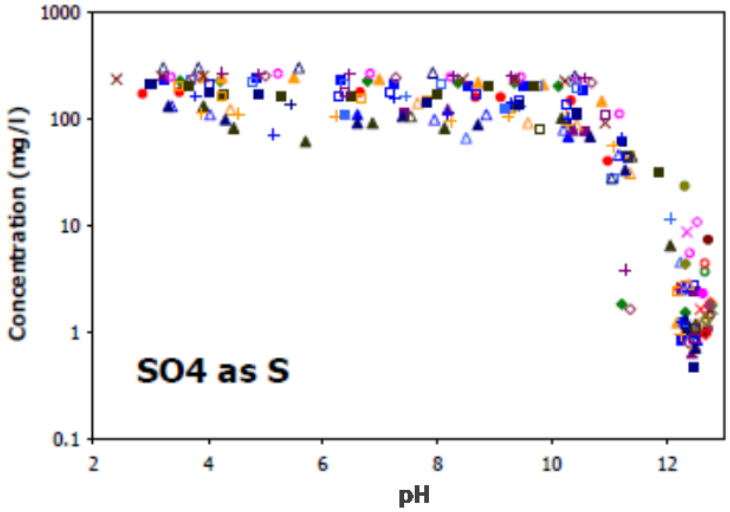

Figure 7.2 Release of SO_4 from cement mortars of worldwide origin and ranging from regular Portland to different types of blended cements (from Meeussen et al, 2010)

The difference is attributed to the difference in pH of the two matrices. Data obtained from a study by Meeussen et al, (2010) are shown in Figure 7.2 and show that release of sulphate in cementitious matrices is high at a pH range 2-10 but reduces at a pH of 12. In addition, Shirley and Black, (2011) suggested that release of SO_4 is tied to the release of Cl, as free Cl ions create a high ionic strength environment, thus reducing the activity of SO_4 ions and increasing release of SO_4. However, CEM I mixes released higher amount of Cl but still exhibited lower SO_4 release compared to GGBS. Therefore the contributors to and differences in ionic strength between GGBS and CEM I mixes requires further investigation.

As with the previous elements, the w/s ratio did not appear to have a significant effect on the release of SO_4 for 50 wt.% mixes. ANOVA tests resulted in *p*-values of 0.46 (F = 0.88) and 0.45 (F = 0.82) for 50 wt.% CEM I and 50 wt.% GGBS mixes respectively. The w/s ratio appears to have a statistically significant effect for 20 wt.% CEM I additions (*p*-value: 0.03, F = 4.1). However, 20 wt.% CEM I mixes at w/s 0.45 and 0.5 exhibited similar 64-day releases of 1,108 and 1,036 mg/m^2 respectively whereas only the mix at w/s: 0.6 had a lower release of 697 mg/m^2. Further investigation is required to establish if this is a real effect or rather attributed to experimental and/or analytical error.

Binder addition (investigated for CEM I mixes) has a more significant effect (*p*-value: 0.04, F = 3.8) compared to the w/s ratio. As with Ca, this is partly attributed to a dilution effect as binder content increases and the amount of APC residues decreases. However, fixation of SO_4^{2-} can occur in hydrates as it will be described below. Therefore increasing the binder content may result in greater amounts of hydration products with the capacity to incorporate and immobilise SO_4^{2-} ions.

Calcium sulphate hemihydrate, a potential source for leaching, was observed in the diffractograms for both CEM I and GGBS products, whereas gypsum ($CaSO_4.H_2O$) was found to adequately describe release of SO_4 in the modelling study. Comparison of leaching results indicates that immobilisation of sulphate may have taken place to a greater extent in CEM I mixes. However, other sulphur-containing minerals such as ettringite or monosulphate were not detected in the diffractograms of either the GGBS or CEM I mixes, though previous studies report formation of ettringite in S/S APC residues (Baur et al, 2001). In addition, modelling results showed that the precipitation of ettringite does not occur during the monolithic leaching test. While high concentrations of chloride have been reported (Birnin-

Yauri and Glasser, 1998; Balonis et al, 2010; Loser et al, 2010) to destabilise monosulphate and ettringite in favour of the production of Friedel's salt, the form of the sulphate and its release mechanisms in the 50 wt.% CEM I S/S products remains an open question. This is also supported by results of the modelling study where predicted release of SO_4 for the 50 wt.% mix was more than twice (133%) as high as the measured value.

Previous studies (Balonis et al, 2010) identified the presence of a Cl and SO_4-containing calcium aluminate hydrate known as Kuzel's salt. Thermodynamic modelling did not identify the formation of Kuzel's salt in S/S APC residues. Glasser et al, (1999) reported that Kuzel's salt is relatively stable relative to mixture of Friedel's salt and sulphate AFm as when these are mixed at a 1:1 ratio react to yield Kuzel's salt. However Kuzel's salt is somewhat soluble in binary combination with either Friedel's salt or sulphate-AFm. In addition, as discussed above the large concentrations of Cl in APC residues may destabilise Kuzel's salt and favour the formation of Cl-AFm phases.

As noted above, AFm phases have been previously identified as sinks for SO_4^{2-} ions which compete with Cl^-, OH^- and CO_3^{2-} ions. XRD analysis for S/S APC residues identified a single calcium aluminate hydrate ($Ca_2Al(OH)_7.H_2O$) for both CEM I and GGBS. Research has shown that the anionic content of AFm phases is sensitive to the concentrations of anions in the pore fluid. In addition, AFm phases often exhibit different hydration states. Although AFm phases with different hydration states are structurally similar (common plan) (Matschei et al, 2007), their individual detailed characteristics and role on incorporation of ions may differ. This study did not attempt to determine stability windows for AFm phases in S/S APC residues as the availability and compositional data used in the modelling study were obtained from the literature and was also deemed beyond the scope of this project. However, the interactions between the different components in the complex system of S/S and the stability of cement hydrates require further investigation.

Given the complexity in the chemistry and mineralogy of S/S APC residues the formation and interaction of AFm phases with anionic constituents of APC residues requires further investigation. Although it is unlikely that high Cl^- contents in APC residues can be immobilised fully by AFm phases, understanding of the interactions between mix constituents in complex environments can have implications for improved mix designs. For example Glasser et al, (1999) reported that the anion bound in AFm phases can affect the

hydration state of the AFm phases which in turn affects its bulk density. This may be associated with expansion effects due to changes in the hydration state of the AFm phases.

g) Minor Elements

Release of other minor elements, such as Fe, Li and Sr is similar for GGBS and CEM I at the same binder addition. Differences in release of Fe and Li between the two binders (50 wt.% addition and w/s: 0.5) were not found to be statistically significant (p-value > 0.05). In contrast, differences in the release of Sr were statistically significant (p-value < 0.05) with higher amounts being release from the CEM I mix. This can be attributed to the increased amounts of Al in GGBS compared to CEM I, which may result in the formation greater amounts of calcium aluminates hydrates ($Ca_2Al(OH)_7$-$2H_2O$). Sr has been previously reported to substitute for Ca in calcium aluminate hydrates (Evans, 2008).

As with all the elements analysed, varying the w/s ratio did not result in statistically significant differences (p-value > 0.05) in the release of Fe, Li and Sr. In addition, varying the binder content did not yield statistically significant differences in release per leaching interval for Li and Sr (p-value > 0.05). In contrast, the binder content was found to have a statistically significant effect on the release of Fe, where the mean release per leaching interval for the 50 wt.% CEM I mix was 2 and 2.6 times higher compared to the 20 and 10 wt.% mixes.

Release of these elements is not fully diffusion-controlled, and different mechanisms (including reactions) may occur throughout the test. Li behaves similarly to Na and K and there is not any indication of fixation in the S/S matrices. It was observed that release of Li increases with increasing CEM I content. This implies that the main source of Li in CEM I mixes is the binder, although the differences in release per leaching interval were not statistically significant. In addition, release of Li from GGBS mixes was greater compared to CEM I mixes which given the release patterns and minimal immobilisation suggests that greater amounts of Li salts are present in GGBS. Therefore release of Li in the case of this study was dependent on the concentration of Li salts in the binder, which in turn was dependent on binder type.

8. ALKALINE/ACID LEACHING

8.1 Introduction

The results from the monolithic leaching test indicate that Cl, Pb and Zn are barriers to the treatment of APC residues through S/S. An attempt was made as part of this study to assess the feasibility of extracting elements of concern from APC residues using a washing (leaching) pre-treatment step. This chapter forms a pre-feasibility study utilising geochemical modelling to evaluate the extraction and recycling potential of valuable elements.

8.2 Experimental and Modelling Procedure

A combined alkaline/acid leaching test was not included in the experimental scope of work of this study. Rouchotas (2001) has previously performed such a leaching procedure on APC residues from the SELCHP plant, the same EfW plant from where APC residues treated in this study were obtained. Data obtained by Rouchotas, as well as available data from other similar studies were utilised to model the combined leaching procedure. The experimental programme used by Rouchotas is briefly described here for completeness.

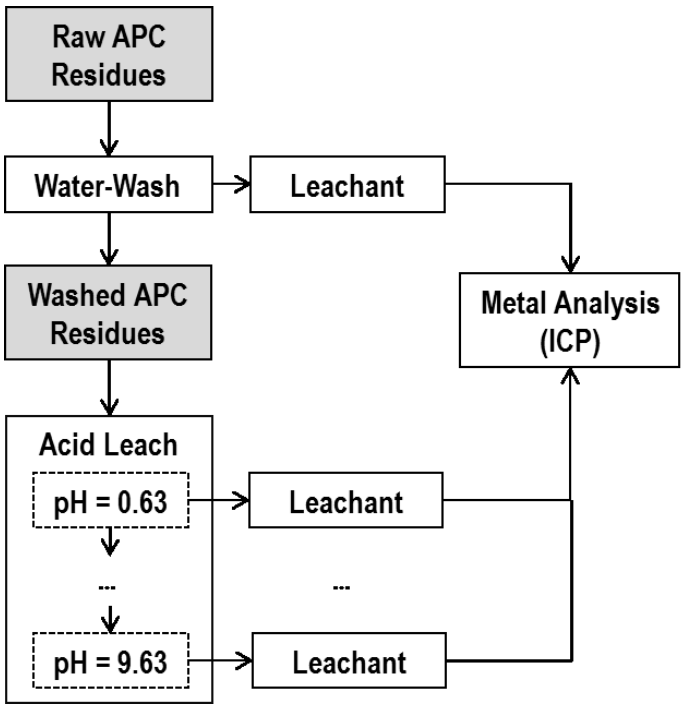

Figure 8.1 Overview of Alkaline/Acid Leaching Performed by Rouchotas

Rouchotas performed a two-step leaching test involving a water-wash step and an acid leaching step. The experimental framework followed is presented in Figure 8.1 and the procedure is detailed in Figure 8.2.

A. Water-Wash Step (Alkaline Leaching)

The water-wash step was conducted at a liquids-to-solids ratio of 20 ml/g. APC residues were placed in beakers and the corresponding amount of distilled water were added in order to achieve the desired L/S. The mixture was agitated by means of a magnetic stirrer for 24 hours. Throughout the experiment pH and conductivity measurements were obtained. The washed APC residues and the leachate were separated via filtration and the latter was analysed for metals via ICP. The washed APC residues were dried at 105^0C for 24 hours and their mineralogy was subsequently assessed via XRD.

B. Acid Leaching Step

The acid leaching step involved a series of parallel batch extractions with increasing acid addition. Eleven centrifuged tubes were stored in nitric acid overnight and subsequently rinsed with nitric acid. Each tube was labelled and 2.5g of washed APC residues were added. The appropriate amounts of 2N HNO_3 were then added to each tube with the total amount of liquids always totalling to 30ml resulting in an L/S of 12. The tubes were manually shaken until the contents appeared mixed and were then rotated end over end for 48 hours at room temperature using a rotary extractor. The tubes were subsequently centrifuged for 10 minutes at 6,000 rpm and the pH of the supernatant was determined.

Figure 8.2 Description of Alkaline/Acid Leaching Performed by Rouchotas

The water-wash step used is a batch extraction leaching procedure similar to EN12457-3, however Rouchotas used an L/S of 20 instead of 10 that is required by EN12457-3. The test can be characterised as an alkaline leaching step due to the inherent alkalinity in APC residues. Rouchotas obtained pH measurements during the water-wash step and observed that the pH was between 12 and 12.2 consistently throughout the test.

The acid leaching procedure for washed APC residues is similar to the EN14429 pH-dependence leaching test, involving a series of parallel batch extractions where sub-samples

are in contact with aqueous solutions with increasing amounts of HNO_3, under agitation for 48 hours. Differences between the test by Rouchotas and the EN14429 include:

- L/S of 12 instead of 10; and
- pH range 0.63-9.63 instead of 4-12.

Both the water-wash and acid leaching results obtained by Rouchotas[10] were converted in the LeachXS database format using 'Material Exchanger', as described previously in section 6.4.1 for the monolithic leaching test. The model input parameters and required information in each case is different due to the difference in the nature of the two tests as well as changes in the composition of APC residues following the water-wash step. The different input parameters are discussed in more detail in the following sections.

8.2.1 Alkaline Leaching Procedure (water-wash)

Rouchotas obtained alkaline leaching data for the majority of elements of interest, apart from chloride which is one of the most problematic elements in APC residues. Chloride extraction data from other studies were obtained and compared in an attempt to estimate potential chloride extraction and input in the LeachXS model. Table 8.1 shows chloride extraction values obtained in four other studies which included a water-wash pre-treatment step. It is observed that chloride extraction among these studies varied between 85 and 91.8%. For modelling purposes, it was assumed that the average of these values (or 88%), would represent a good approximation of the chloride extraction as a percentage of the total available chloride concentration in SELCHP APC residues. Taking into account that chloride availability in SELCHP APC residues is 165,000 mg/kg the estimated chloride release during the alkaline leaching step is estimated to be approximately 145,000 mg/kg.

Apart from the leaching results for the water-wash step, additional data required by LeachXS for modelling a batch extraction test include the type and volume of eluent (ml), the mass (g wet wt.) and moisture content (%) of APC residues used and the pH of the eluate.

[10] The ICP results as obtained by Rouchotas (2001) are presented in Appendix VI

Table 8.1 Chloride extraction values achieved in other studies

Study	Extraction Procedure	L/S	Cl^- Extraction (% of total Cl^-)
Hyks et al, (2007)	6 Wash Steps at L/S: 20	120	>85%
Xingbao Gao et al, (2008)	Single Batch Extraction	5	87.4%
Zheng et al, (2011)	2 Wash Steps at L/S: 1	2	91.8%
Quina et al, (2008b)	DIN38414-S4	10	91.4%

Modelling the water-wash step followed the process presented in Figure 6.1. Data that were converted in the LeachXS database format using Material Exchanger include ICP leaching results (μg/L), the mass (g wet wt.) and moisture content (%) of APC residues tested, the type and volume of eluent (ml) used and finally the pH of the eluate. These parameters are also used to transform the ICP leaching results from emission of mass per litre of eluate (μg/L) to emission of mass per mass of APC residues (mg/kg). The Chemical Speciation Finder was then used to determine an initial relevant mineral set based on the calculation of saturation indices.

Modelling of the alkaline (water-wash) step was then conducted using the Leaching Prediction Wizard in LeachXS and choosing "pH-dependent (equilibrium) cases" for a single material. The alkaline leaching in this case can be considered as a pH-dependent case comprising a single batch extraction at a pH of 12. Input variables at this stage include availability concentrations for different elements, concentrations of solid and dissolved humic acid, clay and HFO, the L/S ratio of the test and the mineral set. A summary of the input variables for the water-wash step is also presented in following sections.

The availabilities for different elements were based on the compositional analysis for the raw APC residues as provided by the SELCHP plant operator (Appendix I). However, for certain elements such as Pb the availability concentration provided by the plant operator was lower compared to the leaching value obtained by Rouchotas and so it was adjusted accordingly. This has also been observed by Quina et al, (2008b) where the amounts of Pb leached were higher compared to the availability concentration. Finally, the initial set of relevant minerals was determined using the Chemical Speciation Finder and it was adjusted thereafter until a good fit with the observed data was obtained for all or the majority of elements.

8.2.2 Acid Leaching Procedure

Modelling of the acid leaching procedure followed a similar process to the alkaline leaching (water-wash step). Apart from the leaching results (μg/L) for each batch extraction, additional data that need to be entered/transferred in the LeachXS (database) format include the mass (g wet wt.) and moisture content (%) of the washed APC residues used, the normality of the HNO_3 solution, the amount of water (ml) and the amount of the HNO_3 solution (ml) added for each batch extraction. These parameters are used to convert leaching concentrations in emission of element mass per mass of APC residues (mg/kg) and also calculate the acid neutralisation capacity of the waste.

Following data entry, the Chemical Speciation Finder was used to establish an initial list of potential solubility controlling minerals by calculating saturation indices. The leaching procedure was then modelled in the same manner as the alkaline leaching step, using the Leaching Prediction Wizard in LeachXS and choosing "pH-dependent (equilibrium) cases" for a single material. Just like the alkaline leaching step, input variables at this stage include availability concentrations for different elements, concentrations of solid and dissolved humic acid, clay and HFO, the L/S ratio of the test and the mineral set.

Rouchotas did not establish the total content or the availabilities of elements in washed APC residues and these had to be estimated prior to performing any modelling runs. Availabilities were estimated based on previous studies on washed APC residues, as well as by taking into account the results of the alkaline leaching step for soluble and availability-controlled elements (Na, K, Cl etc.). Hyks et al. (2007) previously conducted a pH-dependence test on washed and raw APC residues where it was observed that there were no significant differences between release of elements other than Na, K or Cl.

The uncertainty in availability concentrations was assessed by adjusting these values in different modelling runs and assessing the results as part of an uncertainty analysis. However, a thorough uncertainty analysis was constrained by the large number of unknown reactant availabilities (i.e. variables) in the model. Finally one of the key variables was the set of possible solubility-controlling minerals. This was adjusted after each modelling run until a good fit was observed for the majority of elements assessed.

8.3. Results

This section presents the results from the alkaline and acid leaching procedures that were described above. These results aim to provide a preliminary indication of the potential to remove elements that currently prohibit reuse of APC residues. Therefore the results focus predominantly on soluble salts (Na, K and Cl) as well as heavy metals.

8.3.1 Alkaline Leaching Step

The input parameters for modelling the alkaline leaching step are shown in Table 8.2 and the measured and predicted results are shown in Table 8.3. Although the model provides release results over a pH range, only release at the natural pH (i.e. ~12) of APC residues is of interest and is presented at this stage. The selection of relevant minerals predicts the release at the natural pH of APC residues within an order of magnitude. The availability concentrations of Na, K and Cl in raw APC residues as reported by the EfW operator overestimated the release observed by Rouchotas (2001). These were adjusted to 145,000, 18,000 and 14,000 mg/kg for Cl, K and Na respectively in an attempt to match the measured results as release was assumed to be controlled by soluble salts present in raw APC residues. Although this study and the study by Rouchotas used APC residues from the same EfW plant, some differences are expected due to the inherent variability in the composition of the waste.

Table 8.2 Input parameters for modelling the alkaline leaching step by Rouchotas

Mineral Set	***Availability Concentrations (mg/kg)***			
AA_Al[OH]3[am] AA_Brucite AA_Calcite AA_Gibbsite AA_Portlandite Anhydrite Ba[SCr]O4[77%SO4] BaSrSO4[50%Ba] Cd[OH]2[C] Cu[OH]2[s] Ferrihydrite Manganite MgKPO4:6H2O[c] Ni[OH]2[s] $Pb_4(OH)_6SO_4$ Pb2V2O7 Pb3[VO4]2 P-Wollstanite Pyrolusite Willemite	Ca	269,600	Mg	1,845
	Al	4,500	Mn	69.4
	Si	1,507	Pb	955
	H_2CO_3	13,120	Zn	7,200
	SO_4	61,190	V	0.58
	Fe	25.8	Cd	101.1
	Na	14,000	Cr	14.1
	K	18,000	Ni	6.4
	Cl	145,000	Sr	453.8
	Li	8.0	Ba	130
	Cu	98.1	PO_4	51.3
	Other Parameters			
	DOC (kg/l)	0.0001	DHA (fraction)	0.2
	SHA (kg/kg)	0.0001	pH+pe	13
	L/S ratio: 20.17			

Table 8.3 Measured and predicted release at for selected elements after the alkaline leaching step (measured data obtained from Rouchotas, 2001)

Element	Measured (mg/kg)	Predicted (mg/kg)	% Difference
Ca	83,300	161,936	94.4%
K	16,599	18,001	8.4%
Na	12,046	14,007	16.3%
Cl	144,212	144,936	0.5%
SO4	14,623	11,294	-22.8%
Pb	649	650	0.1%
Zn	122.2	149.3	22.2%
Cu	1.8	1.4	-21.6%

Significant amounts of both Ca (83,000 mg/kg) and SO_4 (15,000 mg/kg) are released from the alkaline washing. Release of Ca is overpredicted by using portlandite and calcite as the solubility controlling minerals, although the measured and predicted release were in the same order of magnitude. In contrast, release of SO_4 was found to be controlled predominantly by gypsum.

Significant amounts of soluble salts are also released from the alkaline leaching step although their release was not expected to be affected by pH but by the L/S ratio of the test. However, the effect of the L/S ratio was not investigated in this study. The predicted release during this leaching step was 14, 18 and 145 g/kg for Na, K and Cl respectively. The higher amounts of Cl are attributed to other major soluble minerals in APC residues such as CaClOH. It is evident that the model predicts that all available Na, K and Cl will be released. Assuming that that the availability of Cl in APC residues is as reported by the EfW operator (i.e. 169 g/kg) the release during the alkaline leaching step constitutes an 86% extraction[11]. Even though availabilities of Na and K were reduced in an attempt to meet the measured values, some differences are still observed. The extraction for Na and K were 60 and 72% respectively which were not as high as Cl extraction, which is partly attributed to the presence of other soluble Cl-containing compounds (i.e. CaClOH). However, this also indicates that the fate of Na and K is more complex and incorporation in less soluble minerals or hydrates may partly control release.

Model predictions for the release of heavy metals such as Pb, Zn and Cu agree well with measured values. Release of Pb, Zn and Cu at the natural pH of APC residues was found to

[11] Extraction values are expressed as a percentage of total available and not total present in the waste

be 649, 122 and 1.8 mg/kg respectively. It is interesting to note that release for Zn and Cu at the natural pH of APC residues is lower by almost two orders of magnitude compared to the release at lower (< 6) or higher (>13) pH values. This may affect the removal efficiency if leaching is conducted without any pH adjustment. This will be discussed as part of the acid leaching step which is also not constrained by the lack of results at other pH values.

Release of Pb using the availability values by the EfW operator was under-predicted, despite selection of different potential solubility-controlling minerals. The availability of Pb was adjusted as part of sensitivity analysis. This also assumed that Pb exhibits greater availability in raw APC residues and at high pH values due to formation of soluble minerals such as $Pb_4(OH)_6SO_4$ or $Pb_2(OH)_3Cl$. Adjusting the availability to 650 mg/kg, compared to 73 mg/kg as reported by the operator and using $Pb_4(OH)_6SO_4$ as the controlling mineral resulted in improved agreement between predicted and measured results. It is also noted that a similar study by Hyks et al, (2007) used a concentration of 2,100 mg/kg for Pb whereas Quina et al, (2009c) reported that available concentration for water extraction of Pb ranges between 324 and 483 mg/kg. In contrast, Zn release was described well using the availability provided by the EfW plant operator coupled with willemite as the solubility-controlling mineral.

Leaching of Cu is not problematic as its release from APC residues investigated in this study meets relevant UK WAC. However, it was included here in order to demonstrate the potential to remove such metals from APC residue focusing on recycling. The leaching behaviour of Cu was adequately described by $Cu(OH)_2$. Similar results were also obtained for other metals present in raw APC residues such as Ni, by using the relevant metal hydroxide as the solubility-controlling mineral.

8.3.2 Acid Leaching Step

The input parameters for the acid leaching step are shown in Table 8.3 and the measured and predicted results are shown in Figure 8.4.

Table 8.4 Input parameters for modelling the acid leaching step by Rouchotas

Mineral Set		***Availability Concentrations (mg/kg)***			
AA_3CaO_Fe2O3_6H2O[s]	Pb2V2O7	Ca	220,000	Mg	1,845
AA_Al[OH]3[am]	Pb3[PO4]2[2]	Al	4,500	Mn	69.4
AA_Anhydrite	Pb3[VO4]2	Si	1,507	Pb	73
AA_Brucite	PbCrO4	H_2CO_3	10,000	Zn	7,200
AA_Calcite	PbMoO4[c]	SO_4	32,000	V	0.58
AA_CaO_Al2O3_10H2O[s]	Tenorite	Fe	1,000	Cd	101.1
AA_Fe[OH]3[am]	Willemite	Na	2,500	Cr	14.1
AA_Portlandite	Zn[OH]2[B]	K	2,000	Ni	6.4
Analcime	Jarosite-Na	Cl	5,000	Sr	453.8
Ba[SCr]O4[77%SO4]	Kalsilite	Li	8.0	Ba	130
BaSrSO4[50%Ba]	Manganite	Cu	98.1	PO_4	51.3
Brushite[1]	Mg-Ferrite	***Other Parameters***			
Cd[OH]2[A]	MgKPO4:6H2O[c]	DOC (kg/l)	0.0001	DHA (fraction)	0.2
Celestite	Ni[OH]2[s]	SHA (kg/kg)	0.0001	pH+pe	13
Ettringite	Pb[OH]2[C]	***L/S ratio: 12.1***			
Mg3[PO4]2:22H2O[c]	Jarosite-K				

The washing step can have a marked effect on the mineralogy of APC residues with the formation of different hydrates that may control release. This is evident by comparing the mineral sets between the alkaline and acid leaching steps.

Similarly to the alkaline washing step a high release of Ca and SO_4 is observed during the acid leaching. Release of Ca was found to be controlled predominantly by portlandite and calcite at high pH values (> 10) whereas hydrates that have formed during the alkaline washing step may play a role in controlling release. Hydrates such as ettringite or calcium aluminosilicates have been previously reported to form during washing and control release of Ca (Xingbao Gao et al, 2008; Yangsheng Liu et al, 2009; Quina et al, 2009). Anhydrite was found to control release of SO_4 throughout the pH range acid leaching step although at pH values > 10 ettringite may also play a role in controlling release. Previous studies have also suggested that gypsum may be controlling release of SO_4 (Hyks et al, 2007; Quina et al, 2009).

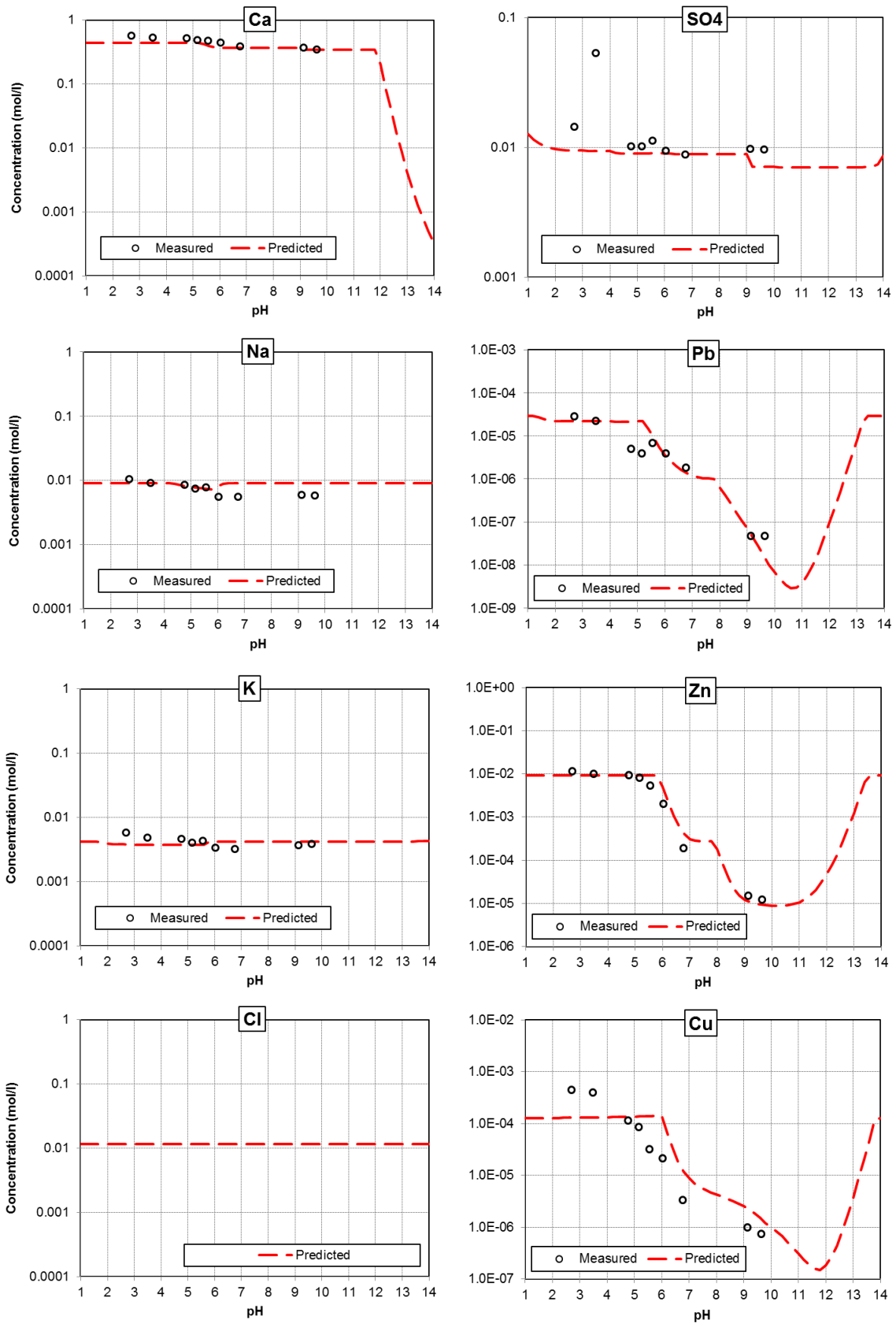

Figure 8.3 Measured and predicted release for selected elements after the acid leaching step (measured data obtained from Rouchotas, 2001)

Although release of Na and K was expected to be controlled by soluble salts remaining in the washed APC residues the release patterns indicate a minor pH dependence on the release of these elements. This may be attributed to their incorporation in phases formed during washing which may be similar to kalsilite, analcime and jarosite-Na or -K. The availability concentrations for Na and K were assumed to be approximately 2,000 mg/kg which is a reduction of approximately 90% compared to their initial availability prior to the alkaline leaching step. Although Rouchotas did not obtain release data for Cl in the acid leaching step, it is assumed that Cl availability would exhibit a similar reduction as discussed above. Remaining chloride could be incorporated in less soluble hydrates such as hydrocalumite which has been previously reported to form during washing (Yangsheng Liu et al, 2009). As shown for the monolithic tank test hydrocalumite-Cl can act as a sink for free Cl^-. The acid leaching stage could act as a supplemental step for removing soluble chloride salts. Chloride release in Figure 8.4 assumes an availability of Cl in the washed APC residues of 5,000 mg/kg. It is noted that more than 95% removal of chloride is desirable, taking into account that requirements for cementitious binders set a 0.1% total concentration limit.

In the case of the acid leaching, using a high availability for Pb (similar to the one used for the alkaline leaching step) overestimated release over the entire pH range regardless of the selection of Pb-containing minerals. This is attributed to the release of readily soluble Pb-containing compounds during the first washing stage. It is assumed that after these compounds are removed during the first (alkaline) washing step release of Pb in subsequent leaching cycles would be controlled by less soluble compounds and would exhibit reduced availability. Moreover, Pb-containing phosphate salts were found to control Pb release at a low pH values.

Release of Zn was adequately described by willemite and calcium zincate. In contrast to Pb the availability of Zn in the acid leaching step was the same as the availability used in the alkaline leaching step. It is noted that this is the total concentration of Zn in APC residues rather than the availability as determined by the EfW operator. When the availability concentration was used it provided the same results for the alkaline leaching step but underestimated release of Zn during the acid leaching step. Moreover, a previous study by Xingbao Gao et al, (2008) showed that the concentration of Zn increased in the washed APC residue by one percentage unit due to the loss of mass during leaching (approximate 31% loss).

Release of Cu in washed APC residues was found to be controlled by tenorite (CuO) but also by the amount of DOC in the pre-treated waste. Due to lack of available data, the default value of 0.0001 kg/L was used in the study. DOC can have an effect on the immobilisation of other metals such as Zn, therefore its role and available quantities in APC residues require further investigation.

In general it is observed that release of heavy metals is high at both extremes of the pH range. Release of Pb, Zn and Cu during the acid leaching step was found to be 73, 9100 and 346 mg/kg respectively, at a pH value of 2.7. In the case of Pb, pH-dependent release of washed APC residues exhibits a V-shape as with alkaline leaching but it is lower by approximately one order of magnitude compared to release during the alkaline washing stage. It is interesting to note that release of Pb at the natural pH of APC residues during the alkaline washing stage was also an order of magnitude greater compared to the release at a pH of 2.7. In contrast release of both Zn and Cu was greater during the acid leaching step indicating that an acid wash may be more suitable for the extraction of these elements. However, according to the V-shaped solubility curve during the alkaline leaching step, it is assumed that a pH higher than the natural pH of APC residues could also maximize yield of Zn during washing.

It is noted that the maximum yield values in the study by Rouchotas (2001) were obtained at pH value of 0.63. This was not modelled in this study based on considerations of commercial applicability due to the large content of acid that would be required to reduce the pH of the highly alkaline APC residues.

8.4 Discussion

This pre-feasibility study was conducted to assess the potential of utilising a single or combined washing process prior to S/S. As previously discussed the goal was to determine the potential for removal of problematic elements such as Cl, Pb and Zn, focusing on both recovery options as well as improving S/S performance.

The amphoteric nature of heavy metals allows for extraction at both the extreme ends of the pH range. Results of the study indicate that greater quantities of Pb may be released during a first stage wash at the natural pH of APC residues or at an acidic pH of less than 4. Similar results were observed by Hyks et al, (2007) where it was found that pH-dependent release of

washed APC residues was approximately an order of magnitude lower compared to raw APC residues. In contrast, release of Zn and Cu were found to be greater at low pH values (< 4) although the V-shaped solubility curves suggest that it may be possible to extract equal amounts of these metals at high pH values (> 13). In addition, more than 85% of the total available chloride can be extracted during a washing step at an L/S of 20. The effect of mixing time requires further investigation in terms of the removal of salts. A recent study by Renbo Yang et al, (2012) used a water-wash process and showed that there is no significant difference in electrical conductivity values (indicative of the presence of salts) between mixing times of 2 and 24 hours.

Release of the individual elements is directly linked to their relevant mineral phases in APC in the raw or washed residues. Although the alkaline washing step in this study focused on minerals that control release at the high natural pH of APC residues, the following discussion presents information from the literature in terms of minerals that control release of elements of concern at other pH levels. Moreover, the washing step has a marked effect on the mineralogy and characteristics of the APC residues and potential changes are also discussed below.

8.4.1 Calcium and Aluminum

The main minerals controlling release of Ca during washing of raw APC residues in this study were found to be portlandite and calcite at pH > 10 whereas anhydrite ($CaSO_4$) may control release at lower pH values. Eighmy et al, (1995) investigated leaching from electrostatic precipitator (ESP) ash from a MSW incinerator, and despite the presence of multiple Ca-containing minerals for Ca, release as a function of pH was found to be controlled by anhydrite. Van der Bruggen et al, (1998) used MINTEQ v.2 to model pH dependent release and found gypsum ($CaSO_4.2H_2O$) as the controlling phase over the entire pH range. Similarly to this study Astrup et al, (2006a, b) showed that for APC residues, gypsum ($CaSO_4.2H_2O$) may predict Ca solution concentration at pH values below 9.5. Quina et al, (2009) also suggested that, hydroxyapatite ($Ca_3(PO_4)_2$), calcite ($CaCO_3$) and dolomite ($CaCO_3.MgCO_3$) may be considered as controlling minerals for high pH. For pH above 9.5, ettringite is likely the controlling phase. For the semi-dry residues, portlandite ($Ca(OH)_2$) shall be the controlling solid at pH 12.5. Calcite ($CaCO_3$) was oversaturated at pH values above 8, which may indicate slow reaction kinetics. Zhang Yan et al, (2008) indicated for

MSWI fly ash that calcium at pH 0–12 is in the solution mostly as Ca^{2+} and $CaCl^{+}$, and $CaOH^{+}$ at pH 12–13. The controlling solids for Ca may be $CaSO_4.2H_2O$ (at pH 0–14) and $Ca_2PO_4(OH)$. In this study also ettringite $Ca_6Al_2(SO_4)_312(OH).26H_2O$ (at pH 11–13) is mentioned as playing a role, as well as $Ca(OH)_2$ (at pH 13–14). Also other studies identified ettringite as a controlling solid (Quina et al, 2009). Dijkstra et al, (2006) evaluated the influence of time in the leaching behaviour and concluded that the steady state of Ca concentrations was not obtained after 168 h in the range of pH 10–12. Thus, a kinetic control on the precipitation of ettringite may occur. Moreover, calcite may also precipitate at pH above 10. An important conclusion strengthened in this study is the fact that the CO_2 uptake may lead to all ettringite solubilisation, with calcite being a possible reaction product (Quina et al, 2009). Although chemical speciation calculations in the present study showed potential equilibrium with elements like Ca and Al with ettringite, the mineral was not considered in modelling pH-dependent release as it was not identified during mineralogical analysis of APC residues. It was considered however for subsequent pH dependent release of washed APC residues as a potential hydration product.

Thermodynamic modelling showed that release of major elements such as Ca and Al in washed APC residues may be partially controlled by formed hydrates, including ettringite that may have formed during washing APC. Xingbao Gao et al (2008) also conducted washing experiments on APC residues with identical mineralogy (in terms of major phases) with the APC residues used in this study. Their study also identified the formation of new mineral calcium aluminosilicate phases and hydrates such as gehlenite ($Ca_2Al_2SiO_7$) and plagioclase ($CaAl_2SiO_8.4H_2O$). The researchers also suggested that as these phases are common in commercial binders, washed ash could be suitable for reuse in cement. Yangsheng Liu et al, (2009) also found that minerals present in washed fly ash were much different from those in the raw waste. In their study many of the soluble minerals like CaClOH, $KCaCl_3$ and $CaCl_2.4H_2O$ had dissolved. Zoisite and gehlenite were the principal aluminosilicates present in the washed fly ash. Moreover their study identified the presence of hydrates such as $CaSO_4(PO_3OH)_4.H_2O$, Hydrocalumite ($Ca_4Al_2O_6Cl_2.10H_2O$), and $Na_{12}[Zn_{12}P_{12}O_{48}].12H_2O$ which were formed during the washing treatment. Hyks et al, (2007) previously suggested that phases such as monosulphate may control release of elements such as Ca and Al. In the present study chemical speciation calculations identified that both monosulphate and ettringite may be in equilibrium with Ca and Al. Given the large concentrations of SO_4, ettringite was selected as a more probable mineral, although selection

of monosulphate did not result in significant differences in the release of Ca and Al. It is noted that due to lack of available data, availability concentrations for all elements were either obtained from the literature or estimated. The available concentrations of elements such as Ca, Al and SO_4 can significantly affect the nature of hydration products and therefore further experimental work is recommended in order to confirm the results of this preliminary modelling study.

8.4.2 Lead

Release of Pb as a function of pH was found to be complex with different possible minerals controlling release at different pH ranges. Results from the present study show that at pH values greater than 10 release of Pb from raw APC residues may be controlled by $Pb_2(OH)_3Cl$ and/or $Pb_4(OH)_6SO_4$. Geysen et al, (2004) conducted simulations with Visual Minteq to model pH dependent release from raw APC residues and concluded that the main controlling phases are: $Pb_2(CO_3)Cl_2$ for pH 4–6, PbClOH for pH 6–12, and $Pb_4(OH)_6SO_4$ for pH > 12. If no sulphate is available for leaching, the Pb solubility above pH 12 may be controlled by $Pb_2(OH)_3Cl$ instead of $Pb_4(OH)_6SO_4$. Therefore, the large amounts of sulphates in APC residues in this study suggest that $Pb_4(OH)_6SO_4$ may play a more important role in controlling release. It is noted however that both minerals exhibit relatively high solubility at the natural pH of APC residues. Astrup et al, (2006a, b) investigated leaching from APC in the absence of high salt levels with and without allowing for carbonation effects. Under these conditions, Pb seems to be controlled by $Pb_2V_2O_7$ for pH below 8–9, and Pb_2O_3 for pH above 9. Cerrusite ($PbCO_3$) and hydrocerrusite have also been suggested to have a role on the Pb solubility (Quina et al, 2009; Hyks et al, 2007; Johnson et al, 1996). This phase was also described by Eighmy et al, (1995) for ESP residues at pH 8–10, whereas anglesite ($PbSO_4$) was found to be a controlling solid at pH 3–8. Hyks et al, (2007) also suggested anglesite as the controlling phase for Pb at low pH values. Van der Bruggen et al, (1998) analysed ESP residues from MSWI, and identified $Pb_5(PO_4)_3Cl$ as the solubility controlling phase for pH lower than 9, whereas $Pb(OH)_2$ is the main phase at higher pH values. However, Van Herck et al, (2000) indicated that $Pb_5(PO_4)3Cl$ controls the solubility only for pH <3.5, while for pH between 3.5 and 9 the controlling mineral is $Pb(OH)_2.Al(OH)_3.2AlPO_4.H_2O$ while for pH > 9, $Pb(OH)_2$ plays a more important role. Pb leaching may be also influenced by sorption processes, being this element referred to in some studies as a sorption/complexation-controlled element (Hyks et al, 2007). At high pH (>11), Pb cations (as well as Ni and Cd)

tend to sorb into reactive surfaces such hydrous iron (hydr)oxides and hydrous aluminium (hydr)oxides (Quina et al, 2009). However, Zhang et al, (2008a) reported that surface complexation has little effect on Pb leaching and that the precipitation/dissolution modelling allowed good adjustment to the experimental values. In their study and at pH above 8, the controlling phase is $Pb(OH)_2$, whereas $Pb_5(PO_4)_3Cl$ is the controlling phase at pH below 8. Hyks et al, (2007) also suggested that the concentration of DOC and complexation with organic ligands can also affect release of Pb. Van der Sloot et al, (2007) used LeachXS to model pH dependent release from MSWI fly ash and found that between pH 8 and 10, up to 20% of the Pb is complexed with DOC (humic acid). Pb speciation in the solid phase was controlled predominantly by mineral solubility and sorption to HFO (between pH 3 and 7). In the pH range from 1 to 7, a significant proportion of Pb is found in the minerals $PbMoO_4$ and, to a much lesser extent, $Pb_3(VO_4)_2$. Above pH 7, there is some sorption to HFO but the mineral $Pb(OH)_2$ is the dominant phase that is controlling Pb solubility in the solid. Binding to solid organic matter (humic acid) was found to be minimal in the pH range from 2 to 6.5.

It is interesting to note that similar minerals were found to control release of Pb in washed APC residues. However, the availability of Pb was considered to be reduced by an order of magnitude. This is attributed to the presence of soluble Cl or SO_4 complexes which are removed during the alkaline washing stage. Indeed inclusion of $Pb_2(OH)_3Cl$ and $Pb_4(OH)_6SO_4$ did not adequately explain release of Pb from washed APC residues. Similar observations were obtained by Hyks et al, (2007). $Pb(OH)_2$ was found to be the main solubility controlling phase at pH > 9 whereas at lower pH (< 5) phases like $PbMo_4$ and lead phosphate salts were found to control release. In addition, measured pH values at the pH range 4-6 for washed APC residues can be explained by $Pb(OH)_2.Al(OH)_3.2AlPO_4.H_2O$. Finally, as in the study by Van der Sloot et al, (2007) and in the pH range 7-10, DOC was found to play an important role in terms of forming complexes with Pb which may be released in solution thereafter. It is noted however, that this study used default LeachXS values for DOC concentrations in the waste and therefore the effect of DOC requires further investigation in order to confirm results of this study.

8.4.3 Zinc

Release of Zn at the natural pH of raw APC residues was found to be described well by willemite. Van der Bruggen et al, (1998) have previously found at pH 6, one third of the total

elemental Zn remains in solution, approximately one third is precipitated as smithsonite ($ZnCO_3$) and the remaining third exists as ZnO.SiO2. The solid $Zn_5(OH)_8C1_2$ was suggested as the controlling phase at pH 6–8 and ZnO at pH 7–13. At low pH, the equilibrium concentration is determined by the maximum amount of zinc that leaches from the waste. When the pH is greater than 13, Zn solubility increases mainly due to the formation of hydroxide complexes (Quina et al, 2009). Van Herck et al, (2000) obtained similar results for Zn, but in their study Zn solubility was controlled by $ZnO.SiO_2$, $ZnCO_3$ and $Zn(OH)_2$. Eighmy et al, (1995) suggested leaching of zinc may be controlled by smithsonite ($ZnCO_3$) over pH 5–10 and $ZnSiO_3$ at low pH values (3–5). Zhang Yan et al, (2008) suggested that only dissolution/precipitation adequately described release of Zn, implying that other processes such as adsorption/complexation are not important. In their study the dominant Zn species in solution were found to be Zn^{2+} and $ZnCl^{+}$ for pH 0–6, $ZnSiO_3$, $ZnOH^{+}$, $Zn(OH)_2(aq)$, $Zn(OH)^{3-}$, and $Zn(OH)_4^{2-}$ for pH 7–13 while above pH 14 the amount of $Zn(OH)_2$ decreased. In their study the main controlling solid was $ZnSiO_3$. Other studies reported that at high pH, Zn does not tend to sorb to reactive surfaces of APC residues such as hydrous iron (hydr)oxides and hydrous aluminium (hydr)oxides (Quina et al, 2009). Astrup et al, (2006a,b) suggested that willemite (Zn_2SiO_4) is the main controlling mineral in the region of pH 7 and in the pH range of 8–10, zincite (ZnO) may play an important role on solubility. At pH 10.5–12, some outliers were described by calcium zincate ($CaZn_2(OH)_6.2H_2O$). Below pH 7, Zn seems to be under-saturated with respect to willemite, and the solubility control may be $ZnSiO_3$.

Results from the pH-dependent release of washed APC residues suggest that there were not any significant mineralogical changes in terms of Zn-containing minerals during washing of raw APC residues. In addition, using the same metal availability concentration for both modelling sessions resulted in predictions that agreed well with experimental data. It is therefore assumed that Zn-chloride or other soluble complexes do not play a significant role in controlling release. It is noted that although willemite was found to control release at pH values < 10, other minerals such as $ZnCO_3$ or $ZnSiO_3$ provided similar results. DOC was not found to have as a significant effect on the release of Zn as in the cases of Pb or Cu. Finally it was observed that higher amounts of Zn are released during at low pH (< 6) and therefore an acid leaching procedure may be more appropriate for the extraction of Zn.

8.4.4 Copper

Copper is not an element of concern in APC residues as leached concentrations meet relevant regulatory requirements for disposal. However, it is considered here with a focus on extraction and recycling. Release of Cu was controlled by $Cu(OH)_2$ for raw APC residues whereas tenorite (CuO) and DOC were found to play a significant role for washed APC residues. Eighmy et al, (1995) also found that model predictions with $Cu(OH)_2$ as the solubility controlling mineral agree well with experimental leaching data for Cu for raw APC residues. Similar observations were also obtained by Hyks et al, (2007) who found that at high pH, release of Cu could be explained by $Cu(OH)_2$ or atacamite ($Cu(OH)_3Cl$). The same study also suggested that at pH 7-10 complexation with DOC becomes more important whereas a pH < 7 release may be controlled by tenorite or atacamite. Johnson et al, (1997) previously investigated the leaching behaviour and solubility of heavy metals in MSWI fly ash. Their study identified that release of Cu exhibited different patterns compared to Pb and Zn. This was attributed to the fact Cu is known to form complexes with organic ligands which can affect release. As noted above, the amount of DOC used in the problem definition was found to affect the model predictions for Cu.

8.5 Conclusions

The above review demonstrates that relatively similar minerals have been previously found to control release of elements of concern from APC residues. The preliminary results from this study suggest that it may be possible to extract heavy metals from APC residues through a single or multiple washing procedure. However, the determining factor for commercial application would be the economics of such a process. The economics would be affected by the cost of the extraction technology as well as the demand for and price of both virgin and recycled metals. In addition, further investigation is required in terms of the hydrometallurgical techniques that would be applicable for the extraction of the metals from the leachate, the potential impact of impurities in the yield and the disposal costs of any non-valuable components remaining.

9. CONCLUSIONS AND RECOMMENDATIONS FOR FURTHER RESEARCH

9.1 Conclusions

The present study aimed at closing a gap in existing knowledge on the effectiveness of S/S of APC residues, not only in terms of heavy metal immobilisation but also considering the role of chloride, the most abundant pollutant in the waste. In addition, the study aimed at obtaining an improved understanding of the performance of high waste/low binder mixes, which are not commonly discussed in the literature.

In order to achieve these objectives, the design of the study included a combined experimental-modelling approach, as shown in Figure 9.1

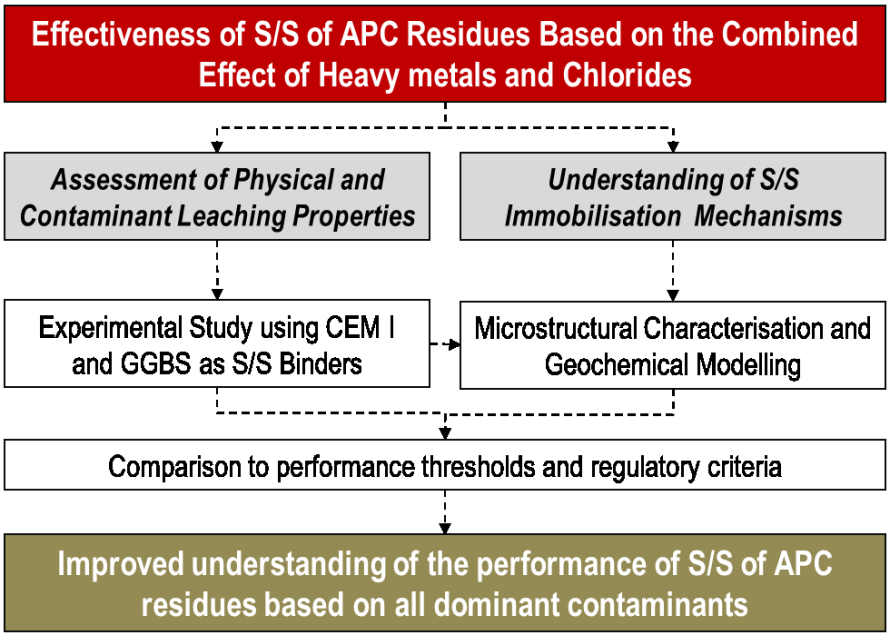

Figure 9.1 High-level study design

The study evaluated the effectiveness of the process utilizing CEM I and GGBS as the S/S binders and varying key parameters such as the waste-to-binder and water-to-solids ratios. Unlike previous studies where an activator (e.g. alkaline solution) was used to activate the GGBS, this study attempted to achieve that by taking advantage of the inherent alkalinity of

APC residues. Physical properties and leaching chacarcteristics of the resulting products were compared to performance thresholds and regulatory criteria. Performance thresholds for S/S products have been previously established by Stegemann and Zhou (2008) and were complimented in this study with UK landfill acceptance criteria as a benchmark for leaching performance as shown below. The UK monWAC were chosen as the absolute ceiling for leaching performance based on disposal options (lower tier of waste management hierarchy). Nevertheless, leaching performance that would favour reuse of APC residues is more desirable.

- Consistence: 175±10 mm
- Initial Setting Time 2< initial setting time < 8 hours
- Final Setting Time < 24 hours
- 28-day Compressive Strength: > 1.0 MPa
- Compliance with UK monWAC

This study showed that treatment of APC residues through S/S is severely hampered bythe large amounts of Cl present in the composition of APC residues, despite partial immobilisation in calcium chloro-aluminate phases. Although S/S matrices achieve mechanical properties that could allow beneficial reuse of APC residues, rapid leaching with respect to Cl prohibits reuse as a building material. Cessation of the three-time derogation of granular WAC as part of the UK hazardous waste management strategy could also render use of S/S impractical even for landfill disposal. Similar findings in terms of reuse of APC residues have been recently reported by Quina et al (2011). Results from this study indicate that a pre-treatment stage would be required prior to S/S to remove the soluble fraction. A single water-wash step could remove more than 90% of total available Cl, as there is limited fixation in APC residues. The high inherent alkalinity of APC residues also favours the extraction of heavy metals during a water-washing step due to the amphoteric nature of key metals present in APC residues. Extraction of heavy metals can be further enhanced with the use of an acid leaching step. Extraction of metals and chlorides as a pre-treatment step can favour recovery of potentially valuable constituents of APC residues while improving the performance of the S/S process.

Specifically and based on the results of this study it can be concluded that:

1. Binder additions greater than 50 wt.% would be required to obtain products that meet UK WAC for monolithic waste for disposal in stable non-reactive waste landfills.

Mixes with lower binder additions (e.g. 10 and 20 wt.%) do not perform well in terms of leaching, as Pb and Zn exceeded relevant WAC. The commercial viability of an S/S process utilising high binder additions (>50 wt.%) and where the end product is destined for landfill is questionable.

2. Although Zn and Pb were effectively immobilised for binder additions of 50 wt.% the fixation mechanisms are not straightforward and several processes may be occurring simultaneously. Geochemical modelling showed that Zn-bearing minerals such as willemite and calcium zincate describe diffusion-controlled release of zinc relatively well. However, these minerals were not identified in the mineralogy of the S/S matrices. Different processes may be taking place such as formation of Zn-containing solid solutions or adsorption to CSH, which along with physical encapsulation contribute to the immobilisation of Zn in the S/S matrix and reduce its availability for leaching. Leaching of Pb was adequately described by $Pb(OH)_2$ or PbO (for lower binder additions) and was affected predominantly by changes in pH. GGBS mixes performed better compared to CEM I in terms of release of Pb and this is attributed to the lower natural pH of the matrix.
3. The Cl content of APC residues is high and is the single most important barrier for the treatment of the waste or its reuse as a cement substitute for structural applications. The fraction of Cl released is in the range of 70-80% and is similar for all mixes regardless of binder type and content. Chloride release exceeds UK monWAC for hazardous waste landfill (20,000 mg/m^2) by up to fifty fold, depending on mix binder content. Release of Cl is availability-controlled and the main parameters that affect release of soluble salts are porosity and tortuosity which pertain to the physical properties of the S/S matrices. The modelling study showed that immobilisation of Cl can occur through the formation of Cl-bearing minerals such as Friedel's salt or hydrocalumite-Cl. This is also supported by the lower release of Cl from GGBS compared to CEM I mixes as the higher amounts of Al in the former contribute to the greater formation of calcium chloro-aluminates. Cl fixation in these minerals however, is affected by competing anions such as OH^-, SO_4^{2-} and CO_3^{2-}.
4. S/S APC residues can achieve compressive strengths that far exceed requirements for landfill disposal and could be suitable for commercial applications (e.g. aggregates, fill material etc.). Binder additions of 50 wt.% resulted in compressive strengths greater than 15 MPa, despite retardation of hydration reactions, and did not exhibit a statistically significant change after immersion in water for 7 days. Structural integrity

and sound mechanical properties improve the prospect of reusing S/S APC residues as long as chlorides are managed appropriately prior to application of S/S.

5. GGBS was successfully activated at 50 wt.% additions using solely APC residues without additional activators. 50 wt.% GGBS mixes achieved physical properties which were comparable to CEM I mixes with the same binder and water content. However, CEM I mixes perform better compared to GGBS at lower binder additions, meeting or exceeding the compressive strength criterion of 1.0 MPa at 28 days. In contrast, 10 and 20 wt.% GGBS mixes had compressive strengths lower than 1.0 MPa and in some cases collapsed during water immersion. The extent and effect of hydration reactions for 10 and 20 wt.% GGBS mixes is therefore questionable.
6. The fine particle size of APC residues coupled with the hygroscopic nature of the salts in their composition result in high water requirement to achieve flowable mixes. Increasing water addition to obtain more flowable mixes had detrimental effects on porosity and compressive strength. However, varying the w/s ratio did not result in statistically significant differences in the leaching of soluble salts. Compromises and trade-offs between workability and matrix performance will need to be assessed as part of a scale-up study prior to commercial application.
7. A preliminary thermodynamic modelling study showed that application of a water washing and/or acid leaching step prior to S/S could result in the removal of more than 90% of Cl in APC residues. In addition, the washing stages can also remove significant amounts of Pb and Zn. Modelling results from this study showed that a simple washing leaching step of 1 kg of APC residues at a L/S ratio of 20 can result in a release of approximately up to 650 mg of Pb and 120 mg of Zn. This enhances the reuse potential of the pre-treated APC residues, but also favours extraction and recovery of these elements for use in manufacturing processes.

9.2 Recommendations for further research

It is recommended that further work on the treatment of APC residues is focused on reuse options and is aligned with UK waste management policy. The cessation of the application of the three-time derogation could have a marked effect on current disposal practices for APC residues as even treated APC residues may not be able to meet the UK WAC for inert landfill disposal. This, coupled with the landfill tax for hazardous or active waste (which is expected to reach £80 per tonne by 2014), should provide an incentive to reduce the amount of APC

residues sent to landfill. According to the UK Technology Strategy Board (2009), the total cost of sending UK's APC residue to landfill was estimated at £24.5 million in 2009.

The recommendations resulting from this study aim to approach APC residues as a resource. Metal-containing waste such as APC residues can be considered as low-grade ores with the potential of recovering their valuable components. Heavy metals in APC residues can be potentially recovered using hydrometallurgy techniques (e.g. leaching). As booming and emerging economies become increasingly resource-intensive, recovery of metals from APC residues may increase the attractiveness of metal recovery technologies.

The fact that 190,000 tonnes of APC residues were generated in the UK in 2009 puts the potential benefit from the extraction of heavy metals in context. Previous studies have used techniques such as electrokinetic extraction (Traina et al., 2009; Ferreira et al., 2008; Ottosen et al., 2006; Pedersen et al., 2005) to recover both heavy metals and chorine by utilising an electrochemical cell. Extraction of metals can also be enhanced by using single or multiple washing steps as demonstrated in this study. Furthermore, the potential presence of rare earth metals in APC residues from other sources such as medical waste incineration (Lijuan Zhao et al., 2008) and techniques for their recovery warrant further investigation.

Recovery of chlorine from APC residues would be advantageous in terms of reusing the Cl-free APC residues while benefiting from selling the recovered chlorine. Chlorine recovery and provision for example for the production of plastics[12] would close the loop for the use of chlorine in this industry. The chlor-alkali process is an example of a well-established commercial procedure for the electrolysis of sodium chloride solutions (brines), resulting in the separation of chlorine and caustic soda (NaOH). The modelling study as part of this research showed that more than 90% of the total Cl content of APC residues can be extracted using a simple washing step. The Cl-rich eluate from the washing process could be further processed to recover chlorine in a form of marketable product. It is therefore recommended that chlorine recovery processes be further investigated for the extraction of chlorine which could be used in commercial chemical production processes thereafter. Limitations for the recovery of chlorine include potentially energy intensive recovery processes (e.g. chlor-alkali

[12] Chlorine is extensively used in the production of commodity and specialty chemicals. A well-known example is the direct chlorination of ethylene to produce ethylene dichloride, a precursor for vinyl chloride monomer which is in turn used for the production of polyvinyl chloride.

process), impurities in the eluate which may hamper recovery of desired components and finally market demand and prices for the product. For example, any recovery process must yield a product with low manufacturing costs that would have competitive price in the global market compared to “virgin” sources of chlorine.

Finally, the rapid leaching of structural elements such as calcium (decalcification) and soluble salts from the S/S matrices investigated in this study and their long-term effect on structural integrity requires further investigation. Such a study would focus on long-term (i.e. > 50 years) changes in mineralogy and physical properties, such as porosity and compressive strength, through laboratory studies (e.g. accelerated decalcification using aggressive solutions) and geochemical modelling. Modelling would form a key part of this study as it would be impractical to assess long-term changes only through laboratory experiments.

10. REFERENCES

Aguiar Del Toro, M., Calmano, W. & Ecke, H. (2009) Wet extraction of heavy metals and chloride from MSWI and straw combustion fly ashes. *Waste Management,* 29, 2494-2499.

Al-Hamdan Z.A. & Reddy R.K. (2008) Electrokinetic remediation modeling incorporating geochemical effects. *Journal of Geotechnical and Geoenvironmental Engineering,* 134, 91-105.

Amutha Rani D., Bocaccini, A.D., Deegan, D. & Cheeseman, C.R. (2008a) Air pollution control residues from waste incineration. Current UK situation and assessment of alternative technologies. *Waste Management,* 28, 2279-2292.

Amutha Rani D., Gomez, E., Bocaccini, A.D., Hao, L., Deegan, D. & Cheeseman, C.R. (2008b) Plasma treatment of air pollution control residues. *Waste Management,* 28, 1254-1262.

Andreola, F., Barbieri, L., Hreglich, S., Lancellotti, I., Morselli, L., Passarini, F. & Vassura, I. (2008) Reuse of incinerator bottom and fly ashes to obtain glassy materials. *Journal of Hazardous Materials*, 153, 1270-1274.

Antemir, A., Hills, C.D., Carey, P.J., Gardner, K.H., Bates, E.R. & Crumbie, A.K. (2010) Long-term performance of aged waste forms treated by stabilization/solidifications. *Journal of Hazardous Materials*, 181, 65-73.

Appelo, C.A.J. & Postma, D. (2005) *Geochemistry, Groundwater and Pollution*. 2nd ed., A.A. Balkema Publishers, The Netherlands.

Asavapisit S. (1998) *Solidification Systems for Metal Containing Hazardous Wastes*. PhD Thesis, Imperial College London.

Asavapisit S., Fowler, G. & Cheeseman, C.R. (1997) Solution chemistry during cement hydration in the present of metal hydroxide wastes. *Cement and Concrete Research*, 27, 1249-1260.

Astrup, T., Dijkstra, J.J., Comans, R.N.J., van der Sloot, H.A. & Christensen, T.H. (2006a) Geochemical modeling of leaching from MSWI air-pollution-control residues. *Environmental Science and Technology*, 40, 3551–3557.

Astrup, T., Mosbæk, H. & Christensen, T.H. (2006b) Assessment of long-term leaching from waste incineration air-pollution-control residues. *Waste Management*, 26, 803–814.

Aubert, J.E., Husson, B. & Vaquier, A. (2004) Use of municipal solid waste incineration fly ash in concrete. *Cement and Concrete Research*, 34, 957-963.

Baciocchi, R., Costa, G., Polettini, A., Pomi, R. & Prigiobbe, V. (2009) Comparison of different reaction routes for carbonation of APC residues. *Energy Procedia*, 1, 4851-4858.

Balonis, M., Lothenbach, B., Le Saout, G. & Glasser, F.P. (2010) Impact of chloride on the mineralogy of hydrated Portland cement systems. *Cement and Concrete Research*, 40, 1009-1022.

Barna, R., Rethy, Z., Imyim, A., Perrodin, Y., Moszkowicz, P. & Tiruta-barna, L. (2000a) Environmental behaviour of a construction made of a mixture of hydraulic binders and air pollution control residues from municipal solid waste incineration Part 1. Physico-chemical characterization and modelling of the source term. *Waste Managemen*t, 20, 741–750.

Barna, R., Rethy, Z., Perrodin, Y., Moszkowicz, P. & Tiruta-barna, L., (2000b) Environmental behaviour of a construction made of a mixture of hydraulic binders and air pollution control residues from municipal solid waste incineration Part 2. Simulation tests and and validation of the source term modelling. *Waste Management*, 20, 751–759.

Barret, P., Ménétrier, D. & Bertrandie, D. (1983) Mechanism of C3S dissolution and problem of the congruency in the very initial period and later on. *Cement and Concrete Research*, 13, 728–738.

Batchelor, B. (2006) Overview of waste stabilisation with cement. *Waste Management*, 26, 689-698.

Batchelor, B. & Wu, K. (1992) Effects of equilibrium chemistry on leaching of contaminants from stabilized/solidified wastes. In: Spence, R.D. (ed) *Chemistry and Microstructure of Solidified Waste Forms*. Lewis Publishers, Boca Raton, Florida.

Baur, I., Ludwig, C. & Johnson, C.A. (2001) The leaching behavior of cement stabilized air pollution control residues: A comparison of field and laboratory investigations. *Environmental Science and Technology*, 35, 2817-2822.

Bayuseno, A.P., Schmahl, W.W. & Müllejans, Th. (2009) Hydrothermal processing of MSWI Fly ash-towards new stable minerals and fixation of heavy metals. *Journal of Hazardous Materials*, 167, 250-259

Bertolini, L., Carsana, M., Cassago, D., Curzio, A.Q. & Collepardi, M. (2004) MSWI ashes as mineral additions in concrete. *Cement and Concrete Research*, 34, 1899-1906.

Birnin-Yauri, U.A. & Glasser, F.P (1998) Friedel's salt, $Ca_2Al(OH)_6(Cl,OH)\bullet 2H_20$: Its solid solutions and their role in chloride binding. *Cement and Concrete Research*, 28, 1713-1723.

Bournonville, B., Nzihou, A., Sharrock, P. & Depelsenaire, G. (2004) Stabilisation of heavy metal containing dusts by reaction with phosphoric acid: study of the reactivity of fly ash. *Journal of Hazardous Materials*, B116, 65-74.

Bullard, J.W., Jennings, H.M., Livingston, R.A., Nonat, A., Scherer, G.W., Schweitzer, J.S., Scrivener, K.L. & Thomas, J.J. (2011) Mechanisms of cement hydration. *Cement and Concrete Research*, 41, 1208-1223.

Caijun Shi, (2004) Hydraulic cement systems for Stabilisation/Solidification. In: Spence, R.D. & Shi, C. (Eds.) *Stabilisation/Solidification of Hazardous, Radioactive and Mixed Wastes*. CRC Press, pp. 49-70.

Chandler, A.J., Eighmy, T. T., Hartlén, J., Hjelmar, O., Kosson, D.S., Sawell, S.E., van der Sloot, H.A. & Vehlow, J. (1997) *Municipal Solid Waste Incinerator Residues: Studies in Environmental Science*, Elsevier.

Chen, J.J., Thomas, J.J. & Jennings, H.M. (2006) Decalcification shrinkage of cement paste. *Cement and Concrete Research*, 36, 801-809.

Chen, Q.Y., Hills, C.D., Tyrer, M., Slipper, I., Shen, H.G. & Brough, A. (2007) Characterisation of products of tricalcium silicate hydration in the presence of heavy metals. *Journal of Hazardous Materials*, 147, 817-825.

Chen, Q.Y., Tyrer, M., Hills, C.D., Yang, X.M. & Carey, P. (2009) Immobilisation of heavy metal in cement-based solidification/stabilisation: A review. *Waste Management*, 29, 390-403.

Chimenos, J.M., Fernández, A.I., Cervantes, A., Miralles, L., Fernández, M.A. & Espiell, F. (2005) Optimizing the APC residue washing process to minimize the release of chloride and heavy metals. *Waste Management*, 25, 686-693.

Chyrsochoou, M. & Dermatas, D. (2006) Evaluation of ettringite and hydrocalumite formation for heavy metal immobilization: Literature review and experimental study. *Journal of Hazardous Materials*, 136, 20-33.

Cinquepalmi, M.A., Mangialardi, T., Panei, L., Paolini, A.E. & Piga, L. (2008) Reuse of cement-solidified municipal incinerator fly ash in cement mortars: Physico-mechanical and leaching characteristics. *Journal of Hazardous Materials*, 51, 585-593.

Collivignarelli, C. & Sorlini, S. (2002) Reuse of municipal solid wastes incineration fly ashes in concrete mixtures. *Waste Management*, 22, 909-912.

Conner, J.A. (1990) *Chemical Fixation and Solidification of Hazardous Wastes*. Van Nostrand Reinhold Publications, New York.

Dajie Zhang, Wenshi Liu, Haobo Hou & Xinghua He (2007) Strength, leachability and microstructure characterisation of Na2SiO3-activated ground granulated blast-furnace slag solidified MSWI fly ash. *Waste Management and Research*, 25, 402-407.

De Windt, L., Badreddine, R. & Lagneau, V. (2007) Long-term reactive transport modelling of stabilized/solidified waste: from dynamic leaching tests to disposal scenarios *Journal of Hazardous Materials*, B139, 529-536.

Dehwah, H.A.F (2006) Effect of sulphate contamination on chloride-binding capacity of plain and blended cements. *Advances in Cement Research*, 18, 7-15.

Department of Environment, Food and Rural Affairs. (2010) *A Strategy for Hazardous Waste Management in England*. Available from http://www.defra.gov.uk/

Dhir, R.K., El-Mohr, M.A.K. & Dyer, T.D. (1996) Choride binding in GGBS concrete. *Cement and Concrete Research*, 26, 1767-1773.

Duchesne, J. & Reardon, E.J. (1995) Measurement and prediction of portlandite solubility in alkali solutions. *Cement and Concrete Research*, 25, 1043-1053.

Eighmy, T.T., Eusden, J., Krzanowski, J., Domingo, D., Stampfli, D., Martin, J. & Erickson, P. (1995) Comprehensive approach toward understanding element speciation and leaching behavior in municipal solid waste incineration electrostatic precipitator ash. *Environmental Science and Technology*, 29, 629–646.

Environment Agency, UK. (2002) *Solid Residues from municipal waste incineration in England and Wales*. Available from http://www.environment-agency.gov.uk/

Environment Agency, UK. (2004) *Guidance on the use of Stabilisation/Solidification for the Treatment of Contaminated Soil*. Available from http://www.environment-agency.gov.uk. Accessed 9 May 2011.

European Commission (2010) *Preparing for the Review of the Thematic Strategy on the Prevention and Recycling of Waste – Final Report*. Available from http://ec.europa.eu/environment/waste/strategy.htm.

European Commission (2011). *Report from the Commission to the European Parliament, the Council, the European Economic and Social Committee and the Committee of the Regions on the Thematic Strategy on the Prevention and Recycling of Waste*. Available from http://ec.europa.eu/environment/waste/strategy.htm. Report number: COM/2011/0013

Eurostat (2013) *Environmental Data Centre on Waste, Municipal Solid Waste*. [Online] Available from http://epp.eurostat.ec.europa.eu. Accessed 25 April 2013.

Evans, N.D.M. (2008) Binding mechanisms of radionuclide to cement. *Cement and Concrete Research*, 38, 543-553.

Fenfen Zhu, Masaki Takaoka, Kazuyuki Oshita, Yoshinori Kitajima, Yasuhiro Inada, Shinsuke Morisawa & Hiroshi Tsuno (2010) Chlorides behavior in raw fly ash washing experiments. *Journal of Hazardous Materials*, 178, 547-552.

Fernandez, Olmo I., Chacon, E. & Irabien, A. (2001) Influence of lead, zinc, iron(III) and chromium(III) oxides on the setting time and strength development of Portland cement. *Cement and Concrete Research*, 31, 1213-1219.

Ferreira, D.C., Jensen, P., Ottosen, L.M. & Ribeiro, A. (2008) Preliminary treatment of MSW fly ash as a way of improving electrodialytic remediation. *Journal of Environmental Science and Health*, A (43), 837-843.

Ferreira, D.C., Ribeiro, A. & Ottosen, L.M. (2005) Effect of major constituents of MSW fly ash during electrodialytic remediation of heavy metals. *Separation Science and Technology*, 40, 2007-2019.

Ferri, V., Ferro, S., Martinez-Huitle, A.C. & De Battisti, A. (2009) Electrokinetic extraction of surfactants and heavy metals from sewage sludge. *Electrochimica Acta*, 54, 2108-2118.

García Lodeiro, I., Macphee, D.E., Palomo, A. & Fernádez-Jiménez, A. (2009) Effect of alkalis on fresh CSH gels. FTIR analysis. *Cement and Concrete Research*, 39, 147-153.

Garrabrants, A.C., Sanchez, F. & Kosson, D.S. (2004) Changes in constituent equilibrium leaching and pore water characteristics of a Portland cement mortar as a result of carbonation. *Waste Management*, 24, 19-36.

Geysen, D., Imbrechts, K., Vandecasteele, C., Jaspers, M. & Wauters, G. (2004a) Immobilization of lead and zinc in scrubber residues from MSW combustion using soluble phosphates. *Waste Management*, 24, 471–481.

Geysen, D., Vandecasteele, C., Jaspers, M. & Wauters, G. (2004b) Comparison of immobilisation of air pollution control residues with cement and silica. *Journal of Hazardous Materials*, B107, 131-143.

Gineys, N., Aouad, G. & Damidot, D. (2010) Managing trace elements in Portland cement – Part I: Interactions between cement paste and heavy metals added during mixing as soluble salts. *Cement and Concrete Composites*, 32, 563-570.

Glasser, F.P. (1993) Chemistry of cement-solidified waste forms. In: Spence, R.D. (ed) *Chemistry and Microstructure of Solidified Waste Forms*. Lewis Publishers, Boca Raton, Florida.

Glasser, F.P., Kindness, A. & Stronach, S.A. (1999) Stability and solubility relationships in AFm phases Part I. Chloride, sulfate and hydroxide. *Cement and Concrete Research*, 29, 861-866.

Glasser, F.P., Marchand, J. & Samson, E. (2008) Durability of concrete – Degradation phenomena involving detrimental chemical reactions. *Cement and Concrete Research*, 38, 226-246.

Halim, C.E., Short, S.A., Scott, J.A., Amal, R. & Low, G. (2005) Modelling the leaching of Pb, Cd, As, and Cr from cementitious waste using PHREEQC. *Journal of Hazardous Materials*, A125, 45-61.

Hall, D.H., Drury, D. & Gronow, J. (2005) Modelling in support of setting the waste acceptance criteria for monolithic waste. In: Al-Tabbaa A., Stegemann J.A (eds.) *Proceedings of the International Conference on Stabilisation/ Solidification treatment and remediation 2005*. A.A. Balkema Publishers.

Hamilton, I.W. & Sammes, N.M. (1999) Encapsulation of steel foundry dusts in cement mortar. *Cement and Concrete Research*, 29, 55-61.

Hewlett, P.C. (1998) *Lea's Chemistry of Cement and Concrete*. 4th ed., Arnold Publications.

Hills, C.D., Sollars, C.J. & Perry, R. (1994) A calorimetric and microstructural study of solidified toxic wastes – Part 2: A model for poisoning of OPC hydration. *Waste Management*, 14, 601-612.

Hui-Sheng Shi, Kai Deng, Feng Yuan & Kai Wu (2009a) Preparation of the saving-energy sulphoaluminate cement using MSWI fly ash. *Journal of Hazardous Materials*, 169, 551-555.

Hui-Sheng Shi & Li-Li Khan (2009b) Leaching behavior of heavy metals from municipal solid wastes incineration (MSWI) fly ash used in concrete *Journal of Hazardous Materials*, 164, 750-754.

Hui-Sheng Shi & Li-Li Khan (2009c) Characteristics of municipal solid wastes incineration (MSWI) fly ash–cement matrices and effect of mineral admixtures on composite system. *Construction and Building Materials*, 23, 2160-2166.

Hyks, J., Astrup, T. & Christensen, T.H. (2007) Influence of test conditions on solubility controlled leaching predictions from air-pollution-control residues. *Waste Management and Research*, 25, 457-466.

IUPAC Compendium of Chemical Terminology, 2nd ed. (1997) Available online at www.iupac.org.

Jain, J. & Neithalath, N. (2009) Analysis of calcium leaching behaviour of plain and modified cement pastes in pure water. *Cement and Concrete Composites*, 31, 176-185.

Jaretun, A. & Aly, G. (1999) New local composition model for electrolyte solutions: single solvent, single electrolyte systems. *Fluid Phase Equilibria*, 163, 175-193.

Jaretun, A. & Aly, G. (2000) New local composition model for electrolyte solutions: multicomponent systems. *Fluid Phase Equilibria*, 175, 213-228.

Jensen, B.S. (1982) *Migration of Radionuclides into the Geosphere*. Harwood Academic Publishers, Switzerland.

Jill R. Pan, Chihpin Huang, Jung-Jen Kuo & Sheng-Huan Lin (2008) Recycling MSWI bottom and fly ash as raw materials for Portland cement. *Waste Management*, 28, 1113-1118.

Johnson, C.A. (2002) *Metal Binding in the Cement Matrix: an Overview of our Current Knowledge*. Department of Water Resources and Drinking Water, Water-Rock Interaction Group, EAWAG, for Cemsuisse, Switzerland.

Johnson, C.A., Kersten, M., Ziegler, F. & Moor, H.C., (1996) Leaching behaviour and solubility – Controlling solid phases of heavy metals in municipal solid waste incinerator ash. *Waste Management*, 16, 129-134.

Johnson, T. (January 2012) The use of thermal plasma technology for treating air pollution control residues. *Waste Advantage Magazine*. p. 22

Kanji, G.K. (1999) *100 Statistical Tests*. Sage Publications Ltd.

Karamanov, A., Pelino, M. & Hreglich, A. (2003) Sintered glass-ceramics from Municipal Solid Waste-incinerator fly ashes—part I: the influence of the heating rate on the sinter-crystallisation. *Journal of the European Ceramic Society*, 23, 827-832.

Kersten, M. (1996) Aqueous solubility diagrams for cementitious waste stabilisation systems. 1. The C-S-H solid solution system. *Environmental Science and Technology*, 30, 2286-2293.

Kirkelund, G.M., Jensen, P.E., Villumsen, A. & Ottosen, M.L (2010) Test of electrodialytic upgrading of MSWI APC residue in pilot scale: focus on reduced metal and salt leaching. *Journal of Applied Electrochemistry*, 40, 1049-1060.

Klich, I., Batchelor, B., Wilding, L.P. & Drees, L.R. (1999) Mineralogical alterations that affect the durability and metals containment of aged solidified and stabilized wastes. *Cement and Concrete Research*, 29, 1433-1440.

Kourti, I., Amutha Rani D., Deegan, D., Boccaccini, A.R. & Cheeseman, C.R. (2010) Production of geopolymers using glass produced from DC plasma treatment of air pollution control (APC) residues. *Journal of Hazardous Materials*, 176, 704-709.

Kung-Yuh Chiang, Jer-Chyuan Jih & Ming-Der Chien (2008) The acid extraction of metals from municipal solid waste incinerator products. *Hydrometallurgy*, 93, 16-22.

Kung-Yuh Chiang & Yu-Hsin Hu (2010) Water washing effects on metals emission reduction during municipal solid waste incinerator (MSWI) fly ash melting process. *Waste Management*, 30, 831-838.

Lancellotti, I., Kamseu, E., Michelazzi, M., Barbieri, L., Corradi, A. & Leonelli, C. (2010) Chemical stability of geopolymers containing municipal solid waste incinerator fly ash. *Waste management*, 30, 673-679.

Lei Wang, Yiying Jin, Yongfeng Nie & Rundong Li (2010a) Recycling of municipal solid waste incineration fly ash for ordinary Portland cement production: A real-scale test. *Resources, Conservation and Recycling*, 54, 1428-1435.

Lei Wang, Yiying Jin & Yongfeng Nie (2010b) Investigation of accelerated and natural carbonation of MSWI fly ash with a high content of Ca. *Journal of Hazardous Materials*, 174, 334-343.

Lei Zheng, Chengwen Wang, Wei Wang, Yunchun Shi & Xingbao Gao (2011) Immobilization of MSWI fly ash through geopolymerisation: Effects of water-wash. *Waste Management*, 31, 311-317.

Li, X.D., Poon C.S., Sun, H., Lo, I.M.C. & Kirk, D.W., 2001. Heavy metal speciation and leaching behaviours of in cement based solidified/stabilised waste materials. *Journal of Hazardous Materials,* A82, 215-230.

Lijuan Zhao, Fu-Shen Zhang & Jingxin Zhang (2008) Chemical properties of rare earth elements in typical medical waste incinerator ashes in China. *Journal of Hazardous Materials*, 158, 465-470.

Lima, A.T., Rodrigues, P.C. & Mexia, J.T. (2010) Heavy metal migration during electroremediation of fly ash from different wastes—Modelling. *Journal of Hazardous Materials*, 75, 366-371.

Loser, R., Lothenbach, B., Leeman, A. & Tuchschmid, M. (2010) Chloride resistance of concrete and its binding capacity – Comparison between experimental results and thermodynamic modelling. *Cement and Concrete Composites*, 32, 34-42.

Lothenbach B. & Winnefeld F. (2006) Thermodynamic modelling of the hydration of Portland cement. *Cement and Concrete Research*, 36, 209-226.

Luna Galiano, Y., Fernández Pereira, C. & Vale, J. (2011) Stabilization/solidification of a municipal solid waste incineration residue using fly ash-based geopolymers. *Journal of Hazardous Materials*, 185, 373-381.

Mangialardi, T. (2003) Disposal of MSWI fly ash through a combined washing-immobilisation process. *Journal of Hazardous Materials*, B98, 225-240.

Mangialardi, T. (2004) Effects of a washing pre-treatment of municipal solid waste incineration fly ash on the hydration behaviour and properties of ash–Portland cement mixtures. *Advances in Cement Research*, 16, 45-54.

Matschei, T., Lothenbach, B. & Glasser, F.P. (2007) Thermodynamic properties of Portland cement hydrates in the system CaO-Al_2O_3-SiO_2-$CaSO_4$-$CaCO_3$-H_2O. *Cement and Concrete Research*, 37, 1379-1410.

Meeussen, J.C.L., Van der Sloot, H.A., Kosson, D.S. & Sarkar, S. (2010) *Demonstration of LEACHXS/ORCHESTRA capabilities by simulating constituent release from a cementitious waste form in a reinforced concrete vault*. Cementitious Barriers Partnership Report number: CBP-TR-2010-007-C1, Rev. 0. Available online from http://sti.srs.gov/fulltext/CBP-TR-2010-007-C1.pdf.

Ore, S., Todorovic, J., Ecke H., Grennberg, K., Lidelöw, S. & Lagerkvist, A. (2007) Toxicity of leachate from bottom ash in a road construction. *Waste Management*, 27, 1626-1637.

Ortego, J.D. (1990) Spectroscopic and leaching studies of solidified toxic metals. *Journal of Hazardous Materials*, 24, 137-144.

Ottosen, M.L., Lima, T.A., Pedersen, J.A. & Ribeiro B.A. (2006) Electrodialytic extraction of Cu, Pb,and Cl from municipal solid waste incineration fly ash suspended in water. *Journal of Chemical Technology and Biotechnology*, 81, 553-559.

Ouki, S.K. & Hills, C.D. (2002) Microstructure of Portland cement pastes containing metal nitrate salts. *Waste Management*, 22, 147-151.

Park, J.Y. & Batchelor, B. (1999a) Prediction of chemical speciation in stabilised/solidified wastes using a general chemical equilibrium model Part I. Chemical representation of cementitious binders. *Cement and Concrete Research*, 29, 361-368.

Park, J.Y & Batchelor, B. (1999b) Prediction of chemical speciation in stabilised/solidified wastes using a general chemical equilibrium model II. Doped waste contaminants in cement porewaters. *Cement and Concrete Research*, 29, 99-105.

Park, J.Y. & Batchelor, B. (2002a) General chemical equilibrium model for stabilized/solidified wastes. *Journal of Environmental Engineering*, 128, 653-661.

Park, J.Y. & Batchelor, B. (2002b) A multi-component numerical leach model coupled with general chemical speciation code. *Water Research*, 36, 156-166.

Pedersen J.A., Ottosen, M.L., & Villumsen, A. (2005) Electrodialytic removal of heavy metals from municipal solid waste incineration fly ash using ammonium citrate as an assisting agent. *Journal of Hazardous Materials*, B122, 103-109.

Peng Zhao, Guohua Ni, Yiman Jiang, Longwei Chen, Mingzhou Chenv& Yuedong Meng (2010) Destruction of inorganic municipal solid waste incinerator fly ash in a DC arc plasma furnace. *Journal of Hazardous Materials*, 181, 580-585.

Peter, M.A., Muntean, A., Meier, S.A. & Böhm, M. (2008) Competition of several carbonation reactions in concrete: A parametric study. *Cement and Concrete Research*, 38, 1385-1393.

Polettini, A., Pomi, R., Sirini, P. & Testa, F. (2001) Properties of Portland cement stabilised MSWI fly ashes. *Journal of Hazardous Materials*, B88, 123-138.

Qian, G.R., Shi, J., Cao, Y.L., Xu, Y.F. & Chui, P.C. (2008) Properties of MSW fly ash-calcium sulfoaluminate cement matrix and stabilization/solidification on heavy metals. *Journal of Hazardous Materials*, 152, 196-203.

Qiao, X.C., Poon, C.S. & Cheeseman, C.R. (2007) Investigation into the stabilisation/ solidification performance of Portland cement through cement clinker phases. *Journal of Hazardous Materials*, B139, 238-243.

Quina, M.J., Bordado, J.C. & Quinta-Ferreira, R.M. (2008a) Treatment and use of air pollution control residues from MSW incineration: An overview. *Waste Management* 28, 2097-2121.

Quina, M.J., Santos, R.C., Bordado, J.C. & Quinta-Ferreira, R.M. (2008b) Characterization of air pollution control residues produced in a municipal solid waste incinerator in Portugal. *Journal of Hazardous Materials*, 152, 853-869.

Quina, M.J., Bordado, J.C.M. & Quinta-Ferreira. R.M. (2009) The influence of pH on the leaching behaviour of inorganic components from municipal solid waste APC residues. *Waste Management*, 29, 2483-2493.

Quina, M.J., Bordado, J.C. & Quinta-Ferreira, R.M., 2010. Chemical stabilisation of air pollution control residues from municipal solid waste incineration. *Journal of Hazardous Materials*, 179, 382-392.

Quina, M.J., Bordado, J.C. & Quinta-Ferreira, R.M. (2011) Environmental impact of APC residues from municipal solid waste incineration: Reuse assessment based on soil and surface water protection criteria. *Waste Management*, 31, 1884-1991.

Rémond, S., Bentz, D.P. & Pimienta, P. (2002) Effects of the incorporation of Municipal Solid Waste Incineration fly ash in cement pastes and mortars. *Cement and Concrete Research*, 32, 565-576.

Renaudin. G., Rapin, J. –P., Elkaim, E. & François, M. (2004) Polytypes and polymorphs in the related Friedel's salt $[Ca_2Al(OH)_6]^+[X.2H_20]^-$ halide series. *Cement and Concrete Research*, 34, 1845-1852.

Renbo Yang, Wing-Ping Liao, & Pin-Han Wu (2012) Basic characteristics of leachate produced by various washing processes for MSWI ashes in Taiwan. *Journal of Environmental Management*, 104, 67-76.

Resource Recovery Forum (2004) *Characterisation of air pollution control residues from MSW energy from waste*. Research report prepared by WRc, available from http://www.resourcesnotwaste.org/

Roether, J.A., Daniel, D.J., Amutha Rani, D., Deegan, D.E., Cheeseman, C.R. & Boccaccini, A.R. (2010) Properties of sintered glass-ceramics prepared from plasma vitrified air pollution control residues. *Journal of Hazardous Materials*, 173, 563-569.

Rouchotas, E. (2001) *Metal removal from air pollution control residues by a water/acid extraction process*. M.Sc. thesis, Imperial College, London.

Röβler, C., Eberhardt, A., Kučerová, H. & Möser, B. (2008) Influence of hydration on the fluidity of normal Portland cement pastes. *Cement and Concrete Research*, 38, 897-906.

Rui Luo, Yuebo Cai, Changyi Wang & Xiaomin Huang (2003) Study of choride binding and diffusion GGBS in concrete. *Cement and Concrete Research*, 33, 1-7.

Sadeghi, R. (2005) New local composition model for electrolyte solutions. *Fluid Phase Equilibria*, 231, 53-60.

Saikia, N., Kato, S. & Kojima, T. (2007) Production of cement clinkers from municipal solid waste incineration (MSWI) fly ash. *Waste Management*, 27, 1178-1189.

Sakai, S. & Hiraoka, M. (2000) Municipal solid waste incinerator residue recycling by thermal processes. *Waste Management*, 20, 249-258.

Sarkar, S., Mahadevan, S., Meeusen, J.C.L., van der Sloot, H. & Kosson, D.S. (2010) Numerical simulation of cementitious materials degradation under external sulphate attack. *Cement and Concrete Composites*, 32, 241-252.

SELCHP (2011) *South East London Combined Heat and Power Facility Guide*. Available online from http://www.selchp.co.uk/. Accessed 4 April 2011.

Shirley, R. & Black L. (2011a) Alkali activated solidification/stabilisation of air pollution control residues and co-fired pulverised fuel ash. *Journal of Hazardous Materials*, 194, 232-242.

Shirley, R. & Black L. (2011b) Alkali activated solidification/stabilisation of air pollution control residues using co-fired pulverised fuel ash: mineralogical characterization. *Advances in Applied Ceramics*, 110, 438-445.

Song, W. & Larson, M.A. (1990) Activity coefficient model of concentrated electrolyte solutions. *AlChe Journal*, 36, 1896 – 1900.

Stegemann, J.A. & Côté, P.L. (1991) *Investigation of test methods for solidified waste evaluation – Cooperative program*. Environment Canada. Report number: EPS 3/HA/8, Ottawa, Ontario, Canada, p.116.

Stegemann, J.A., Caldwell, R.J. & Shi, C. (1997) Response of various solidification systems to acid addition. Waste materials in construction: Putting theory in practice. In: Goumans, J., Senden, J. & Van der Sloot, H. (eds.) *Studies in Environmental Science 71*. Elsevier Science B.V., Amsterdam, pp. 803-814.

Stegemann, J.A., Hodgkin, B. & Shamsaie, A. (2005) *The Influence of Aggregate on Chloride Diffusion from Cement-Based Matrices*. Cement and Concrete Science, Royal Holloway College, September 15-16.

Stegemann, J.A. & Zhou, Q. (2009) Screening tests for assessing treatability of inorganic industrial wastes by stabilisation/solidification with cement. *Journal of Hazardous Materials*, 161, 300-306.

Sung-Yoon Hong & Glasser, F.P. (1999) Alkali binding in cement pastes Part I. The C-S-H phase. *Cement and Concrete Research*, 29, 1893-1903.

Sun-Yu Chou, Shang-Lien Lo, Ching-Hong Hsieh & Ching-Lung Chen (2009) Sintering of MSWI fly ash by microwave energy. *Journal of Hazardous Materials*, 163, 357-362.

Suryavanshi, A.K., Scantlebury, J.D. & Lyon, S.B. (1996) Mechanism of Friedel's salt formation in cements rich in tri-calcium aluminate. *Cement and Concrete Research*, 26, 717-727.

Tashiro, C., Oba, J. & Akama, K. (1979) The effects of several heavy metal oxides on the formation of ettringite and the microstructure of hardened ettringite. *Cement and Concrete Research*, 9, 303-308.

Taylor, H.F.W. (1997) *Cement Chemistry*. 4th ed., Thomas Telford Publishing, London.

Technology Strategy Board (2009) *Innovation Results: Hazardous waste cleans up its act*. Available online from www.innovateuk.org. Accessed 17 October 2012.

Tiruta-Barna, L. (2008) Using PHREEQC for modelling and simulation of dynamic leaching tests and scenarios. *Journal of Hazardous Materials*, 157, 525-533.

Todorovic, J. & Ecke, H. (2006) Demobilisation of critical contaminants in four typical waste-to-energy ashes by carbonation. *Waste Management*, 26, 430–441.

Todorovic, J., Ecke, H. & Lagerkvist, A. (2003) Solidification with water as a treatment method for air pollution control residues. *Waste Management*, 23, 621-629.

Traina, G., Ferro, S. & De Battisti, A. (2009) Electrokinetic stabilization as a reclamation tool for waste materials polluted by both salts and heavy metals. *Chemosphere*, 75, 819-824.

Traina, G., Morselli, L. & Adorno, P.G. (2007) Electrokinetic remediation of bottom ash from municipal solid waste incinerator. *Electrochimica Acta*, 52, 3380-3385.

Trezza, M.A. (2007) Hydration study of Ordinary Portland cement in the presence of zinc ions. *Materials Research*, 10, 331-334.

Trezza, M.A. & Ferraiuelo, M.F. (2007) Hydration study of limestone blended cement in the presence of hazardous wastes containing Cr(VI). *Cement and Concrete Research* 33, 1039-1045.

Trujilo-vazquez, A., Metiver-pignon, H., Tiruta-barna, L. & Piantone, P. (2009) Characterization of a mineral waste resulting from the melting treatment of air pollution control residues. *Waste Management*, 29, 530-538.

UK Cementitious Slag Makers Association (2012) *GGBS Concrete*. Available online at http://www.ukcsma.co.uk/ggbs-concrete.html. Accessed on 25 June 2012.

Van der Bruggen, B., Vogels, G., Van Herck, P. & Vandecasteele, C. (1998) Simulation of acid washing of municipal solid waste incineration fly ashes in order to remove heavy metals. *Journal of Hazardous. Materials*, 57, 127–144.

Van der Sloot, H., van Zomeren, A., Meeusen, J.C.L., Seignette, P. & Bleijerveld, R. (2007) Test method selection, validation against field data and predictive modelling for impact evaluation of stabilised waste disposal. *Journal of Hazardous Materials*, 141, 354-369.

Van Gerven, T., Cornelis, G., Vandoren, E. & Vandecasteele, C. (2007) Effects of carbonation and leaching on porosity in cement-bound waste. *Waste Management*, 27, 977-985.

Van Herck, P., Van der Bruggen, B., Vogels, G. & Vandecasteele, C. (2000) Application of computer modelling to predict the leaching behaviour of heavy metals from MSWI fly ash and comparison with a sequential extraction method. *Waste Management*, 20, 203–210.

Van Jaarsveld, J.G.S & Van Deventer, J.S.J. (1999) The effect of metal contaminants on the formation and properties of waste-based geopolymers. *Cement and Concrete Research*, 29, 1189-1200.

Vespa, M., Dahn, R., Grolimund, D., Harfouche, M., Wieland, E. & Scheidegger, A.M. (2006) Speciation of heavy metals in cement-stabilized waste forms: A micro-spectroscopic study. *Journal of Geochemical Exploration*, 88, 77-80.

Weeks, C., Hand, R.J. & Sharp, H.J. (2008) Retardation of cement hydration caused by heavy metals. *Cement and Concrete Composites*, 30, 970-978.

Williams P.T. (2005) *Waste Treatment and Disposal* 2nd ed., John Wiley & Sons Ltd., Chichester, England.

Xiaomin Li., Fernandez Bertos M., Hills D.C., Carey P.J. & Simon S. (2007) Accelerated carbonation of municipal solid waste incineration fly ashes. *Waste Management*, 27, 1200-1206.

Xingbao Gao, Wei Wang, Tunmin Ye, Feng Wang & Yuxin Lan (2008) Utilisation of washed MSWI fly ash as partial cement substitute with the addition of dithiocarbamic chelate. *Journal of Environmental Management*, 88, 293-299.

Yangsheng Liu, Liting Zheng, Xiaodong Li & Shaodong Xie (2009) SEM/EDS and XRD characterization of raw and washed MSWI fly ash sintered at different temperatures. *Journal of Hazardous Materials*, 162, 161-173.

Yongjie Xue, Haobo Hou, Shujing Zhu & Jin Zha (2009) Utilization of municipal solid waste incineration ash in stone mastic asphalt mixture: Pavement performance and environmental impact. *Construction and Building Materials*, 23, 989-996.

Young-Sook Shim, Young-Keun Kim, Sung-Ho Kong, Seung-Whee Ree & Woo-Keun Lee (2003) The adsorption characteristics of heavy metals by various particles sizes of MSWI bottom ash. *Waste Management*, 23, 851-857.

Yousuf, A., Mollah, A., Hess, T.R., Tsai Y.-N. & Cocke, D.L. (1993) FTIR and XPS investigations of the effects of carbonation on the solidification/stabilisation of cement based system – Portland Type V with zinc. *Cement and Concrete Research*, 23, 773-784.

Zemaitis, Jr. J.F, Clark, D.M., Rafal, M. & Scrivner, N.C. (1986) *Handbook of Aqueous Electrolyte Thermodynamics. Theory and Application*. American Institute of Chemical Engineers, New York: DIPPR.

Zhang Haiying, Zhao Youcai & Qi Jingyu (2011) Utilization of municipal solid waste incineration (MSWI) fly ash in ceramic brick: Product characterization and environmental toxicity. *Waste Management*, 31, 331-341.

Zhang Yan, Jiang Jianguo & Chen Maozhe (2008) MINTEQ modelling for evaluating the leaching behaviour of heavy metals in MSWI fly ash. *Journal of Environmental Science*, 20, 1398–1402.

Zhang Yunsheng, Sun Wei, Chen Qianli & Chen Lin (2007) Synthesis and heavy metal immobilisation behaviour of slag based geopolymer. *Journal of Hazardous Materials*, 143, 206-213.

Zhao Youcai, Song Lijie & Li Guojian (2002) Chemical stabilisation of MSW incinerator fly ashes. *Journal of Hazardous Materials*, B95, 47-63.

Ziegler, F. & Johnson, A.C (2001) The solubility of calcium zincate ($CaZn_2(OH)_6{\cdot}H_2O$). *Cement and Concrete Research*, 31, 1327-1332.

APPENDIX I: APC RESIDUE MINERALOGY AND COMPOSITIONAL DATA BY PLANT OPERATOR

A. XRD DATA

LONDON & SCANDINAVIAN METALLURGICAL CO LIMITED
Fullerton Road, Rotherham, South Yorkshire S60 1DL, England

UKAS TESTING 1091

Attachment to Certificate No: 2604874	Page 1 of 1

XRD

SELCHP/APC/AUG 06 (2617536)

Phases identified		
Major phases	KCl	Potassium Chloride, Sylvite
	CaClOH	Calcium Chloride Hydroxide
Major/Minor phases	NaCl	Sodium Chloride, Halite
	$CaCO_3$	Calcium Carbonate, Calcite
	$Ca(OH)_2$	Calcium Hydroxide, Portlandite
	$CaSO_4$	Calcium Sulphate, Anhydrite
Minor phases	SiO_2	Silicon Dioxide, Quartz
	CaO	Calcium Oxide, Lime

Analysed using documented in-house procedures for X-ray Diffraction	☑ P. S. Cooper, Laboratory Manager ☐ P.W. Hurditch, Chief Chemist
Signed	☐ H. Speakman, Laboratory Business Manager

Registered Office as above. Registered in England No. 345279 V.A.T. No. GB 789 6326 65.

B. XRF DATA

LONDON & SCANDINAVIAN METALLURGICAL CO LIMITED

Fullerton Road, Rotherham, South Yorkshire S60 1DL, England

Certificate No. 2604874
Page 1 of 1

UKAS TESTING 1091

PLEASE NOTE: These results are semiquantitative only. In particular, no reliance should be placed on the summation of the analysis to 100% as this is part of the data processing procedure and will ignore any element lighter than F unless it has been added to the analysis manually.

C:\UQ4\JOB\JOB.901 2006-09-04
SELCHP/APC/AUG 06 Sample H14 Haz

London and Scandinavian Metallurgical Co Ltd PW2404 Rh 60Kv LiF220 Ge111 TlAP
C:\UQ4\ASC\Kdata.asc 2006-08-29 ..\ChData.asc 2005-10-21
Calculated as : Oxides Matrix (Shape & ImpFc) : 1 Teflon
X-ray path = Vacuum Film type = No supporting film
Case number = 0 Known Mass, Area, Rest, Dilution
Eff.Diam. = 25.0 mm Eff.Area = 490.6 mm2
KnownConc = 0 %
Rest = 0 % Viewed Mass = 11706.56 mg
Dil/Sample = 0.200 Cellulose Sample Height = 2.00 mm
< means that the concentration is < 100 mg/kg
<2e means wt% < 2 StdErr.

Z	wt%	StdErr	Z	wt%	StdErr	Z	wt%	StdErr
9 F	0.261	0.046	29 CuO	0.0869	0.0025	52 TeO2	<	
11 Na2O	3.80	0.15	30 ZnO	1.30	0.06	53 I	<	
12 MgO	0.688	0.076	31 Ga2O3	<		55 Cs2O	<	
13 Al2O3	2.16	0.13	32 GeO2	<		56 BaO	0.033	0.011
14 SiO2	4.24	0.10	33 As2O3	<		SumLa..Lu	0.041	0.052
15 P			34 SeO2	<		72 HfO2	<	
15 P2O5	0.617	0.068	35 Br	0.291	0.032	73 Ta2O5	<	
16 SO3	5.45	0.25	37 Rb2O	<		74 WO3	<	
16 S			38 SrO	0.0787	0.0087	75 Re2O7	<	
17 Cl	22.34	0.21	39 Y2O3	<		76 OsO4	<	
18 Ar	<		40 ZrO2	0.0177	0.0018	77 IrO2	<	
19 K2O	4.16	0.22	41 Nb2O5	<		78 PtO2	<	
20 CaO	51.90	0.55	42 MoO3	<		79 Au	<	
21 Sc2O3	<		44 RuO4	<		80 HgO	<	
22 TiO2	0.861	0.040	45 Rh2O3	<		81 Tl2O3	<	
23 V2O5	<		46 PdO	<		82 PbO	0.396	0.044
24 Cr2O3	0.0742	0.0082	47 Ag2O	<		83 Bi2O3	<	
25 MnO	0.0758	0.0038	48 CdO	0.0199	0.0022	90 ThO2	<	
26 Fe2O3	0.817	0.090	49 In2O3	<		92 U3O8	<	
27 Co3O4	<		50 SnO2	0.151	0.014	94 PuO2	<	
28 NiO	<		51 Sb2O3	0.115	0.013	95 Am2O3	<	

===== Lanthanides La..Lu =======

57 La2O3	<		63 Eu2O3	<		68 Er2O3	
58 CeO2	0.0163	0.0057	64 Gd2O3	<		69 Tm2O3	
59 Pr6O11	<		65 Tb4O7	<		70 Yb2O3	
60 Nd2O3	<		66 Dy2O3	<		71 Lu2O3	
62 Sm2O3	<		67 Ho2O3	<			

KnownConc= 0 REST= 0 D/S= 0.200Cellulose
Sum Conc's before normalisation to 100% : 81.4 %

C. LEACHING DATA

All concentrations in mg kg^{-1}	Al	As	B	Ba	Ca	Cd	Co	Cr (total)	Cu	Fe	Hg	K	Mg	Mn	Mo	Na
Total concentrations (metals determined by aqua regia digests)																
APC	14000	9.1	0.9	340	290000	110	14	70	410	3200	9	23000	4100	340	8.2	20000
Potential availability for leaching																
APC	9.89	1.61	61.5	130	269575	101.1	1.0	14.14	98.09	25.83	2.71	23677	1845	69.39	8.57	20807
Leachability in water at L/S ratio 2-10 cumulative (EN123457-3)																
APC	0.65	0.219	<3	33.35	68936	0.006	0.017	0.2	1.04	2.28	0.022	19104	4	<0.16	0.88	18861

Sample All concentrations in mg kg^{-1}	Ni	P	Pb	Sb	Se	Si	Sn	Ti	Tl	V	Zn	Water extractable ions Br	F	Cl	SO_4	CO_3
Total concentrations (metals determined by aqua regia digests)																
APC	23	4100	2800	390	<3	510	310	1000	<10	9	7200	2020	23.3	nd	11200	21300
Potential availability for leaching																
APC	6.41	51.25	72.98	100.5		15067	10.25	0.512	10.25	0.25	4069	1055	738	165025	61192	13120
Leachability in water at L/S ratio of 2-10 cumulative (EN123457-3)																
APC	0.17	<1	686.0	0.002	0.151	135	<0.002	<0.05	<1	0.091	36.8	1656	32.3	77275	3285	<985

APPENDIX II: SEVERN TRENT LABORATORY ELUATE ANALYSIS METHODS

A. LABORATORY METHOD 53F

SEVERN TRENT ENVIRONMENTAL LEADERSHIP STL Leaders in Environmental Testing

ANALYTICAL METHOD STATEMENT

Determinand:
This method determines the metal concentrations of aluminium, boron, cadmium, calcium, chromium, copper, iron, potassium, magnesium, manganese, sodium, nickel, lead and zinc in groundwaters.

Matrix:
Water and related material

Principle of Method:
A portion of the .as received. sample is filtered through a No. 50 filter paper, unless already supplied as a filtered sample. The sample is acidified with nitric acid (4.1) prior to analysis. The concentrations of the metals are determined by the technique of inductively coupled plasma optical emission spectroscopy.

An ICP source consists of a flowing stream of argon gas ionised by an applied radio frequency field. This field is inductively coupled to ionised gas by a water-cooled coil surrounding a quartz `torch' that supports and confines the plasma.

A sample aerosol is generated in a nebuliser and spray chamber and is carried into the plasma through an injector tube. The sample aerosol is injected directly into the ICP subjecting the constituent atoms to temperatures of between 6000 and 8000 K. Because this results in almost complete dissociation of molecules a significant reduction in chemical interferences is achieved.

Sample Preparation
The test is carried out on a filtered portion of the shaken “as received” sample.

Interferences:
Spectral interferences in ICPS analysis - At the concentrations handled, there are no significant inter-element correction factors for the analytes.

Chemical interferences in ICPS analysis - The technique of ICPS analysis reduces the effects of chemical interference on the final analytical measurements to insignificant levels for the elements determined in the acid matrix.

Performance of Method:

Determinand	Range of Application (mg/l)	LOD (mg/l)	Routine Reporting Limit (mg/l)
Aluminium	0.07 – 3	0.0632	0.07
Boron	0.05 – 3	0.0447	0.05
Calcium	0.2 – 400	0.1548	0.2
Cadmium	0.002 – 0.5	0.0013	0.002
Chromium	0.01 – 1	0.0071	0.01
Copper	0.01 – 10	0.0034	0.01
Iron	0.04 – 20	0.0394	0.04
Potassium	0.3 – 20	0.2988	0.3
Magnesium	0.05 – 50	0.023	0.05
Manganese	0.01 – 10	0.0058	0.01
Sodium	0.15 – 200	0.1493	0.15
Nickel	0.01 – 1	0.0051	0.01
Lead	0.01 – 3	0.0085	0.01
Zinc	0.01 – 5	0.0077	0.01

Standards - Precision and bias

Determinand	Low standard			High standard		
	Tot. RSD %	Bias %	Uncert. %	Tot. RSD %	Bias %	Uncert. %
Aluminium	3.68	-0.97	8.33	1.92	-1.55	5.39
Boron	4.82	7.12	16.76	1.59	-0.5	3.68
Calcium	3.26	4.47	10.99	2.4	-1.35	6.15
Cadmium	3.22	9.91	16.35	2.26	-0.25	4.77
Chromium	2.86	6.1	11.82	1.93	-0.88	4.74
Copper	2.91	1.33	7.15	1.55	-1.3	4.40
Iron	3.47	8.55	15.49	1.69	-0.72	4.10
Potassium	7.5	5.37	20.37	1.96	-1.00	4.92
Magnesium	2.62	7.4	12.64	2.24	-0.77	5.25
Manganese	3.05	4.49	10.59	2.51	-1.88	6.90
Sodium	4.83	4.72	14.38	2.08	-1.91	6.07
Nickel	3.11	9.09	15.31	1.95	-0.88	4.78
Lead	3.89	7.83	15.61	2.01	-0.38	4.40
Zinc	2.82	8.59	14.23	1.61	-0.88	4.10

Samples and Spiked Samples

Determinand	Leachate			Groundwater			Surface Water		
	Tot. RSD	Rec. %	Uncert. %	Tot. RSD	Rec. %	Uncert. %	Tot. RSD	Rec. %	Uncert. %
Aluminium	3.4	101.5	8.30	3.49	99.97	7.01	3.4	99.73	7.07
Boron	2.51	100.21	5.23	2.32	99.37	5.27	2.1	99.32	4.88
Calcium	2.94	99.45	6.43	3.54	99.55	7.53	2.43	96.04	8.82
Cadmium	1.93	99.74	4.12	2.01	97.48	6.54	2.04	97.9	6.18
Chromium	2.14	100.12	4.40	2.13	98.44	5.82	1.86	98.69	5.03
Copper	1.98	99.96	4.00	1.73	98.46	5.00	1.9	98.47	5.33
Iron	3.32	100.29	6.93	1.81	98.67	4.95	2.09	99.11	5.07
Potassium	9.85	99.55	20.15	2.78	99.38	6.18	2.21	101.25	5.67
Magnesium	1.96	99.37	4.55	2.05	91.95	12.15	2.05	100.17	4.27
Manganese	1.88	99.92	3.84	3.05	98.38	7.72	2.35	98.78	5.92
Sodium	2.15	96.35	7.95	2.15	94.87	9.43	1.93	96.61	7.25
Nickel	2.05	99.51	4.59	2.08	97.33	6.83	2.23	96.93	7.53
Lead	1.97	99.96	3.98	2.44	97.85	7.03	2.27	97.72	6.82
Zinc	1.97	99.73	4.21	1.94	97.86	6.02	1.88	98.14	5.62

References:

MEWAM Methods for the determination of metals in soils, sediments and sewage sludge and plants by hydrochloric - nitric acid digestion 1986. HMSO. London. ISBN 011 7519081

MEWAM Information on concentration and determination procedures in atomic spectrophotometry 1992. HMSO .London. ISBN 011 7523755

MEWAM Inductively coupled plasma spectrometry 1996. HMSO. London. ISBN011 7532444

B. LABORATORY METHOD 68

SEVERN TRENT ENVIRONMENTAL LEADERSHIP STL Leaders in Environmental Testing

ANALYTICAL METHOD STATEMENT

Determinand:
This method determines the metal concentrations of lithium, silicon, strontium, titanium, tellurium, thorium, thallium, uranium, germanium, gallium, bismuth, sulphur, gold, tin, platinum, palladium and zirconium in ground waters.

Matrix:
Water and a related material.

Principle of Method:
A portion of the "as received" sample is filtered through a No. 50 filter paper, unless already supplied as a filtered sample. The sample is acidified with nitric acid (4.1) prior to analysis. The concentrations of the metals are determined by the technique of inductively coupled plasma optical emission spectroscopy. The sample aerosol is generated in a nebuliser and spray chamber and is carried into the plasma through an injector tube. The sample aerosol is injected directly into the ICP subjecting the constituent atoms to temperatures of between 6000 and 8000 K. As this results in almost complete dissociation of the molecules, a significant reduction in chemical interferences is achieved.

Sample Preparation:
The test is carried out on a filtered portion of the shaken "as received" sample.

Interferences:
Spectral interferences in ICP-OES analysis – At the concentrations handled there are no significant inter-element correction factors for the analytes.

Chemical interferences in ICP-OES analysis – The technique of ICP-OES analysis reduces the effects of chemical interference on the final analytical measurements to insignificant levels for the elements determined in the acid matrix.

Range of Method:

Determinand	Range of Application (mg/l)
Lithium	0.01 – 1
Silicon	0.01 – 10
Strontium	0.002 – 20
Titanium	0.01 – 1
Tellurium	0.08 – 10
Thorium	0.004 – 10
Thallium	0.02 – 10
Uranium	0.02 – 10
Germanium	0.02 – 10
Gallium	0.005 – 10
Bismuth	0.04 – 10
Sulphur	0.1 – 10
Gold	0.008 – 10

Determinand	Range of Application (mg/l)
Tin	0.1 – 10
Platinum	0.08 – 10
Palladium	0.008 – 10
Zirconium	0.003 - 10

APPENDIX III: UK WASTE ACCEPTANCE CRITERIA FOR MONOLITHIC WASTE

	Stable non-reactive hazardous waste in non-hazardous landfill and non-hazardous waste in same cell		Hazardous waste landfill	
Parameter	**Cumulative values ($mg.m^{-2}$)**			
	For compliance (cumulative 4-day leaching)	**For characterisation (cumulative 64-day leaching)**	**For compliance (cumulative 4-day leaching)**	**For characterisation (64-day leaching)**
As (arsenic)	0.325	1.3	5	20
Ba (barium)	11.25	45	37.5	150
Cd (cadmium)	0.05	0.2	0.25	1.0
Cr (chromium total)	1.25	5	6.25	25
Cu (copper)	11.25	45	15	60
Hg (mercury)	0.025	0.1	0.1	0.4
Mo (molybdenum)	1.75	7	5	20
Ni (nickel)	1.5	6	3.75	15
Pb (lead)	1.5	6	5	20
Sb (antimony)	0.075	0.3	0.625	2.5
Se (selemium)	0.1	0.4	1.25	5
Zn (zinc)	7.5	30	25	100
Cl- (chloride)	2,500	10,000	5,000	20,000
F- (fluoride)	15	60	50	200
SO420 (sulphate)	2,500	10,000	5,000	20,000
DOC (dissolved organic C)	must be determined	must be determined	must be determined	must be determined
pH	must be determined	must be determined	must be determined	must be determined
EC ($\mu.cm^{-1}.m^{-2}$)	must be determined	must be determined	must be determined	must be determined

APPENDIX IV: INTERPRETATION OF MONOLITHIC LEACHING RESULTS

A. ANNEX E OF NEN 7375:2004.

Annex E (informative)

Graphical representation of diffusion controlled leaching in special cases.

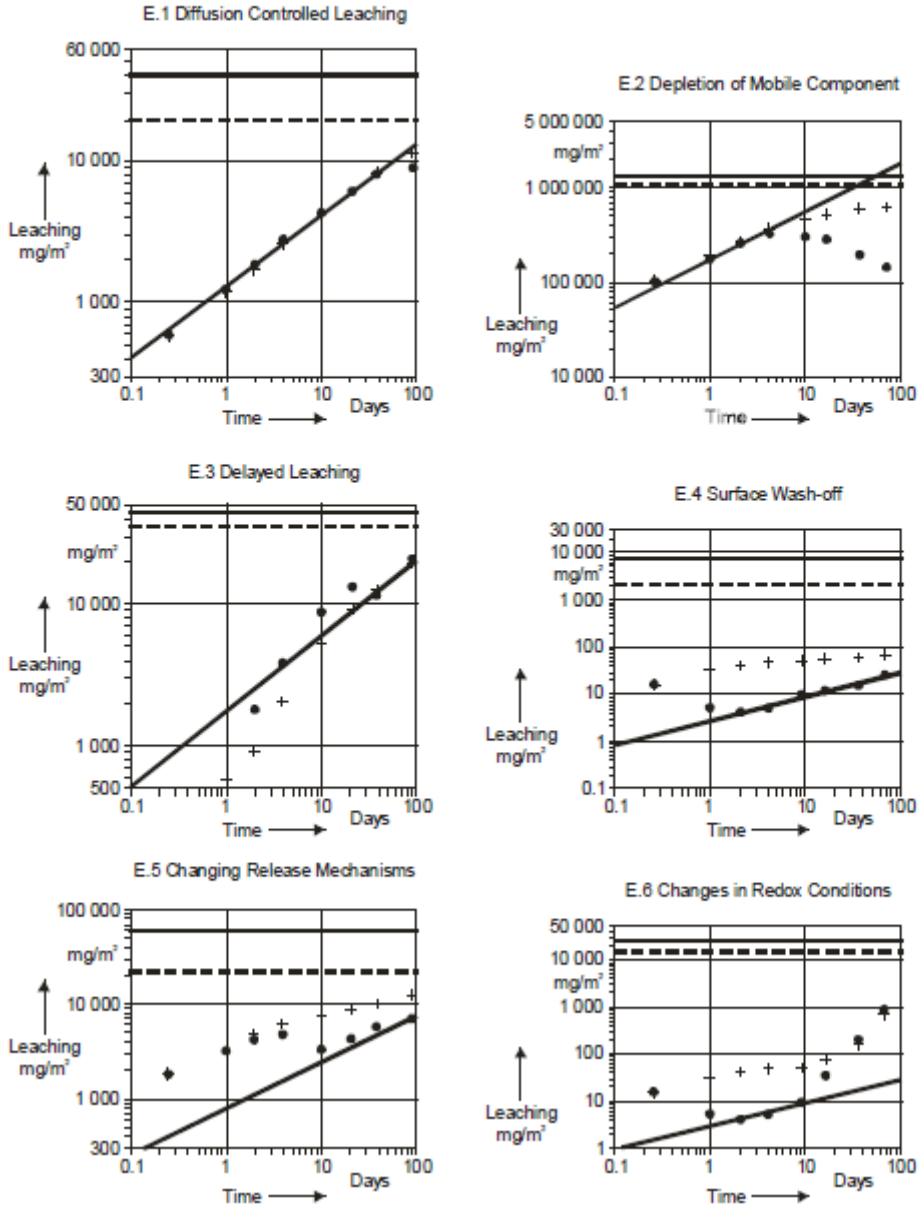

KEY

\+ Cumulative measured leaching, from 8.2.1 equation (4)

• Cumulative measured leaching, from 8.2.2 equation (5)

Slope defined by rc=0.5

Upper limit defined by total content of component

Upper limit based on availability in accordance with NEN 7371

B. SLOPES OF LEACHING INTERVALS

	Slopes of Monolithic Leaching Test Intervals					
Element	***2-7***	***5-8***	***4-7***	***3-6***	***2-5***	***1-4***
Ca						
50% CEMI w/s: 0.5	0.14	0.12	0.06	0.06	0.16	0.55
20% CEMI w/s: 0.5	-0.18	-0.24	-0.56	-0.08	0.10	0.47
10% CEMI w/s: 0.5	-0.24	-0.20	-0.65	-0.25	0.03	0.97
50% GGBS w/s: 0.35	0.27	0.20	0.13	0.22	0.39	0.67
50% GGBS w/s: 0.4	0.32	0.15	0.17	0.21	0.49	0.55
Al						
50% CEMI w/s: 0.5	0.55	0.10	0.07	0.26	0.98	0.28
20% CEMI w/s: 0.5	0.65	0.19	-0.09	0.34	1.16	1.57
10% CEMI w/s: 0.5	1.02	0.31	0.83	1.35	1.19	-0.36
50% GGBS w/s: 0.35	0.30	0.39	0.18	0.20	0.38	0.76
50% GGBS w/s: 0.4	0.28	0.33	0.18	0.20	0.36	0.66
Si						
50% CEMI w/s: 0.5	0.16	0.13	0.24	0.15	0.59	0.53
20% CEMI w/s: 0.5	-0.13	-0.13	-0.55	-0.15	0.28	0.38
10% CEMI w/s: 0.5	0.10	-0.06	-0.13	-0.03	0.44	0.53
50% GGBS w/s: 0.35	0.20	-0.01	0.01	0.16	0.33	0.69
50% GGBS w/s: 0.4	0.17	-0.09	-0.05	0.20	0.35	0.58
Na						
50% CEMI w/s: 0.5	-0.29	-0.39	-0.61	0.07	-0.13	1.35
20% CEMI w/s: 0.5	-0.72	-0.24	-1.07	-0.93	-0.42	0.06
10% CEMI w/s: 0.5	-0.79	-0.35	-1.23	-1.07	-0.37	1.75
50% GGBS w/s: 0.35	0.07	-0.40	-0.10	0.04	0.25	0.37
50% GGBS w/s: 0.4	0.10	-0.44	-0.11	0.00	0.35	0.41
K						
50% CEMI w/s: 0.5	-0.39	-0.44	-0.74	-0.25	-0.20	1.45
20% CEMI w/s: 0.5	-0.83	-0.22	-1.16	-0.92	-0.58	-0.05
10% CEMI w/s: 0.5	-0.85	-0.31	-1.12	-1.10	-0.62	1.70
50% GGBS w/s: 0.35	0.02	-0.38	-0.16	0.05	0.20	0.28
50% GGBS w/s: 0.4	0.11	-0.54	-0.21	0.02	0.48	0.34
Li						
50% CEMI w/s: 0.5	0.005	0.01	0.18	0.09	0.03	0.69
20% CEMI w/s: 0.5	-0.11	-0.06	-0.31	-0.18	0.00	0.30
10% CEMI w/s: 0.5	-0.17	-0.06	-0.32	-0.31	-0.10	0.78
50% GGBS w/s: 0.35	0.16	-0.07	0.02	0.12	0.28	0.43
50% GGBS w/s: 0.4	0.16	-0.10	0.02	0.13	0.32	0.44
Cl						
50% CEMI w/s: 0.5	0.04	0.26	0.37	0.05	0.27	0.46
20% CEMI w/s: 0.5	-0.29	-0.52	-0.70	-0.25	0.14	0.37
10% CEMI w/s: 0.5	-0.56	-0.58	-1.04	-0.50	-0.14	0.34
50% GGBS w/s: 0.35	0.22	-0.07	0.03	0.21	0.41	0.64
50% GGBS w/s: 0.4	0.20	-0.08	0.02	0.19	0.37	0.55
50% GGBS w/s: 0.5	0.29	0.00	0.13	0.27	0.45	0.59
SO4						
50% CEMI w/s: 0.5	0.22	0.08	0.01	0.24	0.31	0.75
20% CEMI w/s: 0.5	-0.03	0.05	-0.20	-0.07	-0.01	0.35
10% CEMI w/s: 0.5	-0.48	-0.29	-0.64	-0.60	-0.42	1.00
50% GGBS w/s: 0.35	0.51	0.58	0.60	0.39	0.43	0.46
50% GGBS w/s: 0.4	0.49	0.51	0.53	0.31	0.49	0.51

	Slopes of Monolithic Leaching Test Intervals					
Element	***2-7***	***5-8***	***4-7***	***3-6***	***2-5***	***1-4***
Zn						
50% CEMI w/s: 0.5	0.41	0.16	0.71	0.21	0.14	0.39
20% CEMI w/s: 0.5	0.31	-0.11	-0.19	0.26	0.97	0.79
10% CEMI w/s: 0.5	0.26	0.14	-0.17	0.10	0.46	0.95
50% GGBS w/s: 0.35	-0.13	1.76	0.07	-0.67	-1.25	0.60
50% GGBS w/s: 0.4	0.17	-0.16	-0.68	0.02	1.02	1.06
Pb						
50% CEMI w/s: 0.5	0.43	0.50	0.55	0.46	0.13	0.01
20% CEMI w/s: 0.5	0.42	0.32	0.37	0.40	0.33	0.27
10% CEMI w/s: 0.5	0.49	0.49	0.54	0.24	0.26	0.64
50% GGBS w/s: 0.35	n/a	n/a	n/a	n/a	n/a	n/a
50% GGBS w/s: 0.4	n/a	n/a	n/a	n/a	n/a	n/a
Fe						
50% CEMI w/s: 0.5	0.14	0.06	0.05	0.06	0.19	0.41
20% CEMI w/s: 0.5	0.13	0.01	-0.14	0.16	0.42	0.44
10% CEMI w/s: 0.5	0.09	0.07	-0.19	0.13	0.23	0.47
50% GGBS w/s: 0.35	-0.03	0.27	-0.12	-0.24	-0.08	0.54
50% GGBS w/s: 0.4	0.20	0.11	-0.10	0.12	0.30	0.77
Sr						
50% CEMI w/s: 0.5	0.08	0.01	0.12	0.20	0.11	0.67
20% CEMI w/s: 0.5	-0.27	-0.26	-0.60	-0.25	0.00	0.30
10% CEMI w/s: 0.5	-0.30	-0.25	-0.64	-0.34	-0.05	0.67
50% GGBS w/s: 0.35	0.19	-0.11	0.04	0.15	0.35	0.45
50% GGBS w/s: 0.4	0.16	-0.12	0.06	0.18	0.30	0.38

APPENDIX V: pH-DEPENDENT RELEASE DATA FOR SURROGATE MATERIAL

A. FRACTION INFORMATION

Fraction	*pH*	*L/S (l/kg)*	*W (kg)*	*V(ml)*
8	3.60	10.0	0.020	200.0
7	4.80	10.0	0.020	200.0
6	6.05	10.0	0.020	200.0
5	7.30	10.0	0.020	200.0
4	7.80	10.0	0.020	200.0
3	9.50	10.0	0.020	200.0
2	10.30	10.0	0.020	200.0
1	11.70	10.0	0.020	200.0

B. CONSTITUENT RELEASE SUMMARY (all values in mg/kg)

Fraction	*8*	*7*	*6*	*5*	*4*	*3*	*2*	*1*
pH	*3.60*	*4.80*	*6.05*	*7.30*	*7.80*	*9.50*	*10.30*	*11.70*
Al	4456	867.3	113.5	0.23	0.68	0.85	1.01	1.77
As	0.15	0.15	0.15	0.15	0.10	0.13	0.15	0.050
B	59.5	53.0	44.9	33.8	24.2	16.2	18.6	0.60
Ba	12.7	17.7	19.2	18.4	19.3	11.1	11.7	1.84
Br	499.7	533.3	564.2	581.3	577.2	593.3	623.2	833.8
Ca	83625	75817	66159	57425	52488	48767	44233	8189
Cd	178.2	165.6	143.5	87.2	17.8	0.35	0.020	0.030
Cl	47252	46764	48091	48160	53500	47746	49055	49185
Co	3.04	2.51	1.92	1.24	0.44	0.030	0.020	0.030
Cr	9.69	0.31	0.060	1.16	1.15	2.05	4.14	1.34
Cu	365.0	184.2	22.0	0.29	0.070	0.050	0.015	0.16
DOC	32.0	31.0	19.0	24.0	22.0	31.0	23.0	30.0
F	1904	1291	535.0	131.7	138.0	143.1	129.6	15.9
Fe	73.9	2.73	0.030	0.030	0.030	0.030	0.030	0.10
K	33815	32602	30681	32039	31005	30960	30875	29812
Li	24.5	18.5	12.8	10.9	9.80	8.80	7.60	6.62
Mg	3903	3242	2824	2112	1262	558.9	390.0	2.13
Mn	174.8	128.4	92.6	62.3	22.6	0.090	0.070	0.080
Mo	0.13	0.15	1.40	2.75	1.32	1.73	4.43	7.70
Na	24966	24775	23095	23807	25626	22787	22473	21027
Ni	9.29	8.07	6.39	3.88	1.61	0.030	0.030	0.030
P	4.74	1.04	0.99	0.73	0.75	1.03	0.84	1.96
Pb	955.1	411.0	42.9	2.69	1.04	0.23	0.28	18.6
S	4282	3623	3683	3548	3774	3945	3774	10656
Sb	2.22	1.14	3.04	3.32	3.11	4.92	3.52	0.090
Se	0.40	0.39	0.30	0.24	0.22	0.38	0.46	0.33
Si	3556	1409	468.2	224.2	78.1	61.7	63.7	6.07
Sn	0.070	0.060	0.070	0.050	0.040	0.060	0.030	
Sr	206.0	184.6	151.3	142.0	128.4	117.2	108.9	49.5
Ti	0.005	0.005	0.005	0.005	0.005	0.005	0.005	
V	0.36	0.13	0.12	0.010	0.080	0.36	0.58	0.040
Zn	8015	7210	6023	618.9	56.7	0.98	1.24	13.5

APPENDIX VI: STATISTICAL ANALYSIS TABLES

A. PHYSICAL PROPERTIES

A1. COMPRESSIVE STRENGTH

Binder Type

GGBS

t-test *on means of 28-day UCS before (UCS28) and after water immersion (UCS28w) for 50 wt.% GGBS addition*

a) w/s: 0.5

```
Paired t test
------------------------------------------------------------------------------
Variable |     Obs        Mean    Std. Err.   Std. Dev.   [95% Conf. Interval]
---------+--------------------------------------------------------------------
   UCS28 |       3          10    .7505554         1.3    6.770621    13.22938
  UCS28w |       3         8.5    .0577352    .1000004    8.251585    8.748415
---------+--------------------------------------------------------------------
    diff |       3         1.5    .7023767    1.216552   -1.522083    4.522083
------------------------------------------------------------------------------
     mean(diff) = mean(UCS28 - UCS28w)                             t =   2.1356
 Ho: mean(diff) = 0                              degrees of freedom =        2

 Ha: mean(diff) < 0           Ha: mean(diff) != 0           Ha: mean(diff) > 0
 Pr(T < t) = 0.9169         Pr(|T| > |t|) = 0.1662          Pr(T > t) = 0.0831
```

b) w/s: 0.4

```
Paired t test
------------------------------------------------------------------------------
Variable |     Obs        Mean    Std. Err.   Std. Dev.   [95% Conf. Interval]
---------+--------------------------------------------------------------------
   UCS28 |       3        12.6    2.007486    3.477067    3.962486    21.23751
  UCS28w |       3    15.66667     .638575    1.106044     12.9191    18.41423
---------+--------------------------------------------------------------------
    diff |       3   -3.066667    2.575742    4.461315   -14.14919    8.015855
------------------------------------------------------------------------------
     mean(diff) = mean(UCS28 - UCS28w)                             t =  -1.1906
 Ho: mean(diff) = 0                              degrees of freedom =        2

 Ha: mean(diff) < 0           Ha: mean(diff) != 0           Ha: mean(diff) > 0
 Pr(T < t) = 0.1780         Pr(|T| > |t|) = 0.3560          Pr(T > t) = 0.8220
```

c) w/s: 0.35

```
Paired t test
------------------------------------------------------------------------------
Variable |     Obs        Mean    Std. Err.   Std. Dev.   [95% Conf. Interval]
---------+--------------------------------------------------------------------
   UCS28 |       3    20.53333    .4096067    .7094597    18.77094    22.29573
  UCS28w |       3    22.13333    1.669664    2.891943    14.94935    29.31732
---------+--------------------------------------------------------------------
    diff |       3   -1.600001    1.792577    3.104835   -9.312839    6.112837
------------------------------------------------------------------------------
     mean(diff) = mean(UCS28 - UCS28w)                             t =  -0.8926
 Ho: mean(diff) = 0                              degrees of freedom =        2

 Ha: mean(diff) < 0           Ha: mean(diff) != 0           Ha: mean(diff) > 0
 Pr(T < t) = 0.2331         Pr(|T| > |t|) = 0.4663          Pr(T > t) = 0.7669
```

t-test *on means of 7-day UCS 7 and 28-day UCS (UCS28w) for 20 and 10 wt.% GGBS addition*

a) 20 wt.% GGBS, w/s: 0.5

```
Paired t test
------------------------------------------------------------------------------
Variable |     Obs        Mean    Std. Err.   Std. Dev.   [95% Conf. Interval]
---------+--------------------------------------------------------------------
    UCS7 |       3          .2           0           0          .2          .2
   UCS28 |       3    .8333333    .0333333    .057735    .6899116    .976755
---------+--------------------------------------------------------------------
    diff |       3   -.6333333    .0333333    .057735    -.776755   -.4899116
------------------------------------------------------------------------------
     mean(diff) = mean(UCS7 - UCS28)                              t = -19.0000
 Ho: mean(diff) = 0                               degrees of freedom =        2

 Ha: mean(diff) < 0           Ha: mean(diff) != 0           Ha: mean(diff) > 0
 Pr(T < t) = 0.0014         Pr(|T| > |t|) = 0.0028          Pr(T > t) = 0.9986
```

b) 20 wt.% GGBS, w/s: 0.6

```
Paired t test
------------------------------------------------------------------------------
Variable |     Obs        Mean    Std. Err.   Std. Dev.   [95% Conf. Interval]
---------+--------------------------------------------------------------------
    UCS7 |       3    .2666667    .0666667    .1154701   -.0201768    .5535102
   UCS28 |       3    .8333333    .0333333     .057735    .6899116     .976755
---------+--------------------------------------------------------------------
    diff |       3   -.5666667    .0881917    .1527525   -.9461249   -.1872084
------------------------------------------------------------------------------
     mean(diff) = mean(UCS7 - UCS28)                              t =  -6.4254
 Ho: mean(diff) = 0                               degrees of freedom =        2

 Ha: mean(diff) < 0           Ha: mean(diff) != 0           Ha: mean(diff) > 0
 Pr(T < t) = 0.0117         Pr(|T| > |t|) = 0.0234          Pr(T > t) = 0.9883
```

c) 20 wt.% GGBS, w/s: 0.7

```
Paired t test
------------------------------------------------------------------------------
Variable |     Obs        Mean    Std. Err.   Std. Dev.   [95% Conf. Interval]
---------+--------------------------------------------------------------------
    UCS7 |       3          .1           0           0          .1          .1
   UCS28 |       3          .5     .057735          .1    .2515862    .7484138
---------+--------------------------------------------------------------------
    diff |       3         -.4     .057735          .1   -.6484138   -.1515862
------------------------------------------------------------------------------
     mean(diff) = mean(UCS7 - UCS28)                              t =  -6.9282
 Ho: mean(diff) = 0                               degrees of freedom =        2

 Ha: mean(diff) < 0           Ha: mean(diff) != 0           Ha: mean(diff) > 0
 Pr(T < t) = 0.0101         Pr(|T| > |t|) = 0.0202          Pr(T > t) = 0.9899
```

d) 10 wt.% GGBS, w/s: 0.5

```
Paired t test
------------------------------------------------------------------------------
Variable |     Obs        Mean    Std. Err.   Std. Dev.   [95% Conf. Interval]
---------+--------------------------------------------------------------------
    UCS7 |       3          .9           0           0          .9          .9
   UCS28 |       3    .4333333    .0333333    .057735    .2899116    .5767551
---------+--------------------------------------------------------------------
    diff |       3    .4666666    .0333333    .057735    .3232449    .6100884
------------------------------------------------------------------------------
     mean(diff) = mean(UCS7 - UCS28)                              t =  14.0000
 Ho: mean(diff) = 0                               degrees of freedom =        2

 Ha: mean(diff) < 0           Ha: mean(diff) != 0           Ha: mean(diff) > 0
 Pr(T < t) = 0.9975         Pr(|T| > |t|) = 0.0051          Pr(T > t) = 0.0025
```

e) 10 wt.% GGBS, w/s: 0.6

```
Paired t test
------------------------------------------------------------------------------
Variable |     Obs        Mean    Std. Err.   Std. Dev.   [95% Conf. Interval]
---------+--------------------------------------------------------------------
    UCS7 |       3    .6666667    .0666667      .11547    .3798232    .9535102
   UCS28 |       3          .3           0           0          .3          .3
---------+--------------------------------------------------------------------
    diff |       3    .3666667    .0666667      .11547    .0798232    .6535102
------------------------------------------------------------------------------
     mean(diff) = mean(UCS7 - UCS28)                               t =   5.5000
 Ho: mean(diff) = 0                             degrees of freedom =        2

 Ha: mean(diff) < 0           Ha: mean(diff) != 0           Ha: mean(diff) > 0
 Pr(T < t) = 0.9842         Pr(|T| > |t|) = 0.0315          Pr(T > t) = 0.0158
```

f) 10 wt.% GGBS, w/s: 0.8

```
Paired t test
------------------------------------------------------------------------------
Variable |     Obs        Mean    Std. Err.   Std. Dev.   [95% Conf. Interval]
---------+--------------------------------------------------------------------
    UCS7 |       3    .1133333    .0466667     .080829   -.0874571    .3141238
   UCS28 |       3    .2333333    .0333333     .057735    .0899116    .3767551
---------+--------------------------------------------------------------------
    diff |       3        -.12         .02     .034641   -.2060531    -.033947
------------------------------------------------------------------------------
     mean(diff) = mean(UCS7 - UCS28)                               t =  -6.0000
 Ho: mean(diff) = 0                             degrees of freedom =        2

 Ha: mean(diff) < 0           Ha: mean(diff) != 0           Ha: mean(diff) > 0
 Pr(T < t) = 0.0133         Pr(|T| > |t|) = 0.0267          Pr(T > t) = 0.9867
```

CEM I vs. GGBS

t-test *on means of 28-day UCS by binder for 50 wt.% binder addition*

a) w/s: 0.4

```
Two-sample t test with equal variances
------------------------------------------------------------------------------
   Group |     Obs        Mean    Std. Err.   Std. Dev.   [95% Conf. Interval]
---------+--------------------------------------------------------------------
    CEMI |       3    17.36667    .6887994    1.193036      14.403    20.33033
    ggbs |       3        12.6    2.007486    3.477067    3.962486    21.23751
---------+--------------------------------------------------------------------
combined |       6    14.98333    1.427216     3.49595    11.31456    18.65211
---------+--------------------------------------------------------------------
    diff |            4.766667    2.122368               -1.12597     10.6593
------------------------------------------------------------------------------
    diff = mean(CEMI) - mean(ggbs)                                t =   2.2459
Ho: diff = 0                                   degrees of freedom =        4

    Ha: diff < 0                 Ha: diff != 0                 Ha: diff > 0
 Pr(T < t) = 0.9560         Pr(|T| > |t|) = 0.0880          Pr(T > t) = 0.0440
```

b) w/s: 0.5

```
Two-sample t test with equal variances
------------------------------------------------------------------------------
   Group |     Obs        Mean    Std. Err.   Std. Dev.   [95% Conf. Interval]
---------+--------------------------------------------------------------------
    CEMI |       3    12.43333    .3666668    .6350855    10.85569    14.01097
    ggbs |       3          10    .7505554         1.3    6.770621    13.22938
---------+--------------------------------------------------------------------
combined |       6    11.21667    .6600084    1.616684    9.520061    12.91327
---------+--------------------------------------------------------------------
    diff |            2.433333     .835331                .1140827    4.752584
------------------------------------------------------------------------------
    diff = mean(CEMI) - mean(ggbs)                                t =   2.9130
Ho: diff = 0                                     degrees of freedom =        4

    Ha: diff < 0                 Ha: diff != 0                 Ha: diff > 0
 Pr(T < t) = 0.9782         Pr(|T| > |t|) = 0.0435          Pr(T > t) = 0.0218
```

Wilcoxon Mann-Whitney test *on means of 28-day UCS by binder for 50 wt.% binder addition*

a) w/s: 0.4

```
Two-sample Wilcoxon rank-sum (Mann-Whitney) test

        bndr |      obs    rank sum    expected
-------------+---------------------------------
        CEMI |        3          15        10.5
        ggbs |        3           6        10.5
-------------+---------------------------------
    combined |        6          21          21

unadjusted variance        5.25
adjustment for ties        0.00
                     ----------
adjusted variance          5.25

Ho: UCS28(bndr==CEMI) = UCS28(bndr==ggbs)
             z =   1.964
    Prob > |z| =   0.0495
```

b) w/s: 0.5

```
Two-sample Wilcoxon rank-sum (Mann-Whitney) test

        bndr |      obs    rank sum    expected
-------------+---------------------------------
        CEMI |        3          15        10.5
        ggbs |        3           6        10.5
-------------+---------------------------------
    combined |        6          21          21

unadjusted variance        5.25
adjustment for ties       -0.15
                     ----------
adjusted variance          5.10

Ho: UCS28(bndr==CEMI) = UCS28(bndr==ggbs)
             z =   1.993
    Prob > |z| =   0.0463
```

Effect of w/s Ratio on Compressive Strength

ANOVA: *Effect of water content on 28-day UCS for 50 wt.% CEM I mixes*

```
           |   Summary of Compressive Strength
Water-to-So |                @28d
 lids Ratio |        Mean   Std. Dev.       Freq.
------------+------------------------------------
         .4 |   17.366667   1.1930355           3
         .5 |   12.433333   .63508552           3
        .55 |          11   .43588992           3
         .6 |   8.6000001    .0999999           3
------------+------------------------------------
      Total |       12.35   3.4009358          12

                      Analysis of Variance
    Source              SS         df      MS            F     Prob > F
------------------------------------------------------------------------
Between groups      123.176669      3   41.0588897     81.04     0.0000
 Within groups      4.05333476      8   .506666845
------------------------------------------------------------------------
    Total           127.230004     11    11.566364

Bartlett's test for equal variances:  chi2(3) =   6.7883  Prob>chi2 = 0.079
```

ANOVA: *Effect of water content on 28-day UCS for 50 wt.% GGBS mixes*

```
           |   Summary of Compressive Strength
Water-to-So |                @28d
 lids Ratio |        Mean   Std. Dev.       Freq.
------------+------------------------------------
        .35 |   20.533333   .70945968           3
         .4 |        12.6   3.4770674           3
         .5 |          10         1.3           3
------------+------------------------------------
      Total |   14.377778   5.1138969           9

                      Analysis of Variance
    Source              SS         df      MS            F     Prob > F
------------------------------------------------------------------------
Between groups      180.648869      2   90.3244347     18.97     0.0025
 Within groups       28.566662      6   4.76111033
------------------------------------------------------------------------
    Total           209.215531      8   26.1519414

Bartlett's test for equal variances:  chi2(2) =   3.8468  Prob>chi2 = 0.146
```

Multivariate Regression Analysis

UCS at 28 days for CEM I mixes

```
      Source |       SS       df       MS              Number of obs =      36
-------------+------------------------------           F(  2,    33) =  427.57
       Model |  693.725523     2  346.862761            Prob > F      =  0.0000
    Residual |  26.7708777    33  .811238718            R-squared     =  0.9628
-------------+------------------------------           Adj R-squared =  0.9606
       Total |    720.4964    35  20.5856114            Root MSE      =  .90069

------------------------------------------------------------------------------
       UCS28 |      Coef.   Std. Err.      t    P>|t|     [95% Conf. Interval]
-------------+----------------------------------------------------------------
 CEMI (wt.%) |   .1513177   .0093853    16.12   0.000     .1322233    .1704122
         w/s |  -37.28788   2.130208   -17.50   0.000    -41.62183   -32.95394
       _cons |   23.79839   1.278285    18.62   0.000      21.1977    26.39908
------------------------------------------------------------------------------
```

UCS at 28 days for all mixes – A binary variable is used for the binder type with 0 and 1 representing GGBS and CEM I respectively

```
      Source |       SS       df       MS              Number of obs =      69
-------------+------------------------------           F(  3,    65) =   92.02
       Model |  1887.86149     3  629.287163            Prob > F      =  0.0000
    Residual |  444.527168    65  6.83887951            R-squared     =  0.8094
-------------+------------------------------           Adj R-squared =  0.8006
       Total |  2332.38866    68  34.2998332            Root MSE      =  2.6151

------------------------------------------------------------------------------
       UCS28 |      Coef.   Std. Err.      t    P>|t|     [95% Conf. Interval]
-------------+----------------------------------------------------------------
      binder |   2.548348   .6316026     4.03   0.000     1.286951    3.809746
 binder_wt.% |   .2156138   .0220374     9.78   0.000     .1716021    .2596255
         w/s |  -19.41722   3.362537    -5.77   0.000    -26.13267   -12.70177
       _cons |   9.781071   2.222475     4.40   0.000     5.342481    14.21966
------------------------------------------------------------------------------
```

A2. POROSITY

Multivariate Regression Analysis

Porosity at 28 days for all mixes – A binary variable is used for the binder type with 0 and 1 representing GGBS and CEM I respectively

```
      Source |       SS       df       MS              Number of obs =      23
-------------+------------------------------           F(  3,    19) =  138.46
       Model |  1414.74185     3  471.580618            Prob > F      =  0.0000
    Residual |  64.7112231    19  3.40585385            R-squared     =  0.9563
-------------+------------------------------           Adj R-squared =  0.9494
       Total |  1479.45308    22  67.2478671            Root MSE      =  1.8455

------------------------------------------------------------------------------
      por28d |      Coef.   Std. Err.      t    P>|t|     [95% Conf. Interval]
-------------+----------------------------------------------------------------
      binder |  -5.482541   .7720138    -7.10   0.000    -7.098384   -3.866697
 binder_wt.% |   -.246529   .0269365    -9.15   0.000    -.3029078   -.1901502
         w/s |   38.68451   4.110061     9.41   0.000     30.08205    47.28696
       _cons |   34.37469   2.716553    12.65   0.000     28.68888     40.0605
------------------------------------------------------------------------------
```

B. MONOLITHIC LEACHING

B1. pH

ANOVA: *Effect of water content on pH for 50 wt.% CEM I mixes*

```
Water-to-So |   Summary of Leaching Fraction pH
 lids Ratio |        Mean   Std. Dev.       Freq.
------------+------------------------------------
         .4 |    11.73875      .11655           8
         .5 |    11.82125   .09387489           8
        .55 |    11.82875    .1144475           8
         .6 |     11.8475   .11029182           8
------------+------------------------------------
      Total |   11.809063    .1120587          32

                      Analysis of Variance
    Source              SS         df      MS            F     Prob > F
------------------------------------------------------------------------
Between groups      .055659289      3   .018553096      1.56     0.2218
 Within groups      .333612396     28   .011914728
------------------------------------------------------------------------
    Total           .389271685     31   .012557151

Bartlett's test for equal variances:  chi2(3) =   0.3638  Prob>chi2 = 0.948
```

ANOVA: *Effect of water content on pH for 20 wt.% CEM I mixes*

```
Water-to-So |   Summary of Leaching Fraction pH
 lids Ratio |        Mean   Std. Dev.       Freq.
------------+------------------------------------
        .45 |    11.80625     .159905           8
         .5 |    11.82375   .14686592           8
         .6 |    11.84125   .15878431           8
------------+------------------------------------
      Total |    11.82375   .14910773          24

                      Analysis of Variance
    Source              SS         df      MS            F     Prob > F
------------------------------------------------------------------------
Between groups      .004899957      2   .002449979      0.10     0.9038
 Within groups      .506461666     21   .024117222
------------------------------------------------------------------------
    Total           .511361623     23   .022233114

Bartlett's test for equal variances:  chi2(2) =   0.0576  Prob>chi2 = 0.972
```

ANOVA: *Effect of water content on pH for 50 wt.% GGBS mixes*

```
Water-to-So |   Summary of Leaching Fraction pH
 lids Ratio |        Mean   Std. Dev.       Freq.
------------+------------------------------------
        .35 |    10.99125   .15569545           8
         .4 |     11.0375   .11732143           8
         .5 |       10.97   .15856489           8
------------+------------------------------------
      Total |   10.999583    .1415897          24

                      Analysis of Variance
    Source              SS         df      MS            F     Prob > F
------------------------------------------------------------------------
Between groups      .019058297      2   .009529149      0.45     0.6420
 Within groups       .44203751     21   .021049405
------------------------------------------------------------------------
    Total           .461095807     23   .020047644

Bartlett's test for equal variances:  chi2(2) =   0.6972  Prob>chi2 = 0.706
```

B2. SOLUBLE SALTS

Chloride (Cl)

ANOVA: *Effect of water content on **Cl** release for 50 wt.% CEM I mixes*

```
Water-to-So |       Summary of Cl in mg/m2
 lids Ratio |        Mean   Std. Dev.       Freq.
------------+------------------------------------
         .4 |   76858.662   20061.155           8
         .5 |   73732.136   25250.289           8
        .55 |   71640.287   33263.397           8
         .6 |   72495.024    40335.66           8
------------+------------------------------------
      Total |   73681.527   29259.403          32

                      Analysis of Variance
    Source              SS         df      MS            F     Prob > F
------------------------------------------------------------------------
Between groups       125369580       3   41789859.9      0.04     0.9873
 Within groups      2.6414e+10      28    943361506
------------------------------------------------------------------------
    Total           2.6539e+10      31    856112637

Bartlett's test for equal variances:  chi2(3) =   3.5621  Prob>chi2 = 0.313
```

ANOVA: *Effect of water content on **Cl** release for 20 wt.% CEM I mixes*

```
Water-to-So |       Summary of Cl in mg/m2
 lids Ratio |        Mean   Std. Dev.       Freq.
------------+------------------------------------
        .45 |   128412.62   74508.409           8
         .5 |   122069.65   70284.153           8
         .6 |   109361.09   75607.206           8
------------+------------------------------------
      Total |   119947.79   70698.557          24

                      Analysis of Variance
    Source              SS         df      MS            F     Prob > F
------------------------------------------------------------------------
Between groups      1.5059e+09      2    752935968      0.14     0.8707
 Within groups      1.1345e+11     21   5.4026e+09
------------------------------------------------------------------------
    Total           1.1496e+11     23   4.9983e+09

Bartlett's test for equal variances:  chi2(2) =   0.0388  Prob>chi2 = 0.981
```

ANOVA: *Effect of water content on **Cl** release for 50 wt.% GGBS mixes*

```
Water-to-So |       Summary of Cl in mg/m2
 lids Ratio |        Mean   Std. Dev.       Freq.
------------+------------------------------------
        .35 |   70587.112   18407.697           8
         .4 |   73978.725   14850.887           8
         .5 |   67692.351   20039.878           8
------------+------------------------------------
      Total |   70752.729    17302.08          24

                      Analysis of Variance
    Source              SS         df      MS            F     Prob > F
------------------------------------------------------------------------
Between groups       158403167       2   79201583.6      0.25     0.7832
 Within groups      6.7269e+09     21    320329629
------------------------------------------------------------------------
    Total           6.8853e+09     23    299361972

Bartlett's test for equal variances:  chi2(2) =   0.5986  Prob>chi2 = 0.741
```

Sodium (Na)

ANOVA: *Effect of water content on **Na** release for 50 wt.% CEM I mixes*

Water-to-Solids Ratio	Summary of Na in mg/m2 Mean	Std. Dev.	Freq.
.4	13948.6	7227.6019	8
.5	15588.437	10929.571	8
.55	15963.4	13934.996	8
.6	15228.475	13072.587	8
Total	15182.228	11036.284	32

Analysis of Variance

Source	SS	df	MS	F	Prob > F
Between groups	18393704.1	3	6131234.69	0.05	0.9868
Within groups	3.7574e+09	28	134192600		
Total	3.7758e+09	31	121799565		

Bartlett's test for equal variances: chi2(3) = 2.9631 Prob>chi2 = 0.397

ANOVA: *Effect of water content on **Na** release for 20 wt.% CEM I mixes*

Water-to-Solids Ratio	Summary of Na in mg/m2 Mean	Std. Dev.	Freq.
.45	24565.037	24309.549	8
.5	24680.037	26333.333	8
.6	16557.1	18862.375	8
Total	21934.058	22677.615	24

Analysis of Variance

Source	SS	df	MS	F	Prob > F
Between groups	346993049	2	173496524	0.32	0.7315
Within groups	1.1481e+10	21	546729259		
Total	1.1828e+10	23	514274239		

Bartlett's test for equal variances: chi2(2) = 0.7511 Prob>chi2 = 0.687

ANOVA: *Effect of water content on **Na** release for 50 wt.% GGBS mixes*

Water-to-Solids Ratio	Summary of Na in mg/m2 Mean	Std. Dev.	Freq.
.35	17352.437	5204.2726	8
.4	16987.887	5409.9929	8
.5	16348.887	5217.9357	8
Total	16896.404	5061.2947	24

Analysis of Variance

Source	SS	df	MS	F	Prob > F
Between groups	4128880.1	2	2064440.05	0.07	0.9288
Within groups	585055302	21	27859776.3		
Total	589184182	23	25616703.6		

Bartlett's test for equal variances: chi2(2) = 0.0125 Prob>chi2 = 0.994

Potassium (K)

ANOVA: *Effect of water content on **K** release for 50 wt.% CEM I mixes*

Water-to-Solids Ratio	Summary of K in mg/m2 Mean	Std. Dev.	Freq.
.4	14448.55	8994.8175	8
.5	15680.938	12574.612	8
.55	14886.013	14825.322	8
.6	14671.037	14475.453	8
Total	14921.634	12293.994	32

Analysis of Variance

Source	SS	df	MS	F	Prob > F
Between groups	6915346.9	3	2305115.63	0.01	0.9977
Within groups	4.6785e+09	28	167089135		
Total	4.6854e+09	31	151142294		

Bartlett's test for equal variances: chi2(3) = 1.8490 Prob>chi2 = 0.604

ANOVA: *Effect of water content on **K** release for 20 wt.% CEM I mixes*[13]

Water-to-Solids Ratio	Summary of K in mg/m2 Mean	Std. Dev.	Freq.
.45	20033	21919.307	8
.5	21072.887	25092.299	8
.6	4027.6475	8189.6197	8
Total	15044.512	20537.163	24

Analysis of Variance

Source	SS	df	MS	F	Prob > F
Between groups	1.4608e+09	2	730390514	1.86	0.1802
Within groups	8.2400e+09	21	392383122		
Total	9.7008e+09	23	421775069		

Bartlett's test for equal variances: chi2(2) = 7.1819 Prob>chi2 = 0.028

ANOVA: *Effect of water content on **K** release for 50 wt.% GGBS mixes*

Water-to-Solids Ratio	Summary of K in mg/m2 Mean	Std. Dev.	Freq.
.35	17376.738	6214.5967	8
.4	15753.038	6427.0477	8
.5	16555.588	4510.071	8
Total	16561.788	5565.5319	24

Analysis of Variance

Source	SS	df	MS	F	Prob > F
Between groups	10546067.4	2	5273033.71	0.16	0.8551
Within groups	701882264	21	33422965		
Total	712428332	23	30975144.9		

Bartlett's test for equal variances: chi2(2) = 0.9233 Prob>chi2 = 0.630

[13] Erratic results were obtained for the mix with w/s: 0.6 resulting in a low mean

CEM I vs. GGBS

***t-test** on means of **Cl** release by binder for 50 wt.% binder addition*

a) w/s: 0.4

```
Two-sample t test with equal variances
------------------------------------------------------------------------------
   Group |     Obs        Mean    Std. Err.   Std. Dev.   [95% Conf. Interval]
---------+--------------------------------------------------------------------
    CEMI |       8    76858.66    7092.689    20061.16    60087.12    93630.21
    ggbs |       8    73978.73    5250.582    14850.89    61563.07    86394.38
---------+--------------------------------------------------------------------
combined |      16    75418.69    4278.906    17115.62    66298.42    84538.96
---------+--------------------------------------------------------------------
    diff |            2879.937    8824.673               -16047.1    21806.98
------------------------------------------------------------------------------
    diff = mean(CEMI) - mean(ggbs)                                t =   0.3264
Ho: diff = 0                                     degrees of freedom =       14

    Ha: diff < 0                 Ha: diff != 0                 Ha: diff > 0
 Pr(T < t) = 0.6255         Pr(|T| > |t|) = 0.7490          Pr(T > t) = 0.3745
```

b) w/s: 0.5

```
Two-sample t test with equal variances
------------------------------------------------------------------------------
   Group |     Obs        Mean    Std. Err.   Std. Dev.   [95% Conf. Interval]
---------+--------------------------------------------------------------------
    CEMI |       8    73732.14    8927.325    25250.29    52622.37    94841.91
    ggbs |       8    67692.35    7085.167    20039.88    50938.59    84446.11
---------+--------------------------------------------------------------------
combined |      16    70712.24    5560.325     22241.3    58860.69     82563.8
---------+--------------------------------------------------------------------
    diff |            6039.786    11397.22              -18404.83     30484.4
------------------------------------------------------------------------------
    diff = mean(CEMI) - mean(ggbs)                                t =   0.5299
Ho: diff = 0                                     degrees of freedom =       14

    Ha: diff < 0                 Ha: diff != 0                 Ha: diff > 0
 Pr(T < t) = 0.6978         Pr(|T| > |t|) = 0.6045          Pr(T > t) = 0.3022
```

***t-test** on means of **Na** release by binder for 50 wt.% binder addition*

a) w/s: 0.4

```
Two-sample t test with equal variances
------------------------------------------------------------------------------
   Group |     Obs        Mean    Std. Err.   Std. Dev.   [95% Conf. Interval]
---------+--------------------------------------------------------------------
    CEMI |       8     13948.6    2555.343    7227.602    7906.173    19991.03
    ggbs |       8    16987.89    1912.721    5409.993    12465.02    21510.75
---------+--------------------------------------------------------------------
combined |      16    15468.24    1590.981    6363.924    12077.15    18859.34
---------+--------------------------------------------------------------------
    diff |           -3039.287    3191.909              -9885.251    3806.676
------------------------------------------------------------------------------
    diff = mean(CEMI) - mean(ggbs)                                t =  -0.9522
Ho: diff = 0                                     degrees of freedom =       14

    Ha: diff < 0                 Ha: diff != 0                 Ha: diff > 0
 Pr(T < t) = 0.1786         Pr(|T| > |t|) = 0.3572          Pr(T > t) = 0.8214
```

b) w/s: 0.5

```
Two-sample t test with equal variances
------------------------------------------------------------------------------
   Group |     Obs        Mean    Std. Err.   Std. Dev.   [95% Conf. Interval]
---------+--------------------------------------------------------------------
    CEMI |       8    15588.44    3864.187    10929.57    6451.087    24725.79
    ggbs |       8    16348.89    1844.819    5217.936    11986.58    20711.19
---------+--------------------------------------------------------------------
combined |      16    15968.66    2070.718    8282.873    11555.03    20382.29
---------+--------------------------------------------------------------------
    diff |            -760.45    4281.974               -9944.37     8423.47
------------------------------------------------------------------------------
    diff = mean(CEMI) - mean(ggbs)                                t =  -0.1776
Ho: diff = 0                                     degrees of freedom =       14

    Ha: diff < 0                 Ha: diff != 0                 Ha: diff > 0
 Pr(T < t) = 0.4308         Pr(|T| > |t|) = 0.8616          Pr(T > t) = 0.5692
```

***t-test** on means of **K** release by binder for 50 wt.% binder addition*

a) w/s: 0.4

```
Two-sample t test with equal variances
------------------------------------------------------------------------------
   Group |     Obs        Mean    Std. Err.   Std. Dev.   [95% Conf. Interval]
---------+--------------------------------------------------------------------
    CEMI |       8    14448.55    3180.148    8994.817    6928.694    21968.41
    ggbs |       8    15753.04    2272.305    6427.048    10379.89    21126.18
---------+--------------------------------------------------------------------
combined |      16    15100.79    1895.502    7582.007    11060.63    19140.96
---------+--------------------------------------------------------------------
    diff |           -1304.488    3908.543               -9687.479    7078.504
------------------------------------------------------------------------------
    diff = mean(CEMI) - mean(ggbs)                                t =  -0.3338
Ho: diff = 0                                     degrees of freedom =       14

    Ha: diff < 0                 Ha: diff != 0                 Ha: diff > 0
 Pr(T < t) = 0.3718         Pr(|T| > |t|) = 0.7435          Pr(T > t) = 0.6282
```

b) w/s: 0.5

```
Two-sample t test with equal variances
------------------------------------------------------------------------------
   Group |     Obs        Mean    Std. Err.   Std. Dev.   [95% Conf. Interval]
---------+--------------------------------------------------------------------
    CEMI |       8    15680.94    4445.797    12574.61    5168.299    26193.58
    ggbs |       8    16555.59    1594.551    4510.071    12785.07     20326.1
---------+--------------------------------------------------------------------
combined |      16    16118.26    2284.268    9137.072    11249.46    20987.06
---------+--------------------------------------------------------------------
    diff |           -874.6498    4723.103               -11004.7    9255.399
------------------------------------------------------------------------------
    diff = mean(CEMI) - mean(ggbs)                                t =  -0.1852
Ho: diff = 0                                     degrees of freedom =       14

    Ha: diff < 0                 Ha: diff != 0                 Ha: diff > 0
 Pr(T < t) = 0.4279         Pr(|T| > |t|) = 0.8557          Pr(T > t) = 0.5721
```

B3. LEAD AND ZINC

Zinc (Zn)

ANOVA: *Effect of water content on **Zn** release for 50 wt.% CEM I mixes*

```
Water-to-So |       Summary of Zn in mg/m2
 lids Ratio |        Mean   Std. Dev.       Freq.
------------+------------------------------------
         .4 |      1.8675    .5776739           8
         .5 |   3.0296975   3.1230372           8
        .55 |   1.5273475   .83493131           8
         .6 |      1.9475   .59492494           8
------------+------------------------------------
      Total |   2.0930112   1.6860135          32

                      Analysis of Variance
    Source              SS         df      MS            F     Prob > F
------------------------------------------------------------------------
Between groups      10.1550839      3   3.38502796      1.22     0.3223
 Within groups      77.9667997     28   2.78452856
------------------------------------------------------------------------
    Total           88.1218836     31   2.84264141

Bartlett's test for equal variances:  chi2(3) =  28.5124  Prob>chi2 = 0.000
```

ANOVA: *Effect of water content on **Zn** release for 20 wt.% CEM I mixes*

```
Water-to-So |       Summary of Zn in mg/m2
 lids Ratio |        Mean   Std. Dev.       Freq.
------------+------------------------------------
        .45 |        4.41   3.3906762           8
         .5 |      4.4025   3.2858038           8
         .6 |   2.2897713   1.5338426           8
------------+------------------------------------
      Total |   3.7007571   2.9222672          24

                      Analysis of Variance
    Source              SS         df      MS            F     Prob > F
------------------------------------------------------------------------
Between groups      23.8907959      2   11.9453979      1.45     0.2562
 Within groups      172.521053     21   8.21528825
------------------------------------------------------------------------
    Total           196.411849     23   8.53964561

Bartlett's test for equal variances:  chi2(2) =   4.2202  Prob>chi2 = 0.121
```

ANOVA: *Effect of water content on **Zn** release for 50 wt.% GGBS mixes*

```
Water-to-So |       Summary of Zn in mg/m2
 lids Ratio |        Mean   Std. Dev.       Freq.
------------+------------------------------------
        .35 |        1.03   .48711983           8
         .4 |     1.50625   1.0873025           8
         .5 |   .90747874   .29231387           8
------------+------------------------------------
      Total |   1.1479096   .72638652          24

                      Analysis of Variance
    Source              SS         df      MS            F     Prob > F
------------------------------------------------------------------------
Between groups      1.60094015      2   .800470074      1.60     0.2264
 Within groups      10.5347195     21   .501653308
------------------------------------------------------------------------
    Total           12.1356596     23   .527637374

Bartlett's test for equal variances:  chi2(2) =  10.9355  Prob>chi2 = 0.004
```

ANOVA: *Effect of binder content on **Zn** release for CEM I mixes at w/s: 0.5*

Waste-to-Binder Ratio	Summary of Zn in mg/m2 Mean	Std. Dev.	Freq.
1	3.0296975	3.1230372	8
4	4.4025	3.2858038	8
9	5.9399999	2.292821	8
Total	4.4573991	3.054319	24

Analysis of Variance

Source	SS	df	MS	F	Prob > F
Between groups	33.915608	2	16.957804	1.97	0.1642
Within groups	180.648273	21	8.60229872		
Total	214.563881	23	9.3288644		

Bartlett's test for equal variances: chi2(2) = 0.9194 Prob>chi2 = 0.631

Lead (Pb)

ANOVA: *Effect of water content on **Pb** release for 50 wt.% CEM I mixes*

Water-to-Solids Ratio	Summary of Pb in mg/m2 Mean	Std. Dev.	Freq.
.4	.6925	.42921023	8
.5	1.0648935	.8322457	8
.55	1.444855	1.2232095	8
.6	1.5348463	1.3518471	8
Total	1.1842737	1.0314299	32

Analysis of Variance

Source	SS	df	MS	F	Prob > F
Between groups	3.57517391	3	1.19172464	1.13	0.3520
Within groups	29.4041056	28	1.05014663		
Total	32.9792795	31	1.06384773		

Bartlett's test for equal variances: chi2(3) = 8.2498 Prob>chi2 = 0.041

ANOVA: *Effect of water content on **Pb** release for 20 wt.% CEM I mixes*

Water-to-Solids Ratio	Summary of Pb in mg/m2 Mean	Std. Dev.	Freq.
.45	5.7524999	3.4922598	8
.5	5.3575001	2.9576138	8
.6	3.549645	3.2922945	8
Total	4.8865483	3.2607665	24

Analysis of Variance

Source	SS	df	MS	F	Prob > F
Between groups	22.0718261	2	11.0359131	1.04	0.3704
Within groups	222.477927	21	10.594187		
Total	244.549753	23	10.6325979		

Bartlett's test for equal variances: chi2(2) = 0.1835 Prob>chi2 = 0.912

ANOVA: *Effect of binder content on **Pb** release for CEM I mixes at w/s: 0.5*

```
Waste-to-Bi |       Summary of Pb in mg/m2
 nder Ratio |        Mean   Std. Dev.       Freq.
------------+------------------------------------
          1 |   1.0648935    .8322457           8
          4 |   5.3575001   2.9576138           8
          9 |   9.0387502   7.9097998           8
------------+------------------------------------
      Total |   5.1537146    5.744045          24

                      Analysis of Variance
    Source              SS         df      MS            F     Prob > F
------------------------------------------------------------------------
Between groups      254.827904      2   127.413952      5.31     0.0136
 Within groups      504.035317     21   24.0016818
------------------------------------------------------------------------
    Total           758.863222     23   32.9940531

Bartlett's test for equal variances:  chi2(2) =  23.6735  Prob>chi2 = 0.000
```

B4. CALCIUM (Ca)

<u>CEM I vs. GGBS</u>

***t-test** on means of **Ca** release by binder for 50 wt.% binder addition*

a) w/s: 0.4

```
Two-sample t test with equal variances
------------------------------------------------------------------------------
   Group |     Obs        Mean    Std. Err.   Std. Dev.   [95% Conf. Interval]
---------+--------------------------------------------------------------------
    CEMI |       8    52394.76     3313.92    9373.182    44558.59    60230.94
    ggbs |       8    29139.45    3305.929    9350.579    21322.17    36956.73
---------+--------------------------------------------------------------------
combined |      16    40767.11    3758.472    15033.89    32756.11     48778.1
---------+--------------------------------------------------------------------
    diff |            23255.31    4680.944                13215.69    33294.94
------------------------------------------------------------------------------
    diff = mean(CEMI) - mean(ggbs)                                t =   4.9681
Ho: diff = 0                                     degrees of freedom =       14

    Ha: diff < 0                 Ha: diff != 0                 Ha: diff > 0
 Pr(T < t) = 0.9999         Pr(|T| > |t|) = 0.0002          Pr(T > t) = 0.0001
```

b) w/s: 0.5

```
Two-sample t test with equal variances
------------------------------------------------------------------------------
   Group |     Obs        Mean    Std. Err.   Std. Dev.   [95% Conf. Interval]
---------+--------------------------------------------------------------------
    CEMI |       8    59244.08    3643.368       10305    50628.88    67859.27
    ggbs |       8    19930.99    4693.966    13276.54    8831.522    31030.45
---------+--------------------------------------------------------------------
combined |      16    39587.53    5830.699     23322.8    27159.69    52015.37
---------+--------------------------------------------------------------------
    diff |            39313.09    5942.007                26568.75    52057.42
------------------------------------------------------------------------------
    diff = mean(CEMI) - mean(ggbs)                                t =   6.6161
Ho: diff = 0                                     degrees of freedom =       14

    Ha: diff < 0                 Ha: diff != 0                 Ha: diff > 0
 Pr(T < t) = 1.0000         Pr(|T| > |t|) = 0.0000          Pr(T > t) = 0.0000
```

Effect of water content

ANOVA: *Effect of water content on **Ca** release for 50 wt.% CEM I mixes*

```
Water-to-So |       Summary of Ca in mg/m2
 lids Ratio |        Mean   Std. Dev.       Freq.
------------+------------------------------------
         .4 |   52394.762   9373.1816           8
         .5 |   59244.075   10305.001           8
        .55 |     60993.9    10197.02           8
         .6 |   62243.775    8580.683           8
------------+------------------------------------
      Total |   58719.128   9942.6834          32

                      Analysis of Variance
    Source              SS         df      MS            F     Prob > F
------------------------------------------------------------------------
Between groups       462967229      3    154322410      1.66     0.1980
 Within groups      2.6016e+09     28   92914225.8
------------------------------------------------------------------------
    Total           3.0646e+09     31   98856953.3

Bartlett's test for equal variances:  chi2(3) =   0.2810  Prob>chi2 = 0.964
```

ANOVA: *Effect of water content on **Ca** release for 20 wt.% CEM I mixes*

```
Water-to-So |       Summary of Ca in mg/m2
 lids Ratio |        Mean   Std. Dev.       Freq.
------------+------------------------------------
        .45 |   113488.65   38744.397           8
         .5 |   105439.45   43597.974           8
         .6 |   72842.725    27627.59           8
------------+------------------------------------
      Total |   97256.941   39873.808          24

                      Analysis of Variance
    Source              SS         df      MS            F     Prob > F
------------------------------------------------------------------------
Between groups      7.4118e+09      2   3.7059e+09      2.67     0.0927
 Within groups      2.9156e+10     21   1.3884e+09
------------------------------------------------------------------------
    Total           3.6568e+10     23   1.5899e+09

Bartlett's test for equal variances:  chi2(2) =   1.3565  Prob>chi2 = 0.507
```

ANOVA: *Effect of water content on **Ca** release for 50 wt.% GGBS mixes*

```
Water-to-So |       Summary of Ca in mg/m2
 lids Ratio |        Mean   Std. Dev.       Freq.
------------+------------------------------------
        .35 |   29309.562   9683.2525           8
         .4 |    29139.45   9350.5789           8
         .5 |   19930.987    13276.54           8
------------+------------------------------------
      Total |   26126.667   11350.176          24

                      Analysis of Variance
    Source              SS         df      MS            F     Prob > F
------------------------------------------------------------------------
Between groups       460753048      2    230376524      1.93     0.1695
 Within groups      2.5023e+09     21    119155070
------------------------------------------------------------------------
    Total           2.9630e+09     23    128826501

Bartlett's test for equal variances:  chi2(2) =   1.0374  Prob>chi2 = 0.595
```

Effect of binder content

ANOVA: *Effect of binder content on **Ca** release for CEM I mixes at w/s: 0.5*[14]

```
Waste-to-Bi |       Summary of Ca in mg/m2
 nder Ratio |        Mean   Std. Dev.       Freq.
------------+------------------------------------
          1 |   59244.075   10305.001           8
          4 |   105439.45   43597.974           8
          9 |   110488.95   60257.677           8
------------+------------------------------------
      Total |   91724.158   47652.367          24

                      Analysis of Variance
    Source              SS         df      MS            F     Prob > F
------------------------------------------------------------------------
Between groups      1.2761e+10      2   6.3807e+09      3.40     0.0528
 Within groups      3.9466e+10     21   1.8793e+09
------------------------------------------------------------------------
    Total           5.2227e+10     23   2.2707e+09

Bartlett's test for equal variances:  chi2(2) =  14.5034  Prob>chi2 = 0.001
```

***t-test** on means of **Ca** release from 50 wt.% and 20 wt.% CEM I mixes at w/s: 0.5*

```
Two-sample t test with equal variances
------------------------------------------------------------------------------
   Group |     Obs        Mean    Std. Err.   Std. Dev.   [95% Conf. Interval]
---------+--------------------------------------------------------------------
       1 |       8    59244.08    3643.368       10305    50628.88    67859.27
       4 |       8    105439.4    15414.21    43597.97    68990.63    141888.3
---------+--------------------------------------------------------------------
combined |      16    82341.76    9700.705    38802.82     61665.2    103018.3
---------+--------------------------------------------------------------------
    diff |           -46195.37    15838.94               -80166.52   -12224.22
------------------------------------------------------------------------------
    diff = mean(1) - mean(4)                                      t =  -2.9166
Ho: diff = 0                                     degrees of freedom =       14

    Ha: diff < 0                 Ha: diff != 0                 Ha: diff > 0
 Pr(T < t) = 0.0056         Pr(|T| > |t|) = 0.0113          Pr(T > t) = 0.9944
```

***t-test** on means of **Ca** release from 50 wt.% and 10 wt.% CEM I mixes at w/s: 0.5*

```
Two-sample t test with equal variances
------------------------------------------------------------------------------
   Group |     Obs        Mean    Std. Err.   Std. Dev.   [95% Conf. Interval]
---------+--------------------------------------------------------------------
       1 |       8    59244.08    3643.368       10305    50628.88    67859.27
       9 |       8    110488.9    21304.31    60257.68    60112.27    160865.6
---------+--------------------------------------------------------------------
combined |      16    84866.51    12359.95     49439.8     58521.9    111211.1
---------+--------------------------------------------------------------------
    diff |           -51244.87     21613.6               -97601.43   -4888.318
------------------------------------------------------------------------------
    diff = mean(1) - mean(9)                                      t =  -2.3710
Ho: diff = 0                                     degrees of freedom =       14

    Ha: diff < 0                 Ha: diff != 0                 Ha: diff > 0
 Pr(T < t) = 0.0163         Pr(|T| > |t|) = 0.0326          Pr(T > t) = 0.9837
```

[14] The result of the ANOVA is influenced by the similar mean release per fraction for mixes with 20 and 10 wt.% CEM I addition. Therefore, *t*-tests comparing these mixes to the mix with 50 wt.% CEM I addition were conducted instead.

***t-test** on means of **Ca** release from 20 wt.% and 10 wt.% CEM I mixes at w/s: 0.5*

```
Two-sample t test with equal variances
------------------------------------------------------------------------------
   Group |     Obs        Mean    Std. Err.   Std. Dev.   [95% Conf. Interval]
---------+--------------------------------------------------------------------
       4 |       8    105439.4    15414.21    43597.97    68990.63    141888.3
       9 |       8    110488.9    21304.31    60257.68    60112.27    160865.6
---------+--------------------------------------------------------------------
combined |      16    107964.2    12718.82    50875.26    80854.68    135073.7
---------+--------------------------------------------------------------------
    diff |           -5049.499    26295.84               -61448.47    51349.48
------------------------------------------------------------------------------
    diff = mean(4) - mean(9)                                      t =  -0.1920
Ho: diff = 0                                     degrees of freedom =       14

    Ha: diff < 0                 Ha: diff != 0                 Ha: diff > 0
 Pr(T < t) = 0.4252         Pr(|T| > |t|) = 0.8505          Pr(T > t) = 0.5748
```

B5. SILICON AND ALUMINIUM

Silicon (Si)

ANOVA*: Effect of water content on **Si** release for 50 wt.% CEM I mixes*[15]

```
Water-to-So |       Summary of Si in mg/m2
 lids Ratio |        Mean   Std. Dev.       Freq.
------------+------------------------------------
         .4 |      31.675   25.773727           8
         .5 |        15.5   5.5312098           8
        .55 |    17.52325   11.186602           8
         .6 |      15.175   7.8182477           8
------------+------------------------------------
      Total |   19.968313   15.714943          32

                       Analysis of Variance
    Source              SS         df      MS            F     Prob > F
------------------------------------------------------------------------
Between groups      1487.73223      3   495.910745      2.25     0.1043
 Within groups      6168.01054     28   220.286091
------------------------------------------------------------------------
    Total           7655.74278     31   246.959444

Bartlett's test for equal variances:  chi2(3) =  17.9560  Prob>chi2 = 0.000
```

ANOVA*: Effect of water content on **Si** release for 50 wt.% CEM I mixes (excluding mix at w/s: 0.4)*

```
                       Analysis of Variance
    Source              SS         df      MS            F     Prob > F
------------------------------------------------------------------------
Between groups      25.9025179      2    12.951259      0.18     0.8372
 Within groups      1518.01535     21   72.2864454
------------------------------------------------------------------------
    Total           1543.91787     23    67.126864

Bartlett's test for equal variances:  chi2(2) =   3.1511  Prob>chi2 = 0.207
```

[15] The inequality of variances is predominantly influenced by the mix at w/s: 0.4 which had a high release during the first fraction of the monolithic leaching test (91.4 mg/m^2). This could be attributed to experimental and given the results for the other 50 wt.% mixes as well for 20 wt.% mixes it is not expected to be a real effect. If the mix at w/s: 0.4 is excluded from the test then the *prob>chi2* value for the equality of variance test is 0.21 and the *p* and *F* values for the test are 0.84 and 0.18 respectively.

ANOVA: *Effect of water content on **Si** release for 20 wt.% CEM I mixes*

```
Water-to-So |       Summary of Si in mg/m2
 lids Ratio |        Mean   Std. Dev.       Freq.
------------+------------------------------------
        .45 |   9.0750002   2.6980153           8
         .5 |      10.075   4.1896982           8
         .6 |   8.0741925   2.8641507           8
------------+------------------------------------
      Total |   9.0747309   3.2788283          24

                      Analysis of Variance
    Source              SS         df      MS            F     Prob > F
------------------------------------------------------------------------
Between groups      16.0129258      2   8.00646288      0.73     0.4951
 Within groups       231.25352     21   11.0120724
------------------------------------------------------------------------
    Total           247.266446     23    10.750715

Bartlett's test for equal variances:  chi2(2) =   1.5938  Prob>chi2 = 0.451
```

ANOVA: *Effect of water content on **Si** release for 50 wt.% GGBS mixes*

```
Water-to-So |       Summary of Si in mg/m2
 lids Ratio |        Mean   Std. Dev.       Freq.
------------+------------------------------------
        .35 |     78.0875   16.394898           8
         .4 |   80.999999   12.595578           8
         .5 |   68.947962   23.960847           8
------------+------------------------------------
      Total |    76.01182   18.229994          24

                      Analysis of Variance
    Source              SS         df      MS            F     Prob > F
------------------------------------------------------------------------
Between groups      632.707695      2   316.353848      0.95     0.4036
 Within groups      7010.94412     21   333.854482
------------------------------------------------------------------------
    Total           7643.65182     23   332.332688

Bartlett's test for equal variances:  chi2(2) =   2.7555  Prob>chi2 = 0.252
```

ANOVA: *Effect of binder content on **Si** release for CEM I mixes at w/s: 0.5*

```
Waste-to-Bi |       Summary of Si in mg/m2
 nder Ratio |        Mean   Std. Dev.       Freq.
------------+------------------------------------
          1 |        15.5   5.5312098           8
          4 |      10.075   4.1896982           8
          9 |   8.0749999   2.5655688           8
------------+------------------------------------
      Total |   11.216667   5.1889234          24

                      Analysis of Variance
    Source              SS         df      MS            F     Prob > F
------------------------------------------------------------------------
Between groups      236.163327      2   118.081663      6.47     0.0065
 Within groups      383.109977     21   18.2433322
------------------------------------------------------------------------
    Total           619.273304     23   26.9249263

Bartlett's test for equal variances:  chi2(2) =   3.5607  Prob>chi2 = 0.169
```

Aluminium (Al)

ANOVA: *Effect of water content on **Al** release for 50 wt.% CEM I mixes*[16]

```
Water-to-So |       Summary of Al in mg/m2
 lids Ratio |        Mean   Std. Dev.       Freq.
------------+------------------------------------
         .4 |    40.47125   52.939894           8
         .5 |    16.18125   8.6976917           8
        .55 |   14.323563   7.7643128           8
         .6 |    11.49885   6.1322023           8
------------+------------------------------------
      Total |   20.618728   28.469631          32

                      Analysis of Variance
    Source              SS         df      MS            F     Prob > F
------------------------------------------------------------------------
Between groups      4292.92087      3   1430.97362      1.92     0.1487
 Within groups      20833.1948     28   744.042672
------------------------------------------------------------------------
    Total           25126.1157     31   810.519861

Bartlett's test for equal variances:  chi2(3) =  42.6649  Prob>chi2 = 0.000
```

ANOVA: *Effect of water content on **Al** release for 20 wt.% CEM I mixes*

```
Water-to-So |       Summary of Al in mg/m2
 lids Ratio |        Mean   Std. Dev.       Freq.
------------+------------------------------------
        .45 |   4.5895413   2.7953909           8
         .5 |       4.745   3.1397316           8
         .6 |   4.3695625   3.2880233           8
------------+------------------------------------
      Total |   4.5680346   2.9484846          24

                      Analysis of Variance
    Source              SS         df      MS            F     Prob > F
------------------------------------------------------------------------
Between groups      .569363652      2   .284681826      0.03     0.9705
 Within groups      199.382552     21   9.49440724
------------------------------------------------------------------------
    Total           199.951916     23   8.69356155

Bartlett's test for equal variances:  chi2(2) =   0.1798  Prob>chi2 = 0.914
```

ANOVA: *Effect of water content on **Al** release for 50 wt.% GGBS mixes*

```
Water-to-So |       Summary of Al in mg/m2
 lids Ratio |        Mean   Std. Dev.       Freq.
------------+------------------------------------
        .35 |    92.71625   41.540542           8
         .4 |    97.94125   36.975827           8
         .5 |   79.964999   35.626099           8
------------+------------------------------------
      Total |     90.2075   37.243289          24

                      Analysis of Variance
    Source              SS         df      MS            F     Prob > F
------------------------------------------------------------------------
Between groups      1368.10842      2   684.054211      0.47     0.6311
 Within groups      30534.3313     21   1454.01578
------------------------------------------------------------------------
    Total           31902.4397     23    1387.0626

Bartlett's test for equal variances:  chi2(2) =   0.1726  Prob>chi2 = 0.917
```

[16] Same observation for inequality of variances as with Si for 50 wt.% mix at w/s: 0.4. Al release for the first test faction was abnormally high (170 mg/m^2) resulting in a high standard deviation.

ANOVA: *Effect of binder content on **Al** release for CEM I mixes at w/s: 0.5*[17]

```
Waste-to-Bi |       Summary of Al in mg/m2
 nder Ratio |        Mean   Std. Dev.       Freq.
------------+------------------------------------
          1 |    16.18125   8.6976917           8
          4 |       4.745   3.1397316           8
          9 |   4.1375001    3.473071           8
------------+------------------------------------
      Total |   8.3545833   7.8561706          24

                      Analysis of Variance
    Source              SS         df      MS            F     Prob > F
------------------------------------------------------------------------
Between groups      736.556735      2   368.278367     11.32     0.0005
 Within groups      682.989837     21   32.5233256
------------------------------------------------------------------------
    Total           1419.54657     23   61.7194162

Bartlett's test for equal variances:  chi2(2) =   8.8292  Prob>chi2 = 0.012
```

***t-test** on means of **Al** release from 20 wt.% and 10 wt.% CEM I mixes at w/s: 0.5*

```
Two-sample t test with equal variances
------------------------------------------------------------------------------
   Group |     Obs        Mean    Std. Err.   Std. Dev.   [95% Conf. Interval]
---------+--------------------------------------------------------------------
       4 |       8       4.745    1.110063    3.139732    2.120119    7.369881
       9 |       8      4.1375    1.227916    3.473071     1.23394     7.04106
---------+--------------------------------------------------------------------
combined |      16     4.44125    .8034228    3.213691    2.728795    6.153705
---------+--------------------------------------------------------------------
    diff |               .6075      1.6553               -2.942765    4.157765
------------------------------------------------------------------------------
    diff = mean(4) - mean(9)                                      t =   0.3670
Ho: diff = 0                                     degrees of freedom =       14

    Ha: diff < 0                 Ha: diff != 0                 Ha: diff > 0
 Pr(T < t) = 0.6404         Pr(|T| > |t|) = 0.7191          Pr(T > t) = 0.3596
```

***t-test** on means of **Al** release from 50 wt.% and 10 wt.% CEM I mixes at w/s: 0.5*

```
Two-sample t test with equal variances
------------------------------------------------------------------------------
   Group |     Obs        Mean    Std. Err.   Std. Dev.   [95% Conf. Interval]
---------+--------------------------------------------------------------------
       1 |       8    16.18125    3.075098    8.697692    8.909798     23.4527
       9 |       8      4.1375    1.227916    3.473071     1.23394     7.04106
---------+--------------------------------------------------------------------
combined |      16    10.15937     2.23065    8.922601    5.404857    14.91389
---------+--------------------------------------------------------------------
    diff |            12.04375    3.311194                4.941944    19.14556
------------------------------------------------------------------------------
    diff = mean(1) - mean(9)                                      t =   3.6373
Ho: diff = 0                                     degrees of freedom =       14

    Ha: diff < 0                 Ha: diff != 0                 Ha: diff > 0
 Pr(T < t) = 0.9987         Pr(|T| > |t|) = 0.0027          Pr(T > t) = 0.0013
```

[17] The inequality of variances is influenced by the similar mean release per fraction for mixes with 20 and 10 wt.% CEM I addition. Results of *t*-tests comparing these mixes to the mix with 50 wt.% CEM I indicate statistically significant differences.

CEM I vs. GGBS

***t-test** on means of **Al** release by binder for 50 wt.% binder addition*

a) w/s: 0.4

```
Two-sample t test with equal variances
------------------------------------------------------------------------------
   Group |     Obs        Mean    Std. Err.   Std. Dev.   [95% Conf. Interval]
---------+--------------------------------------------------------------------
    CEMI |       8    40.47125    18.71708    52.93989    -3.78761    84.73011
    ggbs |       8    97.94125    13.07293    36.97583    67.02869    128.8538
---------+--------------------------------------------------------------------
combined |      16    69.20625    13.29162    53.16648    40.87583    97.53667
---------+--------------------------------------------------------------------
    diff |             -57.47    22.83047               -106.4365   -8.503505
------------------------------------------------------------------------------
    diff = mean(CEMI) - mean(ggbs)                                t =  -2.5172
Ho: diff = 0                                     degrees of freedom =       14

    Ha: diff < 0                 Ha: diff != 0                 Ha: diff > 0
 Pr(T < t) = 0.0123         Pr(|T| > |t|) = 0.0246          Pr(T > t) = 0.9877
```

b) w/s: 0.5

```
Two-sample t test with equal variances
------------------------------------------------------------------------------
   Group |     Obs        Mean    Std. Err.   Std. Dev.   [95% Conf. Interval]
---------+--------------------------------------------------------------------
    CEMI |       8    16.18125    3.075098    8.697692    8.909798     23.4527
    ggbs |       8      79.965    12.59573     35.6261    50.18083    109.7492
---------+--------------------------------------------------------------------
combined |      16    48.07312     10.3456     41.3824      26.022    70.12425
---------+--------------------------------------------------------------------
    diff |           -63.78375    12.96567               -91.59235   -35.97515
------------------------------------------------------------------------------
    diff = mean(CEMI) - mean(ggbs)                                t =  -4.9194
Ho: diff = 0                                     degrees of freedom =       14

    Ha: diff < 0                 Ha: diff != 0                 Ha: diff > 0
 Pr(T < t) = 0.0001         Pr(|T| > |t|) = 0.0002          Pr(T > t) = 0.9999
```

***t-test** on means of **Si** release by binder for 50 wt.% binder addition*

a) w/s: 0.4

```
Two-sample t test with equal variances
------------------------------------------------------------------------------
   Group |     Obs        Mean    Std. Err.   Std. Dev.   [95% Conf. Interval]
---------+--------------------------------------------------------------------
    CEMI |       8      31.675    9.112389    25.77373    10.12762    53.22238
    ggbs |       8          81    4.453209    12.59558    70.46983    91.53017
---------+--------------------------------------------------------------------
combined |      16     56.3375    8.034394    32.13758    39.21259    73.46241
---------+--------------------------------------------------------------------
    diff |             -49.325    10.14232               -71.07812   -27.57188
------------------------------------------------------------------------------
    diff = mean(CEMI) - mean(ggbs)                                t =  -4.8633
Ho: diff = 0                                     degrees of freedom =       14

    Ha: diff < 0                 Ha: diff != 0                 Ha: diff > 0
 Pr(T < t) = 0.0001         Pr(|T| > |t|) = 0.0003          Pr(T > t) = 0.9999
```

b) w/s: 0.5

```
Two-sample t test with equal variances
------------------------------------------------------------------------------
   Group |     Obs        Mean    Std. Err.   Std. Dev.   [95% Conf. Interval]
---------+--------------------------------------------------------------------
    CEMI |       8        15.5    1.955578     5.53121    10.87579    20.12421
    ggbs |       8    68.94796    8.471439    23.96085    48.91619    88.97973
---------+--------------------------------------------------------------------
combined |      16    42.22398    8.077684    32.31073    25.00681    59.44116
---------+--------------------------------------------------------------------
    diff |           -53.44796    8.694225               -72.09522    -34.8007
------------------------------------------------------------------------------
    diff = mean(CEMI) - mean(ggbs)                                t =  -6.1475
Ho: diff = 0                                     degrees of freedom =       14

    Ha: diff < 0                 Ha: diff != 0                 Ha: diff > 0
 Pr(T < t) = 0.0000         Pr(|T| > |t|) = 0.0000          Pr(T > t) = 1.0000
```

B6. SULPHATE

ANOVA: *Effect of water content on SO_4^{2-} release for 50 wt.% CEM I mixes*[18]

```
Water-to-So |       Summary of SO4 in mg/m2
 lids Ratio |        Mean   Std. Dev.       Freq.
------------+------------------------------------
         .4 |    215.9875   392.38404           8
         .5 |   75.049999   20.075286           8
        .55 |   84.788224    23.06607           8
         .6 |    100.2125   18.436798           8
------------+------------------------------------
      Total |   119.00955    195.8912          32

                       Analysis of Variance
    Source              SS         df      MS            F     Prob > F
------------------------------------------------------------------------
Between groups      102892.741      3   34297.5804      0.88     0.4615
 Within groups      1086681.47     28   38810.0527
------------------------------------------------------------------------
    Total           1189574.22     31   38373.3618

Bartlett's test for equal variances:  chi2(3) =  80.7136  Prob>chi2 = 0.000
```

ANOVA: *Effect of water content on SO_4^{2-} release for 20 wt.% CEM I mixes*

```
Water-to-So |       Summary of SO4 in mg/m2
 lids Ratio |        Mean   Std. Dev.       Freq.
------------+------------------------------------
        .45 |    138.5625   48.558976           8
         .5 |       129.5   38.625271           8
         .6 |    87.18465   23.933595           8
------------+------------------------------------
      Total |   118.41572   43.234441          24

                       Analysis of Variance
    Source              SS         df      MS            F     Prob > F
------------------------------------------------------------------------
Between groups        12033.07      2   6016.53501      4.08     0.0318
 Within groups      30958.9185     21   1474.23422
------------------------------------------------------------------------
    Total           42991.9886     23   1869.21689

Bartlett's test for equal variances:  chi2(2) =   3.0524  Prob>chi2 = 0.217
```

[18] Same observation for inequality of variances as with Si and Al for 50 wt.% mix at w/s: 0.4. SO_4^{2-} release for the first test faction was abnormally high (1186 mg/m^2) resulting in a high standard deviation.

ANOVA: *Effect of water content on* SO_4^{2-} *release for 50 wt.% GGBS mixes*

Water-to-Solids Ratio	Summary of SO4 in mg/m2 Mean	Std. Dev.	Freq.
.35	803.8125	615.34085	8
.4	847.49998	617.045	8
.5	529.69137	327.55336	8
Total	727.00128	533.30673	24

Analysis of Variance

Source	SS	df	MS	F	Prob > F
Between groups	474808.819	2	237404.409	0.82	0.4533
Within groups	6066760.64	21	288893.364		
Total	6541569.46	23	284416.064		

Bartlett's test for equal variances: chi2(2) = 2.9218 Prob>chi2 = 0.232

ANOVA: *Effect of binder content on* SO_4^{2-} *release for CEM I mixes at w/s: 0.5*

Waste-to-Binder Ratio	Summary of SO4 in mg/m2 Mean	Std. Dev.	Freq.
1	75.049999	20.075286	8
4	129.5	38.625271	8
9	274.175	253.99261	8
Total	159.575	166.068	24

Analysis of Variance

Source	SS	df	MS	F	Prob > F
Between groups	169457.125	2	84728.5625	3.83	0.0383
Within groups	464850.237	21	22135.7256		
Total	634307.362	23	27578.581		

Bartlett's test for equal variances: chi2(2) = 37.0798 Prob>chi2 = 0.000

t-test *on means of* SO_4^{2-} *release from 20 wt.% and 10 wt.% CEM I mixes at w/s: 0.5*

Two-sample t test with equal variances

Group	Obs	Mean	Std. Err.	Std. Dev.	[95% Conf.	Interval]
4	8	129.5	13.6561	38.62527	97.20847	161.7915
9	8	274.175	89.79995	253.9926	61.83186	486.5181
combined	16	201.8375	47.68615	190.7446	100.1969	303.4781
diff		-144.675	90.83237		-339.4911	50.14107

diff = mean(4) - mean(9) t = -1.5928

Ho: diff = 0 degrees of freedom = 14

Ha: diff < 0 Ha: diff != 0 Ha: diff > 0

Pr(T < t) = 0.0668 Pr(|T| > |t|) = 0.1335 Pr(T > t) = 0.9332

***t-test** on means of SO_4^{2-} release from 50 wt.% and 20 wt.% CEM I mixes at w/s: 0.5*

```
Two-sample t test with equal variances
------------------------------------------------------------------------------
   Group |     Obs        Mean    Std. Err.   Std. Dev.   [95% Conf. Interval]
---------+--------------------------------------------------------------------
       1 |       8       75.05    7.097686    20.07529    58.26664    91.83336
       4 |       8       129.5     13.6561    38.62527    97.20847    161.7915
---------+--------------------------------------------------------------------
combined |      16     102.275    10.23143    40.92571    80.46723    124.0828
---------+--------------------------------------------------------------------
    diff |              -54.45    15.39045               -87.45924   -21.44076
------------------------------------------------------------------------------
    diff = mean(1) - mean(4)                                      t =  -3.5379
Ho: diff = 0                                     degrees of freedom =       14

    Ha: diff < 0                 Ha: diff != 0                 Ha: diff > 0
 Pr(T < t) = 0.0016         Pr(|T| > |t|) = 0.0033          Pr(T > t) = 0.9984
```

CEM I vs. GGBS

***t-test** on means of SO_4 release by binder for 50 wt.% binder addition*

a) w/s: 0.4

```
Two-sample t test with equal variances
------------------------------------------------------------------------------
   Group |     Obs        Mean    Std. Err.   Std. Dev.   [95% Conf. Interval]
---------+--------------------------------------------------------------------
    CEMI |       8    215.9875    138.7287     392.384   -112.0538    544.0288
    ggbs |       8       847.5    218.1584     617.045    331.6375    1363.363
---------+--------------------------------------------------------------------
combined |      16    531.7437    149.1392    596.5568    213.8611    849.6264
---------+--------------------------------------------------------------------
    diff |           -631.5125    258.5319               -1186.008    -77.0168
------------------------------------------------------------------------------
    diff = mean(CEMI) - mean(ggbs)                                t =  -2.4427
Ho: diff = 0                                     degrees of freedom =       14

    Ha: diff < 0                 Ha: diff != 0                 Ha: diff > 0
 Pr(T < t) = 0.0142         Pr(|T| > |t|) = 0.0284          Pr(T > t) = 0.9858
```

b) w/s: 0.5

```
Two-sample t test with equal variances
------------------------------------------------------------------------------
   Group |     Obs        Mean    Std. Err.   Std. Dev.   [95% Conf. Interval]
---------+--------------------------------------------------------------------
    CEMI |       8       75.05    7.097686    20.07529    58.26664    91.83336
    ggbs |       8    529.6914    115.8076    327.5534    255.8499    803.5328
---------+--------------------------------------------------------------------
combined |      16    302.3707    81.15455    324.6182    129.3939    475.3475
---------+--------------------------------------------------------------------
    diff |           -454.6414    116.0249                -703.49   -205.7927
------------------------------------------------------------------------------
    diff = mean(CEMI) - mean(ggbs)                                t =  -3.9185
Ho: diff = 0                                     degrees of freedom =       14

    Ha: diff < 0                 Ha: diff != 0                 Ha: diff > 0
 Pr(T < t) = 0.0008         Pr(|T| > |t|) = 0.0015          Pr(T > t) = 0.9992
```

B7. MINOR ELEMENTS

Iron (Fe)

ANOVA: *Effect of water content on **Fe** release for 50 wt.% CEM I mixes*

Water-to-Solids Ratio	Summary of Fe in mg/m2 Mean	Std. Dev.	Freq.
.4	3.65	1.0169984	8
.5	4.0500001	.9165152	8
.55	3.7821212	.96212941	8
.6	3.35	1.2071217	8
Total	3.7080303	1.0133264	32

Analysis of Variance

Source	SS	df	MS	F	Prob > F
Between groups	2.03188809	3	.677296028	0.64	0.5979
Within groups	29.7998522	28	1.06428043		
Total	31.8317403	31	1.02683033		

Bartlett's test for equal variances: chi2(3) = 0.5984 Prob>chi2 = 0.897

ANOVA: *Effect of water content on **Fe** release for 20 wt.% CEM I mixes*

Water-to-Solids Ratio	Summary of Fe in mg/m2 Mean	Std. Dev.	Freq.
.45	1.5375	.19955307	8
.5	1.4375	.26692694	8
.6	.94490549	.7924393	8
Total	1.3066352	.543075	24

Analysis of Variance

Source	SS	df	MS	F	Prob > F
Between groups	1.61018034	2	.805090172	3.27	0.0581
Within groups	5.17322019	21	.246343818		
Total	6.78340053	23	.294930458		

Bartlett's test for equal variances: chi2(2) = 14.0008 Prob>chi2 = 0.001

ANOVA: *Effect of water content on **Fe** release for 50 wt.% GGBS mixes*

Water-to-Solids Ratio	Summary of Fe in mg/m2 Mean	Std. Dev.	Freq.
.35	4.325	1.5979899	8
.4	3.525	.92543433	8
.5	3.6114451	1.0080541	8
Total	3.8204817	1.2170451	24

Analysis of Variance

Source	SS	df	MS	F	Prob > F
Between groups	3.08435582	2	1.54217791	1.05	0.3692
Within groups	30.9832134	21	1.47539112		
Total	34.0675693	23	1.48119866		

Bartlett's test for equal variances: chi2(2) = 2.4236 Prob>chi2 = 0.298

Lithium (Li)

ANOVA: *Effect of water content on **Li** release for 50 wt.% CEM I mixes*

```
Water-to-So |       Summary of Li in mg/m2
 lids Ratio |        Mean   Std. Dev.       Freq.
------------+------------------------------------
         .4 |        21.6   4.5254834           8
         .5 |       20.75   4.8565125           8
        .55 |    19.47305   6.9759538           8
         .6 |        19.9   6.8702256           8
------------+------------------------------------
      Total |   20.430762   5.6820349          32

                      Analysis of Variance
    Source              SS         df      MS            F     Prob > F
------------------------------------------------------------------------
Between groups      21.3436075      3   7.11453582      0.20     0.8932
 Within groups       979.50752     28   34.9824114
------------------------------------------------------------------------
    Total           1000.85113     31   32.2855202

Bartlett's test for equal variances:  chi2(3) =   1.9818  Prob>chi2 = 0.576
```

ANOVA: *Effect of water content on **Li** release for 20 wt.% CEM I mixes*

```
Water-to-So |       Summary of Li in mg/m2
 lids Ratio |        Mean   Std. Dev.       Freq.
------------+------------------------------------
        .45 |      17.225   5.9227767           8
         .5 |        17.4   7.5191186           8
         .6 |   15.223475   7.5187016           8
------------+------------------------------------
      Total |   16.616158   6.7901092          24

                      Analysis of Variance
    Source              SS         df      MS            F     Prob > F
------------------------------------------------------------------------
Between groups      23.3972973      2   11.6986487      0.24     0.7912
 Within groups      1037.03111     21   49.3824339
------------------------------------------------------------------------
    Total           1060.42841     23    46.105583

Bartlett's test for equal variances:  chi2(2) =   0.4705  Prob>chi2 = 0.790
```

ANOVA: *Effect of water content on **Li** release for 50 wt.% GGBS mixes*

```
Water-to-So |       Summary of Li in mg/m2
 lids Ratio |        Mean   Std. Dev.       Freq.
------------+------------------------------------
        .35 |      26.025   4.3407529           8
         .4 |       28.75   5.5420475           8
         .5 |   27.255949   10.565849           8
------------+------------------------------------
      Total |    27.34365   7.0960794          24

                      Analysis of Variance
    Source              SS         df      MS            F     Prob > F
------------------------------------------------------------------------
Between groups      29.7948151      2   14.8974076      0.28     0.7606
 Within groups      1128.35507     21   53.7311937
------------------------------------------------------------------------
    Total           1158.14988     23   50.3543427

Bartlett's test for equal variances:  chi2(2) =   5.7653  Prob>chi2 = 0.056
```

Strontium (Sr)

ANOVA: *Effect of water content on **Sr** release for 50 wt.% CEM I mixes*

Water-to-Solids Ratio	Summary of Sr in mg/m2 Mean	Std. Dev.	Freq.
.4	610.93752	155.34801	8
.5	602.18752	159.42118	8
.55	684.9315	201.33243	8
.6	607.43751	164.17654	8
Total	626.37351	166.18532	32

Analysis of Variance

Source	SS	df	MS	F	Prob > F
Between groups	36886.736	3	12295.5787	0.42	0.7399
Within groups	819257.601	28	29259.2		
Total	856144.337	31	27617.5593		

Bartlett's test for equal variances: chi2(3) = 0.5917 Prob>chi2 = 0.898

ANOVA: *Effect of water content on **Sr** release for 20 wt.% CEM I mixes*

Water-to-Solids Ratio	Summary of Sr in mg/m2 Mean	Std. Dev.	Freq.
.45	488.70001	165.42402	8
.5	653.68751	381.92058	8
.6	499.7	290.93277	8
Total	547.36251	290.5195	24

Analysis of Variance

Source	SS	df	MS	F	Prob > F
Between groups	136144.079	2	68072.0393	0.79	0.4660
Within groups	1805092.21	21	85956.7719		
Total	1941236.29	23	84401.5778		

Bartlett's test for equal variances: chi2(2) = 4.1544 Prob>chi2 = 0.125

ANOVA: *Effect of water content on **Sr** release for 50 wt.% GGBS mixes*

Water-to-Solids Ratio	Summary of Sr in mg/m2 Mean	Std. Dev.	Freq.
.35	246.675	52.896194	8
.4	239.625	53.764375	8
.5	235.53375	136.64016	8
Total	240.61125	86.230789	24

Analysis of Variance

Source	SS	df	MS	F	Prob > F
Between groups	508.182345	2	254.091172	0.03	0.9692
Within groups	170514.043	21	8119.71633		
Total	171022.225	23	7435.74893		

Bartlett's test for equal variances: chi2(2) = 8.3301 Prob>chi2 = 0.016[19]

[19] The inequality of variances is driven by the mix at w/s: 0.5 which exhibited a low concentration at the first fraction of the leaching test (91.4 mg/m^2) compared to the mixes at w/s: 0.35 and 0.4.

Effect of binder content

ANOVA: *Effect of binder content on **Fe** release for CEM I mixes at w/s: 0.5*

```
Waste-to-Bi |       Summary of Fe in mg/m2
 nder Ratio |        Mean   Std. Dev.       Freq.
------------+------------------------------------
          1 |   4.0500001    .9165152           8
          4 |      1.4375   .26692694           8
          9 |           2   .22677867           8
------------+------------------------------------
      Total |   2.4958334   1.2681652          24

                      Analysis of Variance
    Source              SS         df      MS            F     Prob > F
------------------------------------------------------------------------
Between groups      30.2508351      2   15.1254175     47.14     0.0000
 Within groups      6.73875064     21   .320892888
------------------------------------------------------------------------
    Total           36.9895857     23   1.60824286

Bartlett's test for equal variances:  chi2(2) =  15.6228  Prob>chi2 = 0.000
```

ANOVA: *Effect of binder content on **Li** release for CEM I mixes at w/s: 0.5*

```
Waste-to-Bi |       Summary of Sr in mg/m2
 nder Ratio |        Mean   Std. Dev.       Freq.
------------+------------------------------------
          1 |   602.18752   159.42118           8
          4 |   653.68751   381.92058           8
          9 |   382.71251   202.07141           8
------------+------------------------------------
      Total |   546.19584   281.00052          24

                      Analysis of Variance
    Source              SS         df      MS            F     Prob > F
------------------------------------------------------------------------
Between groups      331330.623      2   165665.311      2.34     0.1206
 Within groups      1484779.11     21    70703.767
------------------------------------------------------------------------
    Total           1816109.73     23   78961.2926

Bartlett's test for equal variances:  chi2(2) =   5.5816  Prob>chi2 = 0.061
```

ANOVA: *Effect of binder content on **Li** release for CEM I mixes at w/s: 0.5*

```
Waste-to-Bi |       Summary of Li in mg/m2
 nder Ratio |        Mean   Std. Dev.       Freq.
------------+------------------------------------
          1 |       20.75   4.8565125           8
          4 |        17.4   7.5191186           8
          9 |       15.95   7.0514437           8
------------+------------------------------------
      Total |   18.033333    6.613206          24

                      Analysis of Variance
    Source              SS         df      MS            F     Prob > F
------------------------------------------------------------------------
Between groups      96.9733332      2   48.4866666      1.12     0.3449
 Within groups      908.920011     21   43.2819053
------------------------------------------------------------------------
    Total           1005.89334     23   43.7344932

Bartlett's test for equal variances:  chi2(2) =   1.3243  Prob>chi2 = 0.516
```

CEM I vs. GGBS

***t-test** on means of **Fe** release by binder for 50 wt.% binder addition*

a) w/s: 0.4

```
Two-sample t test with equal variances
------------------------------------------------------------------------------
   Group |     Obs        Mean    Std. Err.   Std. Dev.   [95% Conf. Interval]
---------+--------------------------------------------------------------------
    CEMI |       8        3.65    .3595632    1.016998    2.799768    4.500232
    ggbs |       8       3.525    .3271904    .9254343    2.751318    4.298682
---------+--------------------------------------------------------------------
combined |      16      3.5875    .2353853    .9415413    3.085788    4.089212
---------+--------------------------------------------------------------------
    diff |               .125    .4861474               -.9176825    1.167682
------------------------------------------------------------------------------
    diff = mean(CEMI) - mean(ggbs)                                t =   0.2571
Ho: diff = 0                                     degrees of freedom =       14

    Ha: diff < 0                 Ha: diff != 0                 Ha: diff > 0
 Pr(T < t) = 0.5996         Pr(|T| > |t|) = 0.8008          Pr(T > t) = 0.4004
```

b) w/s: 0.5

```
Two-sample t test with equal variances
------------------------------------------------------------------------------
   Group |     Obs        Mean    Std. Err.   Std. Dev.   [95% Conf. Interval]
---------+--------------------------------------------------------------------
    CEMI |       8        4.05    .3240371    .9165152    3.283774    4.816226
    ggbs |       8    3.611445    .3564009    1.008054    2.768691    4.454199
---------+--------------------------------------------------------------------
combined |      16    3.830723    .2394658    .9578634    3.320313    4.341132
---------+--------------------------------------------------------------------
    diff |             .438555    .4816863               -.5945593    1.471669
------------------------------------------------------------------------------
    diff = mean(CEMI) - mean(ggbs)                                t =   0.9105
Ho: diff = 0                                     degrees of freedom =       14

    Ha: diff < 0                 Ha: diff != 0                 Ha: diff > 0
 Pr(T < t) = 0.8110         Pr(|T| > |t|) = 0.3780          Pr(T > t) = 0.1890
```

***t-test** on means of **Li** release by binder for 50 wt.% binder addition at w/s: 0.5*

a) w/s: 0.4

```
Two-sample t test with equal variances
------------------------------------------------------------------------------
   Group |     Obs        Mean    Std. Err.   Std. Dev.   [95% Conf. Interval]
---------+--------------------------------------------------------------------
    CEMI |       8        21.6         1.6    4.525483     17.8166     25.3834
    ggbs |       8       28.75     1.95941    5.542047    24.11673    33.38327
---------+--------------------------------------------------------------------
combined |      16      25.175    1.531407     6.12563    21.91088    28.43912
---------+--------------------------------------------------------------------
    diff |           -7.150001    2.529681               -12.57563   -1.724374
------------------------------------------------------------------------------
    diff = mean(CEMI) - mean(ggbs)                                t =  -2.8264
Ho: diff = 0                                     degrees of freedom =       14

    Ha: diff < 0                 Ha: diff != 0                 Ha: diff > 0
 Pr(T < t) = 0.0067         Pr(|T| > |t|) = 0.0135          Pr(T > t) = 0.9933
```

b) w/s: 0.5

```
Two-sample t test with equal variances
------------------------------------------------------------------------------
   Group |     Obs        Mean    Std. Err.   Std. Dev.   [95% Conf. Interval]
---------+--------------------------------------------------------------------
    CEMI |       8       20.75    1.717036    4.856513    16.68985    24.81015
    ggbs |       8    27.25595    3.735592    10.56585    18.42268    36.08922
---------+--------------------------------------------------------------------
combined |      16    24.00297     2.15626    8.625039    19.40702    28.59893
---------+--------------------------------------------------------------------
    diff |           -6.505949    4.111309               -15.32383    2.311931
------------------------------------------------------------------------------
    diff = mean(CEMI) - mean(ggbs)                                t =  -1.5825
Ho: diff = 0                                     degrees of freedom =       14

    Ha: diff < 0                 Ha: diff != 0                 Ha: diff > 0
 Pr(T < t) = 0.0679         Pr(|T| > |t|) = 0.1359          Pr(T > t) = 0.9321
```

*t-test on means of **Sr** release by binder for 50 wt.% binder addition at w/s: 0.5*

a) w/s: 0.4

```
Two-sample t test with equal variances
------------------------------------------------------------------------------
   Group |     Obs        Mean    Std. Err.   Std. Dev.   [95% Conf. Interval]
---------+--------------------------------------------------------------------
    CEMI |       8    610.9375    54.92382     155.348    481.0633    740.8117
    ggbs |       8     239.625    19.00858    53.76438    194.6769    284.5731
---------+--------------------------------------------------------------------
combined |      16    425.2813    55.55242    222.2097    306.8741    543.6884
---------+--------------------------------------------------------------------
    diff |            371.3125    58.12015                246.6572    495.9678
------------------------------------------------------------------------------
    diff = mean(CEMI) - mean(ggbs)                                t =   6.3887
Ho: diff = 0                                     degrees of freedom =       14

    Ha: diff < 0                 Ha: diff != 0                 Ha: diff > 0
 Pr(T < t) = 1.0000         Pr(|T| > |t|) = 0.0000          Pr(T > t) = 0.0000
```

b) w/s: 0.5

```
Two-sample t test with equal variances
------------------------------------------------------------------------------
   Group |     Obs        Mean    Std. Err.   Std. Dev.   [95% Conf. Interval]
---------+--------------------------------------------------------------------
    CEMI |       8    602.1875     56.3639    159.4212    468.9081     735.467
    ggbs |       8    235.5337    48.30959    136.6402    121.2997    349.7678
---------+--------------------------------------------------------------------
combined |      16    418.8606    59.38362    237.5345    292.2874    545.4338
---------+--------------------------------------------------------------------
    diff |            366.6538    74.23413                207.4374    525.8701
------------------------------------------------------------------------------
    diff = mean(CEMI) - mean(ggbs)                                t =   4.9392
Ho: diff = 0                                     degrees of freedom =       14

    Ha: diff < 0                 Ha: diff != 0                 Ha: diff > 0
 Pr(T < t) = 0.9999         Pr(|T| > |t|) = 0.0002          Pr(T > t) = 0.0001
```

APPENDIX VII: LEACHING DATA FROM A COMBINED ALKALINE/ACID LEACHING PROCEDURE

A. ALKALINE (WATER-WASH) LEACHING DATA

Moisture Content (%)	Eluant	Eluant volume (ml)	Contact time (hr)	pH	Sample Weight (g)
0.8	Deionized water	50	24	12	2.5

Element	Al	As	Ba	Ca	Cd	Co	Cr	Cu	Fe	K	Mg	Mn
LOD	10	10	10	200	2	10	10	10	10	200	50	10
Unit	**µg/l**	**µg/l**	**µg/l**	**µg/l**	**µg/l**	**µg/l**	**µg/l**	**µg/l**	**µg/l**	**µg/l**	**µg/l**	**µg/l**
Concentration	*10*	*10*	400	4130000	*2*	*10*	140	87.5	375	823000	1725	175

Element	Na	Ni	P	Pb	Sr	V	Zn	Cl	SO4	Ti	Li
LOD	50	10	50	10	10	10	10	500	10	10	10
Units	**µg/l**	**µg/l**	**µg/l**	**µg/l**	**µg/l**	**µg/l**	**µg/l**	**µg/l**	**µg/l**	**µg/l**	**µg/l**
Concentration	597000	10	250	32200	6640	50	6060	7150000	724988	40	370

B. ACID LEACHING DATA

pH	HNO3 (ml)	Li	Na	K	Be	Mg	Ca	Sr	Ba	Al	La	Ti	V	Cr
	(2N)	(µg/ml)	(µg/ml)	(µg/ml)	(µg/ml)	(µg/ml)	(µg/ml)	(µg/ml)	(µg/ml)	(µg/ml)	(µg/ml)	(µg/ml)	(µg/ml)	(µg/ml)
0.63	30/30	1.19	299	307	3.85E-02	477	25900	37	3.368	1510	0.587	8.43	0.9	5.1
0.8	27/30	1.185	295	300	3.80E-02	477	25700	36.7	3.233	1520	0.55	4.85	0.887	4.975
2.7	24/30	0.955	243	229	3.38E-02	398	22700	33.8	6.85	822	0.687	0.575	0.7	1.925
3.48	22/30	0.855	211	191	1.98E-02	362	21200	31.3	6.55	246	0.525	0.32	0.3125	1
4.76	21/30	0.78	195	180	6.25E-03	346	20900	30	5.89	13	7.50E-02	0.29	2.50E-02	BDL
5.15	19/30	0.675	170	160	5.50E-03	316	19700	28	3.923	5.75	8.75E-02	0.23	5.00E-02	BDL
5.56	18/30	0.69	180	169	4.50E-03	302	18900	27.1	3.148	5	7.50E-02	0.305	3.75E-02	BDL
6.03	16/30	0.505	129	131	5.00E-03	252	17900	25.3	2.965	7.25	5.00E-02	0.215	0.1	BDL
6.76	15/30	0.495	127	127	3.25E-03	239	15400	23.5	3.475	3.5	8.75E-02	0.145	BDL	BDL
9.13	14/30	0.465	138	145	2.50E-03	135	14800	21.2	2.575	2.5	BDL	0.135	BDL	BDL
9.63	13/30	0.445	134	152	2.25E-03	10.8	14000	19.5	3.055	2	BDL	0.11	BDL	BDL

pH	HNO3 (ml)	Mo	Mn	Fe	Co	Ni	Cu	Ag	Zn	Cd	Pb	P	S	As
	(2N)	(µg/ml)	(µg/ml)	(µg/ml)	(µg/ml)	(µg/ml)	(µg/ml)	(µg/ml)	(µg/ml)	(µg/ml)	(µg/ml)	(µg/ml)	(µg/ml)	(µg/ml)
0.63	30/30	0.4	50.1	298	0.5	1.275	52.2	3.50E-02	786	14.2	197	259	589	3.225
0.8	27/30	0.275	50.1	297	0.562	1.325	49.3	4.50E-02	795	14.1	191	261	475	3.075
2.7	24/30	0.2	42.5	197	0.512	1.05	28.6	4.00E-02	750	14	6	64.2	465	0.8
3.48	22/30	0.125	38.2	142	0.3875	0.75	25	1.50E-02	671	13.1	4.575	1.9	1710	BDL
4.76	21/30	0.175	34.6	65.1	0.35	0.675	7.32	2.50E-02	613	10.4	1.05	0.9	326	BDL
5.15	19/30	0.275	29.1	31.4	0.3	0.55	5.49	2.50E-02	533	8.64	0.825	0.65	327	BDL
5.56	18/30	0.25	25.1	1.125	0.275	0.525	2.015	1.50E-02	355	6.66	1.425	1.05	361	BDL
6.03	16/30	0.275	14.6	1.75	0.1625	0.35	1.345	2.50E-02	131	1.112	0.825	1	303	BDL
6.76	15/30	0.275	3.162	1.875	BDL	0.125	0.215	BDL	12.5	0.1875	0.375	0.5	284	BDL
9.13	14/30	0.2	0.1625	0.625	BDL	BDL	6.25E-02	BDL	0.995	BDL	BDL	0.6	314	BDL
9.63	13/30	0.225	7.50E-02	0.5	BDL	BDL	4.75E-02	BDL	0.795	BDL	BDL	0.5	310	BDL

APPENDIX VIII: PHYSICAL PROPERTIES DATA FOR S/S APC RESIDUES

A. CEM I MIXES

	50 wt.% CEM I				20 wt.% CEM I				10 wt.% CEM I			
Water/Solids (ml/g)	**0.4**	**0.5**	**0.55**	**0.6**	**0.45**	**0.5**	**0.6**	**0.65**	**0.5**	**0.55**	**0.6**	**0.65**
UCS **(7d)** (MPa)	11.7	5.9	3.9	3.4	7.6	6.1	2.7	2.5	4.0	2.9	2.1	1.5
UCS **(28d)** (MPa)	17.3	12.4	11.0	8.6	10.4	7.7	3.6	2.0	5.5	4.9	3.8	2.4
UCS at 28d after immersion (Mpa)	15.2	13.3	11.1	9.3	3.5	2.7	1.9	0.4	1.2	0.9	N/A	N/A
Initial Setting (min)	26	41	107	182	48	83	132	162	39	98	110	160
Final Setting (min)	37	84	145	212	88	107	170	237	82	129	140	231
Consistence (mm)	121	146	183	213	106	128	158	170	109	129	146	171
Moisture **(7d)** (%)	21.3	25.9	28.3	29.7	27.1	29.2	33.4	34.3	30.2	33.2	34.2	36.3
Moisture **(28d)** (%)	20.9	24.9	26.6	27.0	27.5	29.0	34.0	35.5	31.1	32.3	33.5	37.6
Bulk Density **(7d)** (g/cm3)	1.85	1.69	1.72	1.68	1.74	1.71	1.64	1.61	1.68	1.65	1.62	1.62
Bulk Density **(28d)** (g/cm3)	1.84	1.73	1.71	1.68	1.75	1.72	1.62	1.58	1.64	1.63	1.62	1.59
Specific Gravity **(7d)** (g/cm3)	2.15	2.12	2.12	2.11	2.08	2.06	2.08	2.06	2.07	2.07	2.06	2.06
Specific Gravity (**28d)** (g/cm3)	2.10	2.08	2.07	2.07	2.08	2.09	2.07	2.07	2.08	2.08	2.08	2.09
Porosity **(7d)** (%)	32.4	41.0	41.6	44.1	38.9	41.3	47.4	48.7	43.3	46.7	48.3	50.0
Porosity **(28d)** (%)	30.7	37.5	39.6	40.8	38.9	41.6	48.2	50.7	45.7	46.8	48.2	52.5

B. GGBS MIXES

	50 wt.% GGBS			20 wt.% GGBS					10 wt.% GGBS				
Water/Solids (ml/g)	**0.35**	**0.4**	**0.5**	**0.4**	**0.5**	**0.6**	**0.7**	**0.8**	**0.4**	**0.5**	**0.6**	**0.7**	**0.8**
UCS **(7d)** (MPa)	0.8	0.7	0.4	1.3	0.2	0.3	0.1	0.1		0.9	0.7	0.1	0.1
UCS **(28d)** (MPa)	20.6	14.6	10.0	1.7	0.8	0.8	0.5			0.4	0.3	0.4	0.2
UCS at 28d after immersion (Mpa)	22.1	15.7	8.5	N/A	N/A	N/A	N/A	N/A	N/A	N/A	N/A	N/A	N/A
Initial Setting (min)	55	70	310	38	60	123	160	310	36	89	107	138	397
Final Setting (min)	85	105	525	68	115	159	250	439	68	117	135	233	595
Consistence (mm)	107	114	149	100	106	117	124	213	100	106	110	122	129
Moisture **(7d)** (%)	23.7	26.4	29.3	29.8	35.1	36.2	39.1	40.6		32.6	34.5	41.8	42.7
Moisture **(28d)** (%)	22.7	24.8	27.9	31.4	36.1	38.7	41.5			38.6	40.1	40.9	45.0
Bulk Density **(7d)** (g/cm3)	1.80	1.68	1.66	1.68	1.59	1.54	1.54	1.58		1.60	1.55	1.45	1.49
Bulk Density **(28d)** (g/cm3)	1.74	1.72	1.67	1.59	1.57	1.52	1.49			1.55	1.48	1.49	1.49
Specific Gravity **(7d)** (g/cm3)	2.24	2.21	2.17	2.17	2.16	2.13	2.15	2.16		2.15	2.15	2.13	2.13
Specific Gravity **(28d)** (g/cm3)	2.03	2.02	2.02	2.05	2.04	2.04	2.04			2.05	2.04	2.01	2.04
Porosity **(7d)** (%)	38.8	43.9	45.9	45.7	52.2	53.8	56.4	56.5		49.9	52.6	60.3	59.9
Porosity **(28d)** (%)	33.7	36.1	40.5	46.8	50.8	54.2	57.3			53.5	56.5	56.3	59.9

APPENDIX IX: MONOLITHIC LEACHING DATA

A. MONOLITHIC LEACHING SAMPLE DATA

The coding of the sample is as follows and an example is shown below.

- The first letter indicates the binder use. *O* stands for CEM I and *G* stands for GGBS
- The second number indicates the APC residue content and waste/binder ratio: 1: 50 wt.%; 4: 80 wt.%; 9: 90 wt.%
- The last two numbers indicate the water-to-solids ratio e.g. 55: 0.55.

O	**1**	**40**
CEM I	50 wt.%	w/s: 0.4

Sample	Fraction	Weight (gr)	Moisture Content (%)	Sample Geometry	Volume (cm^3)	Leaching Surface (cm^2)	pH	Conductivity (mS/cm)	Temperature (°C)	Eluate Volume (ml)
O140	1	235.69	20.9	Block-all sides	131	150	11.52	7420	25	540
O140	2						11.64	7460	25	540
O140	3						11.7	6770	25	540
O140	4						11.79	5910	25	540
O140	5						11.78	7100	25	540
O140	6						11.76	5980	25	540
O140	7						11.89	6260	25	540
O140	8						11.83	6190	25	540
O150	1	224.5	24.9	Block-all sides	128	150	11.72	7410	25	540
O150	2						11.78	6430	25	540
O150	3						11.73	6900	25	540
O150	4						11.78	6580	25	540
O150	5						11.91	7760	25	540
O150	6						11.79	5880	25	540
O150	7						11.99	6130	25	540
O150	8						11.87	7600	25	540
O155	1	220.07	26.6	Block-all sides	127	150	11.65	8640	25	540
O155	2						11.76	8790	25	540
O155	3						11.76	5890	25	540

Sample	Fraction	Weight (gr)	Moisture Content (%)	Sample Geometry	Volume (cm^3)	Leaching Surface (cm^2)	pH	Conductivity (mS/cm)	Temperature (°C)	Eluate Volume (ml)
O155	4						11.81	5650	25	540
O155	5						11.86	7940	25	540
O155	6						11.83	5990	25	540
O155	7						12.02	6280	25	540
O155	8						11.94	7340	25	540
O160	1	214.16	27	Block-all sides	126	150	11.67	9820	25	540
O160	2						11.83	9330	25	540
O160	3						11.76	5880	25	540
O160	4						11.82	5780	25	540
O160	5						11.88	7550	25	540
O160	6						11.85	5890	25	540
O160	7						12.04	6200	25	540
O160	8						11.93	6780	25	540
O445	1	225.14	27.1	Block-all sides	130	150	11.6	14100	25	540
O445	2						11.71	13670	25	540
O445	3						11.64	11090	25	540
O445	4						11.7	10480	25	540
O445	5						11.89	10710	25	540
O445	6						11.95	7470	25	540
O445	7						11.99	6490	25	540
O445	8						11.97	6690	25	540
O450	1	221.66	29.2	Block-all sides	130	150	11.64	13600	25	540
O450	2						11.74	12330	25	540
O450	3						11.68	10600	25	540
O450	4						11.71	9880	25	540
O450	5						11.92	10190	25	540
O450	6						11.94	7120	25	540

Sample	Fraction	Weight (gr)	Moisture Content (%)	Sample Geometry	Volume (cm^3)	Leaching Surface (cm^2)	pH	Conductivity (mS/cm)	Temperature (°C)	Eluate Volume (ml)
O450	7						12.03	6320	25	540
O450	8						11.93	6650	25	540
O460	1	209.84	33.4	Block-all sides	131	150	11.63	13840	25	540
O460	2						11.75	13430	25	540
O460	3						11.7	10510	25	540
O460	4						11.72	9290	25	540
O460	5						11.94	8790	25	540
O460	6						12.03	6510	25	540
O460	7						12.03	6090	25	540
O460	8						11.93	6290	25	540
O950	1	219.77	31.1	Block-all sides	132	150	11.6	16720	25	540
O950	2						11.7	16770	25	540
O950	3						11.67	12870	25	540
O950	4						11.76	11980	25	540
O950	5						11.94	10050	25	540
O950	6						11.98	6870	25	540
O950	7						12.1	6050	25	540
O950	8						11.93	6380	25	540
G135	1	250.42	23.7	Block-all sides	143	160	10.7	3510	25	560
G135	2						10.97	4460	25	560
G135	3						10.85	4460	25	560
G135	4						11.02	4570	25	560
G135	5						11.01	6220	25	560
G135	6						11.08	4480	25	560
G135	7						11.2	5430	25	560
G135	8						11.1	5430	25	560
G140	1	248.95	26.4	Block-all sides	146	160	10.87	4220	25	560

Sample	Fraction	Weight (gr)	Moisture Content (%)	Sample Geometry	Volume (cm^3)	Leaching Surface (cm^2)	pH	Conductivity (mS/cm)	Temperature (°C)	Eluate Volume (ml)
G140	2						10.99	4730	25	560
G140	3						10.9	4710	25	560
G140	4						11.03	4780	25	560
G140	5						11.05	6270	25	560
G140	6						11.12	4620	25	560
G140	7						11.22	5460	25	560
G140	8						11.12	5440	25	560
G150	1	233.38	29.3	Block-all sides	139	160	10.68	3320	25	560
G150	2						10.92	3790	25	560
G150	3						10.86	4010	25	560
G150	4						10.96	4100	25	560
G150	5						10.98	5800	25	560
G150	6						11.08	4510	25	560
G150	7						11.2	5770	25	560
G150	8						11.08	5370	25	560

B. ELUATE ANALYSIS

- Data presented is the average of two duplicates in µg/l
- When data obtained was below the laboratory detection limit, the value of the latter was used. Indicated by values in *italics*.
- Data in bold indicate estimated values

Sample	Fraction	Al	Ca	Fe	K	Mg	Na	Pb	Si	Sr	Zn	Cl	SO4	Li
O140	1	4721.75	1160995	99.4345	188870	188.87	305525	*10*	2538.6	8332.5	36.7	2674170.75	32934.1	816.585
O140	2	138.875	1277650	85.547	761035	62.7715	711040	17.2	205.5	19998	62.8	2674170.75	2163.4	666.6
O140	3	488.84	1722050	87.2135	783255	68.882	666600	17.8	683.3	22775.5	48.9	2249302.5	3245.1	711.04
O140	4	744.37	1149885	96.1015	411070	82.7695	333300	*10*	705.5	14665.2	83.3	2164328.85	2051.9	444.4
O140	5	744.37	1333200	93.8795	366630	69.993	338855	*10*	911	16665	31.1	2499225	2043.6	472.175
O140	6	661.045	1610950	73.8815	366630	*50*	383295	13.9	983.2	19442.5	52.2	2014375.35	2210	566.61
O140	7	877.69	1555400	107.2115	211090	62.7715	211090	25.6	605.5	16109.5	47.2	1824434.25	2334.8	527.725
O140	8	616.605	1833150	166.65	122210	85.547	149985	46.1	405.5	17776	52.8	979696.2	1015.1	594.385
O150	1	822.14	1222100	161.095	49995	73.326	59994	43.3	538.8	11054.45	47.2	2724155.25	1148.3	377.74
O150	2	96.1015	1610950	92.7685	1027675	83.325	905465	13.3	250	17776	78.3	2274294.75	1880.5	749.925
O150	3	277.75	1666500	112.211	744370	72.215	683265	*10*	500	17776	34.4	2484229.65	1930.4	649.935
O150	4	444.4	1610950	122.21	633270	86.658	577720	11.7	538.8	17220.5	38.9	2304285.45	2251.6	622.16
O150	5	566.61	1444300	90.5465	411070	79.992	427735	11.1	633.3	14443	63.9	2749147.5	2376.4	511.06
O150	6	383.295	2222000	92.213	405515	*50*	549945	29.4	266.6	26108.5	38.3	1704471.45	2792.5	738.815
O150	7	716.595	1610950	133.32	138875	84.9915	161095	40.6	472.2	13887.5	294.4	1359578.4	2701	455.51
O150	8	288.86	1777600	94.9905	73881.5	74.9925	98879	76.1	244.4	15554	77.8	784756.65	1597.6	505.505
O155	1	349.965	1388750	110.5445	44440	68.882	47217.5	95	200	12221	52.8	3248992.5	1414.6	311.08
O155	2	144.43	1944250	115.544	1222100	64.438	1122110	15.6	283.3	27219.5	95	3154021.95	2995.5	872.135
O155	3	261.085	2055350	106.1005	827695	78.3255	894355	16.7	338.9	26664	28.9	1804440.45	3078.7	766.59
O155	4	394.405	1277650	76.659	366630	88.88	405515	*10*	405.5	14443	28.9	1614499.35	2334.8	422.18
O155	5	633.27	1499850	102.7675	322190	61.6605	383295	13.9	627.7	14998.5	33.9	2604192.45	1827.3	433.29
O155	6	372.185	1944250	86.1025	344410	99.99	472175	37.8	1049.9	21109	24.4	1609500.9	2725.9	622.16
O155	7	794.365	1722050	161.095	115544	114.9885	138875	42.2	799.9	16665	31.1	1209624.9	2784.2	433.29

Sample	Fraction	Al	Ca	Fe	K	Mg	Na	Pb	Si	Sr	Zn	Cl	SO4	Li
O155	8	233.31	1722050	81.6585	64993.5	*50*	83880.5	88.9	188.9	18887	44.4	674790.75	1680.8	466.62
O160	1	244.42	1444300	83.325	46662	56.661	47773	101.7	166.7	13332	49.4	3798822	2812.5	311.08
O160	2	122.21	1833150	64.438	1166550	76.1035	1049895	11.1	183.3	21109	44.4	3433935.15	3161.9	855.47
O160	3	205.535	1944250	60.5495	838805	58.883	827695	13.9	350	24442	48.3	1774449.75	3078.7	766.59
O160	4	377.74	1555400	76.659	422180	57.772	455510	*10*	450	13332	38.3	1624496.25	2235	494.395
O160	5	438.845	1444300	155.54	327745	151.096	377740	12.2	799.9	13332	37.8	2374263.75	2725.9	466.62
O160	6	333.3	2110900	83.8805	311080	57.772	444400	48.3	294.4	21109	85	1459547.4	3391.6	677.71
O160	7	649.935	1777600	133.32	89991	104.434	111100	49.4	527.7	13887.5	58.9	1044676.05	3017.2	422.18
O160	8	183.315	1722050	86.1025	57216.5	81.103	69993	93.3	599.9	14443	70.5	599814	1847.2	427.735
O445	1	*10*	3944050	39.996	1777600		1999800	116.7	277.8	19442.5	50.6	6123101.25	6640.1	788.81
O445	2	23.8865	4055150	33.33	1077670		1222100	78.9	238.9	16665	54.4	5698233	4659.7	605.495
O445	3	87.769	4166250	42.7735	727705		916575	85.5	244.4	15554	344.4	4598574	4243.7	544.39
O445	4	211.09	3610750	40.5515	388850		622160	93.3	350	13332	76.7	4248682.5	3549.7	444.4
O445	5	158.3175	3666300	47.2175	216645		411070	115	350	16665	96.7	4023752.25	2775.8	449.955
O445	6	166.65	2555300	41.107	83880.5		102212	172.2	138.9	12776.5	107.2	2214313.35	3225.2	344.41
O445	7	155.54	1777600	49.4395	101656.5		106100.5	283.3	172.2	8721.35	127.8	1124651.25	3350	377.74
O445	8	205.535	1444300	47.2175	77770		78881	333.3	244.4	5443.9	122.2	504843.45	2346.5	272.195
O450	1	*10*	3999600	42.7735	1999800		2110900	161.1	444.4	34996.5	52.2	5723225.25	5641.6	861.025
O450	2	13.8875	4277350	31.108	1222100		1388750	78.9	327.7	29441.5	56.1	5073426.75	4659.7	694.375
O450	3	101.6565	3333000	39.996	633270		749925	70	300	19998	92.8	4398636	3411.6	494.395
O450	4	177.76	3777400	33.33	438845		655490	92.2	327.7	21109	109.4	3948775.5	3882.5	516.615
O450	5	127.765	3221900	56.661	211090		327745	99.4	388.9	17776	338.9	4483609.65	2709.3	422.18
O450	6	216.645	2444200	39.996	76103.5		86102.5	150	161.1	9721.25	90	1884415.65	2775.8	288.86
O450	7	155.54	1333200	32.7745	46662		93879.5	244.4	138.9	7388.15	122.2	1174635.75	3017.2	338.855
O450	8	249.975	1044340	42.7735	54994.5		71659.5	294.4	150	4832.85	116.7	439863.6	2679.3	249.975
O460	1	13.8875	2444200	*10*	1155.44		1388750	*10*	344.4	24442	*11.1*	5773209.75	2978.9	777.7
O460	2	39.4405	3166350	21.6645	670932.9		1077670	42.2	288.9	22220	40.6	5603262.45	3328.4	661.045
O460	3	127.765	2666400	28.886	2833.05		672155	59.4	200	20553.5	70	4198698	2546.2	511.06

Sample	Fraction	Al	Ca	Fe	K	Mg	Na	Pb	Si	Sr	Zn	Cl	SO4	Li
O460	4	56.661	1999800	*10*	1133.22		190258.75	*10*	255.5	13887.5	*11.1*	3433935.15	2434.7	372.185
O460	5	66.66	2333100	13.8875	**61216.1**		148874	59.4	244.4	14443	47.2	2794133.55	2193.4	355.52
O460	6	233.31	1388750	24.9975	43329		64438	150	133.3	6443.8	108.9	1469544.3	2359.8	222.2
O460	7	183.315	1105445	19.998	62771.5		78325.5	205.5	100	5221.7	111.1	684787.65	2484.6	272.195
O460	8	249.975	1083225	78.3255	51661.5		58883	250	227.8	3832.95	108.9	344893.05	1048.4	211.09
O950	1	199.98	1388750	62.216	37218.5		41662.5	102.2	200	9776.8	70.5	7822574.25	2646	272.195
O950	2	*10*	5110600	56.1055	2388650		1888700	98.9	200	18331.5	99.4	7772589.75	21800.7	766.59
O950	3	*10*	4499550	46.1065	1444300		1666500	133.3	255.5	16665	133.3	5723225.25	13563.1	666.6
O950	4	22.7755	5110600	62.216	872135		1111000	144.4	194.4	14998.5	261.1	4928471.7	9707.2	555.5
O950	5	93.8795	3333000	55.55	388850		555500	113.3	383.3	10443.4	155.5	3598884	5438.5	394.405
O950	6	136.0975	2388650	54.9945	116099.5		138319.5	222.2	150	7110.4	172.2	1624496.25	3391.6	299.97
O950	7	177.76	1499850	48.884	107767		110544.5	533.3	227.8	4555.1	211.1	654796.95	3017.2	344.41
O950	8	266.64	1222100	59.4385	69993		79992	661	183.3	3166.35	216.6	289910.1	1364.6	244.42
G135	1	1083.225	427735	129.4315	799920	211.09	655490	*10*	1316.5	6999.3	29.4415	1172636.37	12298.3	783.255
G135	2	1777.6	666600	109.989	611050	399.96	577720	*10*	1949.8	6666	34.9965	1684477.65	12148.5	749.925
G135	3	2166.45	688820	222.2	477730	477.73	505505	*10*	2294.2	6388.25	27.2195	1694474.55	10734	688.82
G135	4	2110.9	683265	109.989	438845	416.625	461065	*10*	2149.8	5999.4	44.9955	1726964.475	11371.3	649.935
G135	5	2721.95	1027675	68.3265	616605	311.08	655490	*10*	2688.6	9554.6	15	2699163	20416.1	916.575
G135	6	2610.85	816585	132.7645	394405	283.305	405515	*10*	2538.6	6277.15	23.8865	1909407.9	17537.1	666.6
G135	7	3999.6	1222100	87.2135	422180	161.095	505505	*10*	2777.5	9165.75	28.886	2519218.8	59432.8	916.575
G135	8	4721.75	1166550	127.765	211090	138.875	199980	*10*	2133.1	5332.8	44.9955	1719466.8	39790.5	577.72
G140	1	1444.3	594385	61.105	711040	211.09	627715	*10*	1816.5	7277.05	13.8875	1564514.85	12797.5	833.25
G140	2	2055.35	527725	72.215	351020.5	199.98	466620	*10*	2060.9	7277.05	18.887	1806939.675	12481.3	816.585
G140	3	2333.1	716595	106.1005	499950	449.955	549945	*10*	2294.2	5888.3	29.4415	1796942.775	12897.4	772.145
G140	4	2166.45	638825	127.2095	427735	477.73	455510	*10*	2205.3	5221.7	76.1035	1806939.675	13035.5	683.265
G140	5	2999.7	1061005	86.1025	699930	338.855	694375	*10*	2910.8	9443.5	100.5455	2669172.3	24576.6	1105.445
G140	6	2721.95	794365	139.986	361075	283.305	388850	*10*	2705.3	5943.85	23.331	1984384.65	17037.9	722.15
G140	7	4166.25	1277650	108.878	383295	144.43	511060	*10*	2444.2	8443.6	27.775	2519218.8	61097	994.345

Sample	Fraction	Al	Ca	Fe	K	Mg	Na	Pb	Si	Sr	Zn	Cl	SO4	Li
G140	8	4499.55	1049895	103.323	166650	211.09	188870	*10*	2077.6	5277.25	54.439	1704471.45	39790.5	644.38
G150	1	633.27	165539	122.21	299970	117.2105	238865	*10*	688.8	2610.85	25.553	1179634.2	6806.5	388.85
G150	2	1610.95	305525	82.7695	461065	261.085	399960	*10*	1449.9	3999.6	18.887	1397066.775	9818.7	611.05
G150	3	***2479.2***	***385000***	***70***	***523350***	***356.6***	***476100***	***10***	***1944.3***	***4730***	***15.22***	***1502034.225***	***11144.5***	***691.6***
G150	4	1888.7	338855	91.102	416625	344.41	394405	*10*	1705.4	4221.8	19.4425	1504533.45	9540.7	605.495
G150	5	1944.25	361075	118.3215	438845	399.96	399960	*10*	2244.2	5221.7	39.996	2464235.85	9931.8	633.27
G150	6	2944.15	972125	75.548	749925	316.635	727705	*10*	2649.7	11665.5	26.1085	1934400.15	22363.2	1222.1
G150	7	2721.95	805475	149.985	422180	305.525	488840	*10*	2777.5	8054.75	34.9965	2714158.35	16663.4	855.47
G150	8	4055.15	1222100	119.988	472175	149.985	611050	*10*	2299.8	13332	27.2195	1809438.9	34798	1222.1

APPENDIX X: LIST OF PUBLICATIONS RESULTING FROM THIS WORK

JOURNAL AND CONFERENCE PUBLICATIONS

- **Lampris**, C., Pellizon-Birelli, M., Fowler, G.D., Cheeseman, C.R., 2011. Metal leaching from monolithic stabilised/ solidified air pollution control residues. Journal of Hazardous Materials vol. 185, pp. 1115-1123.

- **Lampris**, C., Stegemann, J.A., Cheeseman, C.R, 2009. Metal leaching from APC residues solidified using Portland cement and granulated ground blast furnace slag. WASCON Conference June 2009, Lyon, France.

- **Lampris**, C., Stegemann, J.A., Cheeseman, C.R., 2009. Solidification/stabilisation of air pollution control residues using Portland cement: Physical properties and chloride leaching. Waste Management vol. 29, pp. 1067-1075.

- **Lampris**, C., Stegemann J.A., Cheeseman, C.R., 2008. Chloride leaching from air pollution control residues solidified using granulated ground blast furnace slag. Chemosphere vol. 73, pp. 1544-1549.

- **Lampris**, C., Stegemann, J.A., Cheeseman, C.R, 2008. Comparison of the physical properties and leaching characteristics of APC residues solidified using Portland cement and granulated ground blast furnace slag. 1st International Conference on Hazardous Waste Management October 2008, Crete, Greece.

- Stegemann, J.A., **Lampris**, C., Pellizon-Birelli, M., Zhou, Q., 2008. Development of process envelopes for generic cement-based stabilisation/solidification of industrial wastes. Concrete Communication Conference, September 2008, Liverpool, UK.